The Regulation of Beta-Dystroglycan Internalization

Robert Piggott

A thesis submitted to the University of Sheffield for the degree of Doctor of Philosophy

Department of Biomedical Sciences,
University of Sheffield

July 2014

TABLE OF CONTENTS

Abbreviations Used

APPL1	DCC-interacting Protein 13-alpha
BMD	Becker Muscular Dystrophy
BODIPY	Boron-dipyrromethene
Cdc42	Cell Division Control Protein 42
CHC	Clathrin Heavy Chain
ChTxB	Cholera Toxin B subunit
DGC	Dystrophin-associated Glycoprotein Complex
DMD	Duchenne Muscular Dystrophy
EEA1	Early Endosome-associated Antigen 1
ECM	Extracellular Matrix
EDTA	Ethylenediaminetetraacetic Acid
EGF	Epidermal Growth Factor
ERK	Extracellular Signal-regulated Kinase
FAK	Focal Adhesion Kinase
FGF	Fibroblast Growth Factor
Grb2	Growth Factor Receptor-bound Protein 2
GM1	Monosialotetrahexosylganglioside
H2K	$H2k^b$ ts-A58 (mouse strain)
LacCer	Lactosylceramide
LDL	Low-density Lipoprotein
LGMD	Limb-girdle Muscular Dystrophy
MAPK	Mitogen-activated Protein Kinase
MAST	Microtubule-associated Serine/Threonine Protein Kinase
MEK2	Dual Specificity Mitogen-activated Protein Kinase Kinase 2

MesNa	Sodium Mercaptoethanesulphonate
miRNA	Micro Ribonucleic Acid
NHS	N-hydroxysuccinimide
NMJ	Neuromuscular Junction
NLS	Nuclear Localization Sequence
nNOS	Neural Nitric oxide Synthase
PAK	P21 Activated Kinase
PBS	Phospho-buffered Saline
PDZ	PSD95, Dlg1, zo-1 (domain)
...R	…receptor (e.g “EGFR”, “FGFR”)
Rac1	Ras-related botulinum toxin substrate 1
SGC	Sarcoglycan Complex
snRNA	Small Nuclear Ribonucleic Acid
Src	Proto-oncogene tyrosine-protein kinase Src
TCEP	Tris(2-carboxyethyl)phosphine
Tfn	Transferrin
Tris	Tris(hydroxymethyl)aminomethane
UGC	Utrophin-associated Glycoprotein Complex
XDLC	X-linked Dilated Cardiomyopathy
Y890	Tyrosine 890
WW	Rsp5-domain (Tryptothan-tryptophan domain)

Abstract

β-dystroglycan is a ubiquitously expressed protein that forms adhesion complexes in various cell and tissue types. In skeletal muscle it is part of the dystrophin-associated glycoprotein complex, which is lost from the sarcolemma in the pathology of Duchenne muscular dystrophy, as well as other muscular dystrophies. The loss of β-dystroglycan from the surface membrane is a key step in the pathology of muscular dystrophies and yet, little is known about the mechanisms governing this process. Before, it was thought that β-dystroglycan is held at the membrane by scaffolding proteins, but recent findings reported in the literature challenge this view. In light of these findings it was hypothesized that the phosphorylation of a single residue, tyrosine 890, prompts the internalization of β-dystroglycan. This process was investigated using $H2k^b$ ts-A58 murine skeletal myoblasts, an established *in vitro* model of skeletal muscle satellite cells. The internalization of β-dystroglycan from the surface membrane in response to tyrosine 890 phosphorylation is described in this thesis. The internalization of β-dystroglycan appears to be critically dependent on this modification, as the unmodified form of the protein remains at the plasma membrane. Tyrosine 890 phosphorylation is also linked to the monoubiquitylation of β-dystroglycan although the exact function of this modification in the internalization process is uncertain. An examination of several common endocytic routes reveals no pathway for the internalization of β-dystroglycan. These findings are supported by data from the $Dag1^{Y890F/Y890F}$: *mdx* mouse, suggesting that the mechanism described in $H2k^b$ myoblasts is also present *in vivo*. These findings have profound implications, not only for the understanding of β-dystroglycan, but for the pathology of muscular dystrophies and the development of new therapies.

Chapter 1:
Introduction

1.1.1 The Dystroglycan Subunits

The dystroglycan gene, *DAG1,* is evolutionarily conserved across mammals (Ibraghimov-Beskrovnaya et al., 1993 ; Yotsumoto et al., 1996) and other phyla of the animal kingdom including nematodes (Grisoni et al., 2002), arthropods (Yatsenko et al., 2009) and chordates (Deyst et al., 1995). In mammals, the gene comprises two exons separated by a single intron and it is strongly conserved between mouse and man (Ibraghimov-Beskrovnaya et al., 1993). The gene encodes a single polypeptide that is post-translationally cleaved to form two subunits, α- and β-dystroglycan (Ibraghimov-Beskrovnaya et al. 1992 ; Deyst et al., 1995). Dystroglycan is ubiquitously expressed in mammalian tissues and together the two subunits form a transmembrane adhesion complex (Ibraghimov-Beskrovnaya et al., 1993 ; Durbeej et al., 1998). α-dystroglycan binds to components of the extracellular matrix (ECM): most notably laminin-α1 and –α2 (Ervasti et al., 1993 ; Sunada et al., 1994 ; Durbeej et al., 1999), but also biglycan (Bowe et al., 2000), agrin (Deyst et al., 1995 ; Moll et al., 2001), heparin (Gee et al., 1993) and perlecan (Peng et al., 1998 ; Hochenester et al., 1999). β-dystroglycan contains a single transmembrane domain and binds to both α-dystroglycan (Yoshida et al., 1994 ; Sciandra et al., 2001) and various cytoskeletal linker proteins (Ervasti et al., 1993 ; Rybakova et al., 1996 ; Cerecedo et al., 2005 ; Rezniczek et al., 2007), via an extracellular and an intracellular domain respectively. In this way, the dystroglycan subunits mediate a physical link between the internal cytoskeleton of cells and the surrounding extracellular milieu. A diagrammatic representation of this, as well as an annotated sequence, is shown below.

Figure 1: (A) The two subunits of dystroglycan arise from a post-translational cleavage event. α-dystroglycan is extracellular and mediates various contacts with the extracellular matrix. β-dystroglycan is composed of an ectodomain, a transmembrane domain and a cytoplasmic domain, which mediates interactions with intracellular proteins. All artwork provided as a generous gift by Sarah Palmer. (B) The amino acid sequence of the mature murine β-dystroglycan protein.

A

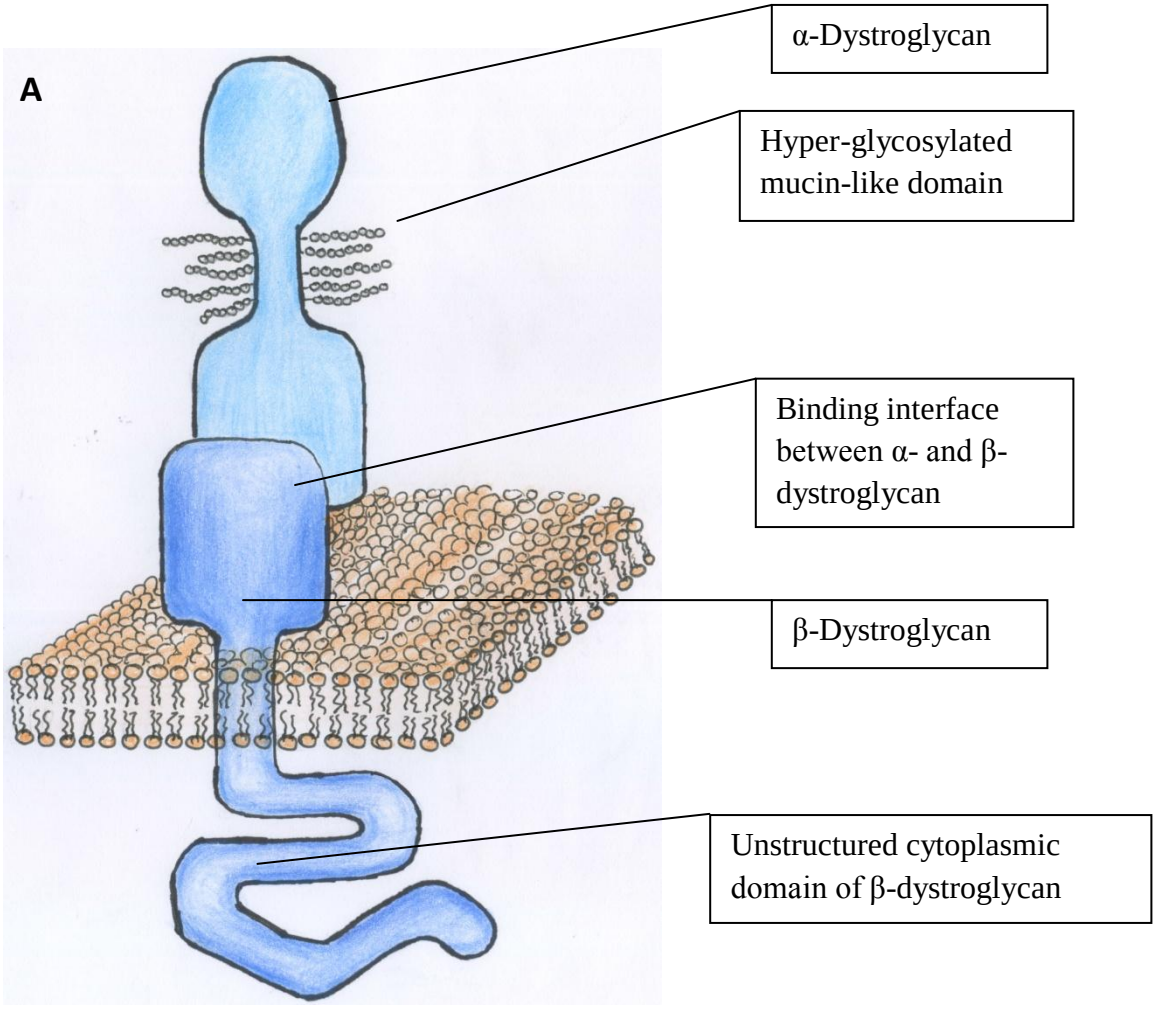

B

---IVVEWTN[660] NTLPLEPCPK[670] EQIAGLSRRI[680] AEDDGKPRPA[690]
FSNALEPDFK[700] ATSITVTGSG[710] SCRHLQFIPV[720] VPPRRVPSEA[730]
PPTEVPDRDP[740] EKSSEDDVYL[750] HTVIPAVVVA[760] AILLIAGIIA[770]
MICYRKKRKG[780] KLTLEDQATF[790] IKKGVPIIFA[800] DELDDSKPPP[810]
SSSMPLILQE[820] EKAPLPPPEY[830] PNQSVPETTP[840] LNQDTMGEYT[850]
PLRDEDPNAP[860] PYQPPPPFTV[870] PMEGKGSRPK[880] NMTPYRSPPPY[890]
VPP[893]

Green – Ectodomain, Pink – Transmembrane domain, Black – Cytoplasmic domain, Orange – Predicted/reported sites of ubiquitylation, Brown – Nuclear localization signal, Blue – Potential sites of tyrosine phosphorylation, Red – Tyrosine 890

1.1.2 Dystroglycan is an Essential Adhesion Protein

In vitro estimates of the interaction between α- and β-dystroglycan predict a K_d of approximately 15μM, suggesting that the interaction is weaker and more dynamic than expected for two molecules acting as a mechanical anchor for cells (Sciandra et al., 2001). However, from *in vivo* findings it is clear that dystroglycan is a component of adhesion complexes (Ervasti et al., 1991_a), and has a critical role in the both the development and stability of various tissues. The deletion of Dag1 results in embryonic lethality in mice, due to a number of defects (Williamson et al., 1997). Although a role for dystroglycan in the correct formation of basement membranes has been proposed (Henry et al., 1998), it is more likely that dystroglycan is involved in the clustering and organization of laminins alongside the integrins, as is evidenced by findings in chimeric $DAG1^{-/-}$ mice and morpholino-treated zebrafish embryos (Cote et al., 1999 ; Cote et al., 2002 ; Parsons et al., 2002). The essential role of dystroglycan is even observed in invertebrates, with dystroglycan gene deletion causing oocyte arrest in *D. melanogaster* (Yatsenko et al., 2009) and muscle weakness in *C. elegans* (Grisoni et al., 2002).

Beyond early development, similar scenarios are encountered within various tissues where dystroglycan-mediated adhesion is critical for further development and growth. Specific examples include: in the development of specific structures within the kidney (Durbeej et al., 1995), in filopodia branching and process formation in differentiating oligodendria (Eyermann et al., 2012), in the formation of the myelin sheath (Nodari et al., 2008), in the repair of prostate lumenal epithelia (Esser et al., 2010), in the formation of the neuromuscular and myotendinous junctions in skeletal muscle (Cote et al. 1999, Goody et al., 2012), and in the maintenance and survival of muscle fibers (Brown et al., 1999 ; Cote et al., 2002 ; Lagenbach et al., 2002). Furthermore, alterations in the levels of α- and β-dystroglycan are linked to the process of tumourigenesis, with decreased protein levels correlating to the emergence of metastasis and reduced chances of patient survival (Sgambato et al., 2007 ; Cross et al., 2008 ; Shen et al., 2011 ; Parberry-Clark et al., 2011).

Consequently, it is unsurprising to find that few examples of dystroglycan mutations are reported in the literature, given the essential nature of this protein in development. A patient with a heterozygous deletion of chromosome 3, which encompasses the DAG1 region, presented symptoms that included facial hypotonia, oral-motor dyspraxia, mild myopathy and white matter abnormalities (Frost et al., 2010). However, whether this is specifically due to the observed reduction in dystroglycan protein levels (approximately 40%) or the deletion of the 62 protein coding genes and 3 miRNAs in this locus is uncertain. Another patient, who presents with mild dystrophy and cognitive impairment, has been reported with a

homozygous T192M mutation in the DAG1 gene (Hara et al., 2011). In this patient, the mutation impaired the glycosylation of α-dystroglycan, preventing normal binding to laminin-α2, and mice harboring the equivalent mutation also exhibited impaired synaptic plasticity and laminin binding (Hara et al., 2011). With this example, one can see both the essential nature of the adhesion mediated by dystroglycan, and how strongly the function of this protein is evolutionarily conserved.

1.1.3 Dystroglycan in the Dystrophin-associated Glycoprotein Complex

The important effects of dystroglycan adhesion are not mediated by the protein alone. Rather, it is the concerted action of a multitude of binding proteins, which scaffold around the dystroglycan adhesion axis, that enable the key functionality of dystroglycan in a variety of situations. In this way, one can draw an important parallel to the multiple effects of adhesion mediated by integrins, which influence the many systems of cellular biology through a large interactome (Zaidel-Bar et al., 2007 ; Sen et al. 2011). A complete exploration of the multiple dystroglycan complexes that have been described to date is beyond the scope of this thesis. However, one can draw many useful inferences and a detailed understanding from an examination of the best characterized example, the dystrophin-associated glycoprotein complex (DGC) (Figure 2).

Early purifications of the DGC from rabbit skeletal muscle describe a tight interaction between the various components. Dystrophin is only dissociated from β-dystroglycan by high molar potassium iodide or alkaline treatments, and chemical cross-linking experiments strongly suggest the existence of a tightly-bound complex (Yoshida et al., 1990 ; Ervasti et al. 1991_a). The extraction of some components by alkaline treatment in the absence of detergent demonstrates that not all components of this complex are integral membrane proteins (Ohlendieck et al., 1991_b). However, immunohistochemical staining reveals a strong sarcolemmal localization, despite not all components being present within the membrane, furthering the argument for a tightly bound complex (Ervasti et al. 1991_b). Detergent treatment of the purified DGC with n-octyl β-D-glucoside separates the components into subcomplexes, but the persistence of these sub-complexes reiterates the notion of a complex held together by strong intermolecular forces (Yoshida et al., 1994). Twenty years after these pioneering experiments, it is now possible to describe a more precise model of the DGC and the protein interactions responsible in the formation of this complex, and it is this that is explored next.

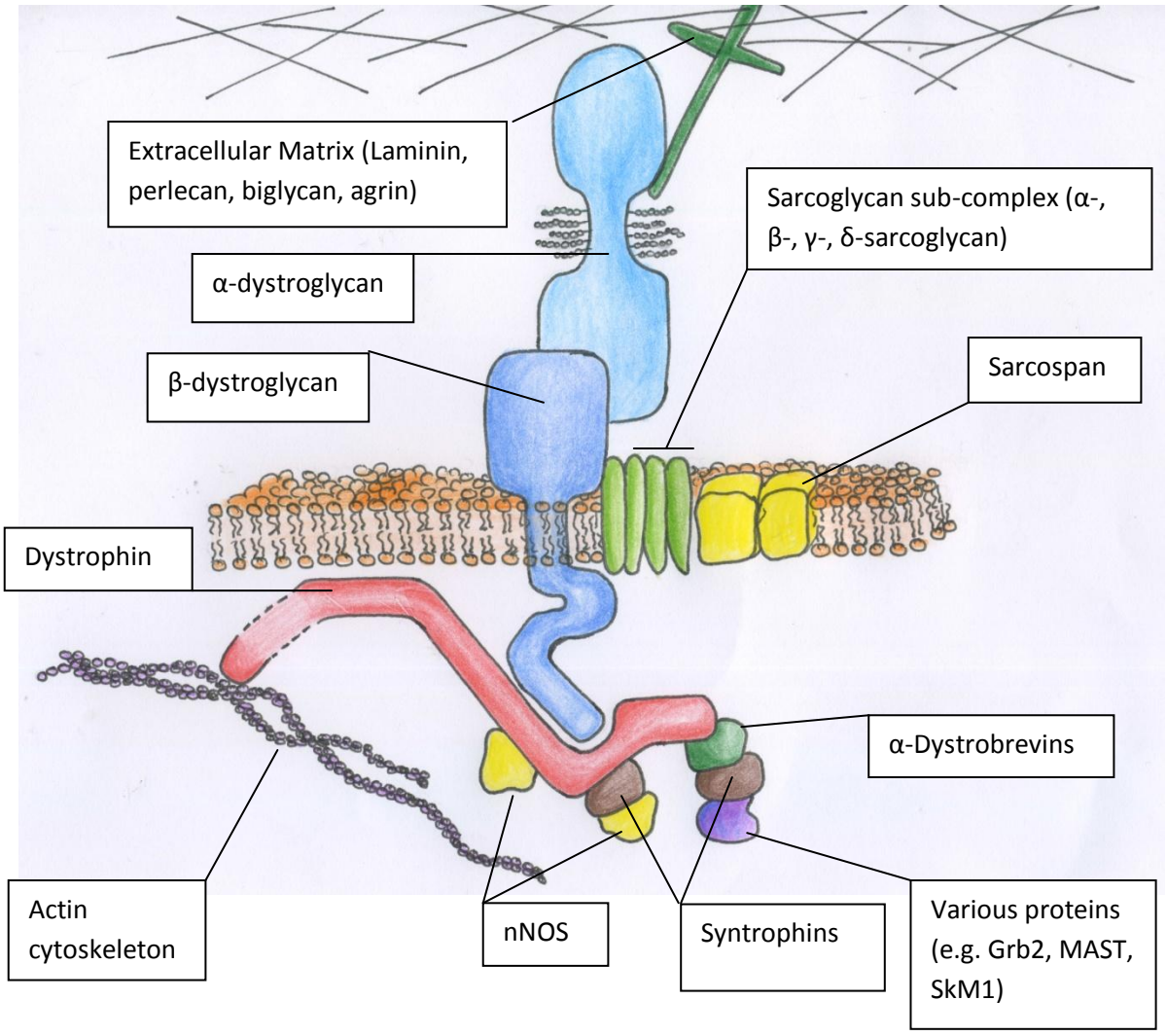

Figure 2: A diagrammatic representation of the dystrophin-associated glycoprotein complex. With dystroglycan at the core, the various components of the DGC enable a mechanical link between the ECM and the cell cytoskeleton, in addition to scaffolding numerous signalling proteins. Note that the organization and stoichiometry of the complex is not exactly as shown, owing to the variable nature of binding by the α-dystrobrevins and syntrophins. In addition, the syntrophins may scaffold any of the associated binding partners at any part of the complex; the organization depicted above is merely for simplicity. All artwork provided as a generous gift by Sarah Palmer.

As is summarized in Figure 2, the recruitment of the many proteins associated with this complex is enabled via interactions with the cytoplasmic domain of β-dystroglycan. The cytoplasmic domain of β-dystroglycan contains several protein-protein interaction motifs and has a high polyproline content (see Figure 1). The flexibility of this domain enables the binding of a wide range of proteins and indeed, numerous examples exist in the literature of this versatility (Yang et al., 1995_a ; Huang et al., 2000 ; James et al., 2000 ; Illsey et al., 2001 ; Zhan et al., 2005 ; Batchelor et al., 2006 ; Higginson et al., 2008). This binding system is analogous to, and even shares components with, the interactome centred around the cytoplasmic tails of the integrins (Zovein et al., 2010). In the case of the DGC, the majority of interactions are mediated by the sarcoglycans and dystrophin, which recruits several key proteins. However, one should note that in other complexes, and particularly in other tissues where these proteins are not expressed, this is not always the case. Hence, either directly, or through additional factors, the cytoplasmic domain of β-dystroglycan scaffolds numerous proteins. It is these numerous proteins that the text now describes in detail.

Dystrophin was first identified as the gene that is mutated in Duchenne and Becker muscular dystrophies, and the full-length form of this gene is expressed in skeletal and cardiac muscle only (Kingston et al., 1984 ; Hoffman et al., 1987 ; Koenig et al., 1987). Dystrophin is part of the spectrin family of proteins, which arose from a common α-actinin ancestor, and, like the other members of this family, it is comprised of an N-terminal actin binding domain, a rod domain (comprised of 24 spectrin-like repeats), a cysteine-rich domain and a C-terminal domain (Hammonds et al., 1987 ; Koenig et al., 1988 ; Hoffman et al., 1989 ; Koenig et al., 1990). The N-terminal actin-binding domain provides a physical link to the actin cytoskeleton (Ervasti et al., 1993 ; Corrado et al., 1994 ; Rybakova et al., 1996 ; Rybakova et al., 2000), whereas the cysteine-rich and C-terminal domains mediate binding to β-dystroglycan via an atypical WW domain interaction (Suzuki et al. 1992 ; Suzuki et al., 1994 ; Jung et al., 1995 ; Rentschler et al., 1999). Owing to the high homology to α-actinin, it was initially proposed that dystrophin functions as an anti-parallel dimer, but subsequent studies have suggested that it is more likely that dystrophin functions as a monomer (Hammonds et al., 1987 ; Rybakova et al., 1996 ; Thomas et al., 1997). Whilst dystrophin is a minor component of skeletal muscle tissue, it is exclusively present at the sarcolemma, where, through dystroglycan, it mediates a physical link between the ECM and the costameric actin cytoskeleton (Ohlendieck et al., 1991_b ; Ervasti et al., 1993 ; Rybakova et al., 2000).

Early purifications of dystrophin identified the presence of several proteins that co-elute with dystrophin and form a strongly associated complex (Yoshida et al., 1990 ; Ervasti et al., 1990 ; Ervasti et al., 1991_b ; Matsumara et al., 1992_a). This complex can be divided into what would be later identified as the dystroglycan and

sarcoglycan sub-complexes, which are membranous, as well as several other intracellular proteins (Ervasti et al., 1991_a ; Roberds et al., 1993_a ; Yoshida et al., 1994 ; Lim et al., 1995). The sarcoglycan complex (SGC) is comprised of four subunits in skeletal muscle: α-, β-, γ- and δ-sarcoglycan (Roberds et al., 1994 ; Nigro et al., 1995 ; Lim et al., 1995 ; McNally et al., 1996). These four subunits are strongly associated and, whilst these proteins are expressed from separate genes and are processed independently, the loss of one subunit results in the complete loss of all subunits from the sarcolemma (Jung et al., 1996 ; Duclos et al., 1998 ; Holt et al., 1998_a ; Araishi et al., 1999 ; Hack et al., 1999). The SGC can be thought of as having two distinct, although not exclusive, functions. The first function of the SGC is to strengthen the association of α- and β-dystroglycan with the DGC, potentially through electrostatic interactions (Roberds et al., 1993_b ; Metzinger et al., 1997 ; Duclos et al., 1998 ; Holt et al., 1998_b ; Araishi et al., 1999 ; Yoshida et al., 2000 ; Matsumara et al., 2005). The second function of the SGC is to provide a scaffold for sarcospan and the α-dystrobrevins.

Sarcospan co-purifies with the DGC and is expressed as either a full-length isoform in skeletal and cardiac muscle, or as a truncated isoform in other tissues (Crosbie et al. 1997). Upon dissociation of the DGC, sarcospan specifically co-sediments with the SGC due to direct binding to the subunits of this complex (Araishi et al., 1999 ; Crobie et al., 1999 ; Miller et al., 2007). Sarcospan has a high degree of sequence similarity to the tetraspannin proteins and, like the tetraspannins, sarcospan oligomerizes and exhibits a membranous localization (Crosbie et al., 1997 ; Miller et al., 2007). Owing to the similarity to tetraspannins, it is postulated that sarcospan oligomers promote the clustering of DGCs, leading to the formation of membrane micro-domains and signalling platforms (Miller et al., 2007). In support of this, there is a growing body of evidence to suggest that sarcospan levels modulate Akt signalling, although exactly how this occurs is currently unclear (Marshall et al., 2012_a ; Marshall et al., 2012_b). In a similar vein, the α-dystrobrevins can bind to the SGC and regulate the signalling capabilities of the DGC (Metzinger et al., 1997 ; Yoshida et al., 2000).

The α-dystrobrevin gene was originally identified by its sequence homology with an 87kDa post-synaptic protein isolated from *T. Californica*, and this gene has a similar gene organization to dystrophin, despite a low level of sequence similarity (Blake et al., 1996 ; Ambrose et al., 1997). Three different protein isoforms, termed α-dystrobrevin 1-3, arise from a single transcript in skeletal muscle, which is post-transcriptionally regulated (Ambrose et al., 1997). Indeed, the sequence of the α-dystrobrevins is further modified by additional alternative splicing events and the removal of variable regions (Ambrose et al. 1997), and transcripts from the skeletal muscle promoter undergo both developmental and spatial regulation (Newey et al., 2001). All 3 isoforms are expressed in skeletal muscle, but only α-dystrobrevin-3 is skeletal muscle specific (Nawrotzki et al., 1998). α-dystrobrevin-

1 and -2 contain dystrophin binding sites and are thought to bind to dystrophin, whereas α-dystrobrevin-3 lacks this site and is proposed to bind to the SGC (Nawrotzki et al., 1998 ; Yoshida et al., 2000). The α-dystrobrevins, along with dystrophin, recruit the syntrophins to the DGC, the signalling function of which is described below. All three α-dystrobrevins contain a constitutive syntrophin binding site, but α-dystrobrevin-1 and -2 can also contain an additional syntrophin binding site as a result of further alternative splicing (Newey et al., 2000_a). This exquisite regulation permits the fine alteration of the signalling capabilities of the DGC, as and where it is required. A notable example of the essential role of α-dystrobrevins is in the maturation of, but not the formation of, the neuromuscular junction in skeletal muscle (Grady et al., 2000).

The syntrophins are PDZ-containing proteins which, through interactions with dystrophin and the dystrobrevins, recruit a multitude of signalling molecules to the DGC. The three syntrophins, α-, β1- and β2-syntrophin are encoded by three separate genes (Adams et al., 1993). Multiple sites within the C-terminus of dystrophin bind the syntrophins *in vitro* (Yang et al., 1995 ; Suzuki et al., 1995) and, as stated above, the dystrobrevins also have constitutive and alternatively spliced syntrophin binding sites (Yang et al., 1995 ; Newey et al., 2000_a). The importance of these interactions is underlined by the loss of syntrophin staining at the sarcolemma when the dystrophin binding site is lost (Roberts et al., 1992), or in α-dystrobrevin null mice (Grady et al., 2000). The syntrophins are proposed to bind to a wide range of signalling and scaffolding molecules including nitric oxide synthase (Brenman et al. 1996), sodium and potassium channels (Gee et al., 1998), the microtubule associated serine/threonine kinase (MAST), (Lumeng et al., 1999) and Grb2 (Oak et al., 2001). That these interactions are functionally important is evidenced by reports of dystrophic patients with deletions in the syntrophin genes (Roberts et al., 1992). Hence, the syntrophins permit the association of signalling molecules with the DGC with important functions beyond adhesion alone.

Finally, there are additional proteins that, despite not co-purifying with the complex in earlier studies (Ervasti et al., 1990), have been shown to interact with members of the complex and are considered to be part of the functional complex. Neural nitric oxide synthase (nNOS) can associate with the DGC via the syntrophins, or via dystrophin, and is thought to regulate calcium homeostasis and the hypertrophic response (Lai et al., 2009 ; Ito et al., 2013_b ; Lai et al., 2013). Syncoilin, a protein associated with intermediate filaments, interacts with α-dystrobrevin-1, extending the adhesive capability of the DGC beyond the actin cytoskeleton (Newey et al., 2001). In addition, various kinases associate with the DGC and are regulated through this interaction (Lagenbach et al., 2002 ; Spence et al., 2004 ; Batchelor et al., 2006). Hence, the function of the DGC extends beyond an immediate, mechanical link to the actin cytoskeleton, to a complex with links to various components of cell adhesion and signalling.

Hence, from the example of a single complex involving dystroglycan, one can draw several important inferences. Whilst adhesion is critically dependent on α- and β-dystroglycan, cytoskeletal linkers, such as dystrophin and syncoilin, enable full linkage between the internal and external environments. Sub-complexes, in this example the SGC and sarcospan, strengthen the adhesive capability of dystroglycan whilst defining the membrane microdomain. Signalling adaptor proteins, chiefly the dystrobrevins and syntrophins, control the number and types of signalling molecules and ion channels associated with the complex. Finally, additional proteins, with perhaps more transient interactions, extend the functionality of the DGC even further. Whilst the proteins specifically associated with dystroglycan in complexes vary between tissues, and even specific membrane domains (for example, the NMJ in skeletal muscle fibres), these general features of complexes involving dystroglycan are the same. However, an understanding of the sarcomeric complex alone does not adequately describe why dystroglycan is so essential in development. Therefore, it is necessary to briefly examine the protein in the context of other tissues and complexes.

1.1.4 Dystroglycan in Other Complexes

The utrophin-associated glycoprotein complex (UGC), which is one example of an "other" dystroglycan complex, is similar to the DGC in organization, but the cytoskeletal linker protein in this case is utrophin. This complex is found in both skeletal muscle and other tissues (Thi Man et al., 1995 ; Deconinck et al., 1997$_a$; Durbeej et al., 1999). Utrophin has a high level of amino acid homology and similar gene structure to dystrophin, and therefore it is predicted that utrophin arose due to gene duplication before vertebrate radiation (Pearce et al., 1993). Utrophin has a widespread tissue distribution and is up-regulated during the earlier stages of mammalian development (Khurana et al., 1990). Utrophin is also up-regulated in necrotic and regenerating muscle fibres (Takemitsu et al., 1991), but upon maturation of the muscle fibre and expression of dystrophin, the expression of utrophin is normally restricted to NMJs and myotendinous junctions (MTJs) (Khurana et al., 1991 ; Gramolini et al., 1997 ; Gramolini et al., 1998). Agrin, which is a ligand of α-dystroglycan and defines NMJs (through acetylcholine receptor clustering), also induces the expression of utrophin, thus allowing site-specific expression (Cohen et al., 1997 ; Gramolini et al., 1998 ; Gramolini et al., 1999).

Functionally, utrophin is comparable to dystrophin: the N-terminal domain is also responsible for actin binding (Winder et al., 1995) and a similar region binds to β-dystroglycan (Chung et al., 1999 ; James et al., 2000). Indeed, the similar nature of the two proteins is verified by the fact that increased utrophin expression can compensate for the loss of dystrophin (Tinsley et al., 1996 ; Tinsley et al., 1998 ;

Rafael et al., 1998). However, two important distinctions should be drawn between the two proteins. First, utrophin does not have the same essential nature as dystrophin: utrophin-null mice exhibit no severe developmental defects and exhibit only small changes to the structure of tissues (Deconinck et al., 1997_a). Second, the promoter region of utrophin is altered with respect to dystrophin: a CpG island permits constitutive expression (Pearce et al., 1993) and an N-box motif boosts expression in response to factors downstream of agrin and heregulin, such as the transcription factor AP-1 (Gramolini et al., 1998 ; Gramolini et al., 1999). Thus, utrophin is expressed in a wide variety of tissues, whereas dystrophin expression is restricted by promoter elements specific for skeletal and cardiac muscle tissue.

The UGC is also found in tissues other than skeletal muscle and involves homologues of the proteins involved in the DGC, which also do not show skeletal muscle specific expression. The presence of a UGC, containing utrophin and dystroglycan, has been reported in kidney cell lines and epithelia (Kachinsky et al., 1999 ; Durbeej et al., 1999), as well as in the myelin sheath of the peripheral nervous system (Matsumara et al., 1993). Interestingly, in the case of the complex present in lung smooth muscle, the presence of a sarcoglycan sub-complex is observed that is associated with the UGC (Durbeej et al., 1999). In this instance, ε-sarcoglycan, the ubiquitously expressed homolog of α-sarcoglycan, functions in place of α-sarcoglycan (Ettinger et al., 1997 ; McNally et al., 1998 ; Durbeej et al., 1999 ; Imamura et al., 2005). Indeed, other components of the UGCs, which are not expressed in skeletal muscle, substitute for the factors in the DGC described earlier. For example, ζ-sarcoglycan replaces γ-sarcoglycan (Shiga et al., 2006) and β-dystrobrevin replaces the α-dystrobrevins (Blake et al., 1998). Like dystrophin and utrophin within the muscle fibre, the presence of complexes involving these homologues within a tissue is not mutually exclusive, as evidence by the presence of complexes containing α- and β-dystrobrevin in renal endothelial and epithelial cells respectively (Loh et al., 2000). The differences in the composition of these complexes are likely to reflect specific, local requirements different from that of the costameric DGC in skeletal muscle. In support of this idea, a differential association of the syntrophins is observed in the various complexes containing α- or β-dystrobrevin in kidney tissue (Loh et al., 2000).

Interestingly, there are several reports in the literature of dystroglycan complexes without the presence of a cytoskeletal linker, such as full-length utrophin or dystrophin. In some cases this is due to the expression of apo-dystrophins, transcripts from the dystrophin gene generated by alternative splicing or transcription initiation sites (Blake et al., 1992 ; Tinsley et al., 1993 ; Schofield et al., 1994). These apo-dystrophins lack the N-terminal actin binding domain, but can bind both β-dystroglycan and the other members of the complex. Therefore, complexes involving apo-dystrophins are thought to have signalling and developmental roles, as full adhesion is not possible (Matsumara et al., 1993 ;

Schofield et al. 1994 ; Loh et al., 2000 ; Cerecedo et al., 2005 ; Judge et al., 2006). Interestingly, there are no apo-utrophins (Man et al., 1995), although an evolutionarily conserved homologue of utrophin and dystrophin, dystrophin related protein 2 (Drp2) has been identified (Roberts et al., 1996). Despite having a low homology to utrophin and dystrophin, Drp2 forms a complex with dystroglycan and periaxin in the peripheral nervous system, which is involved in Cajal band formation and myelination (Sherman et al., 2012). Finally, there are reports in the literature of membranous dystroglycan complexes formed in the absence of dystrophin, the dystrophin homologues or apo-dystrophins (Matsumara et al., 1992_a ; Deconinck et al., 1997_b ; Durbeej et al., 1999). In these instances, other or unknown cytoskeletal linkers may bind β-dystroglycan, such as plectin 1f (Rezniczek et al., 2007). These complexes may also contain other, unknown associated proteins, permitting further, diverse functions for the adhesion complex.

Indeed, the presence of dystroglycan in adhesive structures and other regions of the cell, distinct from that of the costameric DGC of surface membranes, have been reported in multiple systems. This is made possible by the binding of proteins that are not part of the α-actinin family. For example, the cytoplasmic tail of β-dystroglycan can also bind to Grb2 *in vivo* and the proposed binding site overlaps with that of dystrophin (Yang et al., 1995_b ; Russo et al., 2000). However, the estimated K_d of the Grb2 interaction is higher than that of dystrophin and utrophin, suggesting that only non-DGC β-dystroglycan would form this complex (Russo et al., 2000). Nonetheless, the presence of β-dystroglycan in a functional complex with Grb2 and dynamin in cortactin-positive membrane ruffles has been demonstrated (Zhan et al., 2005). β-dystroglycan has also been reported in complexes with ezrin in both filopodia and the cleavage furrow (Cerecedo et al., 2005 ; Batchelor et al., 2007 ; Higginson et al., 2008), and with Tsk5 in podosomes (Thompson et al., 2008), where β-dystroglycan is proposed to scaffold additional factors required for the specific function of these structures. In the case of focal adhesions, it has been observed that β-dystroglycan is not only present in these structures, but binds and recruits components associated with integrin-mediated adhesion (Kramarcy et al., 1990 ; Yoshida et al. 1998 ; Thompson et al., 2008). That there is synergy between the two systems of adhesion involving integrins and dystroglycan is confirmed by the modulation of adhesion to fibronectin (an integrin ligand) in response to dystroglycan levels, and the reciprocal regulation between dystroglycan and integrin expression (Brown et al. 2004 ; Thompson et al., 2010 ; Liu et al., 2011). Furthermore, dystroglycan is observed in, or is proposed to form complexes with, components of various signalling pathways including: RhoA and Rac1 (Chockalingam et al., 2002 ; Oak et al., 2003), ERK and MAPK (Spence et al., 2004), c-Src (Sotgia et al., 2001), FAK (Yoshida et al., 1998 ; Thompson et al., 2008) and Pak1 (Oak et al., 2003). Hence, through the many potential interacting partners of β-dystroglycan, dystroglycan can be involved in a

wide range of complexes with differing signalling capabilities, beyond those defined by the presence of dystrophin or related proteins thereof.

1.1.5 Dystroglycan Complex Formation in Response to the Extracellular Matrix

Shifting the focus from the interactions of the cytoplasmic domain of β-dystroglycan, one finds an additional layer of complexity and regulation in dystroglycan complexes from the interactions between α-dystroglycan and components of the ECM. The mature α-dystroglycan protein is extensively glycosylated and this glycosylation is essential for ligand binding (Ervasti et al., 1991_a ; Gee et al., 1993 ; Sunada et al., 1994). Disrupting the glycosylation of α-dystroglycan in mice produces a dystrophic phenotype, due to impaired laminin-α2 binding (Grewal et al., 2001). Whilst the dystrophic phenotype may have a mechanical basis, due to the loss of linkage between the actin cytoskeleton and the ECM, studies on cell lines suggest this may also have a signalling basis. The blockade of laminin-α2 binding by α-dystroglycan leads to an increased apoptosis of myotubes, due to decreased anti-apoptotic signalling via the Akt pathway (Lagenbach et al. 2002). Furthermore, blockade of the same interaction in myoblasts negatively impacts the differentiation process, resulting in reduced myotube size, myofibril disorganization and the loss of contractile activity (Brown et al., 1999). Conversely, engagement of laminin-α2 is proposed to have an inhibitory effect on ERK-MAPK signalling, due to the sequestering of MEK2 by β-dystroglycan (Spence et al., 2004). In these examples one sees a situation reminiscent of the "outside-in" signalling mediated by integrins: binding to the extracellular α-dystroglycan directly changes the partners bound by the cytoplasmic domain of β-dystroglycan, which affects the maturation, survival and signalling pathways of muscle tissue.

A better characterized example of this phenomenon is found in the agrin-dependent formation of NMJs. Treatment of muscle cultures with agrin causes a redistribution and clustering of acetylcholine receptors and UGCs, which is dependent on tyrosine phosphorylation (Cohen et al., 1997). In addition to binding α-dystroglycan, agrin stimulates the activation of MuSK and transcription of utrophin from nearby myonuclei (Nawrotzki et al., 1998 ; Gramolini et al., 1998). Furthermore, agrin treatment also promotes the recruitment of α-dystrobrevin-1 to NMJs, and α-dystrobrevin-1 co-immunoprecipitates with utrophin, suggesting that these proteins exist in a specialized, agrin-defined UGC (Nawrotzki et al., 1998). The recruitment of α-dystrobrevin-1 is dependent on tyrosine phosphorylation, like the clustering of UGCs (Cohen et al., 1997 ; Nawrotzki et al., 1998), and in the absence of α-dystrobrevin-1 acetylcholine receptor clusters fragment upon removal

of agrin (Grady et al., 2000). Here, the "outside-in" signalling is extended by a subsequent "inside-out" signalling event: agrin treatment specifies the type of dystroglycan complex present at nascent NMJs, but the presence of components of these dystroglycan complexes are required for further maturation of the synapse.

Returning to the glycosylation of α-dystroglycan, one can find further examples of how subtle changes to the ligand binding capacity of this protein impacts the formation of dystroglycan complexes. The binding of biglycan by α-dystroglycan is dependent on the presence of chondrotin sulphate linkages (Bowe et al., 2000), and results in the formation of complexes containing utrophin, β2-syntrophin, and nNOS (Mercardo et al., 2006 ; Amenta et al., 2011). These findings may be criticised on the basis that it is equally plausible that biglycan is exerting these effects on dystroglycan complex formation via another membranous receptor, and that biglycan being an α-dystroglycan ligand is purely coincidental. Nonetheless, assuming that the same kind of process is occurring as is found in the more defined pathways of agrin and NMJ formation, one can conclude that biglycan also influences the formation of dystroglycan complexes. In addition, a minor glycoform of α-dystroglycan, which only binds to β-dystroglycan and no other typical complex components (UGC or DGC), has been described in skeletal muscle (McDearmon et al., 2001). One can postulate that this will influence the formation of another, specific type of dystroglycan complex, but no evidence exists to describe the components involved. Together, the examples of laminin-α2, agrin, biglycan and atypical glycoforms of α-dystroglycan underline an important feature of dystroglycan complexes: that the type of interaction with the ECM is as important as the availability and localization of intracellular binding partners in the definition of the complex.

1.1.6 Summary: Why Dystroglycan is an Essential Protein

Upon molecular examination of the DGC, as well as the other adhesion and signalling complexes that dystroglycan is a component of, it is clear how mutations in *DAG1* have such severe effects in mice and why these are rarely observed in humans. Whilst α- and β-dystroglycan may have a primary function in adhesion, the plethora of proteins associated with dystroglycan complexes, permit a definition of function beyond this role alone. In this manner, dystroglycan can contribute to a wide range of processes in cellular biology. A summary of these interacting proteins is given in Figure 3. Furthermore, by acting as an interface between the extracellular matrix and the cellular microenvironment, dystroglycan has a critical role in not only defining the different complexes it is observed in, but enabling dynamic, regiospecific specialization of the cell. From focal to basement membrane adhesion, and from growth signalling to synaptic function, dystroglycan plays a key role in a multitude of cellular processes and hence, one is able to appreciate why the disruption of the *DAG1* gene has such a profound and negative impact on a wide range of species. It is not surprising then to find that human diseases where this protein is mislocalized, such as DMD, are of a chronic and debilitating nature. What is known about the pathology of this disease, as well as the implications this has for the cellular biology of β-dystroglycan, shall form the following section of this chapter.

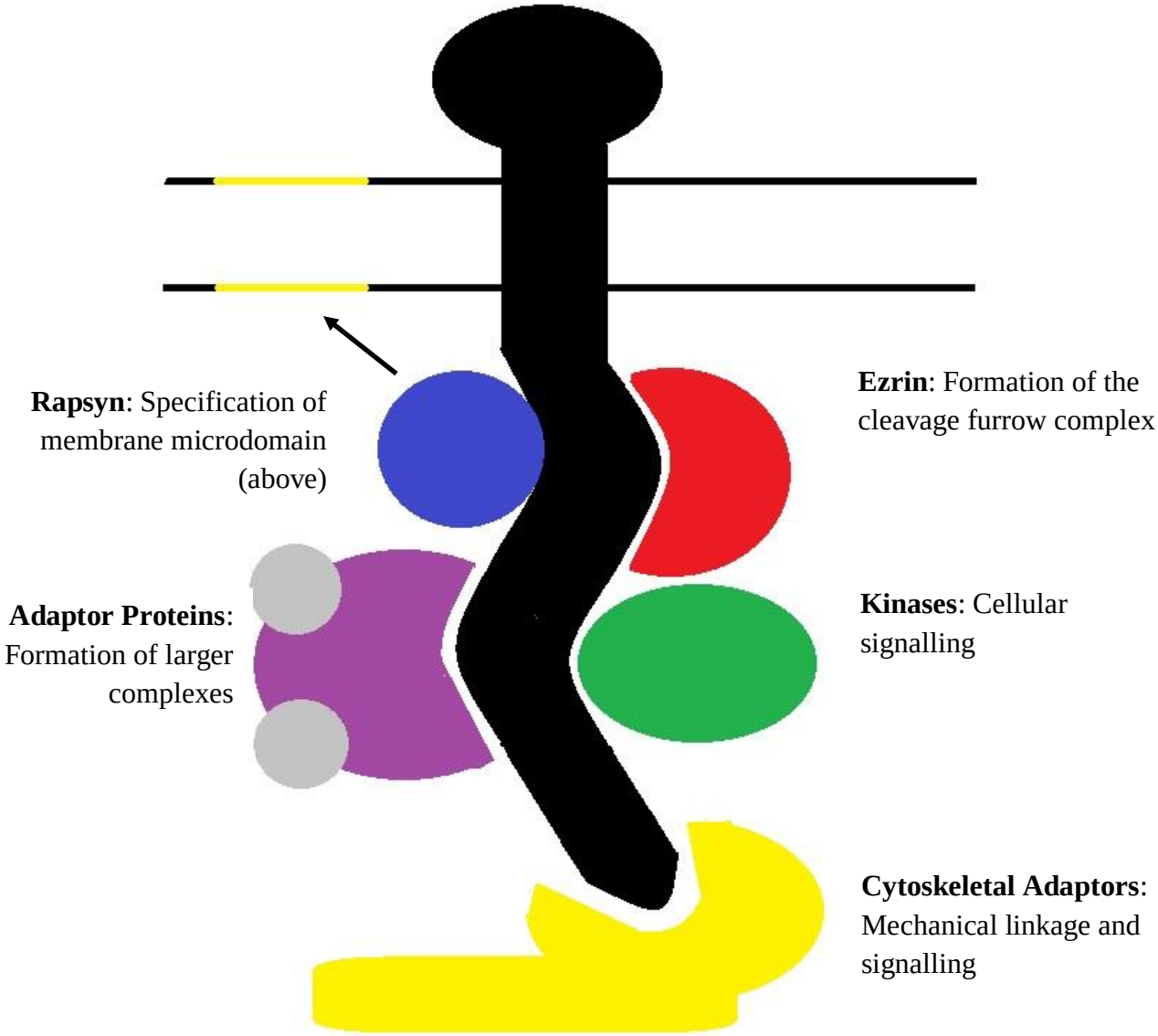

Figure 3: A simplified schematic of the proteins that bind the cytoplasmic tail of β-dystroglycan. Rapsyn (blue), binds to the juxtamembrane region and is thought to specify the neuromuscular junction membrane domain. Similarly, ezrin (red) binds to the juxtamembrane region and specifies the β-dystroglycan complex found at the cleavage furrow. The adaptor protein Grb2 (purple) also binds the cytoplasmic tail to permit the establishment of signalling complexes, such as that containing Sos and JNK1. The signalling kinases ERK and FAK (green) have been shown to have a direct and functional interaction with the cytoplasmic domain. Finally, the adaptor proteins utrophin, dystrophin and dystrophin related protein 2 bind the C-terminus of the protein and provide mechanical linkage to the cytoskeleton.

1.2.1 Duchenne Muscular Dystrophy

DMD is an X-linked disease with an incidence rate of 1 in 3500 male births (Kingston et al., 1984 ; Moser et al., 1984). The disease is primarily characterized by progressive dystrophy of the skeletal muscles and eventual respiratory or heart failure. Clinical manifestations begin between the ages of 3 to 5 years, with a progressive loss of muscle strength that result in a loss of ambulance by the age of 12 years, and death by the age of 20 years (Emery et al., 2003 ; McDonald et al., 2010). Mutations in the *DMD* gene, which codes for dystrophin (see Section 1.1.3), cause DMD, as well as the milder, Becker muscular dystrophy (BMD) (Koenig et al., 1987). BMD patients present with a range of symptoms, which are similar to those of DMD, but less severe: the onset of symptoms occurs between 8 and 12 years of age and, whilst there is progressive muscle weakness, patients can remain ambulatory without assistance to the age of 40 and beyond (Emery et al., 2003).

The *DMD* gene is the largest known gene in humans, spanning over 2.3Mb of genomic DNA, and as such, the gene has a considerably higher mutation rate (mutations/gene unit) than average (Aartsma-Rus et al., 2006). There is a correlation between disease severity and type of mutation, which is broadly explained by the hypothesis proposed by Monaco et al., (1988). "Monaco's Rule" predicts that in-frame mutations produce decreased expression of truncated dystrophins and BMD, whilst out-of-frame and premature stop mutations cause abortive nonsense-mediated decay of the *DMD* transcript and the lack of dystrophin expression typical of DMD patients (Hoffman et al., 1987 ; Bonilla et al., 1988 ; Koenig et al., 1989). However, numerous examples exist that refute this simple explanation.

Chiefly, there is a differential importance in the domains of dystrophin that can be lost due to mutation: large deletions of the rod domain typically result in BMD, whereas small deletions of either the actin binding or the β-dystroglycan binding domains cause DMD (Beggs et al., 1991 ; Helliwell et al. 1992 ; Aartsma-Rus et al., 2006). In fact, estimates from the Leiden DMD mutation database suggest that as many as 9% of BMD/DMD patients do not genetically conform to "Monaco's Rule". In addition to the factors described above, this can be attributed to a variety of post-transcriptional events that are either generated or altered by mutation (Aartsma-Rus et al., 2006 ; Beroud et al., 2007). Consequently, "Monaco's Rule" only applies for the majority of BMD/DMD patients when the site of mutation is examined at the RNA level. However, one cannot rule out other genetic factors that modulate the severity of the disease, as evidenced by the reported variation in symptoms manifested by patients from a family with the same deletion (Melis et al., 1998).

The loss of functional dystrophin expression in the DMD disease state results in several changes to the muscle fibre. First, there is a large reduction in both the sarcolemmal localization and protein levels of components of the DGC, including α- and β-dystroglycan (Matsumara et al., 1992_a ; Ohlendieck et al., 1993 ; Campbell et al., 1995). This loss is specific as the overall levels of other sarcolemmal glycoproteins are unaltered in the absence of dystrophin (Ohlendieck et al., 1991_a ; Ohlendieck et al., 1993). In the absence of the DGC, the sarcolemma ruptures, presumably due to an inability to dissipate the lateral forces generated during muscle contraction. When compared to healthy muscle, muscles fibres from DMD patients have a reduced diameter and are permeable to small dyes such as procion yellow and Evans blue, and also large molecules such as IgM (Bradley et al., 1978 ; Straub et al., 1997 ; Kinali et al., 2011). In this instance, the release of enzymes from the permeable muscle fibres results in elevated serum aldolase and creatine kinase levels, which can be used as a diagnostic marker of the disease (Dreyfus et al., 1953 ; Kinali et al., 2011). As a consequence of this damage, dystrophic fibres undergo continual cycles of degeneration and regeneration, as evidenced by the presence of necrotic and centrally nucleated fibres respectively (Ohlendieck et al., 1993). Interstitial fibrosis is evident at early stages of the disease, but the reduction in large, healthy fibres and eventual expansion of the connective tissue leads to progressive fibrosis of the muscle tissue (Ohlendieck et al., 1993). In this manner the distal, followed by the proximal, skeletal muscles become progressively weakened, until respiratory failure and death occurs, due to the combined weakening of the diaphragm and cardiac tissue (Emery et al., 2003).

The full pathology of DMD is currently uncertain. Genetic studies highlight the importance of the mechanical link between dystroglycan and the actin cytoskeleton formed by the respective binding domains of dystrophin (Beggs et al., 1991 ; Helliwell et al., 1992 ; Aartsma-Rus et al., 2006). Furthermore, attempts at molecular therapy in mouse models have demonstrated the necessity of these domains for amelioration of the disease (Cox et al., 1993 ; Cox et al., 1994 ; Phelps et al., 1995 ; Rafael et al., 1998 ; Judge et al., 2006). Finally, reports of patients with reduced expression of dystrophin suggest that as little as 30% expression is required to protect against dystrophy (Neri et al., 2007 ; Anthony et al., 2011). Collectively, these studies suggest that when the linkage between the actin cytoskeleton and ECM drops below a critical threshold, the extent of myofibrillar necrosis becomes too high, leading to progressive fibrosis and weakness. Indeed, dystrophic muscle tissue tries to overcome this problem by up-regulating the expression of utrophin and reconstitution of the mechanical link. Analyses of muscle biopsies from DMD patients reveal both an extra-junctional, sarcolemmal localization of utrophin as well as increased levels of protein (Voit et al., 1991 ; Man et al., 1995 ; Taylor et al., 1997). Whilst utrophin expression is dominant in regenerating muscle fibres (Khurana et al., 1991 ; Takemitsu et al., 1991), a partial protection of the mature muscle fibre is enabled through

maintenance of the extra-junctional UGC in the dystrophic state, as evidenced by the inverse correlation between utrophin up-regulation and disease severity (Mizuno et al., 1993 ; Taylor et al., 1997). However, what happens when these protective mechanisms fail, as is the case for DMD patients, is still unknown. As such, no curative therapy exists for DMD to date, however further insights into the pathological mechanism have emerged from studies of murine models of Duchenne and other muscular dystrophies and it is these that the next section describes.

1.2.2 The mdx Mouse and Other Models

The *mdx* mutation arose spontaneously in the C57 B1/10 ScSn colony of mice and was later shown to correspond to a missense mutation in the mouse *DMD* gene that results in premature termination and nonsense-mediated decay of the *DMD* transcript (Bulfield et al., 1984 ; Hoffman et al. 1987 ; Sicinski et al., 1989). Despite a similar genetic origin, the pathology of the *mdx* mouse is different to that of DMD patients. *Mdx* mice display no histological differences in muscle tissue architecture, compared to control mice, until 3 weeks of age, whereupon extensive necrosis occurs, leaving very few intact fibres and phagocyte infiltration (Dangain et al., 1984). Following this peak in necrosis, continual cycles of necrosis and regeneration are evident, yet these are not accompanied by the progressive fibrosis observed in DMD patients (Coulton et al. 1988). Furthermore, whilst the variability in fibre diameter does increase, the mean fibre diameter size does not change in the *mdx* mouse, unlike in DMD patients (Coulton et al., 1988). The *mdx* mouse lives until at least one year of age and has increased serum creatine and pyruvate kinase levels, which is a consequence of ruptured or permeable sarcolemma (Coulton et al., 1988). *Mdx* skeletal muscles exhibit a decreased specific force and an increased fatigue in response to repeated contraction, despite an increased muscle mass (Dangain et al., 1984 ; Sacco et al., 1992). The increase in muscle mass observed in *mdx* mice has been suggested to be due to an Akt-dependent hypertrophic protection mechanism, which is not observed in DMD patients (Peter et al., 2006). In a similar vein, the disruption of skeletal muscle tissue architecture in the *mdx* mouse in not uniform across all muscle groups; proximal limb, pelvic and shoulder girdle muscles show a large uptake of Evans blue dye (a marker of membrane permeability), whereas distal limb muscles, such as the tibialis anterior show little or no uptake, suggesting that these muscle groups are protected against sarcolemmal rupture (Straub et al., 1997).

The above findings, when partnered with the comparatively long lifespan and viability of the *mdx* mouse, suggest that the protective mechanisms activated in the absence of dystrophin in mice are more significant than in humans. Indeed, *mdx* muscle fibres show the same compensatory up-regulation of utrophin and retention of dystrophin associated proteins, including dystroglycan, at the sarcolemma, as is

observed in humans (Khurana et al., 1991 ; Ohlendieck et al., 1991_a). Whilst not all dystroglycan is associated with utrophin in UGCs, that functional UGCs are formed is also evident from co-sedimentation analysis (Ohlendieck et al. 1991_c ; Matsumara et al., 1992). In fact, it has been proposed that a stronger up-regulation of this compensatory pathway in the *mdx* mouse is the cause of the protection of cardiac and distal muscle tissue from sarcolemmal rupture (Matsumara et al., 1992_a ; Straub et al., 1997). In support of this, an increase in both utrophin and β-dystroglycan protein levels, relative to proximal muscles, is observed in the tibialis anterior muscle of *mdx* mice (Dowling et al., 2002 ; Dowling et al., 2003). In addition, alternative cytoskeletal linkers that bind β-dystroglycan, such as plectin 1f, are also up-regulated in *mdx* muscle tissue (Rezniczek et al., 2007). Thus, relatively speaking, there is a greater pool of proteins compensating for the loss of dyrtophin in mice than in humans. In turn, there is an enhanced restoration of dystroglycan complexes to the sarcolemma and adhesion to the ECM. This ameliorates the dystrophy caused by the loss of dystrophin expression in the *mdx* mouse. However, with an examination of the *dko* model it becomes apparent that dystroglycan-dependent adhesion, and not merely dystrophin expression, is a requirement to protect against dystrophy.

In the *dko* mouse, both the utrophin and dystrophin genes are disrupted. The resulting dystrophic phenotype is far more severe than that of the *mdx* mouse, with necrosis and fibrosis of muscle tissue by postnatal day 6, and death due to respiratory failure by 20 weeks of age (Deconinck et al., 1997_b). In this instance, the *dko* mouse more closely resembles the pathology of DMD patients, however important exceptions still remain. Despite death by respiratory failure, this is due to weakening of the diaphragm and *dko* mice do not exhibit any cardiomyopathy, unlike DMD patients (Deconinck et al., 1997_a ; Crisp et al., 2011). Furthermore, the same protection of distal muscle groups against sarcolemmal rupture is observed, and the extent of degeneration and regeneration is no different to that of the *mdx* mouse. However, one should note that extra-junctional, sarcolemmal dystroglycan is still observed in the *dko* mouse, making the retention of dystroglycan, potentially via cytoskeletal linkage enabled by alternative proteins, a possible cause for the protection of murine muscle fibres in the absence of both dystrophin and utrophin (Deconinck et al., 1997_b). In other words, the presence of sarcolemmal dystroglycan prevents the pathology of these dystrophic diseases in mice. However, the notion of the singular importance of dystroglycan can be challenged by other features of the dystrophic pathology of both *dko* and *mdx* mice.

As mentioned earlier, there is an increase in Akt protein levels and signalling in the *mdx* mouse, with selective downstream activation of p70S6K, suggesting a protective, hypertrophic response (Peter et al., 2006). That this is the case is confirmed by studies using transgenic, inducible Akt in *mdx* mice, as enhanced Akt

signalling and consequent hypertrophy partially ameliorates muscular dystrophy (Peters et al., 2009). However, an important corollary of this study is that utrophin expression is also up-regulated by inducible transgenic Akt signalling; a finding corroborated by studies in transgenic *mdx* mice that overexpress sarcospan, an activator of the Akt/p70S6K pathway (Marshall et al., 2012_a ; Marshall et al., 2012_b). As utrophin up-regulation occurs downstream of Akt signalling, the hypertrophic protection may only occur as a consequence of enhanced dystroglycan restoration. Both *mdx* mice and DMD patients also exhibit rare revertant muscle fibres, where dystrophin expression is restored due to exon skipping of nonsense mutations (Takemitsu et al., 1991 ; Helliwell et al., 1992 ; Fall et al., 2006 ; Van Deutekom et al. 2007). In these fibres, the internally truncated dystrophin mediates the restoration of DGC components and there is an expansion of these fibres in *mdx* muscle with age (Arechavala-Gomeza et al., 2010). As there is no similar expansion of revertant fibres in DMD patients, one could propose that this expansion is another protective mechanism in the *mdx* mouse. However, this mechanism also ultimately results in the restoration of sarcolemmal dystroglycan, suggesting that dystroglycan localization is critically important in DMD and *mdx* pathology (Arechavala-Gomeza et al., 2010).

Alternatively, up-regulation of the integrin adhesion system may be the cause of protection observed in the *mdx* mouse. Mice lacking both dystrophin and α7-integrin exhibit a considerably shortened lifespan and increased muscle necrosis and regeneration, relative to their single knock out littermates, suggesting that these two adhesion system exert a synergistic effect (Rooney et al., 2006). Indeed, in other mouse models an inverse relationship between β-dystroglycan and α7-integrin expression has been reported (Cote et al., 2002 ; Allikian et al., 2004) and in other muscular dystrophies, both β1-integrin and α-dystroglycan levels inversely correlate with disease severity (Brown et al., 2004). Furthermore, transgenic expression of α7-integrin on the *dko* mouse background increases lifespan and ameliorates the features of dystrophic pathology (Burkin et al., 2001), although this finding is called into question on the basis that β1-integrin levels determine the amount of functional, sarcolemmal α7-integrin protein (Liu et al., 2011). However, a recent trial of α7-integrin overexpression as a therapy for the *mdx* mouse demonstrated little or no improvement in dystrophic pathology (Heller et al., 2013). Moreover, the up-regulation of integrins does not ameliorate the dystrophic features of Dag1 null chimeric mice (Cote et al., 1999 ; Cote et al., 2002). Thus, whilst the integrin system of adhesion may attempt to compensate for the loss of dystroglycan-dependent adhesion, it is unlikely to be the protective mechanism in the *mdx* mouse, owing to the incomplete functional overlap between these two systems of adhesion (Boppart et al., 2006 ; Sen et al., 2011).

Finally, one cannot ignore the involvement of other members of the DGC and UGC, which are also lost from the sarcolemma in DMD, *mdx* and *dko* pathology. A

good example of this is nNOS, which is recruited by binding to either syntrophin or dystrophin (see Figure 2 and Section 1.1.3). In addition to a loss of sarcolemmal localization, nNOS expression is decreased in *mdx* mice and DMD patients (Vaghy et al., 1998 ; Barton et al., 2005 ; Amenta et al., 2011) and nNOS levels also inversely correlate with disease severity in DMD patients (Anthony et al., 2011). Transgenic overexpression of nNOS on the *mdx* background ameliorates features of dystrophic pathology, and this has been proposed to be due to the modulation of intracellular calcium handling (Wehling et al., 2001 ; Ito et al., 2013_b). In support of this proposal, alterations in calcium homeostasis have been proposed to contribute to the necrosis of muscle fibres in dystrophic pathology (Kämper et al., 1992 ; Collet et al., 1999 ; Dowling et al., 2003 ; Batchelor et al., 2006 ; Goonaserka et al., 2011). However, these alterations are proposed to occur downstream of sarcolemmal rupture, and hence probably reflect the later stages of pathology (Collet et al., 1999 ; Tinsley et al., 2011). Furthermore, nNOS activity also causes activation of the Akt/p70S6K pathway, which causes an up-regulation of utrophin expression (Marshall et al., 2012_a ; Marshall et al. 2012_b). Moreover, nNOS-null mice do not exhibit any symptoms of dystrophic pathology, suggesting that the loss of nNOS activity is not causative in *mdx* pathology. (Wehling et al., 2001). Thus, the importance of nNOS activity and calcium homeostasis in dystrophic pathology may be viewed as secondary, when compared to the presence of correctly localized dystroglycan and a functional link to the ECM.

1.2.3 Dystroglycan Disruption and Other Muscular Dystrophies

Whilst an examination of the *mdx* and *dko* mouse models provides evidence for and against the importance of β-dystroglycan in dystrophic aetiology, several other key experiments and observations bring the importance of this protein into sharp focus. As mentioned previously, Dag1-null mice die during embryogenesis (Williamson et al., 1997), yet chimeric Dag1-null mice, which continue to live after birth, have been reported (Cote et al., 1999). These chimeric mice are highly dystrophic and have reduced amounts of DGC proteins including: dystrophin, the SGC, nNOS and α-dystrobrevin-2. The basement membranes and ECM components of surrounding muscle fibres appear to be unaltered, but the dystrophic phenotype partnered with the loss of many DGC components re-affirms the key role of α and β-dystroglycan in both the function and integrity of the DGC (Cote et al., 1999 ; Cote et al., 2002). Given that β-dystroglycan binds dystrophin, and the other components of the DGC through dystrophin, one can infer that the presence of sarcolemmal β-dystroglycan is critical for the correct localization of the complex.

This inference is further supported by observations from the conditional loss of dystroglycan, which appears to serve as a master-switch in the formation of the complex. The conditional disruption of dystroglycan expression in mature skeletal

muscle leads to a familiar loss of the DGC, partnered with the onset of dystrophic necrosis, yet later, re-expression restores the DGC and facilitates regeneration (Cohn et al., 2002). The fact that not all DGC components exert this pivotal effect, as evidenced by the retention of DGC components at the sarcolemma in sarcospan$^{-/-}$ and dy/dy (Laminin $\alpha 2^{-/-}$) mice (Marshall et al., 2012_a ; Ohlendieck et al. 1991_a), only serves to strengthen the idea that dystroglycan is a central scaffold in several adhesion complexes. Indeed the subset of limb-girdle muscular dystrophies that are caused by the loss of any one of the sarcoglycans also exhibit reduced levels of sarcolemmal β-dystroglycan, despite only slight reductions in the levels of dystrophin (Vainzof et al., 1996 ; Metzinger et al., 1997 ; Duclos et al., 1998). These muscular dystrophies, amongst many others, have a common loss of dystroglycan from the sarcolemma, implicating it as a key player in the integrity of the complex. Thus, in addition to the dystrophic pathology of *mdx* and *dko* mice, the loss of β-dystroglycan is common to other dystrophies, as one would expect from the critical dependence of the DGC on the presence of this protein.

1.2.4 Summary: The Loss and Restoration of β-Dystroglycan in DMD Pathology and Therapy

From the findings described above, one can come to several important conclusions. Whilst it is not the cause of DMD, BMD, *mdx* or *dko* pathologies, the secondary loss of β-dystroglycan from the sarcolemma in these diseases is of importance. Levels of sarcolemmal β-dystroglycan correlate with disease severity as much as that of dystrophin or utrophin (Neri et al., 2007 ; Anthony et al., 2011) and, whereas dystrophin can be functionally replaced with other proteins in the *mdx* and *dko* mouse models (Cox et al., 1993 ; Rafael et al., 1998 ; Tinsley et al., 1998 ; Rezniczek et al., 2007), β-dystroglycan can not be functionally replaced, even by the integrins, which share functions and binding partners with dystroglycan complexes (Yoshida et al., 1998 ; Cote et al., 2002 ; Thompson et al., 2010 ; Heller et al., 2013). Furthermore, genetic and molecular studies both point to the critical nature of the binding between dystrophin and β-dystroglycan, and if this link is lost then dystrophic pathology ensues (Beggs et al., 1991 ; Cox et al., 1994 ; Judge et al., 2006 ; Aartsma-Rus et al., 2006). This idea is supported by the fact that almost all trialled therapies for DMD to date involve the restoration of β-dystroglycan to the sarcolemma as a marker of efficacy (Gilbert et al., 1998 ; Wakefield et al., 2000 ; Wang et al., 2000 ; Wehling et al., 2001 ; Gregorevic et al., 2006 ; Van Deutekom et al., 2007 ; Peter et al., 2009 ; Yin et al., 2010 ; Cirak et al., 2011 ; Goemans et al., 2011 ; Tinsley et al., 2011 ; Goyenvalle et al., 2012 ; Taniquiti et al., 2012 ; Miller et al., 2012).

In light of this, there is still a large gap in the understanding of β-dystroglycan function: how is this protein lost from the surface membrane? One might postulate that it is merely the loss of binding to sub-membranous scaffolding proteins, such as utrophin or dystrophin, which results in a destabilization of dystroglycan at the surface membrane, but this hypothesis alone cannot explain why membranous dystroglycan complexes exist that are not associated with these proteins. One can argue that in complexes other than the UGC or DGC, other, poorly-characterized proteins scaffold β-dystroglycan at the surface membrane. Certainly, from an examination of complexes involving β-dystroglycan in non-muscle tissues and cell lines this is likely to be the case. However, recent studies have demonstrated the involvement of direct, post-translational modification in the localization of β-dystroglycan (Sotgia et al., 2001 ; Sotgia et al., 2003_a). These studies, discussed in detail later, strongly suggest that a single residue, Y890, is critical to β-dystroglycan localization. However, they do not discern what effect, if any, this has in the internalization process.

In this thesis the role of this tyrosine residue in the internalization of β-dystroglycan is described. This study was performed in parallel with work in the Winder lab examining the therapeutic potential of knock-in mutagenesis of Y890 to a phospho-null form on the *mdx* background. To substantiate and expand the *in vivo* data from this project, several *in vitro* approaches with a muscle cell line were used for the experiments presented in this thesis. Thus, this introduction concludes with a description of this system, the $H2K^b$-tsA58 myoblast cell line.

1.3.1 The $H2K^b$-tsA58 Myoblast Cell Line

The $H2K^b$-tsA58 myoblast cell line (hereafter referred to as H2K myoblasts) is a conditionally immortal cell line derived from the $H2K^b$-tsA58 mouse (Morgan et al., 1994). H2K mice are derived from embryos implanted with the H2Kb-tsA58 construct: a temperature sensitive form of the SV40 transforming antigen (tsA58) coupled to a major histocompatibility complex promoter (H2Kb) (Jat et al. 1991). The H2Kb promoter permits widespread expression in a manner inducible with interferon-γ (Jat et al., 1991), whereas the tsA58 protein drives conditional immortality, but only at permissive temperatures (Jat et al., 1989). Definitive experiments with murine embryonic fibroblasts demonstrated that shifts to the non-permissive temperature accompany degradation of the tsA58 protein and a switch to differentiation, rather than proliferative growth (Jat et al., 1989). Primary myoblasts were isolated from H2Kb mice *in vitro*, prior to demonstration of these cells to maintain proliferation by injection into mouse muscle, and re-isolation of myogenic clones (Morgan et al., 1994). Growth at non-permissive conditions induces differentiation *in vitro* and *in vivo*, with induction of myogenin, a factor

regulating myogenesis, at 12 hours, and dystrophin at later time points (Wright et al., 1989 ; Morgan et al., 1994).

The advantage of using this cell line over other muscle cell lines, such as C2C12 cells, is that other cell lines are permanently transformed (Morgan et al., 1992). This transformation impairs the capacity for differentiation of these cell lines, as evidenced by the numerous discrepancies between differentiated C2C12 myotubes and adult skeletal muscle described in the literature. For example, caveolin-3 is expressed in primary myoblasts and embryonic mouse muscle tissue, where it is proposed to have a role in the development of the t-tubule system (Parton et al., 1997), yet caveolin-3 expression is only detected in differentiated C2C12 myotubes (Song et al., 1996). Further inconsistencies are observed in the C2C12 system with flotillin-1 and -2 (Volonte et al., 1999), and utrophin expression (McDearmon et al., 2001). Whilst these inconsistencies do not prevent the use of the C2C12 system, the unconditional immortality of these cell lines no doubt has an impact on *in vitro* differentiation, and hence the regulation of expression of certain proteins, which reduces the utility of any experimental observations obtained. On the basis that H2K myoblasts are not tumourigenic (Morgan et al., 1994), one can assume that the expression of proteins in these cells more closely mimics the *in vivo* state, making H2K myoblasts a preferential model of choice.

One important caveat of the H2K myoblast system is that, assuming that the differentiation process mimics the development of skeletal muscle tissue, H2K myoblasts do not express full-length dystrophin. Nonetheless, utrophin, which is up-regulated in developing and regenerating skeletal muscle tissue (Khurana et al., 1990 ; Pearce et al., 1993) is expressed in H2K myoblasts (Thompson et al., 2008). Furthermore, in keeping with the functional similarity between utrophin and dystrophin, utrophin and β-dystroglycan co-localize in adhesion structures in H2K myoblasts, suggesting that the two proteins form a functional adhesive complex, as observed in skeletal muscle tissue (Matsumara et al., 1992_a ; Thompson et al., 2008). The H2K myoblast system has also been extensively used to study the function of β-dystroglycan in cellular adhesion, suggesting that this system is a good approximation of the adhesive complexes that contain dystroglycan *in vivo* (Thompson et al., 2008 ; Thompson et al., 2010). As this thesis chiefly investigates how β-dystroglycan is internalized in cells, a process potentially linked to the loss of adhesion in dystrophic pathology, one can conclude that the H2K myoblast system is a justified *in vitro* model. Owing to the similar nature of the adhesive complexes involved, albeit without the costameric DGC found in skeletal muscle fibres, these data can be further tested by *in vivo* experimentation.

1.4.1 Chapter Summary

β-dystroglycan, together with α-dystroglycan, is part of an essential adhesion receptor. This receptor is evolutionarily conserved and forms complexes with various cellular proteins and components of the ECM. β-dystroglycan is present in a wide range of tissues and fulfils signalling and adhesion functions through its interactions with a large number of ubiquitous and tissue-specific proteins. The DGC is a notable example of a β-dystroglycan complex as it exemplifies the many features of dystroglycan-dependent signalling and adhesion. The essential nature of these features is evidenced by the chronic and degenerative nature of the disease DMD, which is characterized by the loss of this complex from the sarcolemma. Molecular studies, whilst indicating the contribution of various processes to the dystrophic state, underline the singular importance of the loss of sarcolemmal β-dystroglycan as a key step in dystrophic pathology. Relatively little is known about the mechanisms governing the sarcolemmal localization of β-dystroglycan yet, as evidenced by the therapeutic effect of sarcolemmal restoration, an understanding of these mechanisms may provide a target for future intervention, as well as extend the current understanding of this protein. In this thesis the role of Y890 in this regard is examined. The work presented here was performed in parallel with a study of the *DAG1*$^{Y890F/Y890F}$ knock-in mouse. As such, the H2K myoblast cell line was chosen as an experimental model, to more closely mimic studies performed *in vivo*. Through the combination of these approaches the mechanism governing β-dystroglycan localization, as well as the importance of this mechanism in dystrophic pathology could be investigated.

Chapter 2:
Materials and Methods

Please note that all buffer formulations are given in full upon first mention in the text, but for ease of reference all buffer formulations are also given in Table 2.6.1.

2.1 Bacterial Methods

2.1.1 Preparation of Competent Bacteria

E.coli DH5α or BL21(DE3) were taken from a frozen glycerol stock and plated on to solid (+4% (w/v) agarose) 2xYT media (1% (w/v) Yeast Extract, 1.6% (w/v) Tryptone, 0.5% (w/v) NaCl) containing no antibiotic. The plated *E.coli* were placed in an incubator and grown at 37°C overnight. The following morning single, isolated colonies were picked with a sterile pipette tip and used to inoculate 10ml of sterile 2xYT media. This starter culture was placed in a rotating incubator set at 37°C and 175rpm and left to grow overnight. The following morning, 200µl of the overnight culture were used to inoculate 20ml of sterile 2xYT media. This culture was placed in a rotating incubator set at 37°C and grown until the OD_{600} reached 0.6 AU. The bacteria were pelleted by centrifugation at 700 x *g* for 10 minutes at 4°C. The supernatant was removed and the pellet was resuspended in 10ml of ice-cold, sterile 0.1M $CaCl_2$. The resuspended cells were incubated on ice for 2 hours, before centrifugation as before. The supernatant was removed and the pellet was resuspended in 2ml ice-cold sterile 0.1M $CaCl_2$. Glycerol stocks of competent bacteria were made by addition of glycerol to a final concentration of 10% (v/v) prior to freezing and storage at -80°C.

2.1.2 Plasmid Purification

E.coli DH5α, which had been successfully transformed with the desired plasmid, were used to produce all the DNA used in this study. DNA was purified using either Mini or Maxi kits (QIAGEN) using the manufacturer's protocol. Purified DNA was re-suspended in sterile distilled water and assayed by A_{260} measurement using a quartz 1cm path-length cuvette (Unico) and a 7315 spectrophotometer (Jenway). Once the concentration of DNA had been determined, aliquots were either stored at 4°C for 6 weeks or less, or stored at -20°C for 6 weeks or more.

2.1.3 Transformation of Competent Bacteria

A glycerol stock aliquot of competent *E.*coli DH5α (for DNA purification) or *E.*coli BL21(DE3) (for protein purification) bacteria was removed from storage at -80°C and thawed on ice. 0.5µg of plasmid DNA were added to the *E.coli* and the mixture was vortexed briefly, before incubation for 20 minutes on ice. The *E.coli* were then transformed by incubation at 42°C for 1 minute, before incubation for a further 20 minutes on ice. 100µl of sterile 2xYT media were added to the transformed *E.coli* and the mixture was vortexed briefly before incubation at 37°C for 1 hour. Following incubation, the cells were plated on to solid YT + agar containing the appropriate antibiotic for selection of the plasmid DNA and placed in an incubator set at 37°C to grow overnight. Following incubation, and checking for the presence of single, isolated colonies, the plates were used immediately for DNA or protein purification, or were stored at 4°C for future use.

2.2 Protein Methods

2.2.1 Growth and Induction of Recombinant Proteins

E.coli BL21(DE3), which had been successfully transformed with the desired plasmid, were used to produce all the recombinant proteins used in this study. Plates of transformed *E.coli* were scraped into 1l of sterile 2xYT media containing kanamycin or ampicillin, at a concentration of 30µg/ml or 100µg/ml respectively, to maintain selection during growth. The inoculated media was placed in a rotating incubator set at 37°C and 175rpm and grown until the OD_{600} reached 0.6 AU. Isopropyl β-D-1-thiogalactopyranoside was then added to the media to a final concentration of 1mM and the *E.coli* were returned to the rotating incubator for induction. The time period for induction varied between the different recombinant proteins expressed, so preliminary induction curves were generated prior to the purifications described here. In general, all recombinant proteins in this study were induced for 4 hours or less at 37°C. Following induction, the *E.coli* were centrifuged at 12,000 x *g* for 15 minutes. The supernatant was removed and the pellet was stored at -20°C for future purification.

2.2.2 WW Domain GST Fusion Purification

Pellets of induced *E.coli* BL21(DE3) were thawed on ice before resuspension in 20ml of chilled PBS (0.8% (w/v) NaCl, 0.02% (w/v) KCl, 0.144% (w/v) Na_2HPO_4, 0.024% (w/v) KH_2PO_4, pH 7.4) . Following the addition of protease inhibitors (1mM sodium orthovanadate, 100nM Calyculin A, 1mM phenylmethanesulfonylfluoride, 10µM tosyl phenylalanyl chloromethyl ketone, 10µM leupeptin, 1µM pepstatin, 10µg/ml aprotinin, 10µg/ml benzamidine), cells were lysed by sonication on ice and thoroughly vortexed, before centrifugation at 21,000 x *g* for 45 minutes at 4°C. The supernatant was mixed with 0.5ml glutathione-Sepharose (GE Healthcare), which had been pre-equilibrated in PBS. The slurry was mixed on a roller for 1 hour at 4°C, prior to transfer to a column in a cold-room. Once settled on the column, the beads were washed with 10ml chilled PBS containing 1% (v/v) Triton-X, then 10ml chilled high salt buffer (150mM NaCl, 50mM Tris (pH 7.4), 1mM dithiothreitol and 1mM EDTA). GST-tagged proteins were then eluted from the beads with 1ml of chilled elution buffer (10mM reduced glutathione in 50mM Tris (pH 8)). 100µl fractions were collected on ice and used for subsequent experiments or stored at -20°C. The peak elution fractions were determined by SDS-PAGE and Coomassie staining, prior to pooling of the peak fractions and determination of final protein concentration by Bradford assay.

2.2.3 Multi-Dsk Protein Purification

Purification was similar to the protocol used above, but with the modifications made by Wilson et al. (2012), owing to the expression of the protein in inclusion bodies. Pellets were resuspended in 20ml chilled STE buffer (10mM Tris pH 8, 1mM EDTA, 100mM NaCl) with 100µg/ml lyzosyme and incubated on ice for 15 minutes. Dithiothreitol and N-lauryl sarcosine were added to final concentrations of 5mM and 1.5% (v/v) respectively and the mixture was sonicated gently on ice. Following sonication and further mixing, the mixture was filtered through cheesecloth and Triton-X was added to the filtrate at a final concentration of 3% (v/v). The filtrate was mixed with 0.5ml glutathione-Sepharose (GE Healthcare), which had been pre-equilibrated in STE buffer. The slurry was mixed on a roller for 3 hours at 4°C, prior to transfer to a column in a cold-room. Once settled on the column, the beads were washed with 50ml chilled wash buffer 1 (450mM NaCl, 10% glycerol (v/v), 0.1mM EDTA, 0.1% Triton-X (v/v) and 2mM DTT in PBS), followed by 25ml chilled wash buffer 2 (50mM NaCl, 10% glycerol (v/v), 1mM 2-Mercaptoethanol, 0.2% Triton-X (v/v) in 50mM KPhos buffer (40.1mM K_2HPO_4, 9.9mM KH_2PO_4, pH 7.4)). The beads were then resuspended in chilled PBS with 1mM sodium azide and stored at 4°C.

2.2.4 Bradford Assay

Duplicate aliquots of 0, 2.5, 5, 7.5 and 10µg of BSA in 100µl of 0.15M NaCl were prepared. The solutions to be assayed were also prepared in duplicate at 1:10, 1:100 and 1:500 dilutions in 0.15M NaCl. 1ml of Coomassie brilliant blue solution (0.1mg/ml Coomassie brilliant blue G-250, 4.5% ethanol (v/v), 8.5% phosphoric acid (v/v)) was added to each of the aliquots before vortexing and incubation at room temperature for 2 minutes. The solutions were transferred to 1-cm pathlength polystyrene cuvettes and the A_{595} for each solution was measured using a spectrophotometer (7315 model, Jenway). After correcting for baseline absorbance, the A_{595} values for the control samples were used to generate a standard curve, from which the concentration of the unknown samples could be interpolated. In the event of the unknown samples having corrected A_{595} values outside the standard curve range, the assay was repeated with different dilutions of the test solution.

2.2.5 Sodium Dodecyl Sulphate Polyacrylamide Gel Electrophoresis (SDS-PAGE)

For SDS-PAGE analysis, an equal volume of 2x Laemmli buffer (20% (v/v) glycerol, 100mM Tris (pH 6.8), 4% (w/v) SDS, 0.2% (w/v) bromophenol blue, 2% (v/v) 2-mercaptoethanol) was added to the samples. The samples were vortexed and then incubated at 95°C for 5 minutes. After cooling, the samples were vortexed and run on SDS-PAGE mini-gels. Mini-gels (10cm x 1cm x 1cm) were run using the Bio-Rad mini-gel system. Mini-gels were either prepared individually using the Bio-Rad casting system or were purchased pre-poured (Mini-protean TGX, Bio-Rad). The mini-gels comprised of 10% or 12% resolving gels with 5% stacking gels (Table 2.6.3). The mini-gels were run in Bio-Rad chambers filled with SDS running buffer (200mM glycine, 25mM Tris, 0.1% (w/v) SDS) according to the manufacturer's instruction. After loading of the sample, mini-gels were run at the fixed voltages of 100V through the stacking gel, and 150V through the resolving gel.

2.2.6 Electroblotting of Proteins

For western blotting, proteins were electroblotted from SDS-PAGE mini-gels to PVDF (polyvinylidene fluoride) membrane (Immobilon-P, Millipore) using the Bio-Rad Mini Trans-Blot system. Prior to transfer, gels were soaked in Towbin transfer buffer (25mM Tris, 192mM Glycine and 20% methanol (v/v)) for at least 5 minutes. The PVDF membrane was wetted in methanol and then immersed in the Towbin transfer buffer with the gel, so that all components of the blot were in chemical equilibrium. Finally, chromatography paper (Whatman) was also immersed in the equilibrated Towbin transfer buffer. All components were assembled into the Bio-Rad Mini Trans-Blot system and the chamber was filled with equilibrated Towbin transfer buffer, as per the manufacturer's instructions. Membranes were blotted at a fixed voltage of 100V for 75 minutes. Following blotting, membranes were removed from the blotting stack and immediately immersed in TBSTw (50mM Tris (pH 7.5), 150mM NaCl, 0.5% (v/v) Tween).

2.2.7 Western Blotting

Electroblotted membranes were blocked with 5% (w/v) skimmed milk powder (Tesco) in TBSTw for 1 hour at room temperature. Membranes were then incubated with a primary antibody at the appropriate dilution (Table 2.6.2) in TBSTw with 5% (w/v) skimmed milk powder for either 2 hours at room temperature, or overnight at 4°C. Following primary antibody incubation, membranes were washed 4 times for 15 minutes with TBSTw at room temperature and then incubated with secondary antibody at the appropriate dilution (Table 2.6.2) in TBSTw with 5% (w/v) skimmed milk powder for 1 hour at room temperature. Following secondary antibody incubation, membranes were washed 3 times for 10 minutes with TBSTw at room temperature. A chemiluminescent signal was generated by incubating the membranes with freshly mixed ECL solution (100mM Tris (pH 8.5), 1.25mM luminol, 0.2mM p-Coumaric acid, 0.02% (v/v) H_2O_2) for 30 seconds. The membranes were then transferred to the Bio-Rad Chemidoc XRS system, where the chemiluminescent signal was recorded for up to 30 minutes.

Please note that for western blots using extravidin-peroxidase as a secondary antibody 5% (w/v) bovine serum albumin was used as a blocking agent instead of skimmed milk powder.

2.2.8 Peptide Arrays

Peptide arrays representing the entire cytoplasmic domain of β-dystroglycan, as 15 residue oligomers with a single residue step, were purchased from Intavis AG. Arrays were wetted with analytical grade ethanol prior to three washes in TBSTw. The arrays were blocked with 5% (w/v) skimmed milk powder in TBSTw for 30 minutes at room temperature, and then incubated with purified protein at 20µg/ml and 5% (w/v) skimmed milk powder in TBSTw overnight at 4°C. Following protein incubation, arrays were rinsed three times in TBSTw and then washed a further three times in TBSTw for 5 minutes per wash. Arrays were incubated with anti-GST at a dilution of 1:5000 in 5% (w/v) skimmed milk powder in TBSTw for 2 hours at room temperature. Following primary antibody incubation, arrays were rinsed three times in TBSTw and then washed a further three times in TBSTw for 5 minutes per wash. Arrays were then incubated with anti-rabbit IgG-HRP at a dilution of 1:10000 in 5% (w/v) skimmed milk powder in TBSTw for 1 hour at room temperature. Following secondary antibody incubation, arrays were rinsed three times in TBSTw and then washed a further three times in TBSTw for 5 minutes per wash. Arrays were drained of excess TBSTw and a chemiluminescent signal was generated and recorded as described for western blotting (section 2.2.7).

2.3 Cell Culture and Assays

2.3.1 Growth of H2K Myoblasts

H-2K^{b}-tsA58 myoblasts (Jat et al., 1991; Morgan et al., 1994) were maintained in DMEM Glutamax^{TM} (+4.5g/L D-glucose, -pyruvate) media (Gibco BRL), supplemented with 20% (v/v) foetal bovine serum (Gibco BRL), 2% (v/v) chick embryo extract (Sera Lab), 2% (v/v) penicillin-streptomycin (Gibco BRL), and 20U/ml Interferon-γ. Myoblasts were maintained in an incubator (Galaxy S, Biohit) at 33°C and 10% CO2. Myoblasts were passaged using 1% (v/v) trypsin-EDTA (Sigma), followed by centrifugation (11030 rotor, Sigma) at 80 x *g* for 3 minutes and resuspension in growth media. Myoblasts were then re-seeded at dilutions suitable for further growth or specific experimental requirements.

2.3.2 Preparation of Lysates

For all experiments, dishes of H2K myoblasts were placed on ice, washed once with chilled PBS, then lysed with RIPA buffer (50mM Tris (pH 7.5), 150mM NaCl, 1mM EGTA, 1mM EDTA, 1% (v/v) Triton-X, 0.5% (w/v) sodium deoxycholate, 0.1% SDS (w/v), 1mM azide) supplemented with protease and phosphatise inhibitors (1mM sodium orthovanadate, 100nM Calyculin A, 1mM PMSF, 10µM TPCK, 10µM leupeptin, 1µM pepstatin, 10µg/ml aprotinin, 10µg/ml benzamidine). A cell scraper was used to ensure complete lysis and collection of sample. Following collection, lysates were centrifuged at 18,000 x *g* for 15 minutes at 4°C.

2.3.3 Immunoprecipitation

H2K myoblast lysates were sonicated for 10 seconds on ice, before centrifugation at 18,000 x *g* and 4°C for 15 minutes. The supernatant was incubated with either protein A Sepharose or protein G Sepharose, pre-equilibrated as a 50% slurry in RIPA buffer, at a ratio of 100µl/1000µl sample. The mixture was incubated for 1 hour at 4°C on a roller. Protein A or G Sepharose was removed by centrifugation at 10,000 x *g* for 1 minute at 4°C. The supernatant was incubated with primary antibody at the appropriate dilution (Table 2.6.2) and placed on a roller overnight at 4°C. The supernatant was then incubated with either protein A Sepharose or protein G Sepharose, pre-equilibrated as a 50% slurry in RIPA buffer, at a concentration of 50µl/1000µl sample. The mixture was incubated for 1 hour at 4°C on a roller. Following centrifugation at 10,000 x *g* for 1 minute at 4°C the supernatant was removed and stored on ice and the beads were washed 3 times in 10 volumes of chilled RIPA buffer. Finally, pellet and supernatant samples were mixed with equal volumes of 2x Laemmli buffer (see section 2.5.2) and were incubated for 5 minutes at 95°C. After cooling to room temperature, samples were either processed immediately, or stored at -20°C for future use.

2.3.4 Orthovanadate Treatment of H2K Myoblasts

H2K myoblasts were incubated with serum-free growth media containing 1mM sodium orthovanadate and 2% (v/v) H2O2 for 30 minutes at 33°C. Following incubation, H2K myoblasts were brought to ice and lysed in RIPA buffer as described in section 2.3.2.

2.3.5 Biotinylation Assay

H2K myoblasts were seeded on to dishes and allowed to adhere in the growth incubator overnight. The dishes were removed from the incubator and placed on ice and washed 3 times with chilled PBS before incubation with chilled biotinylation buffer (0.5 mg/ml EZ-link Sulfo-NHS-ss-biotin (Pierce) in PBS) for 30 minutes. The dishes were then washed once with chilled PBS and twice with chilled serum-free growth media containing 0.2% (w/v) BSA. The dishes were returned to the incubator, to allow endocytosis to occur, for varying amounts of time. After this, dishes were removed from the incubator and placed on ice. The dishes were washed 3 times for 20 minutes with chilled stripping buffer (50mM Tris (pH 8.6), 100mM NaCl, 1mM EDTA, 100mM MesNa and 0.2% (w/v) BSA). The dishes were then washed once for 10 minutes with 100mM iodoacetamide in chilled PBS, before 3 washes in chilled PBS and lysis in RIPA buffer as described (see section 2.3.2). To each lysate, 50µl of streptavidin-Sepharose (50% slurry, preequilibrated in RIPA) was added and the mixture was incubated for 1 hour on a roller at 4°C. Following centrifugation at 10,000 x *g* for 1 minute at 4°C the supernatant was removed and stored on ice and the beads were washed 3 times in 10 volumes of chilled RIPA buffer. Finally, pellet and supernatant samples were mixed with an equal volume of 2x Laemmli buffer (see section 2.5.2) and were incubated for 5 minutes at 95°C. After cooling to room temperature, samples were either processed immediately, or stored at -20°C for future use.

2.3.6 Transferrin Uptake Assay

Transferrin uptake experiments were performed in a manner similar to the method of Semerdjieva et al. (2008). H2K myoblast cells were seeded onto 13mm coverslips in dishes and left to adhere overnight. On ice, the growth media was removed from the dishes and replaced with chilled growth media containing Texas Red transferrin (Invitrogen) at a final concentration of 10µg/ml. The dishes were returned to the incubator, to allow endocytosis to occur, for various times. Following this incubation, the dishes were returned to ice and washed once in chilled PBS, followed by a wash in chilled transferrin stripping buffer (50mM glycine (pH 3.0), 2M urea and 100mM NaCl) for 5 minutes. Coverslips were then processed for microscopy as described in “Preparation of Cells For Microscopy”.

2.3.7 Cholera Toxin Uptake Assay

Cholera toxin uptake assays were performed as described in Marks et al. (2005). H2K myoblast cells were seeded onto 13mm coverslips in dishes and left to adhere overnight. On ice, the growth media was removed from the dishes and replaced with growth media containing Alexa fluor 594-cholera toxin B subunit (Invitrogen) at a final concentration of 1µg/ml and the dishes were returned to the incubator to allow endocytosis to occur for various times. Following this incubation, the dishes were returned to ice and washed once in chilled PBS, followed by 3 washes in chilled stripping buffer (500mM glycine (pH 2.2)) for 30 seconds each. Coverslips were then processed for microscopy as described in "Preparation of Cells For Microscopy".

2.3.8 Lysotracker™ Staining and Ammonium Chloride Treatment

Lysotracker staining was performed in a manner similar to the method of Gotink et al. (2011). H2K myoblast cells were seeded onto 13mm coverslips in dishes and left to adhere overnight. On ice, the growth media was removed from the dishes and replaced with chilled growth media containing Lysotracker™ Red DND-99 (Molecular Probes) at a final concentration of 500mM and the dishes were returned to the incubator for 15 minutes. Following this incubation, the dishes were returned to ice and washed once in chilled PBS. The coverslips were then processed for microscopy as described in "Preparation of Cells For Microscopy". For experiments using ammonium chloride treatment, the protocol followed was exactly the same except that H2K myoblasts were pre-treated with growth media containing 50mM NH_4Cl for 2 hours prior to the experiment.

2.3.9 H2K Myoblast Transfection

For all transfections of H2K myoblasts the Neon™ Transfection System (Invitrogen) was used, as described by the manufacturer's instructions pertaining to adherent cells. H2K myoblasts were trypsinized with 1% (v/v) trypsin-EDTA (Sigma) and centrifuged at 80 x *g* for 3 minutes, before resuspension in growth media and counting using an improved Neubauer haemocytometer (Weber). The myoblasts were washed in sterile PBS twice, before resuspension in sterile PBS at a concentration of 2x10^6 cells/ml. Plasmid DNA (see section 2.1.2) was added to the suspended cells at a final concentration of 75µg/ml and the mixture was gently inverted before incubation at room temperature for 5 minutes. The myoblast/DNA mixture was transferred to a 100µl Neon™ tip before electroporation with a single

1400V pulse for 30ms. The electroporated myoblasts were seeded onto dishes containing antibiotic-free growth media (see section 2.3.1). The dishes were returned to the incubator and the transfected myoblasts were left to adhere and express recombinant proteins for 24 hours prior to further processing.

2.4 Microscopy Techniques

2.4.1 Preparation of Cells for Microscopy

H2K myoblast cells on 13mm coverslips were placed on ice and carefully washed 3 times with chilled PBS. The coverslips were then removed from ice and gently immersed in fixative solution (3.7% (v/v) formalin in PBS) for ten minutes at room temperature. Following fixation, the coverslips were immersed in permeabilizing solution (0.05% (w/v) saponin in PBS) for 1 minute at room temperature. The coverslips were washed with PBS three times at room temperature before blocking by inverting the coverslips onto 20µl of blocking buffer (5% (v/v) FBS, 3% (w/v) BSA, in PBS) on parafilm. The inverted coverslips were placed in a dark, humid chamber and blocked for 1 hour at room temperature. Primary antibody solutions were prepared by mixing primary antibody at the appropriate dilution (Table 2.6.2) in blocking buffer. The coverslips were removed from the humidity chamber, drained of excess blocking buffer, and inverted onto 20µl of primary antibody solution on parafilm. The inverted coverslips were returned to the dark, humid chamber and incubated for 1 hour at room temperature or overnight at 4°C. Secondary antibody solutions were prepared by mixing secondary antibody at the appropriate dilution (Table 2.6.2) in blocking buffer. Following primary antibody incubation, the coverslips were removed from the parafilm and washed by gentle, triplicateimmersions in PBS, before draining of excess PBS and inversion onto 20µl of secondary antibody solution on parafilm. The inverted coverslips were returned to the dark, humid chamber and incubated for 1 hour at room temperature. Following the secondary antibody incubation, the coverslips were removed from the parafilm and washed by gentle, multiple immersions in PBS, before draining of excess PBS and mounting on to glass slides using a preservative mounting solution (2.5% (w/v) 1,4-diazabicyclo[2.2.2]octane (Sigma) and 100ng/ml 4',6-diamidino-2-phenylindole (Sigma) in Hydromount^{TM} (National Diagnostics)). The coverslips were allowed to set in a dry, dark, chamber for 2 hours at room temperature and were then either used immediately or stored at 4°C in the dark.

2.4.2 Epifluorescence Microscopy

Slides were viewed using a Leica DMIRE2 inverted fluorescent microscope powered by a Leica CTRMIC controller. Images were obtained with a Leica HCX PL 63X/1.32 oil-immersion objective lense, with a 50W Osram mercury illumination source and an Ebq isolated lamp power supply. Leica narrow pass filters were used to prevent bleed-through: A4, DAPI, blue (excitation at 360nm, emission at 400nm); L5 FITC/GFP, green, (excitation at 480nm, emission at 505nm); N2.1, rhodamine/Texas Red/Alexa fluor-594, red (excitation at 515-560nm, emission at 580nm). Images were acquired using the Leica QFluoro software package running on a Leica Q550FW Pentium II computer, supported by Microsoft Windows 2000 Professional.

2.4.3 Confocal Microscopy

Slides were viewed using a Leica TCS SP confocal microscope, fitted on to a Leica DMRE upright stand with a motorised stage, under the control of Microsoft Windows 7. Confocal images were obtained using a 63X PL Apo oil-immersion objective lens with a 50W HBO ACL1 illumination source, and Scan Electronics Argon-ion 100mW gas laser, emitting lines at 458, 477, 488 and 514nm, and a 25mW Kryton-ion gas laser emitting light at 568nm in conjunction with Leica Confocal Suite software.

2.5 Computer Aided Analysis of Data

2.5.1 Gel and Blot Analysis

All gels and blots were analyzed for densitometry using Image J v.1.47 (Schneider et al., 2012). Densitometry was performed as described in Ferreira et al., (2012), but is described here in brief. Following manual definition of lanes (Analyze > Gels > Select First Lane/Select Next Lane), the signal intensities were plotted as a function of vertical distance (Analyze > Gels > Plot Lanes). Using the straight line tool, the baseline intensity was defined for each plotted signal intensity peak. The wand tool was then used to find the integrated area under each peak and this number was recorded used for further analysis.

All gels and blots were analyzed for molecular weight estimation, using the "Image Lab" (Bio-Rad) software package, v.3.0. For molecular weight estimation, lanes were manually defined and bands were detected automatically. Following definition of the protein markers, the "Report" function was used to estimate the molecular weight of bands.

2.5.2 Image Processing

Adobe Photoshop CS (Adobe Inc.) and ImageJ were used for the production of all figures and images. Single channel images were first converted to monochrome 8-bit images using Image J (Image > Type > 8-bit). The images were then scaled (Analyze > Set Scale), cropped (Selection, Image > Crop) and depicted with scale bars (Analyze > Tools > Scale Bar). The processed monochrome images were then saved as TIFF files. False colour merged images were then generated (Image > Color > Merge Channels), converted to RGB format (Image > Type > RGB Colour) and saved as TIFF files. Single channel and false colour merged TIFFs were opened in Adobe Photoshop CS2 (Adobe) and manually adjusted for intensity levels and gamma settings, without addition or subtraction of visual data. The final, processed images are presented in this thesis.

2.5.3 Co-localization Analysis

All co-localization analysis was performed using the JaCoP plug-in for Image J (Bolte et al., 2006). Following manual thresholding, the manders coefficients (M1 and M2) were calculated for each pair of images (Manders et al., 1993). The mean manders coefficient (defined as M1+M2/2) was calculated for each pair of images within a data set. After calculation of the mean manders coefficient for a set of data, the data set was subjected to statistical analysis (described below) prior to graphical presentation within the thesis. Where appropriate, the mean of individual manders coefficients (M1 or M2) are used, as stated in the text.

2.5.4 Statistical Analysis

All statistical testing was performed using the statistical software "Minitab" v.15 (Minitab Inc.). Where appropriate, the normality of data sets was confirmed using the Anderson-Darling test or histographical analysis. Data sets which were of a normal distribution were tested parametrically, whereas data sets of a non-normal distribution were tested non-parametrically. Graphs were generated using "Prism" v.5 software (Graphpad Software).

2.6 Tables

2.6.1 Buffers and Solutions

Buffer/Solution Name	Components	Solvent and Notes	Relevant Section
Biotinylation Buffer	0.5 mg/ml EZ-link Sulfo-NHS-ss-biotin	PBS	Cell Culture and Assays
Blocking Buffer (Immunofluorescence)	5% (v/v) FBS, 3% (w/v) BSA	PBS	Microscopy Techniques
Blocking Buffer (western blotting)	5% (w/v) skimmed milk powder	TBSTw	Protein Methods
ChTxB Stripping Buffer	500mM glycine-HCl (pH 2.2)	Distilled Water	Cell Culture and Assays
Coomassie Brilliant Blue/Bradford Reagent	0.1mg/ml Coomassie brilliant blue G-250, 4.5% ethanol (v/v), 8.5% phosphoric acid (v/v)	Distilled Water	Protein Methods
ECL Solution	100mM Tris (pH 8.5), 1.25mM luminol, 0.2mM p-Coumaric acid, 0.02% H_2O_2	Distilled Water	Protein Methods
Elution Buffer	10mM reduced glutathione in 50mM Tris-HCl (pH 8)	Distilled Water	Protein Methods
Fixative Solution	3.7% (v/v) formalin	PBS	Microscopy Techniques
High Salt Buffer	150mM NaCl, 50mM Tris-HCl (pH 7.4), 1mM DTT and 1mM EDTA	Distilled Water	Protein Methods

H2K Myoblast Growth Media	20% (v/v) foetal bovine serum, 2% (v/v) chick embryo extract, 2% (v/v) penicillin-streptomycin, 20U/ml Interferon-γ	DMEM Glutamax™ (+4.5g/L D-glucose, -pyruvate)	Cell Culture and Assays
50mM KPhos Buffer (pH7.4)	40mM K_2HPO_4, 10mM KH_2PO_4	Distilled Water	Protein Methods
Laemmli Buffer (2x)	20% (v/v) glycerol, 100mM Tris (pH 6.8), 4% (w/v) SDS, 0.2% (w/v) bromophenol blue, 2% (v/v) 2-mercaptoethanol	Distilled Water	Protein Methods, Cell Culture and Assays
PBS	0.8% (w/v) NaCl, 0.02% (w/v) KCl, 0.144% (w/v) Na_2HPO_4, 0.024% (w/v) KH_2PO_4, pH 7.4	Distilled Water	All
Permeabilizing Solution	0.05% (w/v) saponin	PBS	Microscopy Techniques
Preservative Mounting Solution	2.5% (w/v) DABCO, 100ng/ml DAPI	Hydromount™	Microscopy Techniques
RIPA Buffer	50mM Tris (pH 7.5), 150mM NaCl, 1mM EGTA, 1mM EDTA, 1% (v/v) Triton-X, 0.5% (w/v) sodium deoxycholate, 0.1% SDS (w/v), 1mM azide	Distilled Water	Protein Methods, Cell Culture and Assays
SDS Running Buffer	200mM glycine, 25mM Tris, 0.1% (w/v) SDS	Distilled Water	Protein Methods
STE	10mM Tris-HCl (pH 8), 1mM EDTA, 100mM NaCl	Distilled Water	Protein Methods

TBSTw	**50mM Tris (pH 7.5), 150mM NaCl, 0.5% (v/v) Tween**	**Distilled Water**	**Protein Methods**
Towbin Transfer Buffer	25mM Tris, 192mM glycine, 20% MeOH	Distilled Water	Protein Methods
Transferrin Stripping Buffer	50mM glycine (pH 3.0), 2M urea and 100mM NaCl	Distilled Water	Cell Culture and Assays
Wash Buffer 1	450mM NaCl, 10% glycerol (v/v), 0.1mM EDTA, 0.1% Triton-X (v/v), 2mM DTT	Distilled Water	Protein Methods
Wash Buffer 2	50mM NaCl, 10% glycerol (v/v), 1mM 2-Mercaptoethanol, 0.2% Triton-X (v/v)	50mM KPhos buffer (pH7.4)	Protein Methods
2xYT	1% (w/v) Yeast Extract, 1.6% (w/v)Tryptone, 0.5% (w/v) NaCl	Distilled water	Bacterial and Protein Methods

2.6.2 Antibodies

Antibody Name	Protein Target	Source	Species	Dilution Used		
				WB	IF	IP
MANDAG2	Beta-dystroglycan	Thi Man & Morris (gift)	Mouse	1/100	1/10	1/10
1709	Beta-dystroglycan (pY890 form)	In house	Rabbit	1/500	1/150	1/30
Anti-EEA1 610456	EEA1	BD Biosciences	Mouse	N/A	1/100	N/A
Anti-Nedd4 (#2740S)	Nedd4	Cell Signalling	Rabbit	1/100	N/A	N/A
Anti-α-Tubulin (T5168)	α-Tubulin	Sigma	Mouse	1/2000	N/A	N/A
Anti-GFP (11814460001)	GFP	Roche	Mouse	1/1000	N/A	N/A
Anti-GST (1011/1012)	GST	VASCAM	Rabbit	1/5000	N/A	N/A
Transferrin Receptor (236-15375)	Transferrin Receptor	Invitrogen	Mouse	1/5000	N/A	N/A
Anti-Clathrin Heavy Chain	Clathrin Heavy Chain	Philipe Feraria (gift)	Mouse	N/A	1/10	N/A
Anti-Ubiquitin(P4D1)	Ubiquitin	Enzo Life Sciences	Mouse	1/100	N/A	N/A
Biotinylated Concanavalin A*	Various (α-D-mannosyl and α-D-glucosyl groups)	Vector Labs	N/A	1/4000	N/A	N/A
Texas Red Anti-mouse	Mouse IgG	Vector Labs	Goat	N/A	1/100	N/A
Texas Red Anti-rabbit	Rabbit IgG	Vector Labs	Goat	N/A	1/100	N/A
FITC Anti-mouse	Mouse IgG	Vector Labs	Goat	N/A	1/100	N/A
FITC Anti-rabbit	Rabbit IgG	Vector Labs	Goat	N/A	1/100	N/A
HRP Anti-mouse (A4416)	Mouse IgG	Sigma	Goat	1/10000	N/A	N/A
HRP Anti-rabbit (A0545)	Rabbit IgG	Sigma	Goat	1/10000	N/A	N/A
HRP Extravidin (E2886)	Biotin	Sigma	Goat	1/20000	N/A	N/A

*Please note that this is technically a lectin, and not an antibody. It is used in the same way, so it is presented here.

2.6.3 Gel Formulations

	Separating Gel		Stacking Gel
	10%	12%	5%
30% Acrylamide	1.675ml	2.075ml	0.8ml
Gel Stock	1.875ml	1.875ml	0.625ml
Water	1.425ml	1.000ml	3.525ml
TEMED	2.5µl	2.5µl	15µl
10% Ammonium Persulfate	50µl	50µl	50µl
Bromophenol Blue	(-)	(-)	(+)

Seperating Gel Stock: 1.5M Tris (pH 8.8), 0.4% (v/v) SDS

Stacking Gel Stock: 0.5M Tris (pH 6.8), 0.4% (v/v) SDS

2.6.4 Plasmids

Construct Name	Plasmid Backbone	Selection	Other Notes	Reference
WW Domain Plasmids	pHH0013 (derivative of pGEX)	Ampicillin	GST- and His-tagged, cloned for bacterial expression	Haiming Huang, personal communication
Lamp1-mcherry	pcDNA3-EGFP	Kanamycin	Cloned for mammalian expression	Jim Norman, personal communication
Sialin-GFP	pcDNA3-EGFP	Kanamycin	Cloned for mammalian expression	Jim Norman, personal communication
HA-UQ	pcDNA3.1	Ampicillin	Cloned for mammalian expression	http://www.addgene.org/18712/
Dystroglycan GFP	pcDNA3-EGFP	Kanamycin	Cloned for mammalian expression	Chen et al., 2002
Dystroglycan (Y890E) GFP	pcDNA3-EGFP	Kanamycin	Cloned for mammalian expression	Winder lab, unpublished
Dystroglycan (Y890F) GFP	pcDNA3-EGFP	Kanamycin	Cloned for mammalian expression	Winder lab, unpublished
Beta-dystroglycan (cytoplasmic only)	Pinpoint™ Xa-1 Vector	Ampicillin	Biotin-tagged, cloned for bacterial expression	Thompson et al., 2008

Chapter 3:

Phosphorylation of Y890 and -the Internalization of β-Dystroglycan

3.1.1 Introduction

To understand the importance of the c-terminus, and in particular Y890, in the localization of β-dystroglycan it is first necessary to return to the interaction with dystrophin described in the introduction (see Chapter 1, Section 1.1.3). As previously described (see Chapter 1, Sections 1.2.1-1.2.4), this interaction is lost in Duchenne muscular dystrophy (DMD), causing the loss of β-dystroglycan from the sarcolemma.

3.1.2 The Importance of the Interaction Between β-dystroglycan and Dystrophin

Within the DGC, the interaction between the c-termini of β-dystroglycan and dystrophin is critical for the stability of the complex as a whole and as such, is well defined and evolutionarily conserved. *In vitro* binding assays map the interaction of dystrophin to a region between residues 3026-3264 and residues 3265-3442, which together largely encompass the cysteine-rich region (Suzuki et al., 1992 ; Suzuki et al., 1994). The first region, which encompasses a WW domain binds to the c-terminal 15 amino acids of β-dystroglycan, whilst the second region, which contains EF hand and ZZ domains stabilizes this interaction (Jung et al., 1995 ; Rentschler et al., 1999). This mode of binding extends to other dystrophin-family proteins, including utrophin and α-dystrobrevin, and these regions not only show high homology, but high conservation between species (Koenig et al., 1988 ; Chung et al., 1999). This interaction is central to a large number of complexes containing β-dystroglycan. A crystal structure of the WW domain of dystrophin bound to the c-terminus of β-dystroglycan reveals the biochemical reasons for this: both the C-terminal PPPY motif, which contains Y890, and R887 of β-dystroglycan are pivotal in binding and the EF hand and ZZ domains of dystrophin support this interaction and provide specificity (Huang et al., 2000). These *in vitro* data are further confirmed by *in vivo* studies. Not only can the binding domains of dystrophin and utrophin immunoprecipitate β-dystroglycan from skeletal muscle preparations (Jung et al., 1995 ; Chung et al., 1999), but confocal immunofluorescence microscopy and freeze-fracture electron microscopy reveal a close association (≤10nm) between the c-termini of dystrophin and β-dystroglycan (Cullen et al., 1998 ; Stevenson et al., 1998).

The potential of truncated dystrophins and utrophins in therapies for DMD underlines the importance of the interaction with the c-terminus of β-dystroglycan. Transgenic or adenoviral-mediated expression of truncated versions of dystrophin, which retain the β-dystroglycan and actin binding domains, ameliorate dystrophic pathology and restore the DGC in both the mdx and dko mouse models of DMD

(Phelps et al, 1995 ; Rafael et al., 1998 ; Gregorovic et al., 2006). It is of interest to note that these studies are based on the observation that patients with the milder, Becker muscular dystrophy (BMD) often express truncated dystrophins of a similar nature, although the relationship between mutation and phenotype is not as consistent in humans as it is in mice (Aartsma-Rus et al., 2006). These findings have are also replicated with adenoviral and peptide delivery of utrophins, which are truncated in a similar manner (Rafael et al., 1998 ; Gilbert et al., 1998 ; Wakefield et al., 2000 ; Sonnemann et al., 2009). However, it is important to reiterate that these truncated proteins all retain the actin-binding regions of dystrophin and utrophin. Transgenic overexpression of Dp71, an isoform of dystrophin lacking the actin-binding region, results in a restoration of DGC components to the sarcolemma with little improvement in mdx pathology (Cox et al., 1994 ; Straub et al., 1997). Here, one can distinguish between the importance of a functional link to the cytoskeleton in dystrophic aetiology, and the stabilization of β-dystroglycan and the DGC at the sarcolemmal membrane mediated by the cysteine-rich regions of dystrophin and utrophin.

Finally, unusual patients and revertant expression of truncated dystrophins provide evidence for the importance of the interaction with the c-terminus of β-dystroglycan. Severe DMD patients have been described in the literature with in-frame deletions of the cysteine-rich region of dystrophin (Bies et al., 1992 ; Aartsma-Rus et al., 2006 ; Beroud et al., 2007). Despite correct sarcolemmal localization of dystrophin, the inability of this protein to bind the C-terminus of β-dystroglycan leads to a severe pathology. In addition, an analysis of 17 BMD patients expressing various levels of truncated dystrophin, which all maintain the cysteine-rich domain, demonstrates a correlation between the levels of dystrophin and β-dystroglycan present at the sarcolemmal membrane (Anthony et al., 2011). In addition, biopsies from DMD patients containing revertant fibres, which produce similar, truncated dystrophins, also exhibit correct sarcolemmal localization of β-dystroglycan and α-sarcoglycan (Arechavala-Gomeza et al., 2010).

The summation of these findings leads to the established view of the sarcolemmal localization of β-dystroglycan: that it is dependent on the presence of dystrophin, or proteins containing similar binding domains, to scaffold β-dystroglycan. However, the molecular analysis of dystrophic pathology, as well as other evidence, can also be used to propose that the residues within the c-terminus of β-dystroglycan are critical for its stabilization at the membrane, and that the same residues may play a pivotal role in its loss. In this instance, the interaction with dystrophin and related proteins retain the importance suggested by numerous studies to date, but instead this interaction serves to protect, rather than scaffold, the c-terminus of β-dystroglycan. Thus, one can postulate that these proteins only scaffold β-dystroglycan because they block internalization.

3.1.3 The Effect of Y890 Phosphorylation

Despite the extensive characterization of the interaction with dystrophin, the loss of β-dystroglycan from the plasma membrane can not be explained by any model that solely deals with this interaction, or interactions of a similar nature, exerting a scaffolding function. Biopsies from limb-girdle muscular dystrophy 2C-F patients, who lack the SGC, exhibit reduced levels of β-dystroglycan at the plasma membrane despite near normal levels of sarcolemmal dystrophin (Metzinger et al., 1997). An early characterization of the *mdx* mouse demonstrated the existence of dystroglycan complexes that were not associated with utrophin or other proteins in the DGC (Matsumara et al., 1992), and even when utrophin is significantly up-regulated in the *mdx* disease state, there is no strict correlation between the levels of utrophin and sarcolemmal β-dystroglycan (Dowling et al., 2002). Furthermore, there is significant data to suggest the existence of membranous dystroglycan in other tissues lacking these cytoskeletal linker proteins (Durbeej et al., 1999 ; Loh et al., 2000) and at the sarcolemma of mice lacking both utrophin and dystrophin (Deconinck et al., 1997_a). Whilst it is not possible to rule out the action of other, uncharacterized proteins acting in the place of dystrophin and utrophin, as is exemplified by the substituting role of plectin 1f in the *mdx* disease state (Rezniczek et al., 2007), there could to be an additional factor controlling the localization of β-dystroglycan to membranous complexes. The phosphorylation state of Y890 is a candidate in this regard, as Y890 is part of the PPPY motif bound by the WW domains of dystrophin and utrophin.

The phosphorylation of Y890 is also linked to an altered localization of β-dystroglycan within a separate, intracellular compartment. This non-sarcolemmal distribution is also observed in murine skeletal muscle and β-dystroglycan with this post-translational modification is separate from that found at the plasma membrane (Sotgia et al., 2001 ; Sotgia et al., 2003_a). Interestingly, phosphorylation at this residue also blocks the interaction with dystrophin and utrophin, presumably due to disruption of the WW domain binding site (James et al., 2000 ; Illsey et al., 2001). A caveat of this and earlier work is that phosphorylation of this residue was not measured directly and may be caused by artefacts of the experimental systems used, such as the overexpression of c-Src (Sotgia et al., 2001). However, phosphorylation of this tyrosine has been reported in other cell lines in response to adherence, and in the association with Tsk5 (James et al., 2000 ; Thompson et al., 2008), which, along with the presence of intracellular puncta in muscle fibres, suggests that this is a normal, physiological process (Sotgia et al., 2003_a). As well as abrogating the interaction with dystrophin or utrophin, the phosphorylation of Y890 would itself be blocked by the binding of these proteins (Jung et al., 1995 ; Huang et al., 2000) and hence, Y890 phosphorylation could have a role in dystrophic pathology by acting as a molecular switch in the function of β-dystroglycan.

This idea is not without precedent: phosphorylation of the cytoplasmic tail of β-dystroglycan, albeit at different residues, also changes the signalling properties of this molecule, by altering the kinases bound by this protein (Spence et al., 2004). Accounting for this also provides an explanation for why some β-dystroglycan remains at the plasma membrane in the absence of dystrophin, utrophin or both these proteins: presumably because phosphorylation is a requirement for the initiation of internalization (Deconinck et al., 1997_a ; Sotgia et al., 2003_a). Given the unstructured nature of the cytoplasmic domain of β-dystroglycan, which is largely attributable to a high proline content, a post-translational modification such as phosphorylation can have a large impact on the molecular activity of this protein by the generation, or removal, of binding sites for other proteins. Thus, it would seem that Y890 phosphorylation may be crucial for a model describing the loss of β-dystroglycan from the plasma membrane.

3.1.4 Hypothesis: Y890 Phosphorylation is Required for the Internalization of β-Dystroglycan in H2K Myoblasts

Given that Y890 phosphorylation prevents the interaction with cytoskeletal linker proteins found in cell adhesion structures, is only possible in the absence of binding by dystrophin or utrophin, and could promote the recruitment of other binding proteins, it was hypothesized that this modification would play a key role in the loss of β-dystroglycan from the plasma membrane. Also, given the exclusive separation of β-dystroglycan with this modification from membranous β-dystroglycan, it seemed logical that this modification would exclusively drive internalization, whereas the unmodified form would remain at the plasma membrane. Experiments were performed in H2K myoblasts, which have been previously demonstrated to be amenable for the molecular study of β-dystroglycan (Thompson et al., 2008 ; Thompson et al., 2010) as well as providing an ideal compromise between a cell line and skeletal muscle tissue (see Chapter 1, Section 1.3.1).

3.1.5 1709 and MANDAG2: Specific Information on the Antibodies Used in This Study

The study of the phosphorylation of Y890 and how this affects β-dystroglycan was made possible by the use of two antibodies available in the Winder lab. Owing to the similar nature of the epitopes, and the important nature of the antibodies in the analyses of the following data, a brief, detailed explanation of the two antibodies is given here. Both antibodies are raised against the last 15 residues at the c-terminus of β-dystroglycan, KNMTPYRSPPPYVPP, and hence, recognize exactly the same region. However, 1709 was raised against a peptide containing an additional phosphate on Y890, or KNMTPYRSPPPpYVPP. Hence the two epitopes for these antibodies are not identical. Both antibodies have been demonstrated to bind their target epitopes on peptide arrays (Figure 1) and do not recognize their cognate phosphorylated or unphosphorylated epitopes. One can draw a useful parallel here between the binding of MANDAG2 and the WW domain of dystrophin/utrophin, which is also abrogated upon phosphorylation of this residue. Consequently, 1709 and MANDAG2 can be thought of as specific sensors for the phosphorylation state of Y890. Importantly, β-dystroglycan that is phosphorylated on tyrosines outside of this region is also detected by these antibodies, but the implications of this will be discussed later.

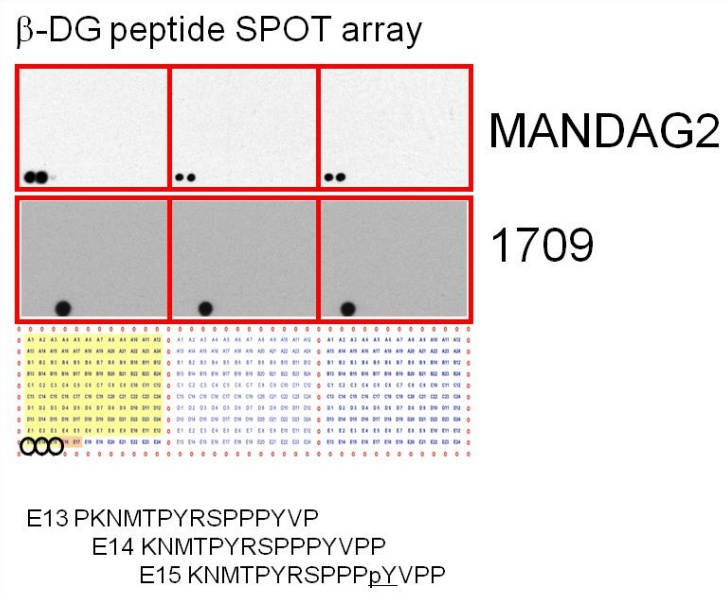

Figure 1: Peptide arrays (Invatis) representing the cytoplasmic domain of β-dystroglycan and a phospho-peptide of the last 15 amino acids were probed with the two antibodies used in this study. In triplicate, MANDAG2 bound the sequence KNMTPYRSPPPYVP whereas 1709 bound the sequence KNMTPYRSPPPpYVPP. Importantly, both antibodies are specific for the two phosphorylation states of Y890. All experiments performed by Dr. Chris Moore and data is reproduced with permission

3.2.1 Phosphorylation of Y890 is Linked to a Change in the Cellular Localization of β-Dystroglycan

To begin, a brief examination of the localization of β-dystroglycan in H2K myoblasts was conducted. Following on from the results of Sotgia et al. (2003), if the hypothesis that phosphorylation of Y890 causes internalization of β-dystroglycan was correct, then this would be reflected by a difference in the cellular staining pattern of Y890-phosphorylated β-dystroglycan when visualized by immunofluorescence. H2K myoblasts were co-stained with MANDAG2 (unphosphorylated form) and 1709 (pY890 form) antibodies. Figure 2 contains representative epiflourescent images showing a distinct punctuate staining pattern of pY890 β-dystroglycan. Owing to the limited resolution of epifluorescence microscopy, it is not possible to conclude that the 1709 stain is internal, however it does show a clear separation from the unphosphorylated form and the punctuate nature of the stain, reminiscent of intracellular vesicles, does not disprove the initial hypothesis.

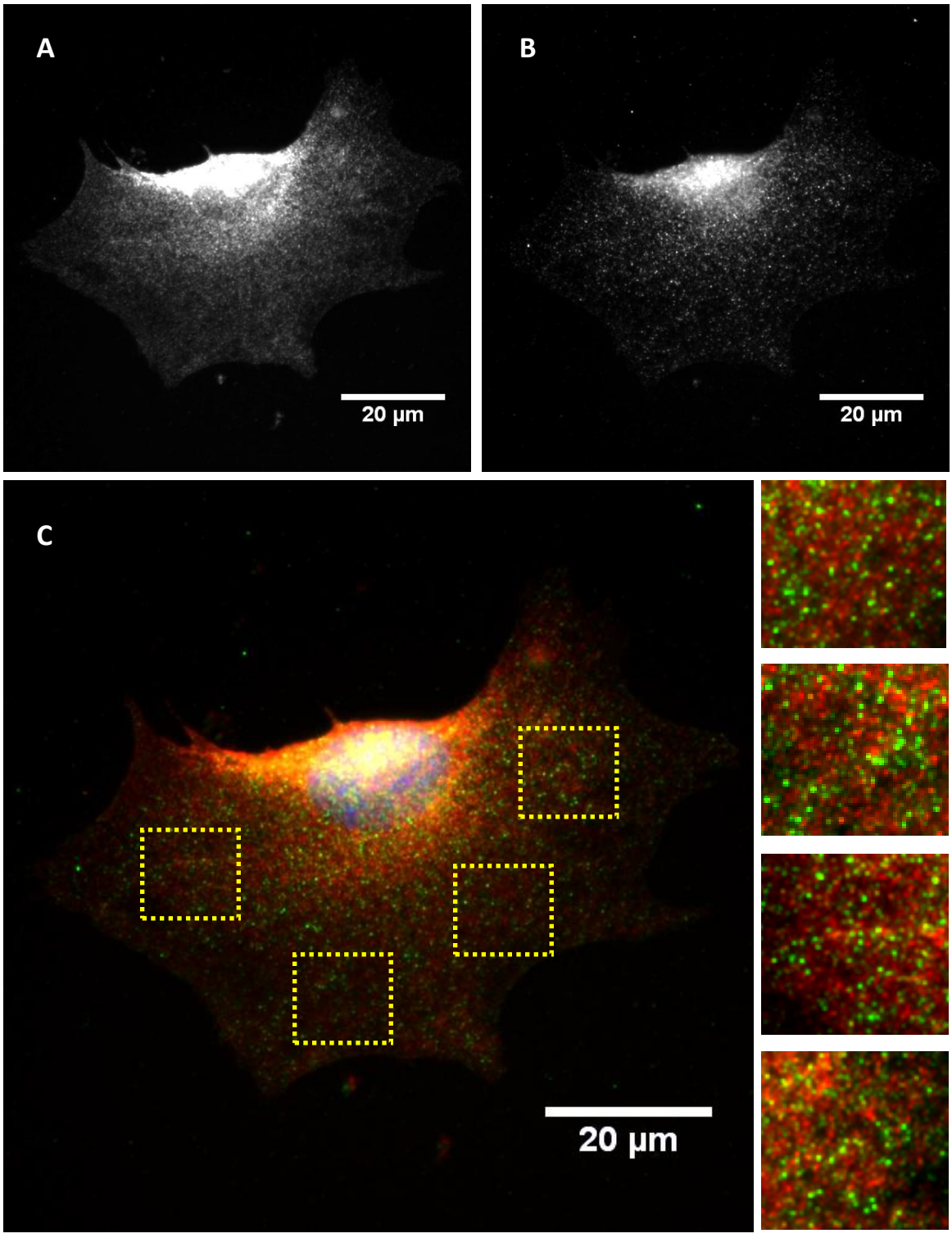

Figure 2: Reprentative images of an H2K myoblast fixed and immunostained with MANDAG2 (A) and 1709 (B). Shown are single channel fluorescence images (A,B) and (C) false colour merged images with MANDAG2 in red, 1709 in green and DAPI in blue. The two stains, whilst showing some overlap, generally show separate staining patterns. To the right are contrast-enhanced versions of the boxes in (C), which permit easier visualization in the difference of the two stains.

3.2.2 Development of Biotinylation Assay: Optimization of Biotinylation Buffer

To further probe the link between Y890 phosphorylation and internalization, a routine, biotinylation assay for endocytosis was employed (Smythe et al., 1992). The biotinylation assay for internalization requires the covalent modification of extracellular lysines of plasma membrane proteins with biotin attached by a disulfide linker (sulfo-NHS-ss-biotin). Following incubation at a temperature permissive for endocytosis, modified proteins that have been internalized are protected from washes in reducing agents, such as glutathione. Hence, internalized proteins retain the biotin modification, whereas proteins that remain at the plasma membrane lose this modification. Following lysis, proteins can be separated into internalized and membranous fractions based on streptavidin chromatography. As this assay had been used with various cell lines, but not H2K myoblasts, conditions suitable for this study were first elucidated. Fortunately, one paper had been published employing this assay to study β-dystroglycan and thus, this was used as a starting point for the development of the assay with H2K myoblasts (Sgambato et al., 2006).

As a first step, the concentration of sulfo-NHS-ss-biotin that gave saturating labelling of β-dystroglycan was determined. Given the range of concentrations used to study various proteins, concentrations of 0.05-0.5mg/ml were initially tested. As the aim was to determine maximal surface labelling, the steps involving incubation at 33°C and washing with reducing agents were omitted from the biotinylation protocol (see Chapter 2, Section 2.3.5). From densitometric analysis of western blots probed for β-dystroglycan, it is clear that saturation of the system is reached at 0.3mg/ml sulfo-NHS-ss-biotin (Figure 4). To account for potential sources of error between experiments, such as variation in cell density or variations in the purity of sulfo-NHS-ss-biotin between batches, a concentration of 0.5mg/ml sulfo-NHS-ss-biotin was used in the biotinylation buffer for all subsequent experiments.

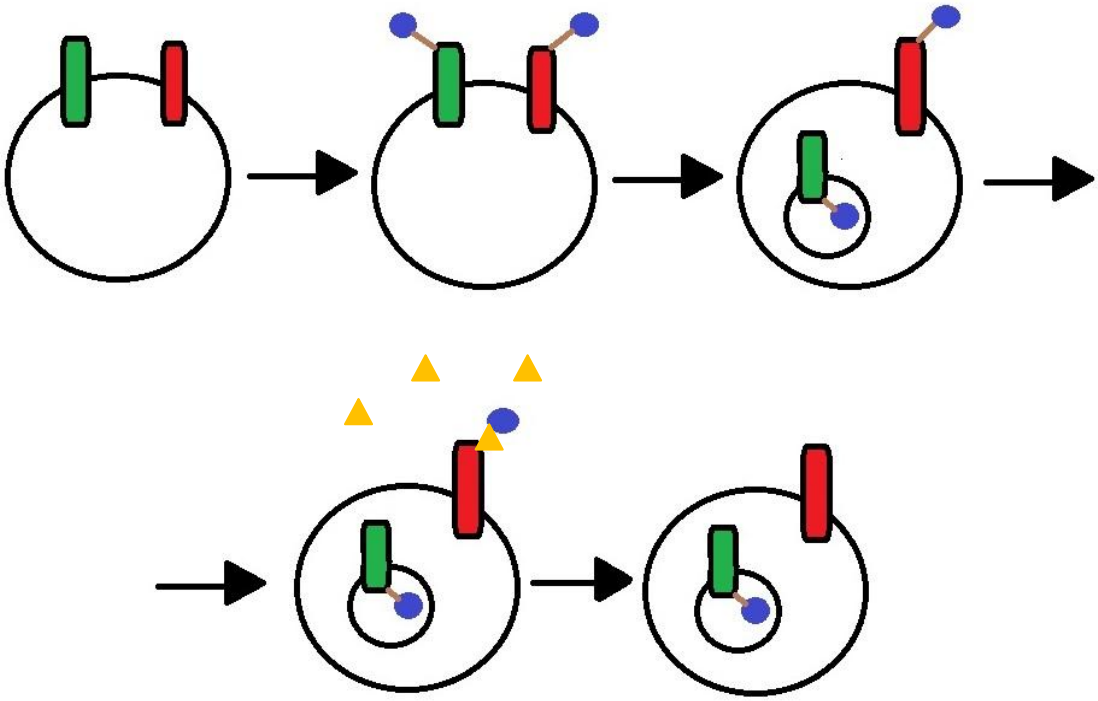

Figure 3: An outline of the biotinylation assay for endocytosis. In this simplified outline there are two membrane proteins, one of which undergoes endocytosis (green), and one which does not (red). Both membrane proteins are covalently bound to a disulphide linker (brown) bound to biotin (blue). After allowing membrane proteins to internalize at a temperature permissive for endocytosis, an excess of reducing agent (yellow triangles), which is membrane impermeable, is added and the disulphide links are broken. The excess reducing agent and free biotin molecules are then washed away, leaving the only the internalized proteins labelled.

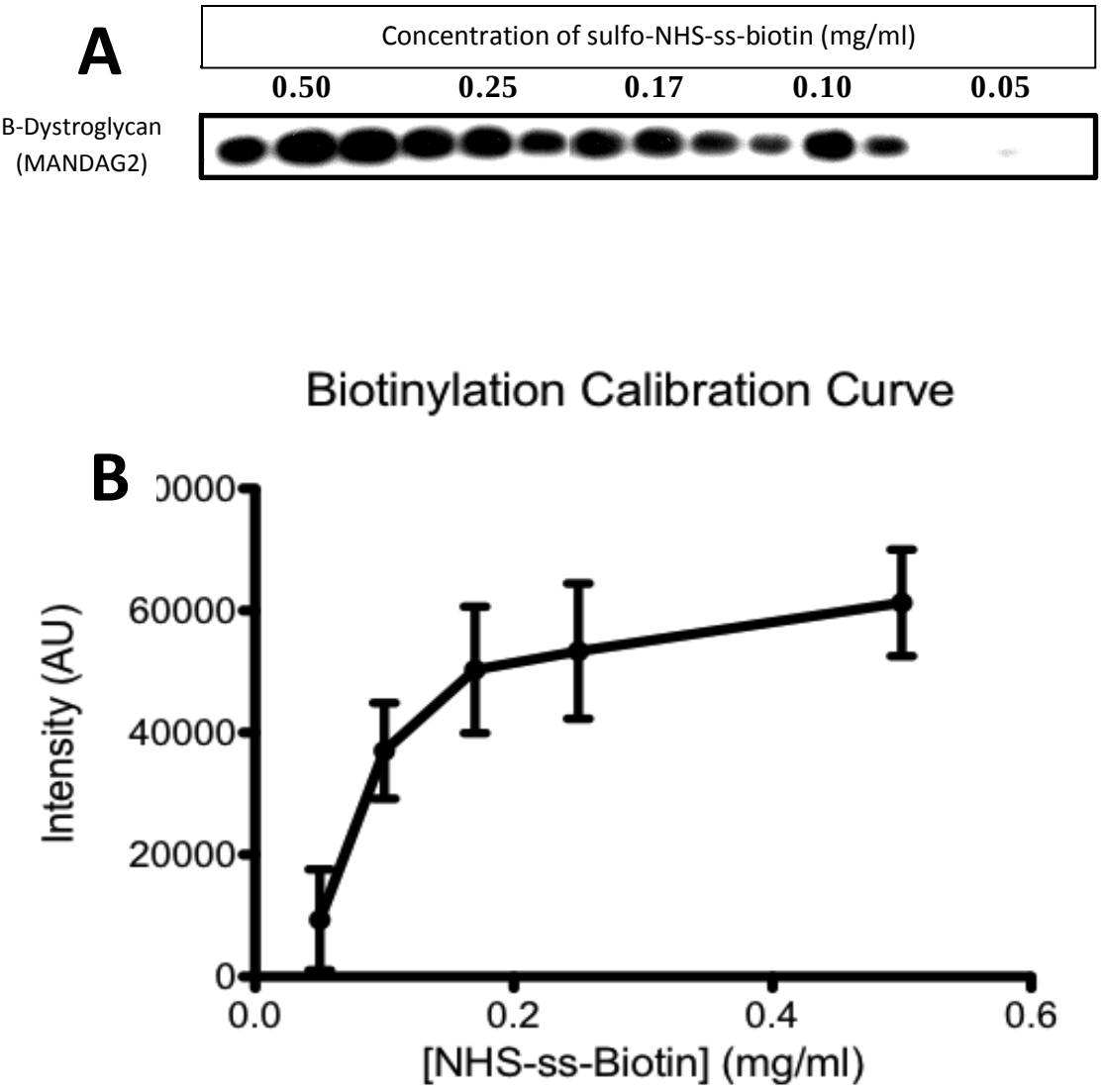

Figure 4: Estimating the concentration of sulfo-NHS-ss-Biotin at which saturating labelling of beta-dystroglycan occurs. H2K myoblasts were treated with various concentrations of sulfo-NHS-ss-Biotin for 30 minutes. After quenching, cells were lysed and the lysates were mixed with streptavidin-Sepharose. Following streptavidin chromatography, the pelleted proteins were resolved on SDS-PAGE gels, prior to western blotting with MANDAG2. The blots were scanned and analyzed by densitometry. A representative blot scan (A) and a curve of the data (B) are depicted. All treatments were performed in triplicate, error bars represent S.E.M.

3.2.3 Development of Biotinylation Assay: Optimization of Stripping Washes

The second problem that needed to be addressed was what conditions, if any, would give suitable reduction of the disulfide linkers, and thus, stripping of the biotin tag, to ensure proper discrimination between internalized and membranous β-dystroglycan. Reagents that are fit for this purpose need to have a high reducing potential, be membrane impermeable and have a low cytotoxicity. Initially, a solution of 50mM reduced glutathione (pH 7.75) was used for this purpose, however it became clear from preliminary results that this was not sufficient. Table 1 details a progressive iterative search, through several reducing agents, wash times and frequencies to find an ideal solution for this purpose. To establish if a particular set of washes were adequate, the biotinylation protocol was performed, except any incubation at 33°C was omitted. The rationale for this choice was that a "complete" reduction would remove all biotin tags on the cell surface after a saturating labelling step, or, in practical terms, any pellet immunoreactivity on western blots probed for β-dystroglycan (MANDAG2). Hence, a percentage stripping efficiency could be estimated from the immunoreactivity of the supernatant fraction divided by the total (supernatant plus pellet fraction) immunoreactivity, as determined by densitometry, for each wash condition. In this manner, the relative effectiveness of each wash trial could be compared.

Treatment	**Estimated Stripping Efficiency (%)**
PBS, 3x20 minute washes (Control)	2
50mM Glutathione in PBS (pH 7.75), 2x20 minute washes	50
50mM Glutathione in PBS (pH 7.75), 3x20 minute washes	55
50mM Glutathione in 75mM NaCl, 75mM NaOH, 1% (w/v) BSA, 3x20 minute washes	51
50mM Glutathione in 150mM NaCl, 1mM $CaCl_2$, 1mM $MgCl_2$, 3x20 minute washes	69
15mM TCEP in 50mM HEPES (pH7.5), 150mM NaCl, 1mM $CaCl_2$, 1mM $MgCl_2$, 2x30 minute washes	10
50mM TCEP in 50mM HEPES (pH7.5), 150mM NaCl, 1mM $CaCl_2$, 1mM $MgCl_2$, 2x30 minute washes	50
100mM TCEP in 50mM HEPES (pH7.5), 150mM NaCl, 1mM $CaCl_2$, 1mM $MgCl_2$, 2x30 minute washes	50
150mM TCEP in 50mM HEPES (pH7.5), 150mM NaCl, 1mM $CaCl_2$, 1mM $MgCl_2$, 2x30 minute washes	52
200mM TCEP in 50mM HEPES (pH7.5), 150mM NaCl, 1mM $CaCl_2$, 1mM $MgCl_2$, 2x30 minute washes	62
250mM TCEP in 50mM HEPES (pH7.5), 150mM NaCl, 1mM $CaCl_2$, 1mM $MgCl_2$, 2x30 minute washes	61

300mM TCEP in 50mM HEPES (pH7.5), 150mM NaCl, 1mM $CaCl_2$, 1mM $MgCl_2$, 2x30 minute washes	68
50mM MesNa in 50mM Tris-HCl (pH8.6), 100mM NaCl, 1mM EDTA, 0.2% (w/v) BSA, 2x30 minute washes	90
100mM MesNa in 50mM Tris-HCl (pH8.6), 100mM NaCl, 1mM EDTA, 0.2% (w/v) BSA, 2x30 minute washes	86 93
150mM MesNa in 50mM Tris-HCl (pH8.6), 100mM NaCl, 1mM EDTA, 0.2% (w/v) BSA, 2x30 minute washes	99
200mM MesNa in 50mM Tris-HCl (pH8.6), 100mM NaCl, 1mM EDTA, 0.2% (w/v) BSA, 2x30 minute washes	100 100
250mM MesNa in 50mM Tris-HCl (pH8.6), 100mM NaCl, 1mM EDTA, 0.2% (w/v) BSA, 2x30 minute washes	
300mM MesNa in 50mM Tris-HCl (pH8.6), 100mM NaCl, 1mM EDTA, 0.2% (w/v) BSA, 2x30 minute washes	
50mM MesNa in 50mM Tris-HCl (pH8.6), 100mM NaCl, 1mM EDTA, 0.2% (w/v) BSA, 3x20 minute washes	93
100mM MesNa in 50mM Tris-HCl (pH8.6), 100mM NaCl, 1mM EDTA, 0.2% (w/v) BSA, 3x20 minute washes	99 100
150mM MesNa in 50mM Tris-HCl (pH8.6), 100mM NaCl, 1mM EDTA, 0.2% (w/v) BSA, 3x20 minute washes	

Table 1: A summary of all the stripping conditions tested and their estimated efficiencies for the biotinylation assay. H2K myoblasts were washed on ice with chilled biotinylation buffer (0.5mg/ml sulfo-NHS-ss-biotin in PBS) and then immediately treated with the various stripping conditions. H2K myoblasts were kept on ice throughout the stripping washes and subsequent lysis to prevent internalization. The lysates were then mixed with streptavidin-Sepharose. Following streptavidin chromatography, the pellet and supernatant proteins were resolved on SDS-PAGE gels, prior to Western blotting with MANDAG2. The blots were scanned and analyzed by densitometry. "Estimated Stripping Efficiency" is defined as the supernatant immunoreactivity, divided by the total (supernatant and pellet) immunoreactivity and is expressed as a percentage.

Changes to the number of washes with, and the composition of, the reduced glutathione solution exhibited some improvements in stripping efficiency; however these improvements were still far below the required level. Adopting the method of Rojek et al. (2008), tris(2-carboxyethyl)phosphine (TCEP) was tested next as a potential stripping agent. The concentration taken from the literature, 15mM, gave the lowest stripping efficiency of all reagents tested (apart from PBS), so a series of higher concentrations up to 300mM were tested. Whilst this approach generated a considerable improvement, the maximal level of stripping (68% with 300mM, Table 1) was comparable to that observed with reduced glutathione (69%, Table 1), and therefore an alternative reducing agent was trialled. An initial trial with 100mM 2-mercaptoethane sulfonate (MesNa), which used the buffer conditions and wash frequencies of Carter et al., (1993), gave a high stripping efficiency (86%, Table 1). A range of concentrations up to 300mM were subsequently tested, and concentrations of 200mM and above gave complete stripping (99% and above, Table 1).

A subtle difficulty with the use of MesNa, and reducing agents in general, is that concentrated solutions can exert a cytotoxic effect, due to the additional reduction of the extracellular domains of adhesion proteins and consequent loss of adherent cells from the dish surface (Liz Smythe, personal communication). This problem was also observed with H2K myoblasts, which are an adherent cell line, and at higher concentrations of MesNa losses of up to 90% of cells were observed (data not shown). To ameliorate this experimental difficulty, a final series of triplicate washes with lower concentrations of MesNa were examined, with the reasoning that an additional wash would increase the stripping efficiencies without causing loss of H2K myoblasts. From the higher stripping efficiencies observed (Table 1 and Figure 5) and reduced or absent loss of cells (data not shown), it seems that this was the case. This series also served as a verification of the high efficiencies obtained with the original series of MesNa concentrations. As a result, triplicate 20 minute washes with 100mM MesNa were used for all subsequent biotinylation experiments. As an additional precaution, all subsequent experiments were also performed in parallel with a stripping control using the same experimental procedure to estimate stripping efficiency. On the occasion that the stripping control failed, the data set was discarded and not used for the analysis presented in this thesis.

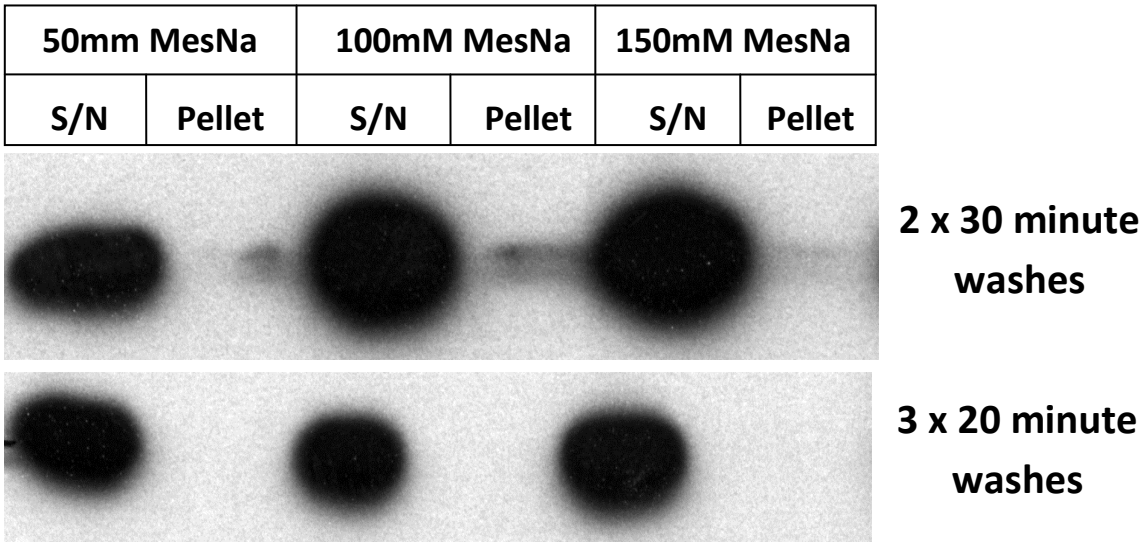

Figure 5: Testing combinations of MesNa concentration and wash conditions for optimum stripping. H2K myoblasts were biotinylated and stripped as indicated. Following lysis and streptavidin chromatography the supernatant (S/N) and pellet samples were resolved on SDS-PAGE gels and western blotted with MANDAG2 (β-dystroglycan). The presence of immunoreactivity in the pellet lanes indicates incomplete or sub-optimal stripping. As shown here, the stripping efficiency with lower concentrations of MesNa can be improved by increasing the frequency of washes. It is also interesting to note that, to the eye, 3x20 minute washes with 50mM MesNa is sufficient to remove all pellet immunoreactivity. However, as shown in Table 1, densitometric analysis reveals that there is residual reactivity.

3.2.4 Development of Biotinylation Assay: A Loading Control for Pellet Fractions

The final problem that required resolution was the need for a loading control for the pellet fractions upon western blotting. Normally, ubiquitous proteins such as tubulin or actin are used, and this was the case for the supernatant fractions. However, owing to the nature of the biotinylation experiment, these proteins would not make suitable loading controls. Other membrane proteins, which would be biotinylated and internalized in the course of the experiment, would make poor loading controls as these would be subject to endocytic regulation and hence, the levels of these proteins would vary between incubations. Natively biotinylated intracellular proteins were initially proposed as ideal loading controls, however western blotting of pellet fractions with extravidin-HRP produced no discernible bands (data not shown). Presumably this is because these proteins are either absent in H2K myoblasts or are present at levels below the detection limit of western blotting.

As an alternative a biotinylated lectin, concanavalin A, was used to probe Western blots of pellet fractions. Concanavalin A binds to several sugar moieties present in glycoproteins (Lei et al., 2009). Assuming that H2K myoblasts contain such a protein, it would be possible to use this as a loading control specific for the pellet fractions. Figure 6 contains images of both a concanavalin A blot and Coomassie stained gel showing several low molecular weight bands which are specific for the pellet fraction and invariant between various incubation times. These bands were consistently resolved at around 15kDa and are therefore unlikely to reflect spurious reactivity at the gel front. Whilst the exact nature of these proteins is unknown, the identity of these proteins was considered to be beyond the scope of investigation. As concanavalin A blotting gave a robust, repeatable and pellet-specific response it was used as a loading control for later experiments. It is also interesting to note that a slower migrating band appeared to be specific for the supernatant samples. Hence, the presence of this band in pellet fractions could be used as a marker for supernatant contamination and thus, provided an additional control for the purity of all pellet samples analyzed.

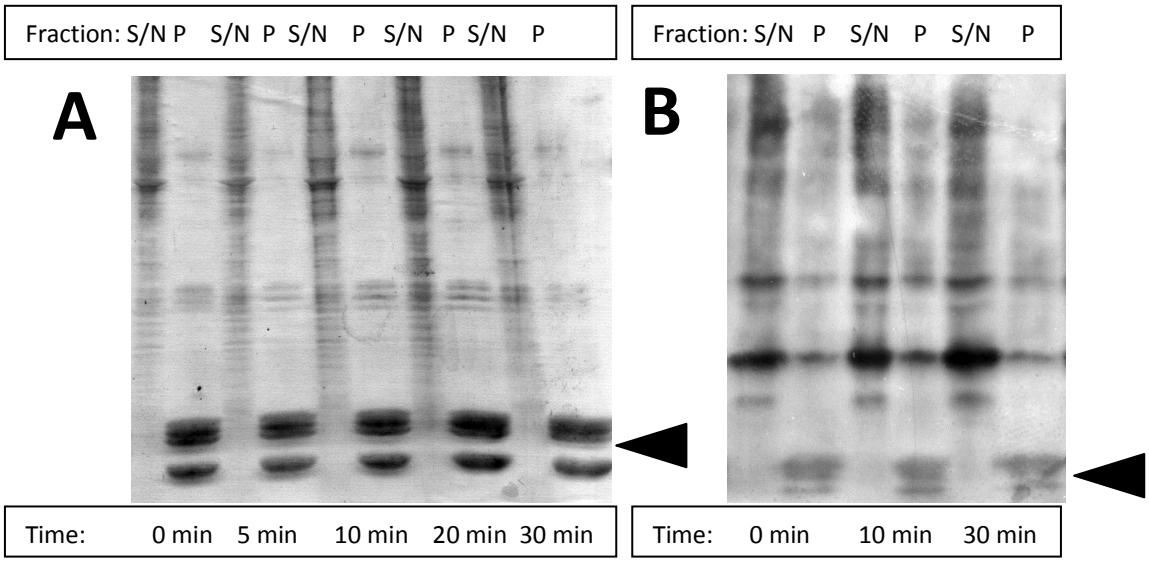

Figure 6: (A) Coomassie stained gel and (B) Concanavalin A blot of the supernatant (S/N) and pellet (P) lanes of a biotinylation experiment. Only two concanavalin A reactive bands (marked by arrowheads) appear to be specific to the P (pellet) lanes. The strong bands (or "doublet") seen at the bottom of the coomassie stained gel are also detected upon Western blotting. As these bands appear to be specific for the pellet lane and did not vary over the course of incubation times used in these experiments, they were used as pulldown and loading controls for later work.

3.2.5 The pY890 Form of β-Dystroglycan is Selectively Internalized in H2K Myoblasts

Having developed the biotinylation assay for internalization to the desired level, it was now possible to test if the change in cellular distribution observed with immunofluorescence microscopy was supported by the internalization of pY890-modified β-dystroglycan from the plasma membrane. The internalization assay was performed as described in materials in methods (Section 2.3.5) and replicate samples for 10, 20 and 30 minutes of internalization at 33°C were collected. Representative Western blots corresponding to this time course are shown in Figure 7.

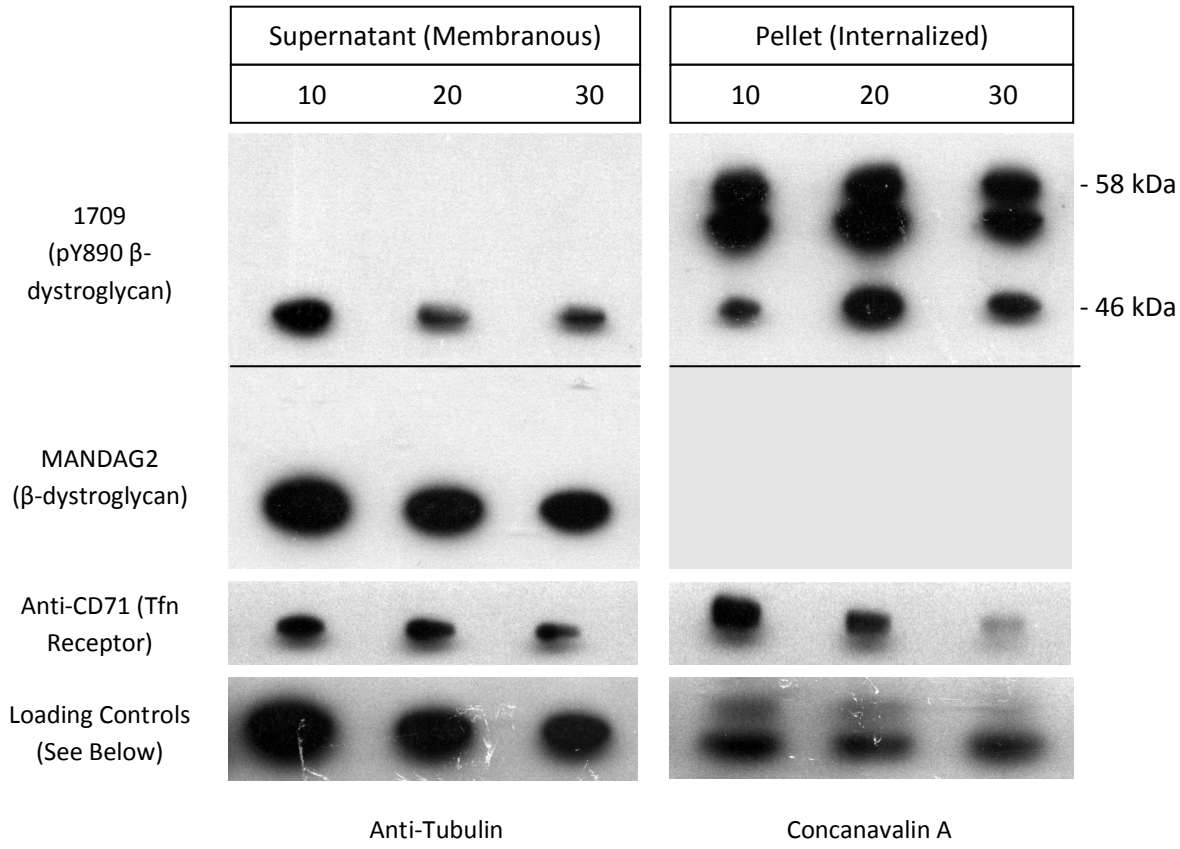

Figure 7: A time course of β-dystroglycan internalization in H2K myoblasts at 33°C. H2K myoblasts were treated for the biotinylation assay (as described in Chapter 2, Section 2.3.5), prior to lysis and streptavidin chromatography. Supernatant and pellet samples were resolved on SDS-PAGE gels prior to western blotting with the antibodies indicated. Y890-phosphorylated β-dystroglycan is specifically internalized and appears to peak at the 20 minute time point. Blotting for the transferrin receptor serves as a control for the experimental technique.

The most striking finding from these data is that the pY890-modified form of β-dystroglycan can be detected in the internalized fractions, whereas the unphosphorylated form is not. Whilst this does not strictly suggest a causative link, it certainly shows that the phosphorylation of this residue is linked to the process of β-dystroglycan internalization. Furthermore, as no unphosphorylated β-dystroglycan is detected in the internalized fractions, one can conclude that this pY890-modification persists for the duration of the time course, and that the native form of the protein is not left unmodified if it is internalized. It is possible to draw this conclusion as the two antibodies used to discriminate the two forms of β-dystroglycan both bind to the same 15-amino acid region (Figure 1). It was also interesting to see the presence of a doublet, which migrated more slowly than full-length β-dystroglycan, specifically on blots of the pY890-modified and internalized form of β-dystroglycan. The potential identity of these bands will be discussed later.

In addition to the loading controls, blotting for the transferrin receptor (anti-CD71, Cell Signalling) gave a control for the experimental system. The transferrin receptor is a classic marker of endocytic studies and is known to undergo constitutive cycling between the plasma membrane and internal compartments (Ghosh et al., 1994). By comparing the ratio of internal to membranous immunostaining, it would appear that peak internalization of this receptor occurred within 10 minutes and that subsequent recycling back to the plasma membrane occurred after this time point. Whilst there is significant variation in the temporal dynamics of transferrin receptor internalization and recycling between different cell and tissue systems, this observation is in keeping with findings in the literature (Hopkins et al., 1983 ; Klausner et al., 1983) and with immunofluorescence studies on H2K myoblasts (see Chapter 5).

By comparing the ratio of internal and membranous pY890-modified β-dystroglycan in these blots, one can also conclude that the peak β-dystroglycan internalization occurs at around 20 minutes at 33°C. At the later, 30 minute time point this ratio has reduced. This could be due to recycling of β-dystroglycan back to the plasma membrane, loss of the pY890 modification or degradation of the protein. Unfortunately, this time course was difficult to replicate in entirety due to technical limitations: namely the loss of cells from dishes during the stripping washes, the amount of material required and the time taken to perform the experiment and subsequent analysis. Owing to these difficulties, the peak of internalization at twenty minutes was used to test the hypothesis instead.

As shown in Figure 8, the findings of the initial time course experiments could be robustly verified: the internalized β-dystroglycan was phosphorylated on Y890, whereas the unmodified form was found exclusively at the membrane. Repeating the assay without internalization, or with 0 minutes of incubation at 33°C, shows that the biotin tag is not protected by a non-endocytic mechanism or anomaly of

the experimental system. Presumably these pools of β-dystroglycan exist in separate membrane domains or quickly separate upon internalization, as there is no internalized, unmodified β-dystroglycan present after 20 minutes. However, the possibility that unmodified β-dystroglycan is internalized, if only due to bulk effects, cannot be excluded: the levels of this form may be below the detection limits of the system. Nonetheless, the fact that pY890-modified β-dystroglycan is selectively internalized from the plasma membrane is conclusively demonstrated by these data.

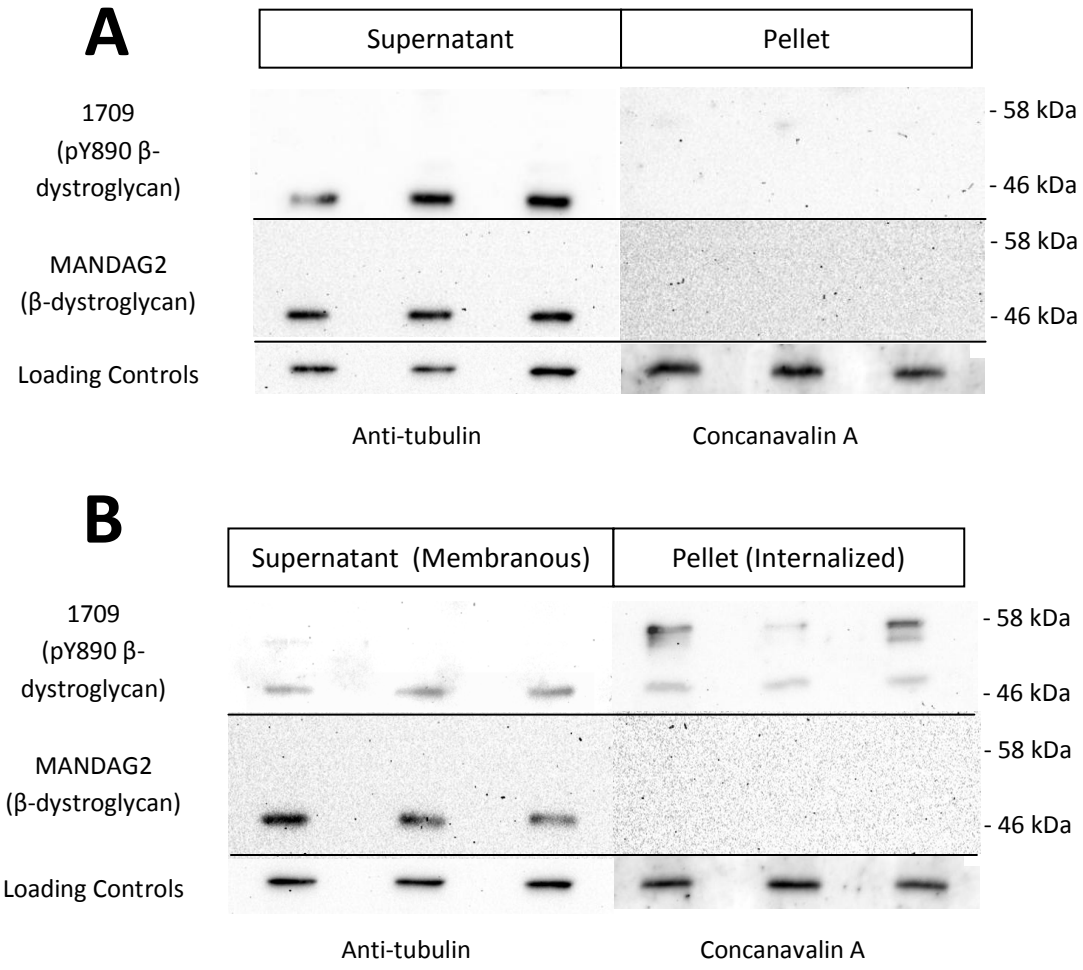

Figure 8: Replicates of the 0 (A) and 20 (B) minute time points of the biotinylation assay. H2K myoblasts were assayed as described (see Chapter 2, Section 2.3.5), prior to lysis and streptavidin chromatography. Post-chromatography samples were resolved on SDS-PAGE gels prior to western blotting for the proteins indicated. Whilst the specific internalization of Y890-phosphorylated β-dystroglycan is clear, the presence of slowly migrating bands, which is suggestive of further post-translational modification, is less consistent yet still apparent.

3.2.6 Hyperphosphorylation is not Solely Responsible for the Modification of Internalized β-Dystroglycan

The slow-migrating doublet present on the 1709 blots of the internal fractions, which can also be seen in the earlier time course experiments (Figure 7), is also seen in these data, although the intensity of immunoreactivity is variable. This doublet corresponds to a protein approximately 10kDa larger than the full-length (43 kDa) form of β-dystroglycan, which runs at 43kDa. Interestingly, these bands are only observed after 10 or 20 minutes of incubation (Figures 7 and 8) and are not observed at the 0 minute time point, which collectively suggests that they are the product of further modification of β-dystroglycan, after internalization has occurred. The cytoplasmic domain of β-dystroglycan contains multiple tyrosine residues that could be potential sites for phosphorylation. Thus, it can be hypothesized that the slower bands may be the result of hyperphosphorylation of β-dystroglycan on residues other than Y890.

Whilst this hypothesis has some credence in the literature (Moraz et al., 2012 and see below), it is unlikely to be the case in this experimental system. Orthovanadate treatment of cells is a means of causing hyperphosphorylation of proteins, including β-dystroglycan, due to the inhibition of tyrosine phosphatases present in the cell (James et al., 2000). Figure 9 shows the effects of a 30 minute treatment of H2K myoblasts in serum free media with or without 1mM orthovanadate The shifts in the electrophoretic mobility of both the unphosphorylated and pY890-modified forms of β-dystroglycan, when visualized by western blotting, strongly suggest that other sites in the cytoplasmic domain are phosphorylated in H2K myoblasts. One should note that the MANDAG2 blot is detecting the phosphorylation of these other sites, and not the Y890 residue, as phosphorylation at the Y890 would abrogate binding of the antibody (Figure 1). However, the fact remains that hyperphosphorylation does not cause the same magnitude of shift in electrophoretic mobility that is observed on western blots of the internalized fractions of β-dystroglycan (Figures 7 and 8). One can then conclude that some other form of post-translational modification is responsible for these species and is potentially linked to the internalization of β-dystroglycan, although the presence of a doublet suggests that this modification may also be partnered with additional phosphorylations.

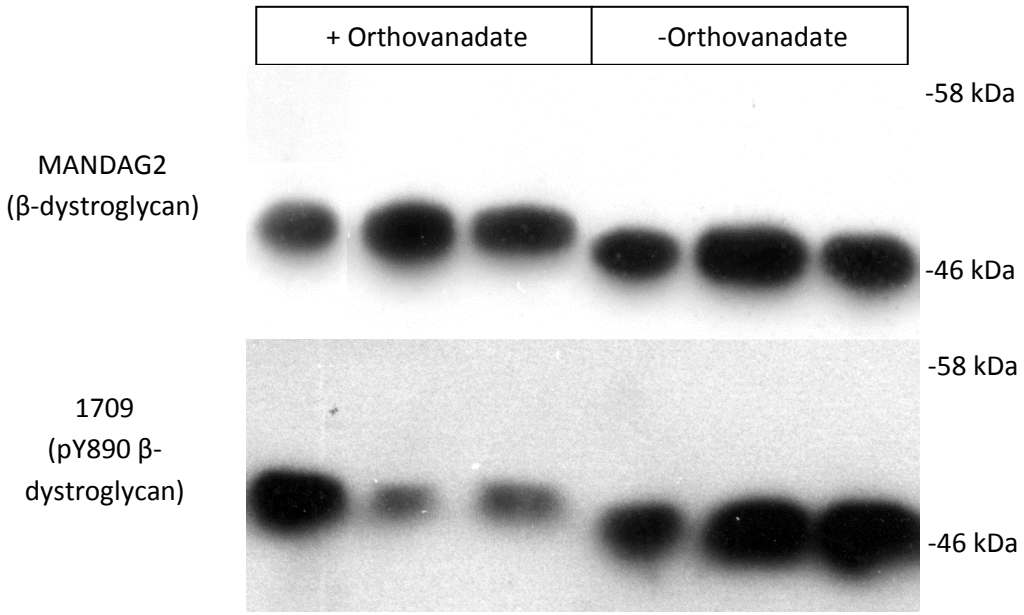

Figure 9: H2K myoblasts were treated with 1mM orthovanadate for 1 hour prior to lysis. Samples were resolved on SDS-PAGE gels and western blotted with either 1709 or MANDAG2. Whilst orthovanadate treatment caused a shift in the electrophoretic mobility of β-dystroglycan detected with both antibodies, which suggests that other tyrosine residues within the cytoplasmic domain are phosphorylated, this shift was not as large as observed in the biotinylation experiments (Figures 7 and 8).

3.3.1 Discussion

β-dystroglycan is traditionally thought of as part of the DGC, a static, costameric adhesion structure in muscle fibres (Yoshida et al., 1990 ; Ervasti et al., 1991_a ; Rybakova et al., 2000). Despite the strong association of β-dystroglycan with dystrophin in the DGC (Anderson et al., 1996), and related proteins in other cell types, the maxim that a membranous localization of this protein is solely dependent on interactions with these proteins can be called into question (Matsumara et al., 1992 ; Deconinck et al., 1997_a ; Durbeej et al., 1999 ; Loh et al., 2000 ; Dowling et al., 2002). When β-dystroglycan is phosphorylated on Y890, both the interaction with dystrophin and utrophin is blocked (James et al., 2000 ; Illsey et al., 2001) and the localization is altered (Sotgia et al., 2003_a). It was therefore hypothesized that Y890 phosphorylation would drive internalization of β-dystroglycan from the plasma membrane in H2K myoblasts.

Whilst MANDAG2 is a relatively robust and well-characterized antibody, a description of 1709 is required. 1709 is a polyclonal antiserum obtainined by immunization of a rabbit with the β-dystroglycan C-terminal phosphopeptide KNMTPYRSPPpYVPP. It is routinely used and was previously characterized without further affinity purification (Illsey et al., 2001; Miller et al., 2012). A number of lines of evidence support the notion that the antiserum specifically recognizes the Y890-phosphorylated form of β-dystroglycan. Firstly, peptide epitope mapping indicates that, when used at the appropriate dilutions, the highest affinity antibodies within the antiserum recognize the phosphor- but not the dephospho-form of the peptide used (Figure 1 and Miller et al., 2012). Secondly, 1709-reactive bands are observed on western blots of muscle tissue lysates from wildtype and Dag1+/Y890F mice, but these bands are not observed in lysates from Dag1Y890f/Y890F mice. To be clear, the mutation of the pivotal tyrosine residue in the sequence, against which the 1709 antisera is raised, abolishes any binding to β-dystroglycan, and hence any detection on a western blot. In a similar vein, immunostaining of cross-sections of fixed muscle tissue from wildtype and Dag1+/Y890F mice results in an observable signal, whereas staining of Dag1Y890F/Y890F tissue cross-sections does not. Limited epitope mapping data suggest that both the N- and C-terminal elements surrounding the phosphorylated residue are required for epitope recognition, and bioinformatic analysis of relevant databases indicates a paucity of proteins that are likely to cross react with this antiserum when used at a high dilution. However, to detect such cross-reactive species one would have to use a significantly lower dilution of primary antibody and, as detailed in Chapter 2 (section 2.6.2), 1709 is used at a comparable dilution to the dilutions used in previously published work (Illsey et al., 2001; Miller et al., 2012). Taken together, these data strongly support the notion that the cross-reacting material identified by immunoblotting and by immunofluorescence in this thesis using this antibody represents phosphorylated forms of β-dystroglycan.

There remains the possibility, in the absence of affinity purification against the immunogen, that other antibodies present in the antisera may generate signals that are distinct from β-dystroglycan. A detailed characterisation of such species by mass spectrometry was beyond the scope of this thesis, but could be undertaken in the future.

3.3.2 Y890 Phosphorylation Changes the Cellular Localization of β-Dystroglycan

By using antibodies specific for either the pY890-modified or native form of β-dystroglycan, it is possible to visualize a change in the distribution of this protein in H2K myoblasts, in response to this modification, with immunofluorescence microscopy (Figure 2). It should be stressed that not all the β-dystroglycan molecules were segregated as spots of co-localization were apparent, however this may be attributable to the poor resolving power of epifluorescence microscopy within the Z-plane. Furthermore, the degree of co-localization is low enough to suggest that the two different phospho-forms of β-dystroglycan examined are distinctly separated, at least within the cell as a whole. This idea is not without precedent, as β-dystroglycan has previously been demonstrated to be present in many different adhesive and signalling structures (Thompson et al., 2008 ; Thompson et al., 2010).

Within the cell, or muscle fibre, β-dystroglycan contributes to other forms of adhesion and so, one might expect particular modifications to be associated with changes in cellular localization. Components of the DGC are found within focal adhesions with integrin, and these are phosphorylated in response to adhesion (Yoshida et al., 1998 ; Kramarcy et al., 2000). β1-integrin shares adhesive components with β-dystroglycan present in focal adhesions (Yang et al., 1995_a ; Oak et al., 2003 ; Cerecedo et al., 2008) and engagement of ECM ligands causes a change in the phosphorylation state of dystroglycan (Spence et al., 2004). The co-dependence of the dystroglycan- and integrin-mediated systems of adhesion is exemplified by studies of mouse muscles depleted for components of either, or both (Rooney et al., 2006). α7-integrin expression is up-regulated when β-dystroglycan is absent (Cote et al., 2002 ; Allikian et al., 2004) and transgenic overexpression (Burkin et al., 2001) or retroviral-mediated delivery (Heller et al., 2013) ameliorates symptoms of muscular dystrophy in the *mdx* mouse model. Although these findings can be called into question on the basis that levels of β1-integrin are of equal, if not greater, importance than α7-integrin (Brown et al., 2004 ; Liu et al., 2012), the co-operative nature of these systems is readily apparent, with a similar co-dependency in other tissues and experimental systems (Nodari et al., 2008).

β-dystroglycan is also found in other types of cellular adhesion, besides focal and fibrillar adhesions. These structures include: membrane ruffles (Spence et al., 2004), filopodia (Batchelor et al., 2007), podosomes (Thompson et al., 2008) and the cleavage furrow (Higginson et al., 2008). These structures occur at specific sites, adapted to their particular functions and are also highly dynamic (Cox et al., 2011). It then follows that different forms of β-dystroglycan, which are involved in all these different adhesive processes, would exhibit some degree of separation. Hence, the fact that the 1709 (pY890) and MANDAG2 (unphosphorylated) stains of H2K myoblasts show such a marked difference is not an unexpected finding. Indeed, a valid criticism of the H2K myoblast system is that components of many adhesive structures may not be expressed at a high enough level to enable this (Sen et al., 2011). Therefore, the expectation of such separation would seem unfounded. Fortunately a previous study, which uses perturbations in the levels of β-dystroglycan to modulate cell spreading and adhesion in H2K myoblasts, discounts this possibility (Thompson et al., 2010).

3.3.3 Developing the Biotinylation Assay for Internalization in H2K Myoblasts

The need for dynamic changes in localization in the kinds of structures mentioned above, partnered with other observations suggesting an intracellular localization of the protein (Sotgia et al., 2003_a), strongly suggest a requirement for the internalization of β-dystroglycan. Furthermore, the microscopy data, whilst not conclusive, did not rule out the possibility that pY890-modified β-dystroglycan puncta were intracellular, owing to the separate localization from unmodified, presumably membranous β-dystroglycan (Figure 2). Hence, a method for biochemically distinguishing between internalized and membranous proteins was required, so that the importance of Y890 phosphorylation in this regard could be addressed. To this end the biotinylation assay was developed for use in the H2K myoblast system.

The method of selectively biotinylating surface proteins and following their internalization is a well developed technique in the field of endocytosis (see section 15.4.3 in "Current Protocols in Cell Biology", 2nd Ed.), and there are examples of its use in the literature concerning adhesion proteins (Le et al., 1999) and even β-dystroglycan (Sgambato et al., 2006). Whilst establishing saturating labelling in the experimental system was relatively simple (Figure 4), it quickly became apparent from preliminary experiments that achieving a suitable level of stripping of biotin tag from surface β-dystroglycan, which had not been internalized over the course of the experiment, was difficult. This problem was compounded by the fact that stronger stripping conditions, often with higher

concentrations of stripping agents, caused a detachment of cells from the substratum and their consequent loss (data not shown). Presumably this is due to the reduction of disulphide linkages in other membrane proteins that contribute to adhesion. Thus, a balance was struck between reduction efficiency and cell loss. Beyond reduced glutathione, TCEP (tris(2-carboxyethyl)phosphine) and MesNa (sodium mercaptoethane sulphonate), which both have been previously used in the literature, were trialled (Rojek et al., 2008 ; Smythe et al., 1992). With various adjustments, a final washing step was reached that gave practically complete stripping (99%, see Table 1 and Figure 5). However, although reduced, cell loss from the dish surface was a consistent technical problem that confounded replication and requires further optimization.

3.3.4 The pY890 Form of β-dystroglycan is Internalized From the Plasma Membrane

Despite these technical difficulties, it was possible to perform a time course of internalization, with further replication of the 20 minute time point (Figures 7 and 8). The most striking feature of these experiments is that the unphosphorylated form of β-dystroglycan is not internalized. Given that the pY890 form is present at the membrane (data not shown), this means that it is somehow selectively internalized and that this post-translational modification is not lost during any subsequent trafficking. It should be noted that it is still possible for the unphosphorylated form of β-dystroglycan to be internalized, or for this specific modification to be lost, however the detection of this is below the sensitivity of the experimental system. This is a distinct possibility, given that only a small proportion of the total β-dystroglycan within H2K myoblasts is absent from the membrane and therefore, despite enrichment with streptavidin chromatography, internalized biotinylated species are difficult to detect.

The time course and subsequent assays are also verified by the internalization and recycling of the transferrin receptor, which served as a control for the experimental system (Figure 7). Unfortunately, there are no data in the literature regarding the kinetics of transferrin receptor recycling in H2K myoblasts. However, it is possible to infer that typical internalization and subsequent recycling is occurring from the peak internalization time, as defined by the time at which the ratio of internal protein levels are at their highest, relative to membrane protein levels. This peak internalization time for the transferrin receptor occurs at the earliest timepoint of 10 minutes, which is in agreement with findings in other experimental systems (Hopkins et al., 1983 ; Klausner et al., 1983 ; Ghosh et al., 1994). The loss of pellet immunoreactivity at subsequent timepoints is largely due to recycling back to the plasma membrane where the biotin tag is cleaved and again, this is in

agreement with estimates of recycling times under 30 minutes for the transferrin receptor (Liz Smythe, personal communication). In a similar way, the pY890-modified β-dystroglycan also exhibits a peak of internalization at the 20 minute timepoint. Unlike the recycling of the transferrin receptor, which is a well documented process, it is not possible to say whether the decline of internalized β-dystroglycan is due to recycling to the plasma membrane or subsequent degredation. Both ideas have precedence in the literature and the case for each is discussed below.

The internalization of β-dystroglycan has been proposed to be part of a degradation mechanism (Sotgia et al., 2001) and the blockade of proteasomal degradation in *mdx* mice and DMD patient explants causes the restoration of β-dystroglycan to the sarcolemmal membrane (Bonnucelli et al., 2003 ; Assereto et al., 2005 ; Bonnucelli et al., 2007), suggesting that the two processes are linked. However, estimates for the lifetime of β-dystroglycan in mammary epithelial cells suggest a half-life of approximately 12 hours (Sgambato et al., 2006). Thus it would seem that the kinetics of degradation and internalization are not the same. This does not mean that the two processes are not linked: the loss of β-dystroglycan from the plasma membrane may be a pre-requisite for degradation, although only a minority of the internalized protein may be eventually degraded, with the majority being recycled back to the plasma membrane. Indeed, the studies involving proteasomal inhibition examine the effects of treatment over large timescales (24 hours – 8 days, Bonnucelli et al., 2003 ; Assereto et al., 2005 ; Bonnucelli et al., 2007), therefore the restoration of β-dystroglycan to the membrane may be the result of a slow, long-term process. Taking this into account, it seems logical to propose that the diminution in internal β-dystroglycan at later time points in these data is primarily due to recycling. This proposal is in better agreement with the involvement of β-dystroglycan in dynamic adhesion structures, mentioned earlier, although whether this is exactly the case will ultimately require further testing.

The internalization of full-length pY890-modified β-dystroglycan is also accompanied by the internalization of other forms of this protein, which share this modification, as determined by the presence of additional bands on western blots of the internalized fractions (Figures 7 and 8). These bands have a slower electrophoretic mobility, suggesting that these represent species of β-dystroglycan with additional modifications, beyond the phosphorylation of Y890. The presence of other species of β-dystroglycan, with a slower electrophoretic mobility, has been previously described in the literature (James et al., 2000 ; Fernandez et al., 2010 ; Lara-Chacon et al., 2010) and is a subject of continuing investigation in the Winder lab. The cytoplasmic domain of β-dystroglycan contains other tyrosine residues, which have also been implicated in the internalization of the protein (Moraz et al., 2012). Furthermore, Moraz et al. propose that phosphorylation of Y890 is not linked to nor required for internalization. Hence, whilst the importance

of Y890 phosphorylation may be disputed, the potential involvement of other phosphorylations could not be ignored in this system.

To test if a shift in the electrophoretic mobility of full-length dystroglycan, identical to that observed in the internalization assay, could be produced by hyper-phosphorylation H2K myoblasts were treated with orthovanadate. Treatments of this kind involving β-dystroglycan have been previously used in the literature (James et al., 2000), as well as in the similar C2 myoblast system (Nawrotzki et al., 1998). Treatment of H2K myoblasts with orthovanadate does produce a shift in the electrophoretic mobility of β-dystroglycan on MANDAG2 and 1709 blots (Figure 9). However, this shift is only a few kDa and is not of the same magnitude (approximately 10kDa) as is observed for internalized β-dystroglycan (Figures 7 and 8). This, along with the absence of any bands detected with MANDAG2, which one would expect to see if other sites of phosphorylation were responsible for internalization, suggest that the additional bands detected on blots for Y890-phosphorylated β-dystroglycan are due to another, subsequent form of post-translational modification. Nonetheless, it should be noted that these bands are a closely migrating doublet, suggesting that they may represent another form of modification with and without additional phosphorylations. Furthermore, the data presented in this chapter do not exclude the possibility that internalized β-dystroglycan is phosphorylated on residues other than Y890; they suggest instead that phosphorylation of Y890 is exclusively linked to internalization.

An alternative method to test this hypothesis would have involved the use of Y890 mutants, such as the phosphomimetic Y890E or phospho-null Y890F on a dystroglycan null, or knocked down background. Such H2K myoblasts were available, however preliminary experiments with Y890 mutants (expressed as GFP fusion proteins) were inconclusive (data not shown). Whilst there were alterations in the kinetics of internalization, the Y890F-GFP mutant was able to internalize in a manner that was not significantly different to the Y890E-GFP mutant or the unmodified counterpart (Y890-GFP). This effect is potentially attributable to c-terminal tagging with GFP, which may sterically exclude regulatory factors associated with internalization, or otherwise promote internalization in the absence of phosphorylation. Hence, GFP-tagged constructs are not suitable for internalization assays involving β-dystroglycan. Due to time constraints this approach was not pursued further, however future tests of this hypothesis could involve mutagenesis of Y890 to examine the contribution of phosphorylation to internalization.

3.3.5 Y890 Phosphorylation and β-Dystroglycan Internalization in Other Systems

The implications of the data presented in this chapter extend to the realm of cellular biology *in vivo*. Whilst the hypothesis that Y890 phosphorylation leads to internalization in a more native state, such as a muscle fibre, has not been directly addressed, there is evidence to support the argument that the same mechanisms exist in muscle fibres as well as in H2K myoblasts. Data from mice harbouring both the *mdx* and β-dystroglycan Y890F mutations suggest that this residue is critical for internalization (Miller et al., 2012). On the *mdx* background, the loss of dystrophin would normally result in a loss of other DGC components, including β-dystroglycan (Ohlendieck et al., 1991_a), however with the Y890F mutation several components of the DGC, including β-dystroglycan, are retained at the sarcolemmal membrane (Miller et al., 2012). Assuming that the Y890F mutation does not alter the expression levels of any proteins, beyond that typical of the *mdx* disease state, one can conclude that the phosphorylation of Y890 has an important mechanistic effect: namely the internalization, and subsequent degradation, of β-dystroglycan. The data presented in this chapter is certainly in agreement with the former if not both ideas.

Beyond this, in current estimates of protein stoichiometries in healthy human muscle, it is suggested that there are ten molecules of β-dystroglycan for every dystrophin molecule (Jim Ervasti, personal communication). Given that β-dystroglycan binds to dystrophin with a 1:1 stoichiometry (Ervasti et al., 1993), that leaves nine 'free' β-dystroglycan molecules for every DGC. Some of the other β-dystroglycan molecules will be involved in other structures with alternative scaffolding proteins, such as utrophin at the neuromuscular junctions (Khurana et al., 1991 ; Gramolini et al., 1997), or be part of other, adhesion and signalling complexes such as focal adhesions (Thompson et al., 2010), but, within a muscle fibre, it is not impossible to imagine a pool of free β-dystroglycan. Importantly, β-dystroglycan that is not bound by or scaffolding any other proteins would be a substrate for phosphorylation on Y890. This would subject 'free' β-dystroglycan to internalization and recycling to other parts of the fibre where needed, so that the dynamic, changing needs of the muscle fibre were met. Again, the data presented in this chapter is compatible with this hypothesis.

Finally, the argument for phosphorylation as a regulator of the internalization of β-dystroglycan can be furthered by a consideration of the conditions that promote a loss of β-dystroglycan from the plasma membrane: namely the altered signalling state of dystrophic muscle. The levels and activity of Akt kinase are significantly altered in *mdx* muscle (Peters et al., 2006), and normalizing these levels has potential as a therapy for muscular dystrophy due to the restoration of DGC components, including β-dystroglycan, to the sarcolemmal membrane (Peters et al.,

2009). In addition, the levels of signalling around the paxillin-FAK-MAPK nexus are also altered in *mdx* muscle (Sen et al., 2011). These changes may be an effect, rather than a cause, of the loss of the DGC from the sarcolemmal membrane in dystrophic pathology (Marshall et al., 2012_a ; Marshall et al., 2012_b). However, in all cases the phosphorylation state of a dystrophic fibre is not the same as a healthy counterpart. The effects of this are apparent beyond the typical hallmarks of dystrophy and exhibit peculiar phenotypes, such as the fragmentation of the golgi apparatus, which can be attributed to the altered activity of c-Src (Percival et al., 2007 ; Weller et al., 2010). Whilst there is currently no conclusive evidence for direct targeting of β-dystroglycan by c-Src, that it is a downstream target of c-Src dependent phosphorylation is evident (Sotgia et al., 2001 ; Thompson et al., 2008 ; Daniel Leocadio Victoria, personal communication). Hence, when one considers the altered phosphorylation state of dystrophic fibres, at least within the *mdx* model, it is possible to speculate how the phosphorylation of β-dystroglycan may contribute to the dramatic loss of this protein, along with the DGC, from the sarcolemmal membrane. On this account, the kinase(s) responsible for Y890 phosphorylation and the mechanisms and stimuli governing this process are of interest and importance for future research.

3.3.6 Summary

The data presented in this chapter can be summarized as follows:

1. The phosphorylation of Y890 of β-dystroglycan is linked to a change in the cellular localization of this protein.
2. In the context of Y890, the phosphorylated form of β-dystroglycan is internalized, whereas the unphosphorylated form is retained at the plasma membrane.
3. Following internalization, β-dystroglycan is modified by further post-translational modification. This modification may include the phosphorylation of other tyrosine residues, but only when partnered with another form of unidentified modification.

Chapter 4:

Phosphorylation of Y890 and the Ubiquitylation of β-Dystroglycan

4.1.1 Introduction

From the data presented in the previous chapter, it seems that β-dystroglycan internalization is linked to to phosphorylation of Y890 (Chapter 3, Figures 5 and 6). However, this phosphorylation is partnered with additional post-translational modifications, which can not be solely attributed to the phosphorylation of other tyrosine side chains within the cytoplasmic domain (Chapter 3, Figure 7). The current understanding of the diversity and varying functions of post-translational modifications, beyond phosphorylation, is limited, however modifications including ubiquitylation (Goldstein et al., 1975), neddylation (Kumar et al., 1993) and sumoylation (Matunis et al. 1996 ; Mannen et al., 1996) are all subjects of intense investigation. It was hypothesized that one of these forms of modification is responsible for the higher bands observed on western blots of internalized, pY890-modified β-dystroglycan.

4.1.2 Identifying a Candidate for the Post-Translational Modification of β-Dystroglycan

In general, it is possible to propose candidates for a particular modification based on criteria elucidated from the known substrates and responses involving that modification. Owing to the infancy of the current understanding of alternative post-translational modifications, the list of "known substrates and responses" is limited, however general rules, or dogmas, have emerged that can be used to inform and direct scientific enquiry. For example, modifications associated with the immune response and lymphoid cells (ISG15, FAT10 and MNSFβ), autophagosomes (ATG8), megakaryoctye and erythroid differentiation (Ufm1), tRNA thiolation and oxidant exposure (URM1) and splicing in yeast (Hub1) are poor candidates for the modification of an adhesion protein in a skeletal muscle cell line (van der Veen et al., 2012). Neddylation, another form of modification, is usually restricted to components of E3 ubiquitin ligases, such as the cullin protein family and the IAPs (inhibitor of apoptosis proteins), where it enhances the activity of these ligases and promotes ubiquitylation (Rabut et al., 2008). As there is no evidence supporting the presence of β-dystroglycan in such a complex, this post-translational modification may also be dismissed as a candidate.

An interesting candidate for the modification of internalized β-dystroglycan is sumoylation. Sumoylation is usually associated with translocation to, or retention within, the nuclear compartment (Lin et al., 2003 ; Matunis et al., 1996 ; Yurchenko et al., 2006) or specific sub-compartments of the nucleus, as is suggested for the VHL (Von-Hippel Lindau) and PTP1B (protein tyrosine phosphatise 1B) proteins (Cai et al., 2009 ; Yip et al., 2012). There is a strong

body of evidence for the presence and function of full-length and truncated β-dystroglycan within the nucleus (Fuentes-Mara et al., 2006 ; Oppizzi et al., 2008 ; Lara-Chacon et al., 2010 ; Martinez et al., 2013 ; Mitchell et al., 2013), but given the apparent cytoplasmic location and rapid modification of pY890-modified β-dystroglycan (see Chapter 3, Figure 1 and Chapter 5), as well as the proposed nuclear localization of the sumoylating E1 and E2 ligases (Matunis et al., 1996 ; Rodriguez et al., 2001 ; Truong et al., 2012), it seems unlikely that this modification is responsible for the changes observed here (Chapter 3, Figure5).

Yet there is still precedent for the cytoplasmic sumoylation of β-dystroglycan. Recent studies have identified several membrane proteins within the central nervous system that present an intracellular, cytoplasmic localization in response to sumoylation (reviewed in Silveirinha et al., 2013). Furthermore, the sumoylating enzymes, despite having a predominantly nuclear localization, also show peripheral, dendritic localization in cultured neurons (Martin et al., 2007 ; Wilkinson et al., 2012). In particular, the GluK2 subunit of the kainate receptor is sumoylated in the cytoplasm (Martin et al., 2007). This sumoylation event occurs downstream of phosphorylation of S868 by protein kinase C (Konopacki et al., 2011 ; Wilkinson et al., 2012). Importantly, inhibition of the phosphorylation or sumoylation of GluK2 decreases the internalization of the kainate receptor in response to kainate treatment (Martin et al., 2007). Here, one can draw a parallel with β-dystroglycan, which is phosphorylated and further modified upon internalization.

However, one can not necessarily draw a parallel between the systems of neuronal signalling and myoblast adhesion. The sumoylation and internalization of the kainate receptor may represent a very specific response, as sumoylation has no effect on kainate receptor endocytosis in response to NMDA treatment (Martin et al., 2007 ; Wilkinson et al., 2012). Indeed, sumoylation has been postulated to be part of both protective and degenerative mechanisms in neurons, as well as a part of long-term potentiation (Jaafari et al., 2012 ; Silveirinha et al., 2013). Furthermore, changes in the activity, and not the localization, of sumoylated proteins have been reported in the literature (Dou et al., 2010 ; Dou et al., 2011), and it may be that the sumoylation of the GluK2 subunit is a means of modulating MLK3-JNK3 signalling (Zhu et al., 2012). Examples also exist in the literature of membrane proteins that are protected from sumoylation upon phosphorylation, such as the progesterone receptor (Knutson et al., 2012). Nonetheless, one cannot discount the possibility of the sumoylation of Y890-phosphorylated β-dystroglycan on account of a cytoplasmic or membranous localization.

Alternatively, ubiquitylation may be the cause of the slower migrating bands observed in the internalized fractions of β-dystroglycan. The ubiquitylation of proteins is normally associated with degradation in an ATP-dependent manner (via the 26S proteasome) (Wilkinson et al., 1981). To quote Stefan Jentsch: "...the ubiquitin/proteasome system also detects and eliminates abnormal proteins that would otherwise be part of a larger complex, but fail to find their partners" (Jentsch et al., 1995). Given that pY890-modified β-dystroglycan is unable to bind its normal anchoring proteins, dystrophin and utrophin (James et al., 2000 ; Illsey et al., 2001) and is lost from the sarcolemmal membrane, where other components of the DGC are typically found (Ohlendieck et al., 1991_a ; Ohlendieck et al., 1993 ; Sotgia et al., 2003_a), it would seem logical to think of internalized β-dystroglycan as an "abnormal protein that would otherwise be part of a larger complex" and hence, a likely target for ubiquitylation. In support of this, inhibition of the proteasome, with either MG-132, velcade or mln273, in *mdx* mice or patient explants leads to a restoration of β-dystroglycan to the sarcolemmal, suggesting an involvement of ubiquitin in the loss of this protein from the membrane (Bonnucelli et al., 2003 ; Assereto et al., 2005 ; Bonnucelli et al., 2007). However, this argument has opposition from the fields of both DMD and proteasome research.

Whilst significantly enhanced protein degradation is reported in the muscle fibres of *mdx* mice (Kämper et al., 1992), this has been attributed to the increased activity of calcium-dependent proteases and altered calcium homeostasis (Spencer et al., 1995 ; Collet et al., 1999 ; Badalamente et al., 2000). In models of cardiac hypertrophy and ischemic injury, which are both associated with the DMD disease state, there is evidence to suggest a link between β-dystroglycan levels and protease activity (Armstrong et al., 2003 ; Daicho et al., 2009). Furthermore, with the loss of components of the DGC, in this case in the muscle fibres of mice that lack α- or β-SG, there is an enhanced proteolysis and loss of β-dystroglycan from the sarcolemma, which can be reversed by treatment with calpain inhibitors (Duclos et al., 1998 ; Araishi et al., 1999). In a similar vein, the enhanced levels of matrix metalloproteinase (MMP) activities in the *mdx* disease state have been linked to an enhanced proteolysis of β-dystroglycan (Michaluk et al., 2007 ; Daicho et al., 2009). Although the exact MMP(s) responsible for the cleavage of β-dystroglycan is currently unresolved (Delfin et al., 2011), the general inhibition of MMPs by treatment with suramin can cause a restoration of β-dystroglycan to the sarcolemma in the *mdx* mouse (Taniquiti et al., 2012). Together, these form an argument against β-dystroglycan being degraded by the proteasome, or at least, make this possibility less likely.

A valid criticism of these studies is that they may reflect general changes in dystrophic pathology, and that the effects of calpain or MMP inhibition on β-dystroglycan represent an indirect mechanism, rather than direct cleavage. In support of this, the levels of the muscle-specific calpain CANP3 are altered in LGMD2A patients, but with no change in β-dystroglycan levels (Spencer et al., 1997). However, an argument made in this manner is equally applicable to the effects of proteasome inhibition mentioned earlier, making a resolution between the mechanisms that mediate the loss of β-dystroglycan from the sarcolemma difficult. Furthermore, the treatment of *mdx* mice with MG-132 also causes an increase in muscle calpain activity, suggesting that these mechanisms are both potentially responsible for the loss of β-dystroglycan from the sarcolemma (Bonnucelli et al., 2003). Thus, when one takes into account the full evidence surrounding the degradation of β-dystroglycan, any conclusions drawn in support of the ubiquitylation of β-dystroglycan are indirect at best.

Returning to the field of ubiquitin research, there is also a further issue with drawing inferences between proteasomal inhibition and the loss of β-dystroglycan from the membrane. A central dogma of proteasomal degradation is that polyubiquitylation, with 4 or more ubiquitin proteins covalently linked in a chain, is a prerequisite (Thrower et al., 2000). Although this dogma is challenged by the suggestion that monoubiquitylation is sufficient for the proteasomal degradation of substrates with 150 residues or less (Shabek et al.,2012), this would not be the case for full-length β-dystroglycan, which is approximately 240 residues in length. The observed shift in the electrophoretic mobility of internalized β-dystroglycan on western blots equates to approximately 10kDa (Chapter 3, Figures 5 and 6), therefore one would expect that mono or possibly diubiquitylation is occurring, but certainly not the tetraubiquitylation that is required for proteasomal processing. Thus, by ascertaining the criteria for ubiquitylation from the process of targeting for degradation, it seems unlikely that β-dystroglycan is modified in this manner. However, degradation is not the only process associated with the ubiquitylation of a substrate.

4.1.3 Monoubiquitylation and the Internalization of β-Dystroglycan

In the literature, there is a growing body of evidence suggesting that monoubiquitylation on particular or multiple lysine side chains can cause the trafficking of a substrate, as opposed to proteasomal degradation (Nichols et al., 2001). Monoubiquitylation of the PDGF, EGF, FGF and interferon-α receptors drives internalization of these proteins and, in a manner to analogous to β-dystroglycan, this internalization is coupled to tyrosine phosphorylation (Karlson

et al., 2006 ; Kumar et al., 2007 ; Hayes et al., 2011). The importance of monoubiquitylation in trafficking can be questioned, as neddylation is suggested to also play a role in the internalization of the EGF receptor (Oved et al., 2006). However, this particular study may be criticised on the basis that neddylation is driven by Nedd8 overexpression, which can lead to the identification of false substrates owing to non-specific neddylation by ubiquitin E3 ligases (Rabut et al., 2008).

Monoubiquitylation is also proposed to cause the cytoplasmic retention, or the nuclear export, of substrate proteins, often in an antagonistic manner to sumoylation (Cai et al., 2010 ; Wang et al., 2012). The monoubiquitylation of p53 by MDM2 leads to the nuclear export of the protein, whereas proteasomal degradation is initiated by polyubiquitylation (Li et al., 2003). Similarly, the VHL and CTP:phosphocholine cytidylyltransferase (CTT) proteins are retained in the cytoplasm by monoubiquitylation, and in the case of CTT this is thought to be due to masking of the nuclear localization sequence (NLS) by ubiquitin (Chen et al., 2009 ; Cai et al., 2010). An important exception to these studies is that monoubiquitylation can drive the nuclear import of the PTEN tumour suppressor (Trotman et al., 2007). Nonetheless, the prevailing consensus is that monoubiquitylation is linked to protein trafficking within the cytoplasm and, in this regard, ubiquitylation is therefore an ideal candidate for the additional post-translational modification of internalized β-dystroglycan.

4.1.4 Hypothesis: Y890 Phosphorylation is Required for the Ubiquitylation of β-Dystroglycan in H2K Myoblasts

To this end, it was initially hypothesized that β-dystroglycan could also be ubiquitylated and that it was this that was responsible for the shift in electrophoretic mobility observed on western blots of internalized β-dystroglycan. Given the rapid emergence of this modification during internalization (Chapter 3, Figure 5), the predominantly cytoplasmic distribution of the presumably internalized puncta observed with epifluorescence microscopy (Chapter 3, Figure 2and Chapter 5), as well as previous work in the literature suggesting a link between β-dystroglycan internalization and proteasomal degradation, ubiquitylation was an ideal candidate modification. Owing to the lack of any additional bands observed on western blots for the unphosphorylated form of β-dystroglycan, it was also hypothesized that ubiquitylation would be exclusively linked to Y890 phosphorylation.

4.2.1 Enrichment of Cellular Ubiquitin by Affinity Tagging

Assuming that the ubiquitylation of β-dystroglycan is a constitutive process, like internalization, this hypothesis could be tested by enrichment of proteins conjugated with ubiquitin and probing with modification specific antibodies against β-dystroglycan. Owing to the availability of antibodies in the Winder lab, initial experiments utilized the transient transfection of H2K myoblasts to express exogenous, HA-tagged ubiquitin, so that immunoprecipitation with anti-HA could be used to enrich for ubiquitylated proteins. This approach is widely used (Yurchenko et al., 2006 ; Rabut et al., 2008 ; Cai et al., 2010) and is thought to cause minor perturbations to the cell ubiquitylation and degradation systems (Love et al., 2013). However, poor expression of this plasmid and unexpectedly high levels of cell death following transfection prevented the use of this approach to test the initial hypothesis in H2K myoblasts.

4.2.2 Enrichment of Cellular Ubiquitin with the MultiDsk Protein

The MultiDsk system was used as an alternative method to enrich ubiquitylated proteins from H2K myoblast lysates. The MultiDsk protein is an artificial recombinant protein containing five Dsk ubiquitin binding domains, which are linked by flexible spacers, with N-terminal GST and C-terminal 6xHis fusion tags (Figure 1).

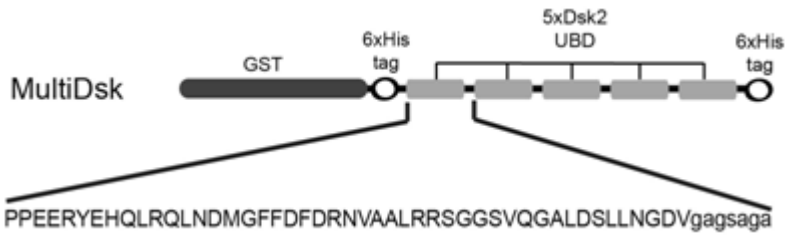

Figure 1: A schematic representation of the GST-MultiDsk fusion protein. Included are the sequence of a single Dsk domain (upper case) and the sequence of a spacer (lower case). Reproduced with permission from Marcus Wilson.

The MultiDsk protein is designed to bind all mono-ubiquitylated and poly-ubiquitylated proteins and does so with a high level of avidity and specificity (Wilson et al., 2012). In this manner it is similar to other, previously published recombinant proteins designed for a similar purpose, such as the GST-Dsk2 and

TUBE-1 proteins (Hjerpe et al., 2009). As little information is available in the literature concerning the expression of this protein, induction and purification data are presented in Figure 2. When induced in *E.coli* BL21 (DE3), the GST-MultiDsk protein is expressed in inclusion bodies, hence an atypical purification protocol is used (Wilson et al., 2012). Details of this protocol are in Chapter 2 (Section 2.2.3). Although contaminant cleavage products and dimers were observed, high yields of relatively pure GST-MultiDsk protein were reproducibly obtained (Figure 2, C and D). By retaining the purified GST-MultiDsk protein on glutathione-Sepharose, the beads could be used for the subsequent pulldown and enrichment of ubiquitylated proteins from H2K myoblast lysates.

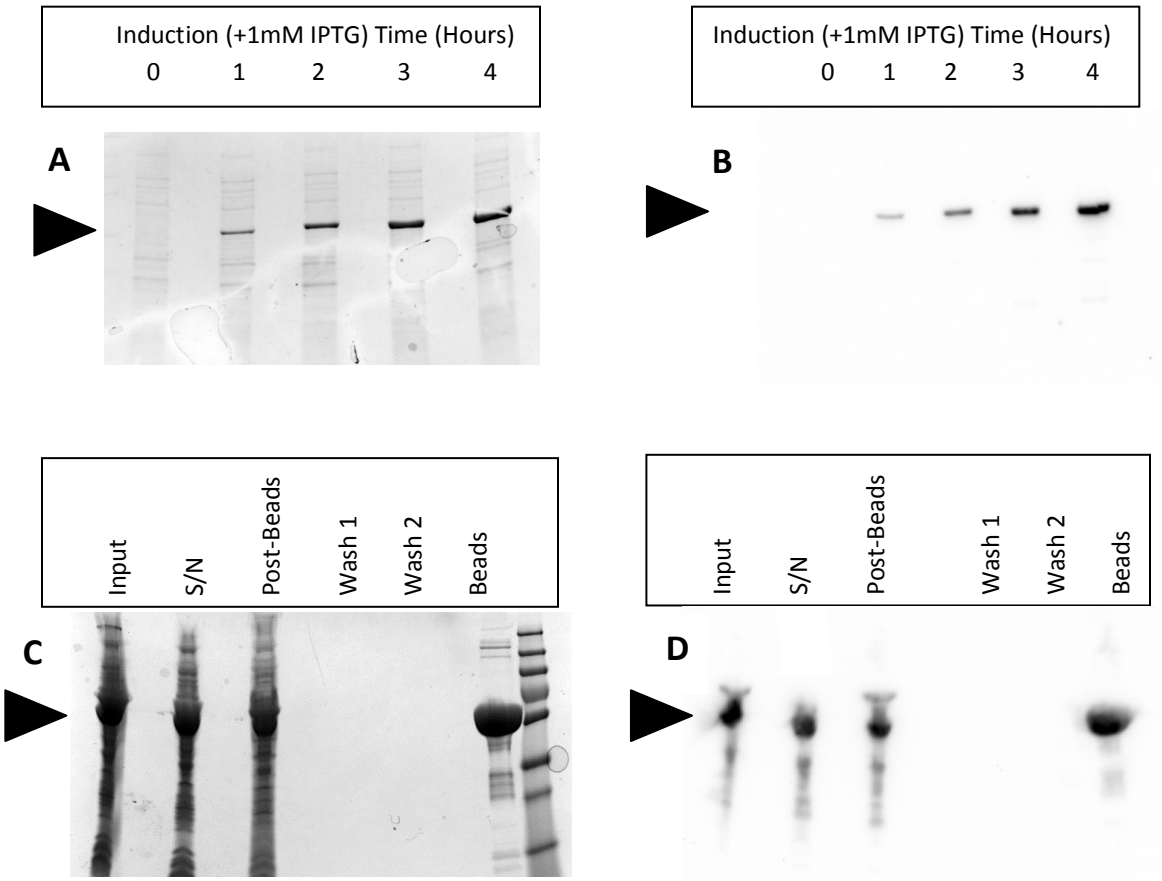

Figure 2: Coomassie stained gels (A and C) and anti-GST immunoblots (B and D) of MultiDsk induction and purification. The MultiDsk (arrowheads) protein is rapidly induced to sufficiently high levels within 3 hours at 37°C (A and B) and migrates as a band at approximately 60kDa. Purification of the MultiDsk protein yields a large amount of full-length protein with some smaller cleavage products (D) and larger bands that migrate at approximately 130kDa (C).

Next, the ability of the GST-MultiDsk protein to specifically enrich ubiquitylated proteins from H2K myoblast lysates was tested. To examine the effect of background binding or non-specific pulldown of proteins, unconjugated glutathione-Sepharose was used as a control for these experiments and all subsequent enrichments. The presence of the MultiDsk protein enabled the enrichment of ubiquitylated proteins from H2K myoblast lysates, with no non-specific pulldown of ubiquitylated or anti-GST immunoreactive proteins mediated by the unbound glutathione-Sepharose (Figure 3). For a full or complete enrichment of ubiquitylated proteins, one would expect to see a smear of immunoreactivity in the pellet lane of the MultiDsk pulldown upon blotting with an anti-ubiquitin antibody. However, this is not observed in the data presented here. That there is enrichment is evident: a comparison of the two treatments reveals a reciprocal shift of immunoreactivity from the supernatant to the pellet lanes in the presence of MultiDsk protein that is not observed for glutathione-Sepharose alone. Therefore, the lack of a regular smear may be due to the anti-ubiquitin antibodies used rather than incomplete enrichment, with other, lower bands being below the detection limit of the system. In support of this, the same banding pattern is observed in the supernatant lanes of the anti-ubiquitin western blots shown in Figure 5, indicating this is a reproducible result of the anti-ubiquitin antibody used. Furthermore, successful anti-ubiquitin antibodies are notoriously hard to generate, and this is why alternative methods for the detection of ubiquitin, such as tagging with HA, are commonly used in the literature (Love et al., 2013). Nonetheless, despite the inherent limitations of detection, one can conclude that the GST-MultiDsk fusion protein elicits a specific enrichment of ubiquitylated proteins from H2K myoblast lysates, as is reported for yeast extracts (Wilson et al., 2012).

4.2.3 Y890 Phosphorylation is Linked to the Ubiquitylation of β-Dystroglycan

Having established the use of the GST-MultiDsk fusion protein as a method for enriching ubiquitylated proteins, it was now possible to test the hypothesis that the pY890 form of β-dystroglycan is ubiquitylated. H2K myoblasts were incubated with Sepharose-bound MultiDsk or glutathione-Sepharose alone and the supernatant and pellet fractions were immunoblotted with MANDAG2 and 1709. As shown in Figure 4, western blotting for the pY890-modified form of β-dystroglycan reveals the presence of a large band with the same electrophoretic mobility as the doublet observed in the previous internalization assays (Chapter 3, Figures 5 and 6). As this band is only present in the pellet fraction of the GST-MultiDsk fusion protein pulldown, one can conclude that it is a ubiquitylated form of β-dystroglycan that has been enriched. The absence of such a band, or indeed

any bands, in the pellet fraction of the control pulldown strengthens the notion that this is a specific pulldown of a ubiquitylated species of β-dystroglycan. Furthermore, the lack of observable bands in the pellet fractions upon detection of the unmodified form of β-dystroglycan suggests with MANDAG2 that ubiquitylation is exclusively coupled to the phosphorylation of Y890 (Figure 4). This is expected, given that forms of β-dystroglycan with electrophoretic mobilities slower than that of the full-length protein were only observed on western blots for the pY890-modified form of the protein previously (Chapter 3, Figures 5 and 6).

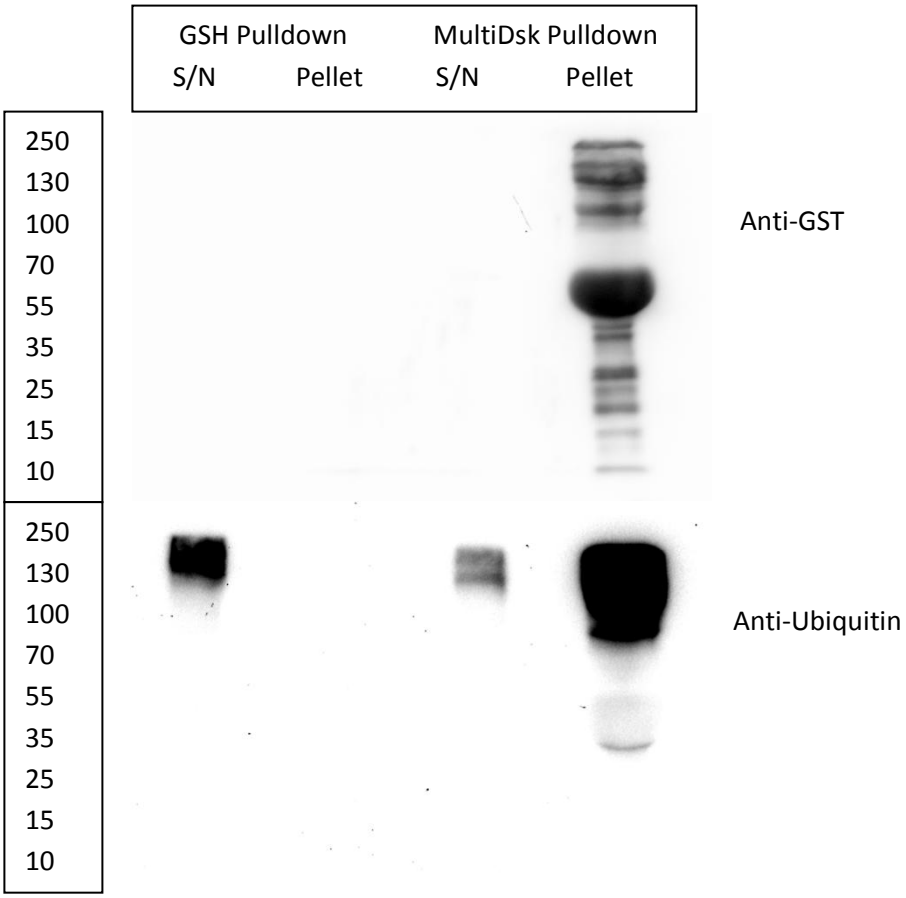

Figure 3: Control experiments for the MultiDsk pulldown and ubiquitin enrichment of H2K myoblast lysates. Glutathione-Sepharose alone does not enrich ubiquitin nor any other GST-containing proteins. By comparison, pulldown with the MultiDsk protein bound to glutathione-Sepharose causes a significant enrichment of ubiquitylated proteins. The bands with a slower and faster electrophoretic mobility than the GST-MultiDsk fusion protein (approximately 60kDa) probably represent dimers and cleavage products respectively.

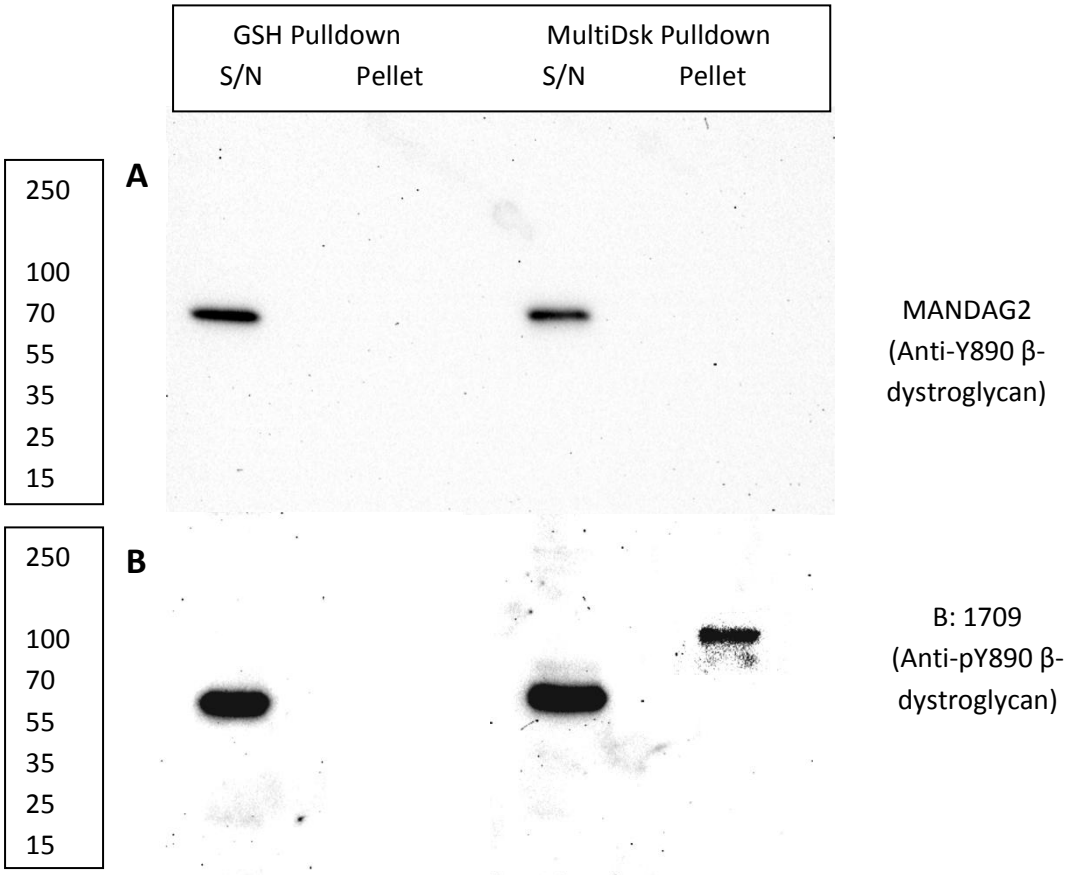

Figure 4: Glutathione-Sepharose and GST-MultiDsk pulldowns of H2K myoblasts. Supernatant and pellet samples were separated by SDS-PAGE and western blotted for pY890-modified β-dystroglycan (1709, B) or the unphosphorylated counterpart (MANDAG2, A).

The hypothesis that Y890 phosphorylation and the ubiquitylation of β-dystroglycan are coupled was further tested by means of reciprocal immunoprecipitation and detection. In this instance, the pY890-modified form of β-dystroglycan was immunoprecipitated from H2K myoblast lysates and detected with anti-ubiquitin immunoblotting (Figure 5). Immunoprecipitation in the absence of 1709 antibody and western blotting with 1709 were used as controls for the pulldown. The presence of a band in Figure 5, specifically enriched by 1709 pulldown, with the same electrophoretic mobility as that in the reciprocal blot (Figure 4) is detected upon western blotting for ubiquitin. The presence of this band is difficult to discern in the 1709 control blot due to spurious IgG heavy chain reactivity. However, that enrichment has occurred is clear when one compares the absence of immunoreactive bands in the control pellet lane of both the 1709 and anti-ubiquitin

blots. As it was possible that the enriched band detected on the anti-ubiquitin blot was an artefact of secondary antibody detection (possibly due to limited cross-reactivity for rabbit IgG heavy chain), an additional control blot was performed using only the same anti-mouse IgG. The lack of immunoreactivity on this blot (Figure 5, C) strongly suggests that the band observed on the anti-ubiquitin immunoblot is not an experimental artefact and does represent ubiquitylated β-dystroglycan. Thus, the hypothesis that Y890 phosphorylation and ubiquitylation are linked is not disproved by this experiment and together the reciprocal pulldowns provide strong evidence that this is indeed case.

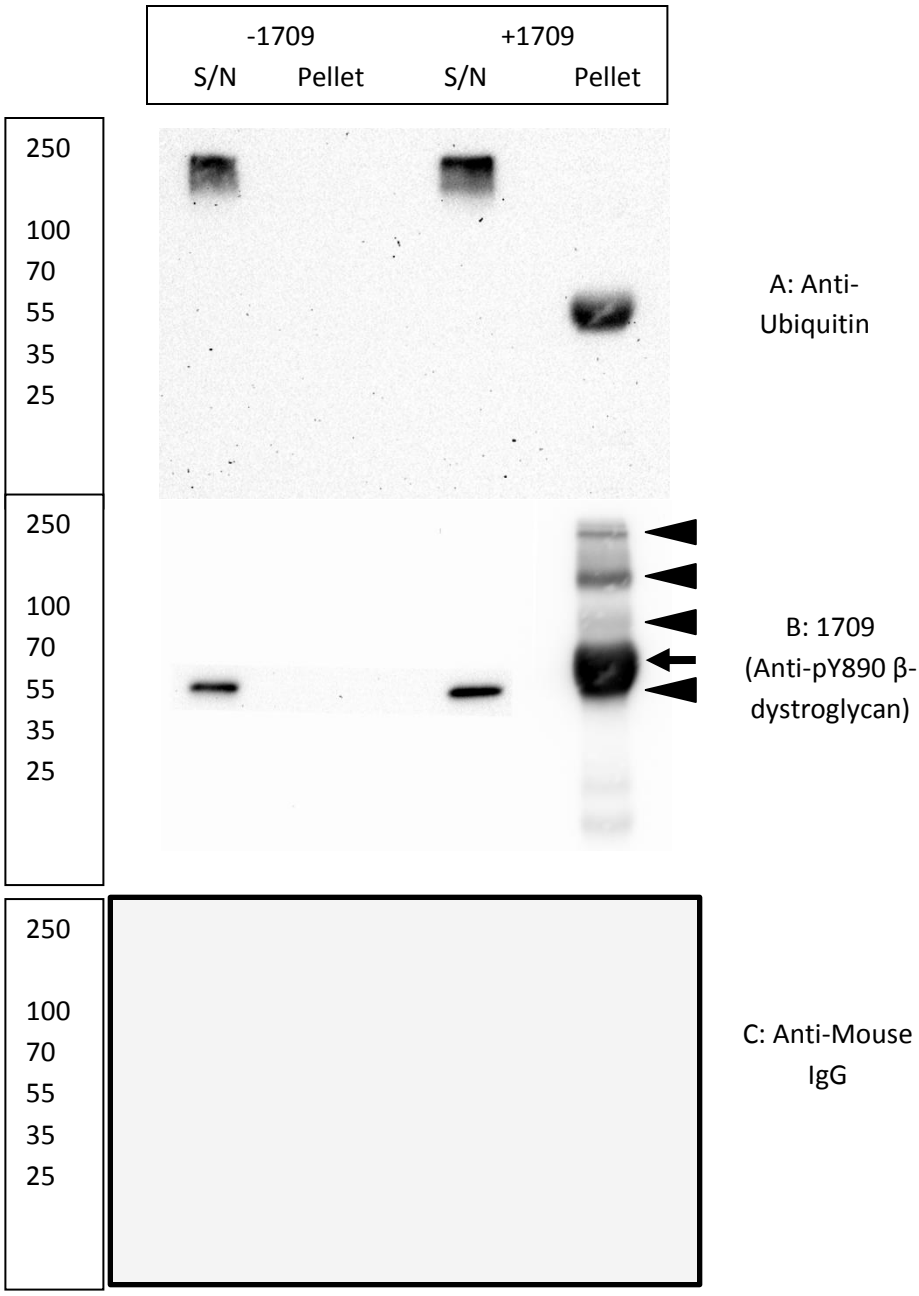

Figure 5: Immunoprecipitation of pY890-modified β-dystroglycan from H2K myoblasts. Western blots of lysates immunoprecipitated with 1709 and with protein A beads alone (See Chapter 2, Section 2.2.3) and probed with anti-ubiquitin (A), 1709 (B) or anti-Mouse IgG (C). Arrowheads represent forms of pY890-modified β-dystroglycan, whereas the arrow represents immunoreactivity due to rabbit IgG chains.

4.2.4 Identification of the Ligase Responsible for the Ubiquitylation of β-Dystroglycan

Having established that β-dystroglycan could be ubiquitylated, it was of interest to identify the ligase responsible next. Fortunately, two likely candidates for this role were available: the E3 ubiquitin ligases Nedd4 and Nedd4L. Nedd4 and Nedd4L are members of a family of HECT domain ubiquitin ligases that includes the yeast essential protein Rsp5 (Yang et al., 2010). Nedd4 and Nedd4L are closely related, owing to a gene duplication event, and possess a similar overall domain organization (Figure 6). WW domains 1 and 3 of Nedd4 and domains 3 and 4 of Nedd4L have been previously shown to bind the cytoplasmic domain of β-dystroglycan *in vitro* and there is a strong conservation of key residues both between domains and between species (Pirozzi et al., 1997 ; Yang et al., 2010). A previous yeast two-hybrid screen in the Winder lab also identified Nedd4L as a potential binding partner of the cytoplasmic tail of β-dystroglycan (Jane Illsey, PhD Thesis, 2001). Data from phage library screens had also identified the consensus targets of these WW domains and, with the exception of the first WW domain of Nedd4, these all preferentially bind canonical WW domain target motifs: specifically, LPxY and PPxY (Gary Bader, personal communication). Figure 7 shows the predicted target motifs of each WW domain, as well as the degree of degeneracy, and phylogenetic relation of these WW domains to each other. The cytoplasmic domain of β-dystroglycan contains several of these motifs, and any or several of these may be bound by one or multiple WW domains of these proteins (Ibraghimov-Beskrovnaya et al., 1992 ; Chen et al., 1995 ; Kay et al., 2000 ; Illsey et al., 2002).

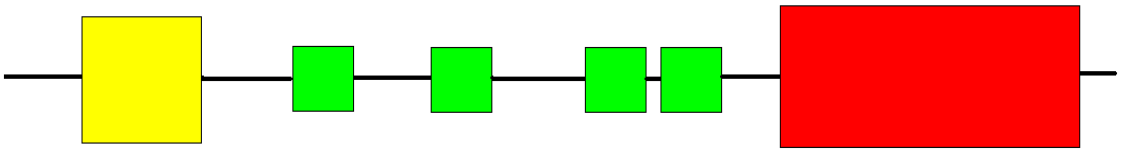

Figure 6: The general domain organization of Nedd4 and Nedd4L: C2 domain (yellow), WW domains (green), HECT domain (red). Figure not drawn to scale.

As multiple binding sequences could be identified within β-dystroglycan, it was necessary to use a method that allowed the visualization of specific binding sequences. To this end, CelluSpots™ peptide arrays representing the entire cytoplasmic domain of β-dystroglycan in 15-residue sections with a single residue step between spots were purchased from Intavis. pUC18 vectors expressing the separate WW domains as recombinant fusion proteins with GST and 6xHis tags were provided as a generous gift (Haiming Huang, Siddhu Lab). Following bacterial expression and purification, elution fractions containing the largest amounts of protein, as judged by Coomassie staining and spectrophotometry, were pooled and used for subsequent binding experiments with peptide arrays. Figure 8 contains two elution profiles of the second WW domain of Nedd4L. These images are representative of all WW domains purified in this study in that a high (approximately 50% of total protein) level of cleavage is apparent, with equally dense bands migrating at the masses corresponding to the uncleaved fusion protein (approximately 35kDa) and the GST fusion tag alone (approximately 30kDa). Despite several attempts to rectify the problem, this phenomenon was uncontrollable, and most likely represents an inherent instability of these particular fusion proteins. For further information on the purification of these fusion proteins, please consult Section 2.2.2.

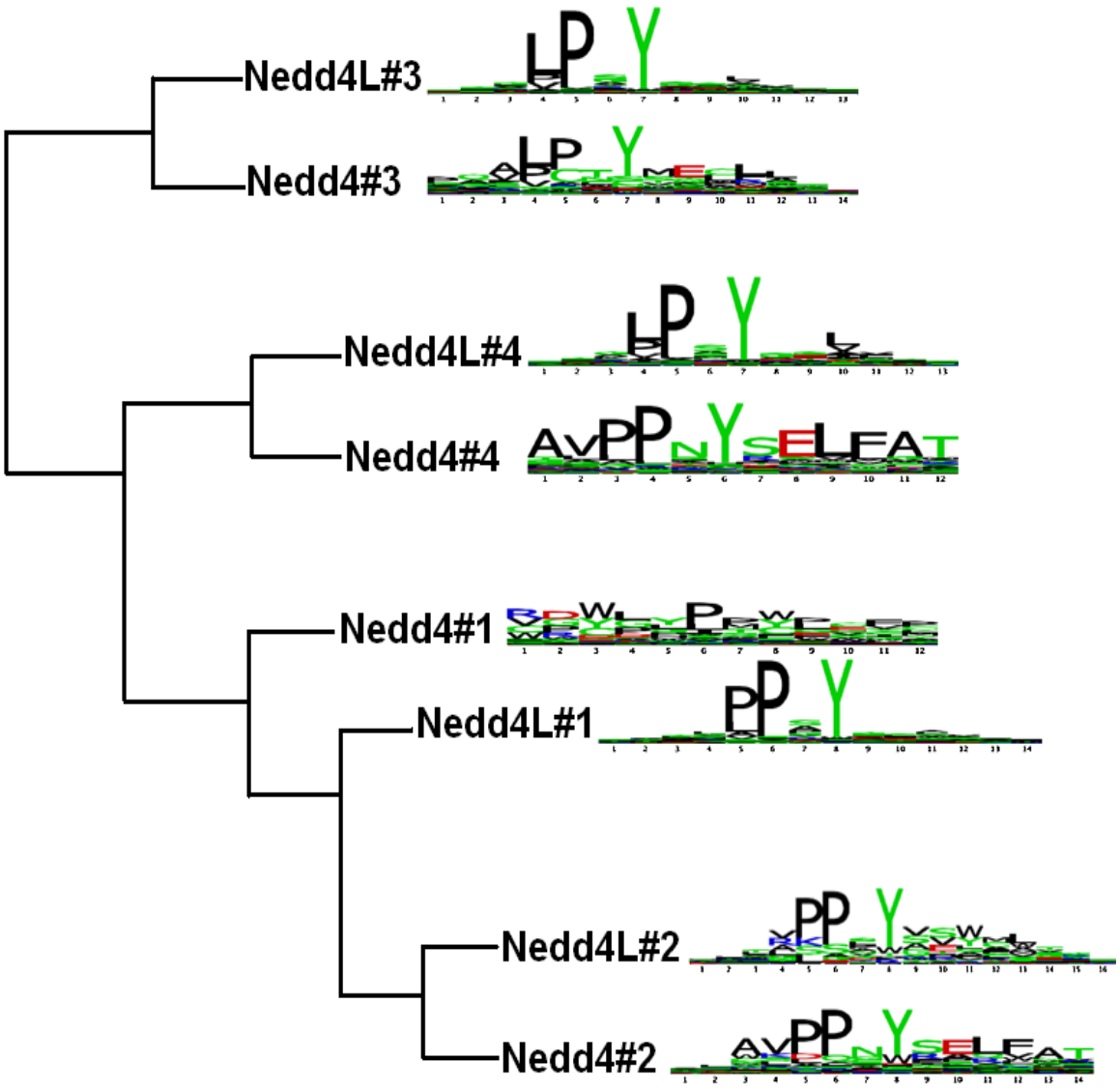

Figure 7: A phylogenetic tree of the WW domains of Nedd4 and Nedd4L with the target sequences, as determined by phage display screening depicted. The tree is not drawn to scale and all data is generously provided by Gary Bader (personal communication).

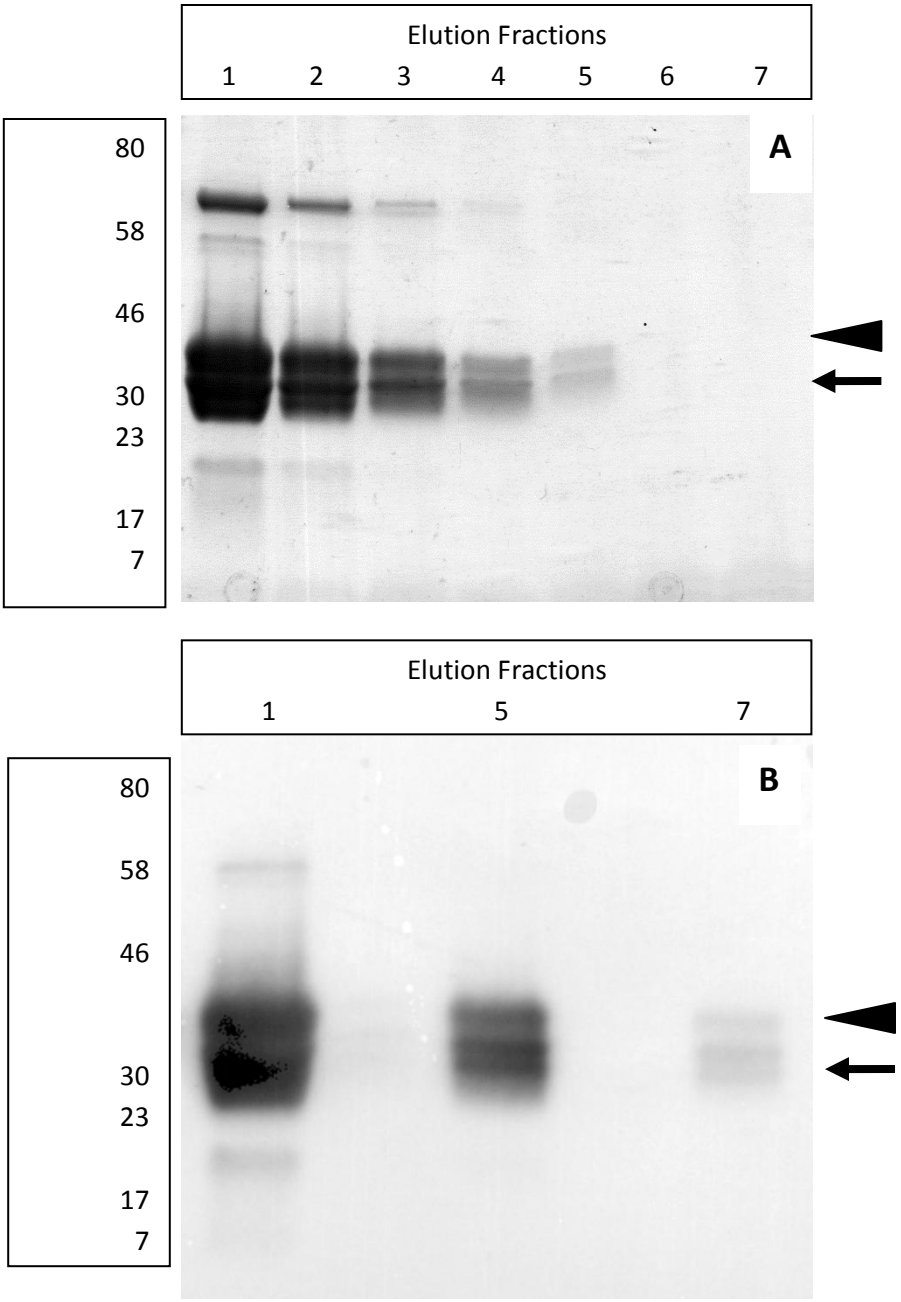

Figure 8: Representative elution profiles of a GST-WW domain fusion protein: (A) A Coomassie stained gel of the elution fractions and (B) An anti-GST immunoblot of elution fractions 1, 5 and 7. On both the gel and the blot the presence of two bands with electrophoretic mobilities corresponding to approximately 35 and 30kDa is apparent. These bands correspond to the full-length fusion protein (arrowheads), and the GST tag alone (arrows). The spurious bands with electrophoretic mobilities of approximately 60 and 70kDa are presumed to be dimers, whereas the fastest migrating band is presumably a cleavage product.

After purification, the recombinant WW domain proteins were loaded onto peptide arrays at a concentration of 20µg/ml. Owing to the large amount of cleavage, and as a control, purified GST protein alone was also loaded onto an array at the same concentration. Following the incubation with recombinant protein, the arrays were washed and immunoblotted with anti-GST. Figure 9 contains images of the arrays after exposure with ECL solution, with the detected binding sequences displayed underneath. Unfortunately, as is evident from comparison with the GST control, there was a large amount of GST-dependent binding for all experiments. Why this is the case is uncertain as previous experiments of a similar nature have failed to detect any binding of GST to the cytoplasmic domain of β-dystroglycan (Rentschler et al., 1999). Nonetheless, any binding to the motif EGKGSR was excluded from further analysis, owing to the clear binding to this motif mediated by GST alone (Figure 9). In spite of this technical difficulty, WW domains 1 and 2 of Nedd4L also exhibited separate binding to another motif within the cytoplasmic domain, LEDQATFIKKGVPI (Figure 9). Although this motif is not a typical WW domain target (Kay et al., 2000 ; Illsey et al., 2002), and is not in agreement with the target motif predicted by phage display screening (Figure 7), the absence of any binding to this motif by GST protein suggests that this motif is specifically bound by these WW domains *in vitro*.

One should also note that WW domains 1 and 2 of NEdd4 also exhibit some weaker, less consistent binding to this motif (Figure 9). This is unsurprising, given the close phylogenetic relationship of these domains (Figure 7). However, this binding was deemed too weak or inconsistent to merit further investigation. Whether this is due to the nature of the experimental system, transient binding by the WW domains, or a combination of both factors remains unresolved.

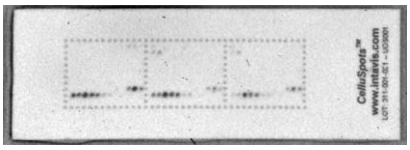

Nedd 4 WW domain #1: EGKGSR

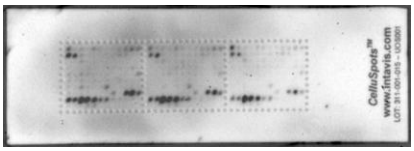

Nedd4L WW domain #1: LEDQATFIKKGVPI, EGKGSR

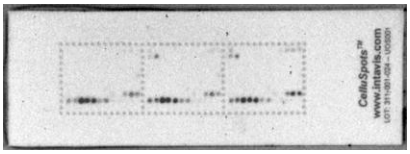

Nedd 4 WW domain #2: PMEGKGSR

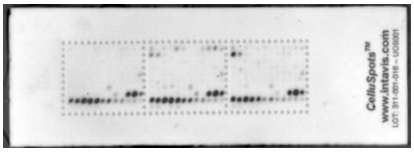

Nedd4L WW domain #2: LEDQATFIKKGVPI, EGKGSR

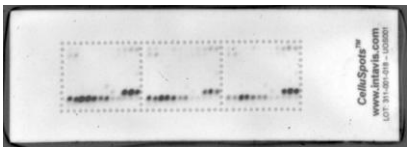

Nedd4 WW domain #3: EGKGSR

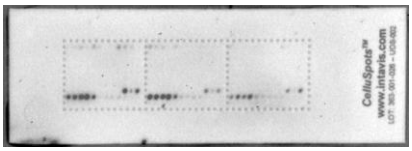

Nedd4L WW domain #3: EGKGSR

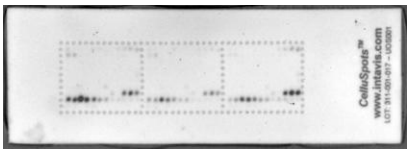

Nedd4 WW domain #4: EGKGSR

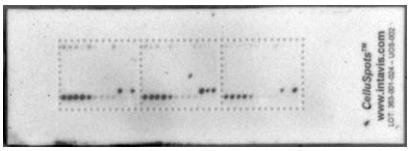

Nedd4L WW domain #4: EGKGSR

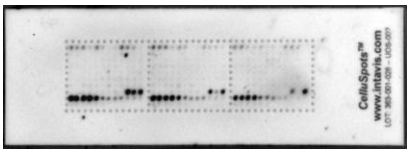

GST: EGKGSR

Figure 9: Peptide array images with the corresponding consensus binding sequences underneath. Peptide arrays were loaded with 20µg/ml of fusion protein and immunoblotted with anti-GST. Each box on the arrays represents a repeat unit, thus all binding sequences are the results of triplicate experiments.

To substantiate these findings, it was necessary to examine if this interaction was also true in the context of H2K myoblasts. Owing to the limited availability of Nedd4L antibodies, an antibody with cross-reactivity to Nedd4 was used. Unfortunately, this antibody was also raised in the same species as 1709, the antibody used to detect the pY890-modified form of β-dystroglycan, so the hypothesis of an interaction with the pY890-modified form could not be tested easily. Since the proposed binding site for Nedd4L was outside of the c-terminal residues of β-dystroglycan, it was assumed that binding of the ligase may not be strictly dependent on phosphorylation. Furthermore, whilst the data so far had suggested a link between Y890 phosphorylation and ubiquitylation, there was nothing to suggest that phosphorylation was causative of Nedd4L binding or subsequent ubiquitylation. Thus, immunoprecipitation of β-dystroglycan from H2K myoblasts with MANDAG2 was performed, with the view that an interaction with Nedd4L could still be tested in this manner. Despite a significant pulldown and enrichment of β-dystroglycan, no Nedd4L protein was detected in the pellet fraction upon western blotting with anti-Nedd4/4L (Figure 10). From the high levels of immunoreactivity in the supernatant fractions one can conclude that Nedd4 and Nedd4L are expressed in H2K myoblasts, but the data from this experiment suggest that the interaction of Nedd4/4L with the unmodified form of β-dsytroglycan is not significant *in vivo*.

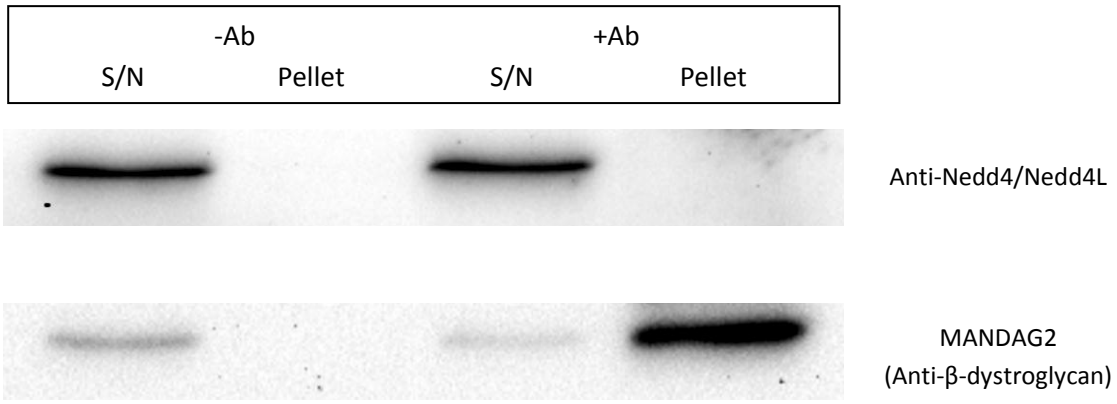

Figure 10: Immunoprecipitation of unmodified (non-pY890) β-dystroglycan from H2K myoblasts. Lysates were immunoprecipitated with or without MANDAG2 and the supernatant and pellet fractions were separated on SDS-PAGE gels and western blotted with MANDAG2 or Anti-Nedd4/Nedd4L.

The apparent binding of the WW domains to the cytoplasmic domain of β-dystroglycan *in vitro* could represent an artifact of the experimental system used: the presentation of this domain as 15 residue peptides, out of the context of flanking residues found in the full amino acid sequence, may permit binding that is not usually possible due to steric or energetic barriers. Similarly, the apparent absence of an interaction *in vivo* could be attributed to a dependence on Y890 phosphorylation for recruitment and binding of the Nedd4L protein. To address the former argument, and to further test the hypothesis that Nedd4L binds to β-dystroglycan, an alternative *in vitro* approach was used. The cytoplasmic domain of β-dystroglycan was expressed as a recombinant protein in *E. coli* BL21(DE3) and purified for use in a far western blot with the GST-WW domain fusion proteins of Nedd4L. As shown in Figure 11, the cytoplasmic domain of β-dystroglycan could be expressed and purified as a relatively pure protein, with minor contaminants and degradation. However, after resolution on SDS-PAGE gels and far western blotting, this protein was not bound by any of the WW domains of Nedd4L including domains 1 and 2, which had both been previously shown to bind to a specific motif on the peptide arrays (Figure 9). Instead, presumably through non-specific or spurious interactions, the GST-WW domain fusion proteins bound to residual, contaminant proteins present in the purified, cytoplasmic β-dystroglycan samples. Hence, given the lack of any interaction with the LEDQATFIKKGVPI motif in the context of the entire cytoplasmic domain, these data collectively suggest that Nedd4L does not bind β-dystroglycan, and may not be the ligase responsible for its ubiquitylation.

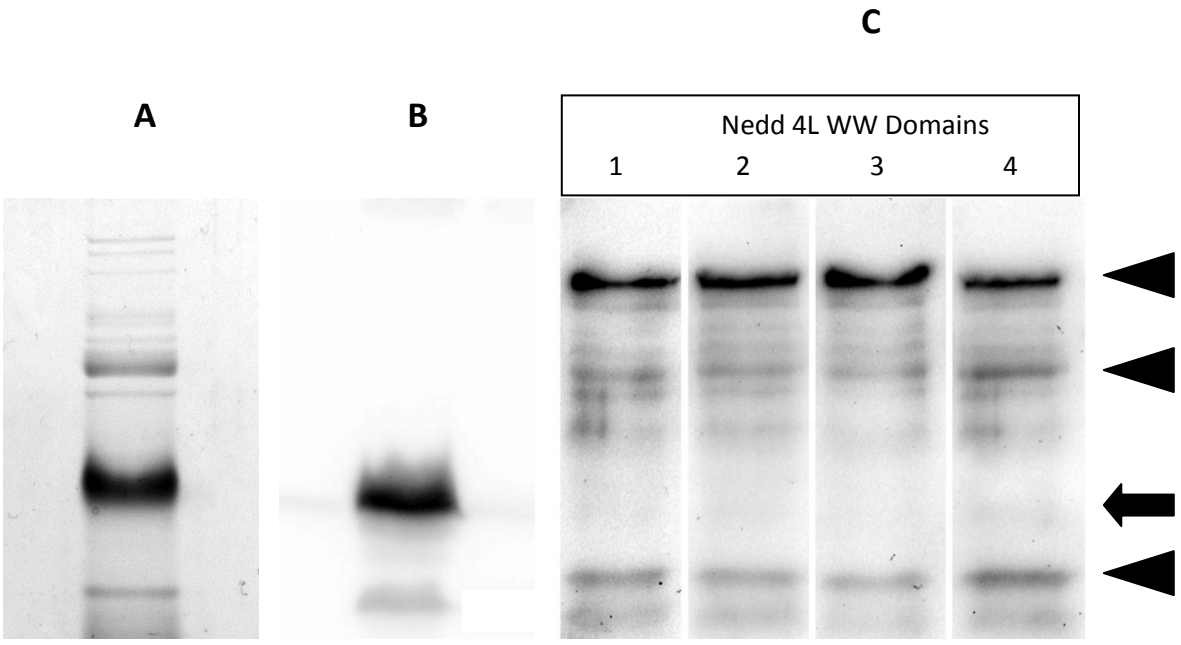

Figure 11: Purification of the cytoplasmic domain of β-dystroglycan and far western blots with the WW domains of Nedd4L. (A) A coomassie stain of the purified cytoplasmic domain of β-dystroglycan. Some contaminating proteins are clearly present, but the cytoplasmic domain has a relatively higher yield. (B) Western blot of the cytoplasmic domain of β-dystroglycan with MANDAG2. A large band with the expected electrophoretic mobility is observed, confirming the observations of (A), as well as several bands with a faster electrophoretic mobility. These faster, immunoreactive bands are presumably cleavage products. (C) Far western blots of the cytoplasmic domain of β-dystroglycan with the GST-fusion, WW domains 1-4 of Nedd4L and anti-GST. Despite high levels of non-specific binding (arrowheads), no immunoreactivity at the expected position of the cytoplasmic domain of β-dystroglycan (arrow) is observed.

4.3.1 Discussion: Establishing the Use of the MultiDsk Protein

Initial attempts to transfect H2K myoblasts with a plasmid containing the HA-ubiquitin fusion gene, with the aim of using affinity purification to enrich the cellular pool of ubiquitylated proteins, were unsuccessful. The expression of HA-tagged ubiquitin, as well as HA-tagged forms of other post-translational modifications, is a procedure that is routinely used in the literature (Yurchenko et al., 2006 ; Rabut et al., 2008 ; Cai et al., 2010 ; Love et al., 2013), and exactly why this approach failed with H2K myoblasts is uncertain. Electroporation of H2K myoblasts with the HA-ubiquitin construct resulted in abnormally high levels of cell death (data not shown), which are normally attributable to excess salt or a volume of DNA in the electroporation mixture larger than 10% (v/v) (Neon™ Transfection System User Manual, Invitrogen). However, attempts to desalt or reduce the volume of DNA used were unsuccessful as evidenced by persistent cell death or low transfection efficiency (data not shown). The Neon™ transfection system is successfully used elsewhere in this thesis, so why it does not give adequate transfection of H2K myoblasts with HA-ubiquitin remains uncertain. Fortunately, another method of ubiquitin enrichment became available: the MultiDsk system.

The recombinant MultiDsk protein relies on the activity of the c-terminal ubiquitin binding (UBA) domain of the *S. cerevisiae* protein Dsk2, which binds both ubiquitin and polyubiquitin chains with a relatively high affinity (Raasi et al., 2005). The MultiDsk protein consists of five Dsk2 UBA domains in tandem, separated by 8-amino acid flexible linkers (Wilson et al., 2012). In a manner similar to another recombinant protein comprised of 4 UBA domains in tandem, the commercial TUBE protein (Hjerpe et al., 2009), the MultiDsk protein both binds ubiquitylated proteins and protects these proteins from deubiquitylation and proteasomal degradation, presumably through steric hindrance of the enzymes responsible (Wilson et al., 2012). Furthermore, the MultiDsk protein does not exhibit any non-specific interactions with non-ubiquitylated proteins, which is a common technical problem for GST-UBA fusion proteins (Kang et al., 2007 ; Wilson et al., 2012). Fortunately, both the tertiary structure and key residues of the ubiquitin protein are well conserved between species and even kingdoms, making the purification of ubiquitylated proteins from a murine cell line with an *S. cerevisiae* protein domain possible (Goldstein et al., 1975 ; Vijay-Kumar et al., 1987).

Due to the presence of an N-terminal GST tag, both the purification of the MultiDsk protein from *E.coli* BL21(DE3), and the pull down of ubiquitylated proteins from H2K myoblast lysates, were possible (Figures 2 and 3). Importantly, control pull downs with glutathione-Sepharose did not result in any enrichment of ubiquitylated proteins (Figure 3) or the forms of β-dystroglycan studied in this

thesis (Figure 4). Whilst little information concerning the MultiDsk protein was available in the literature at the time of these experiments, the data presented here, along with successful preliminary results from other labs, confirms its use in the specific enrichment of ubiquitylated proteins. Although not tested in these experimental conditions, pull downs with the GST-MultiDsk fusion protein are not thought to result in the enrichment of sumoylated or neddylated proteins (Marcus Wilson, personal communication). Together, these data suggest that the GST-MultiDsk fusion protein can be used to specifically enrich the pool of ubiquitylated proteins present in H2K myoblasts.

4.3.2 The Link Between Y890 Phosphorylation, Ubiquitylation and Internalization

Having established a method to enrich ubiquitylated proteins from H2K myoblasts, it was then possible to test the hypothesis that phosphorylation of Y890 was linked to ubiquitylation. Western blots of GST-MultiDsk and GSH control pull downs of H2K myoblast lysates with antibodies against the pY890-modified and unmodified forms of β-dystroglycan reveal a striking difference; Y890 phosphorylation is linked to the presence of a slowly migrating, presumably ubiquitylated, band with a mass of approximately 55kDa (Figure 4). That this band represents a ubiquitylated form of pY890-modified β-dystroglycan is confirmed by the detection of the same, or very similar, protein species in a reciprocal pull down experiment (Figure 5). Furthermore, the inability to detect this band with MANDAG2, akin to the western blots of unmodified β-dystroglycan presented in chapter 3 (Figures 5 and 6), suggest that the ubiquitylation event is linked to Y890 phosphorylation. The inability to detect β-dystroglycan with an antibody against the unphosphorylated form of the protein after MultiDsk enrichment does not necessarily preclude the idea that it can be ubiquitylated, as this form of the protein may be below the detection limits of the system. However, the data presented here certainly suggest a strong link between the events of Y890 phosphorylation and ubiquitylation.

These findings lend themselves to the natural question: is ubiquitylation responsible for the higher bands observed on western blots of internalized, pY890-modified β-dystroglycan? Unfortunately, experiments designed to directly address this question were inconclusive and could not be fully developed due to time constraints. However, it is possible to speculate that this is indeed the case. To begin, both the slowly migrating bands described in the internalization assay and the ubiquitylated bands reported in this chapter all migrate at the same position, which equates to approximately 55kDa. Whilst the bands observed previously clearly migrated as a doublet (Chapter 3, Figures 5 and 6), the bands observed in

Figures 4 and 5 do not appear to do so. However, in both western blots, there is the presence of faint, additional immunoreactivity, suggesting that these bands may in fact be unresolved doublets. This may reflect variation in the SDS-PAGE gel system used between experiments and so, one can not exclude the idea that these bands are equivalent species of β-dystroglycan. Additionally, as mentioned in the introduction to this chapter, monoubiquitylation is linked to the internalization of several surface membrane proteins (Karlson et al., 2006 ; Kumar et al., 2007 ; Hayes et al., 2011). Given that full-length, pY890-modified β-dystroglycan migrates at an approximate mass of 43kDa on SDS-PAGE gels, one would conclude that the electrophoretic mobility shift observed in these data is due to modification with a single ubiquitin. Hence, given the potential involvement of monoubiquitylation with the internalization of β-dystroglycan, one could speculate that the approximately 55kDa band observed in these experiments is related to those observed in the internalized fractions earlier (Chapter 3, Figures 5 and 6). Although a conclusive answer to this question will ultimately require further experiments, these data certainly form a strong basis for future enquiry.

4.3.3 The Proposed Interaction of β-Dystroglycan and Nedd4/Nedd4L

Having established that β-dystroglycan is ubiquitylated, it was of interest to determine the E3-ubiquitin ligase responsible. Fortunately, several lines of evidence made the HECT domain ligases Nedd4 and Nedd4L promising candidates. Both proteins are expressed in murine skeletal muscle and satellite cells, and are both thought to be involved in both the formation of the pre-synaptic membrane of neuromuscular junctions and the response to skeletal muscle atrophy (Yang et al., 2010 ; Nagpal et al., 2012). Using a dual-specificity antibody, the presence of either one, or both, of these proteins in H2K myoblasts was also verified by western blot (Figure 8). Both these ligases are predicted to bind to their substrates by one or several of the four, closely related WW domains that each protein possesses. These domains are typically thought to bind PPXY and LPSY motifs present in membrane proteins, although this idea has been questioned recently (Lin et al., 2008 ; Yang et al., 2010 ; Hayes et al., 2011). Nonetheless, the cytoplasmic domain of β-dystroglycan is a candidate target as it contains two PPxY motifs, as well as several closely related sequences, all of which could be the binding target of a WW domain. In support of this, several WW domains of these proteins have been demonstrated to bind polyproline regions of the cytoplasmic domain of β-dystroglycan *in vitro* (Pirozzi et al., 1997) and phage display screening data indicates an interaction of these WW domains with PPXY or LPXY motifs (Gary Bader, personal communication). Hence, an interaction

between the WW domains of Nedd4 and Nedd4L with β-dystroglycan was examined in closer detail.

Unfortunately, the binding data from peptide arrays representing the cytoplasmic domain of β-dystroglycan chiefly reveals the presence of a binding site for GST, which was used as a fusion protein for the purified WW domains used in this study (Figure 9). The binding motif for GST, EGKGSR, and any binding of GST to the cytoplasmic domain of β-dystroglycan have not been reported in previous studies using similar experimental approaches (Suzuki et al., 1994 ; Chung et al., 1999 ; Rentschler et al., 1999 ; Russo et al., 2000). Given that the proteins used to probe the arrays in these experiments were free from unexpected contaminants (Figure 8), one can conclude that the apparent binding of GST represents an *in vitro* artefact, which is possibly the result of loading at too high a concentration. Indeed, a loading concentration of 20µg/ml was used due to the high (approximately 50%) levels of untagged WW domain protein present in the purified fractions. Future experiments of a similar nature may benefit from establishing concentrations of GST which do not give such prominent non-specific binding.

In spite of these technical difficulties, potential binding sites for the first and second WW domains of Nedd4L were detected using the peptide array approach (Figure 9). The binding site contains the consensus sequence LEDQATFIKKGVPI and is located between residues 783-796 of the Dag1 sequence (Ibraghimov-Beskrovnaya et al., 1992). Whilst this binding motif is very different from the motif predicted by phage display (Gary Bader, personal communication), as well as those typically reported in the literature (Yang et al., 2010), the presence of unusual, or non-canonical binding motifs for Nedd4L, which do not conform to the PPXY or LPSY consensuses, have been reported (Hayes et al., 2011). Thus, the motif identified could represent a novel binding site for these WW domains. Conversely, binding to this motif could represent an *in vitro* artifact, similar to that observed for GST (Figure 9), which highlights the importance of recognizing caveats associated with this experimental approach and the need for subsequent alternative experiments.

As the binding data generated by the peptide arrays could be biased by the presentation of the cytoplasmic domain as 15-residue peptides, which are out of the correct context of any surrounding sequence, alternative approaches to test the interaction between Nedd4L and β-dystroglycan were employed. Testing an interaction within the context of H2K myoblasts by co-immunoprecipitation is a favourable technique, as it permits examination within the context of the full sequence and any additional co-factors that may be involved in the putative interaction. Despite the successful immunoprecipitation of β-dystroglycan with MANDAG2, Nedd4L does not co-immunoprecipitate, suggesting that no direct or indirect interaction exists between these proteins (Figure 10). Ideally, one would test co-immunoprecipitation of Nedd4L with both the pY890-modified and

unphosphorylated forms of β-dystroglycan. However, due to limitations described in the results section, only an interaction with the unphosphorylated form could be tested. Arguably, testing the dependence of Nedd4L binding on Y890 phosphorylation might not be necessary, as the proposed binding site identified from the peptide array data is separated from Y890 by at least 100 residues that are predicted to be unstructured, due to a high proline content. Nonetheless, phosphorylation of Y890 may generate a binding site for additional scaffolding factors, which then recruit Nedd4L and permit binding to the motif identified in this study. Hence, especially in light of the proposed link between Y890 phosphorylation and ubiquitylation (Figures 4 and 5), the data generated by this approach does not fully resolve the question of whether Nedd4L binds β-dystroglycan, but suggest that this is not true for the unphosphorylated form of the protein.

Whilst testing the hypothesis that Nedd4L and β-dystroglycan interact in H2K myoblasts by co-immunoprecipitation was limited by antibody usage, it was possible to further verify the peptide array data with an additional *in vitro* experiment. A pinpoint vector containing the cytoplasmic domain of β-dystroglycan was expressed in BL21 (DE3) *E.coli* and purified by streptavidin chromatography. Due to the inherent instability of the cytoplasmic domain of β-dystroglycan when expressed in bacteria (Steve Winder, personal communication), it was only possible to obtain sufficiently high yields of protein together with the presence of several, unidentified contaminants (Figure 11, A). However, the purification of the cytoplasmic domain allowed the testing of the potential WW domain interactions by far-western blotting, in a manner similar to the approach used for the peptide arrays. This approach allows testing of the interaction with the predicted binding motif, LEDQATFIKKGVPI, but within the context of a more complete sequence. Despite successful detection of the purified cytoplasmic domain with MANDAG2 (Figure 11, B), which suggests that the cytoplasmic domain is amenable to protein binding after electroblotting, no specific binding is observed for any of the WW domains of Nedd4L. Thus, it is possible to conclude that neither Nedd4 nor Nedd4L directly binds to β-dystroglycan with a high level of specificity or affinity *in vitro*, which in turn makes it less likely that these are ligases responsible for the ubiquitylation of β-dystroglycan.

Nonetheless, it is not possible to dismiss an interaction between β-dystroglycan and either of these proteins, despite the data presented here strongly suggesting that no such interaction exists. As stated earlier, the phosphorylation of Y890, potentially along with the additional phosphorylations reported by Moraz et al., (2012) in response to internalization, may create a binding platform for a factor which recruits Nedd4 or Nedd4L. In support of this, a family of proteins termed arrestin related transporters (ARTs) have been identified in *S. cerevisiae*, which function as adaptor proteins for E3 ubiquitin ligases that modify plasma membrane

proteins (Lin et al., 2008). It is of particular interest that in Lin et al. (2008), ART1 binds to plasma membrane proteins and then recruits the WW domain containing E3 ubiquitin ligase Rsp5, which is the yeast homologue of Nedd4, via a PPXY motif. Hence, similar substrate adaptors could play a role in the ubiquitylation of β-dystroglycan by Nedd4 or Nedd4L. So, whilst a direct interaction between the WW domains of the Nedd4 and Nedd4L proteins and β-dystroglycan is unlikely, the possibility of an indirect interaction involving one or several adaptor proteins is worthy of future investigation.

4.3.4 Summary

The data presented in this chapter can be summarized as follows:

1. The pY890-modified and not the unphosphorylated form of β-dystroglycan is monoubiquitylated.
2. Monoubiquitylation of pY890-modified β-dystroglycan can explain the presence of additional protein species observed upon internalization of this protein.
3. The WW domains of the E3 ubiquitin ligases Nedd4 and Nedd4L do not directly interact with the unmodified cytoplasmic domain of β-dystroglycan, but may interact in the presence of post-translational modifications or adaptor proteins.

Chapter 5:

Phosphorylation of Y890 and the Endocytosis of β-Dystroglycan

5.1.1 Introduction

Having established that phosphorylation of Y890 is linked to the internalization (Chapter 3) and ubiquitylation (Chapter 4) of β-dystroglycan, it was of interest to examine where exactly in the cell this form of the protein traffics to. An understanding of which pathway(s) and endosomal compartments are involved in this process would give insights into how, as well as why, the internalization and ubiquitylation of pY890-modified β-dystroglycan occurs. Furthermore, an understanding of the endocytic routes and mechanisms associated with this process would enhance the current understanding of the pathology of DMD (and other dystrophic diseases), as well as increase the potential for therapeutic applications of this research. Hence, the work presented here focussed on understanding the internalization and endocytosis of pY890-modified β-dystroglycan.

5.1.2 The Co-localization of pY890-modified β-Dystroglycan with the Clathrin-mediated Endocytic Pathway

Returning to one of the key references for this thesis, Sotgia et al. (2003_a) describe the internal localization of pY890-modified β-dystroglycan, which is in agreement with the results presented in this thesis (see Chapter 3). pY890-modified β-dystroglycan is present in an internal membranous compartment (Sotgia et al., 2003_a), and the authors note a co-localization with compartments containing the transferrin receptor and early endosomal antigen 1 (EEA1), suggesting the presence of β-dystroglycan in early and recycling endosomes. From the co-localization of pY890-modified β-dystroglycan with these compartments, one could conclude that β-dystroglycan internalizes and recycles via the clathrin-mediated endocytic pathway described for the transferrin receptor, with sequential migration from clathrin- and rab5-positive vesicles, to rab5- and EEA1-positive tubulovesicular compartments, and finally to rab-11 positive vesicles (Harding et al., 1983 ; Mu et al., 1995 ; Trischler et al., 1999).

However, this conclusion is challenged by the existence of alternative pathways, which mediate the delivery of alternative cargoes to the same compartments used by the transferrin receptor. For example, BODIPY-LacCer (boron-dipyrromethene-lactosylceramide), a marker of lipid rafts (Marks et al., 2005), internalizes in a clathrin- and rab5-independent manner, but co-localizes with transferrin receptors in the early endosomal compartment (Sharma et al., 2003). Conversely, neuropilin 1 (NRP1) internalizes in a clathrin-dependent manner, but within ten minutes is transferred to an alternative, GM1-positive (monosialotetrahexosylganglioside) compartment due to the action of Transient Axonal Glycoprotein 1 (TAG1) (Dang et al., 2012). Hence, the co-localization with a particular set of compartments

during the endocytic process does not necessarily describe the mechanism of internalization of pY890-modified β-dystroglycan.

A further, criticism of the Sotgia et al. (2003_a) paper is that the overexpression of exogenous, alkaline phosphatase-tagged β-dystroglycan is used for the co-localization experiments described above. The levels of specific proteins and endocytic components can influence the mechanism by which a protein internalizes. For example, β1-integrin normally internalizes via a mechanism dependent on lipid-rafts and caveolin-1, which is activated downstream of c-Src activation (Sharma et al., 2005 ; Shi et al., 2008 ; Shi et al., 2010). However, clustering of β1-integrin, which is caused by the perturbation of protein levels, antibody cross-linking, changes in local cholesterol levels, or a combination of these factors, can also cause internalization (Sharma et al., 2005). Indeed, the internalization of the β subunit of the cholera toxin protein (ChTxB), a marker of the pathway used by β1-integrins, is dependent on an ability to cross-link multiple GM1 gangliosides (Singh et al., 2003). Hence, it is no surprise that modulating the levels of proteins may cause experimental artefacts that do not represent typical endocytosis and recycling. Therefore, in the context of overexpression, the endocytosis of β-dystroglycan described in Sotgia et al. (2003_a) could be altered and not represent the normal trafficking of the protein.

Unfortunately, beyond the findings of Sotgia et al., (2003_a), there is little information in the literature regarding the endocytosis of β-dystroglycan and as such, any endocytic mechanism may be involved in the internalization and trafficking of the protein. This work uses the H2Kb-tsA58 myoblast cell line as an experimental model, but H2K myoblasts have not been used previously for endocytic studies. Thus, it is unknown which endocytic pathways are active in this model and one can not suggest a likely pathway, or at least eliminate a non-existent pathway, on this basis. However, one can form tentative suggestions based on the findings of previous studies. For example, the presence of a caveolar-dependent endocytic apparatus is suggested by the predominantly sub-sarcolemmal localization and association of either caveolin-1 or caveolin-3 with known components of the endocytic pathway in mammalian myoblasts and skeletal muscle (Parton et al., 1994 ; Song et al., 1996 ; Parton et al., 1997).

Whilst the caveolins are thought to have structural roles within skeletal muscle, such as the biogenesis of t-tubules (Parton et al., 1997), there are plenty of examples of these proteins mediating typical caveolar-dependent endocytosis, suggesting that this pathway is present in H2K myoblasts (Parton et al., 2007 ; Hernández-Deviez et al., 2008 ; Cai et al., 2009; Hertzog et al., 2012). Although other endocytic pathways have not been studied in H2K myoblasts, the presence of early, late, recycling and lysosomal endosomes has been verified (Kaisto et al. 1999). Furthermore, endocytic proteins such as the transferrin receptor (Kaisto et al., 1999) and the flotillins (Volonte et al., 1999) are present in mature skeletal

muscle fibres suggesting that these pathways are also active, as one would expect from their ubiquitous nature (Pearse et al., 1976). Hence, whilst the clathrin-mediated endocytosis of pY890-modified β-dystroglycan in cell lines and muscle tissue is a possibility, whether it is the case for the internalization described in this thesis is uncertain.

5.1.3 Alterations to the Membrane within the Dystrophic State

Additional clues concerning the internalization of β-dystroglycan may instead be deduced from studies of the changes to muscle fibres that accompany the mdx/DMD disease state, as well as dystrophic pathologies in general. *Ex vivo*, *mdx* muscle fibres show an increased susceptibility to stretch-induced sarcolemmal breakage and *mdx* myotubes have a reduced stiffness, relative to their wildtype counterparts (Petrof et al., 1993 ; Pasternak et al., 1995). These changes are partnered by alterations to the cholesterol content of the fibre, which may represent a compensatory mechanism in DMD pathology. Indeed, electron micrographs of digitonin-labelled muscle fibres from DMD patients show an increase in sarcolemmal cholesterol levels with age (Fischbeck et al., 1983), and cholesterol depletion reduces the fatigue resistance of *ex vivo* muscle fibres in response to eccentric contraction, a feature typical of DMD and *mdx* pathology (Dellorusso et al., 2002 ; Sonnemann et al., 2009 ; Vega-Moreno et al., 2012). These changes, by themselves, may not be part of a cellular readjustment of endocytosis, but the notion that they would have no impact on endocytosis can be challenged.

Caveosomes are endocytic pit structures present at the surface membrane, which are decorated by caveolins and require cholesterol for correct formation and function (Chang et al., 1992 ; Rothberg et al., 1992 ; Rodal et al., 1999). When visualized by freeze-fracture electron microscopy, these structures are distinguishable from clathrin coated pits, owing to the distinct lattice formation that coats the latter structures (Larkin et al., 1986). Electron microscopic analysis of dystrophic chicken and DMD patient muscle fibres reveals an increase in both the number and size of caveosomes at the sarcolemma, as well as a loss of the normal I-band localization of these structures (Costello et al., 1979 ; Bonilla et al., 1981 ; Repetto et al., 1999). A possible explanation for this is an increase in the cholesterol content of the sarcolemma. Hence, changes to the cholesterol content of dystrophic sarcolemma may have an impact on caveolar-mediated endocytosis, with the formation of aberrant and mislocalized caveosomes as described above.

Given that endocytosis is altered or impaired in dystrophic pathology, one would expect to see causative links to the expression of endocytic proteins. In support of this hypothesis, caveolin-3 expression is increased in the fibres of DMD patients,

and caveolin-3 knockout mice exhibit a dystrophic phenotype (Repetto et al., 1999 ; Gazerro et al., 2010). Furthermore, other forms of endocytosis, which are dependent on cholesterol levels, but not clathrin or caveolae, may also be effected by the changes in the dystrophic sarcolemma (Shogomori et al., 2001 ; Kokuba et al., 2003 ; Glebov et al., 2006). Hence, in DMD pathology, where the loss of sarcolemmal proteins is associated with alterations to components of the endocytic machinery, one can suggest that these altered pathways may play a role in the internalization of β-dystroglycan.

The chief difficulty with this suggestion, at present, is the inability to discriminate between what is truly cause and effect in the aetiology of DMD and dystrophic pathologies in general. To take one of the arguments presented in Data Chapter 1 as an example: the changes in phosphorylation signalling that accompany dystrophic pathology could promote the internalization of β-dystroglycan, or could be a result of the loss of this protein, which scaffolds several kinases (Chockalingham et al., 2002 ; Oak et al., 2003 ; Spence et al., 2004 ; Sen et al., 2011). Similarly, changes to the sarcolemmal cholesterol content could promote the endocytosis of β-dystroglycan, or could be a mechanical response to the loss of the protein instead, such as the up-regulation of integrin expression (Cote et al., 2002 ; Allikian et al., 2004 ; Rooney et al., 2006 ; Sen et al., 2011 ; Liu et al., 2012). A pre-requisite for these altered pathways having a causative impact is the presence of β-dystroglycan in lipid rafts, as it is these, whether in caveolae clathrin-coated pits, or other vesicles, that are critically dependent on the cholesterol content of the plasma membrane.

In support of this there are reports of β-dystroglycan in cold, Triton-X-100 insoluble membrane fractions (Vega-Moreno et al., 2012), which is a common method of lipid raft purification (Shogomori et al., 2001 ; Sotgia et al., 2003_b), however similar experiments in both the Winder and other labs have produced a negative result (Steve Winder, personal communication). Furthermore, viruses that use α-dystroglycan as a surface receptor internalize in a cholesterol-dependent manner, but the presence of either α- or β-dystroglycan in lipid rafts has not been detected in cell lines that can be infected by these viruses (Kunz et al., 2003 ; Shah et al., 2006 ; Pasqual et al., 2011). Therefore, the argument for altered sarcolemmal cholesterol levels driving the internalization of β-dystroglycan in DMD pathology, or for endocytosis of this protein using lipid-rafts, is not without strong criticism.

5.1.4 The Interaction with Caveolin-3 and Dystrophic Pathology

Nonetheless, the contribution of endocytosis to the pathology of muscular dystrophies, including DMD, should not be overlooked. Mutations in caveolin-3 are associated with limb-girdle muscular dystrophy 1C, as well as several similar diseases affecting skeletal muscle (Gazerro et al., 2010) and can cause the mislocalization of several proteins, including components of the DGC (Herrmann et al., 2000 ; Sotgia et al., 2003_b ; Sotgia et al., 2003_c). In particular, the dysferlin-dependent repair response is critically dependent on the trafficking mediated by caveolin-3 (Hernandez-Davies et al., 2007 ; Cai et al., 2009). In addition to having a role in endocytosis, Caveolin-3 multimers provide a sub-sarcolemmal scaffold for several proteins (Song et al., 1996 ; Hezel et al., 2010 ; Whiteley et al., 2012). Importantly, the levels of caveolin-3 mRNA and protein are increased in the *mdx* mouse disease state (Vaghy et al., 1998), which, when partnered the altered phosphorylation state of dystrophic muscle tissue, could influence the internalization of this protein, as is the case for functionally equivalent caveolin-1 in other tissues (Parton et al., 1994 ; Aoki et al., 1999 ; Pelkmans et al., 2002). Indeed, the internalization of β1-integrin by caveolin-1 is dependent on phosphorylation of both proteins, downstream of c-Src activation (Sharma et al., 2005 ; Shi et al., 2008), and several of the kinases associated with β-dystroglycan regulate caveolar-mediated endocytosis (Pelkmans et al., 2005). Furthermore, the loss of integrin adhesion has been proposed to act as a trigger for caveolar-dependent uptake of this protein (Hertzog et al., 2012). Hence, whether it is due to a global, genetic changes or a local phenomenon within the muscle fibre, the loss of adhesion in the absence of dystrophin binding could stimulate a similar caveolar-dependent internalization of β-dystroglycan.

Unfortunately, this hypothesis has several key problems, which make the caveolar-dependent endocytosis of β-dystroglycan a less distinct possibility, despite the potential parallel with β1-integrin internalization. The hypothesis requires an interaction between β-dystroglycan and caveolin-3 multimers and, whilst co-sedimentation of the two proteins is observed in myoblasts (Song et al., 1996) and an interaction with the c-terminus of β-dystroglycan has been reported (Illsey et al., 2002), these interactions are deemed to be indirect or transient owing to the inability to co-purify caveolin-3 with the DGC (Crosbie et al., 1998). In a similar vein, caveolin-3 may only have a scaffolding role in the localization of β-dystroglycan, as is the case for caveolin-3 and components of neuromuscular junctions (Hezel et al., 2010), and caveolin-3 and the ryanodine receptor (Whiteley et al., 2012). Interestingly, caveolin-3 has been reported to bind both a Y890-phosphorylated and an unphosphorylated motif present at the c-terminus of β-dystroglycan *in vitro* (Illsey et al., 2002). However, the overexpression of

caveolin-1 or -3 in cell lines blocks the phosphorylation of β-dystroglycan on Y890, suggesting that caveolin-3 scaffolds would block the internalization of this protein, rather than facilitate entry into the cell (Sotgia et al., 2003_a). Thus, one can not infer how β-dystroglycan might be internalized from the compartments it is localized to, an understanding of analogous adhesion systems, a knowledge of the pathways present in H2K myoblasts, or the changes to endocytic components within the dystrophic state: for all potential hypotheses there is either insufficient evidence, or worse, conflicting data.

5.1.5 Hypothesis: pY890-modified β-Dystroglycan Internalizes from the Plasma Membrane in a Clathrin-dependent Manner in H2K Myoblasts

Using the results described in Sotgia et al. (2003_a) as a starting point for enquiry, it was initially hypothesized that pY890-modified β-dystroglycan internalized from the plasma membrane of H2K myoblasts in a clathrin-dependent manner. Whilst there was little data to support this hypothesis, there were also few findings that negated this possibility, unlike other potential endocytic mechanisms. To test this hypothesis 3 different general techniques could be employed: RNAi screening of endocytic proteins and associated signaling kinases, as performed in Pelkmans et al. (2005); treatment or transfection of H2K myoblasts with endocytic inhibitors, similar to that used in Pasqual et al. (2011); or co-localization of the pY890-modified form of β-dystroglycan with endocytic markers, as visualized by immunofluorescence microscopy. All 3 approaches would have caveats, however given the previous use of the technique to visualize the clear punctate staining of pY890-modified β-dystroglycan, as well as the ability to directly extend the key findings of Sotgia et al. (2003_a), immunofluorescence microscopy of H2K myoblasts was used.

5.2.1 Controls For Immunofluorescence Experiments

Prior to all immunofluorescence microscopy described in this chapter, secondary control experiments were performed. As shown in Figure 1, all secondary antibodies used in this study exhibited a low level of non-specific binding to H2K myoblasts, resulting in low levels of fluorescent signal. Background fluorescence of this kind is routinely observed in experiments of this nature. Fortunately, the levels of these non-specific backgrounds were low compared to the signals generated upon primary antibody or fluorescent dye incubation. Hence, for each set of experiments, the contrast and exposure settings of the microscope were adjusted to exclude this background fluorescence. For each data set, the modified contrast and exposure settings were maintained throughout the acquisition of data.

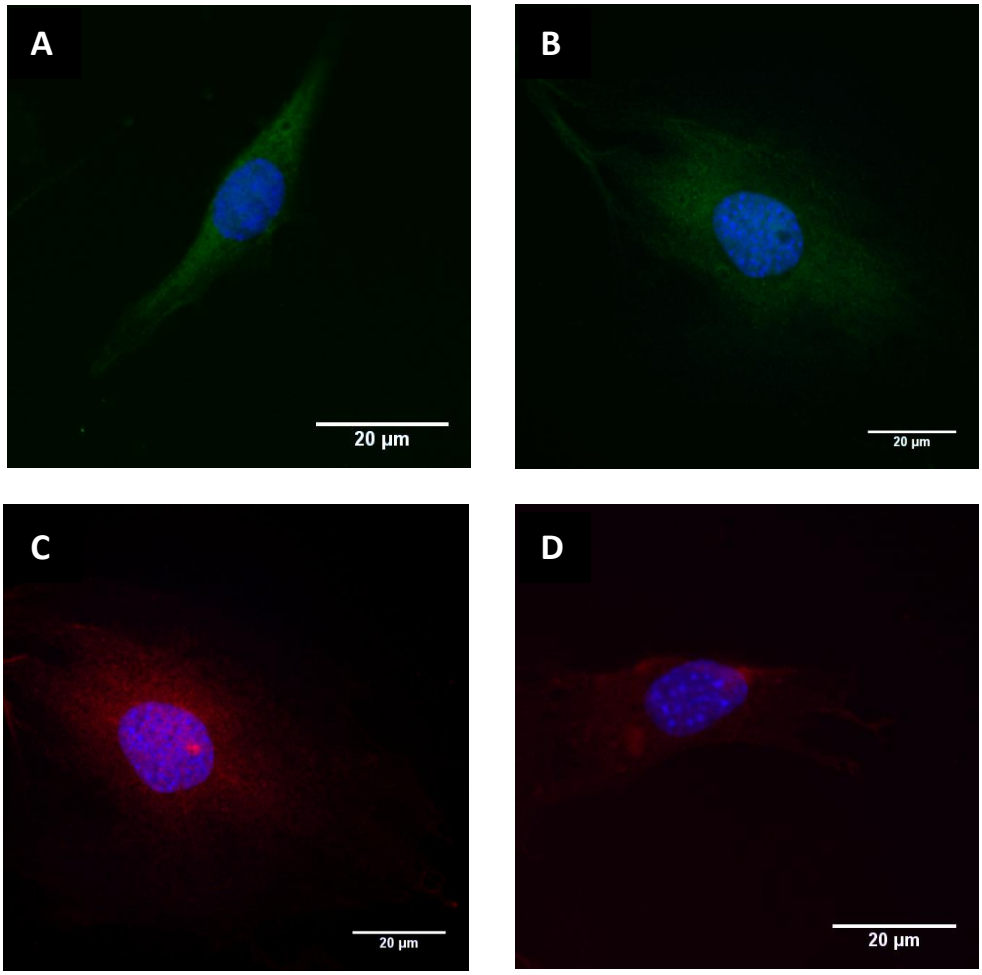

Figure 1: Controls for the secondary antibodies used extensively in this study. Antibodies used are: (A) FITC anti-mouse IgG, (B) FITC anti-rabbit IgG, (C) Texas Red anti-mouse IgG, and (D) Texas Red anti-rabbit IgG. In all cases, faint, background reactivity is observed throughout the cell that is highest in the perinuclear regions. Contrast and exposure settings were adjusted on the microscope to discount this immunoreactivity for all images presented.

5.2.2 Establishing the Use of Transferrin-568 in H2K Myoblasts

The initial hypothesis that β-dystroglycan internalizes and traffics via a clathrin-mediated pathway was tested in H2K myoblasts. To replicate the experiments of Sotgia et al. (2003_a) as closely as possible, transferrin-568 (Molecular Probes) was used to label the transferrin receptors present in H2K myoblasts, which are known to internalize in a clathrin-dependent manner (Harding et al., 1983). Labelling was performed in a pulse-chase manner: H2K myoblasts were incubated with 10µg/ml transferrin-568 in growth medium for one minute at 37°C, prior to switching to growth media without transferrin-568 and subsequent incubation at 37°C. In this way, the overall endocytosis of the transferrin receptor (internalization, recycling or degradation) could be visualized by formalin fixation after various incubation times. As the endocytosis of the transferrin receptor is well characterized in other cell lines, but not in H2K myoblasts, an initial characterization of the endocytic pathway was performed.

Figure 2 presents a series of representative images of the transferrin-568 fluorescence observed in H2K myoblasts after various pulse-chase incubation times. With time, there were progressive changes in the visual phenotype of transferrin-568 stain observed, indicative of progression through compartments of the endocytic pathway described for the transferrin receptor in other cell systems. As no co-staining was used for these experiments, exact definitions of the endocytic compartments harbouring these fluorescent puncta could not be elucidated. However, general changes in the visual phenotype exhibited by transferrin-568 staining of H2K myoblasts could be defined. These definitions were: “cytosolic”, a diffuse punctuate stain between the nucleus and periphery of the cell with little or no perinuclear accumulation (1, 2 and 3 minute time points, Figure 2) ; “perinuclear”, an accumulation of punctuate staining around the nucleus of the cell (10 minute time point, Figure 2); and “mixed” an intermediate of “cytosolic” and “perinuclear” staining with predominant staining both around the nucleus and throughout the cell (5, 15, 20 and 30 minute time points, Figure 2). Importantly, relatively few puncta were observed in control experiments, where transferrin-568 had been allowed to bind to surface receptors before acidic stripping without any internalization, indicating that the majority of fluorescent puncta observed at the various time points were internal (0 minute time point, Figure 2). Hence, these definitions could be used to describe the transferrin-568 staining observed in the experimental system.

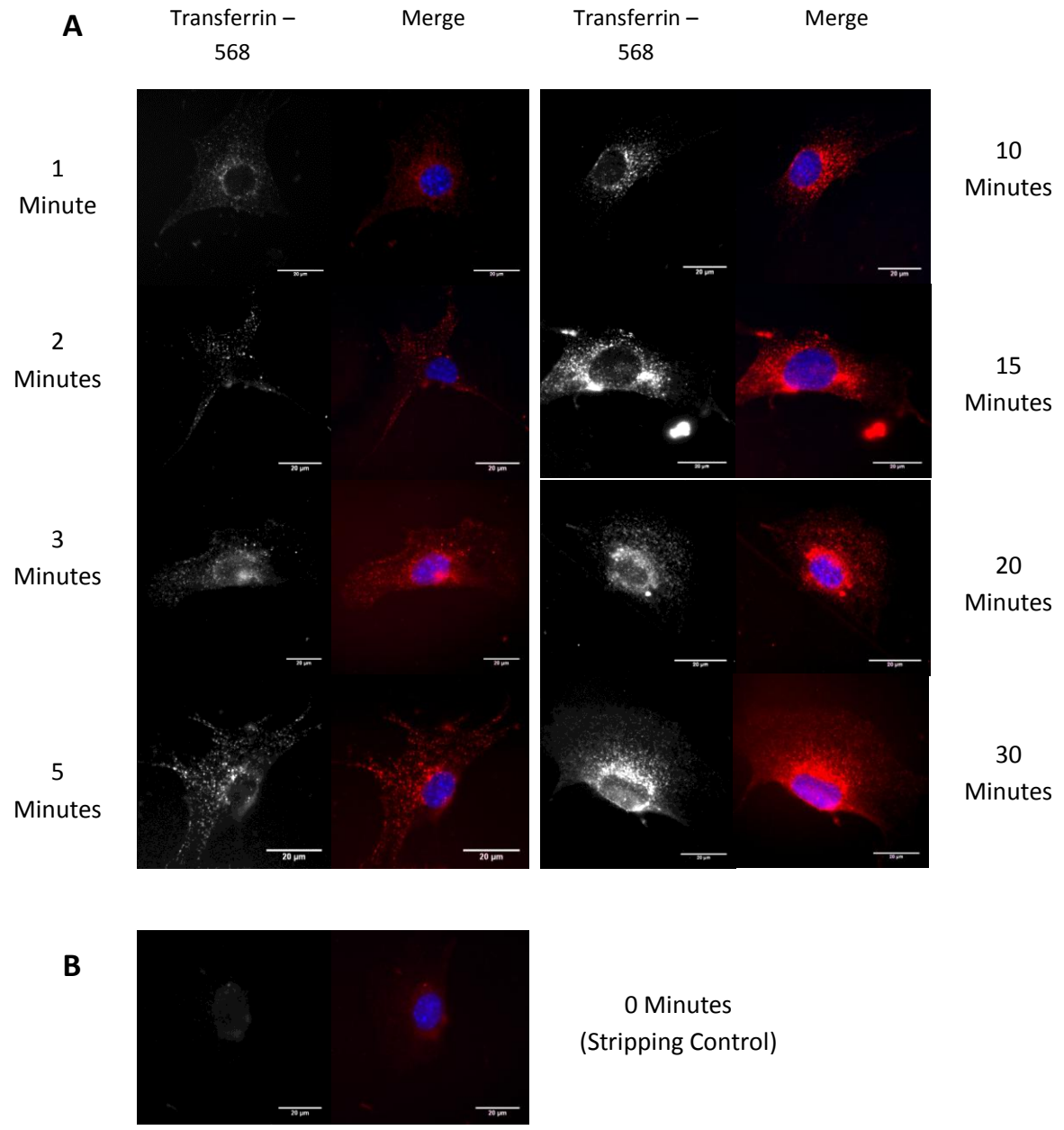

Figure 2: (A) Representative images of a time course of transferrin-568 internalization and recycling in H2K myoblasts. H2K myoblasts were incubated with a saturating concentration of transferrin-568 for 1 minute at 37°C prior to washing with growth media and subsequent incubation at 37°C. Following incubation, H2K myoblasts were stripped of surface bound transferrin-568 at 4°C and processed for immunofluorescence microscopy. Displayed are red channel (transferrin-568) and false colour merged (transferrin-568 and DAPI) images of the time points indicated.

(B) Stripping control for these experiments. H2K myoblasts were incubated with transferrin-568 for 1 hour at 4°C, prior to stripping and processing as described in part (A).

Although the images shown in Figure 2 are representative of the main visual phenotype observed at each time point, a distribution of phenotypes were in fact observed at all time points. This is to be expected, owing to the heterogeneous nature of endocytosis between individual cells. Hence, an equal number of H2K myoblasts were imaged and scored for visual phenotype at each incubation time point, in order to better estimate the progression of transferrin receptor endocytosis in this experimental system. Figure 3 contains a graphical representation of these data, with the percentage of cells exhibiting each of the defined visual phenotypes for each time point. The data shows several overall changes in the predominant visual phenotype of H2K myoblasts pulse-chased with transferrin-568, which can be equated to what is known about this receptor in other experimental systems.

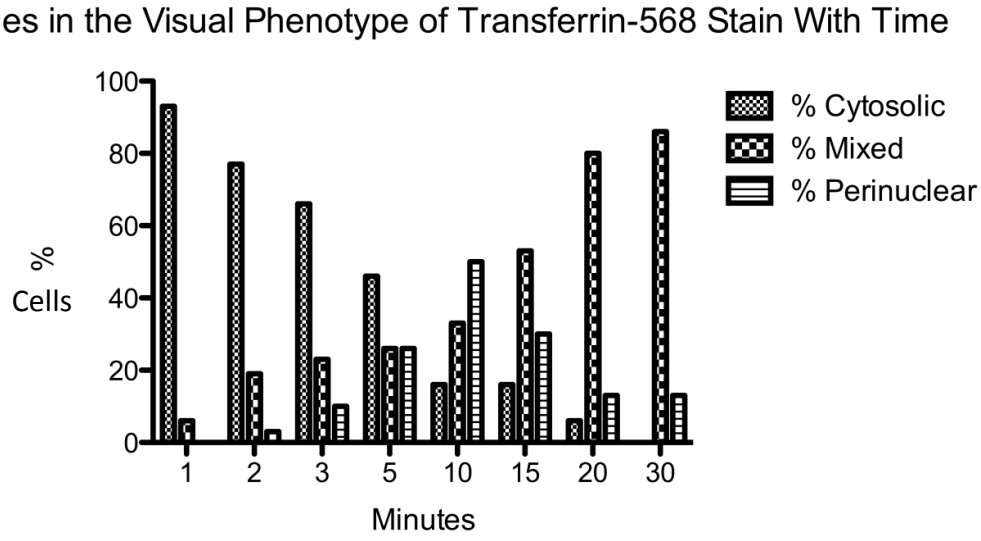

Figure 3: Changes in the visual phenotype of transferrin-568 staining during internalization and subsequent recycling in H2K myoblasts. 30 images were scored per time point for one of the 3 visual phenotypes. The percentage of cells exhibiting each visual phenotype was then plotted against the pulse-chase incubation time.

Initially, transferrin-568 puncta are “cytosolic”, suggesting a localization to sub-membranous or early endosomes within the endocytic system. Clathrin-mediated endocytosis begins with dynamin-dependent scission from the plasma membrane and delivery of endocytic vesicles to the early endosomal compartment (Mu et al., 1995 ; Trischler et al., 1999). Hence, the “cytosolic” phenotype probably represents localization of labelled transferrin receptors within these compartments. In other experimental systems the transferrin receptor then follows various

pathways, which function to either recycle or degrade the protein, via recycling or late endosomal compartments. Whilst direct recycling could not be discerned, as this would contribute to the "cytosolic" visual phenotype, trafficking to the late endosomal compartment could be visualized as this compartment is known to be perinuclear (Piper et al., 2001). It is interesting to note that at the 10 minute time point, both the "mixed" and "perinuclear" visual phenotypes replace "cytosolic" as the dominant staining pattern, suggesting that delivery of pulse-chased transferrin receptors to the late endosomal compartment has occurred. Whilst the majority of stained H2K myoblasts exhibited a "perinuclear" visual phenotype at the 10 minute time point, this shifted to a "mixed" phenotype at subsequent time points, with loss of "cytosolic" and "perinuclear" staining. This could represent either trafficking via the recycling or degradation compartments, or even subsequent internalization of exocytosed transferrin-568. It is important to note that saturation of the system, presumably with recycling of transferrin receptor to the plasma membrane, occurs between 15-30 minutes (Figure 2 and 3), which is in agreement with both estimates from other systems (Harding et al., 1983 ; Hopkins et al., 1983 ; Klausner et al., 1983) and the biochemical data presented earlier (Figure 5, Data Chapter 1). Thus, one can conclude that transferrin receptor endocytosis, as visualized by transferrin-568 pulse-chase staining, is not significantly different from other experimental systems.

5.2.3 β-Dystroglycan Does Not Traffic with the Transferrin Receptor

Having established that transferrin-568 pulse-chase staining could be used in H2K myoblasts, co-localization of pY890-modified β-dystroglycan with the compartments marked by this stain was tested by co-staining with 1709 (Figure 4). Co-localization was examined at the 3, 10, 15 and 30 minute time points, which correspond to the time points used by Sotgia et al., (2003_a), as well as the earlier stages of clathrin-dependent endocytosis (Figure 3 and Trischler et al., 1999). At all time points examined little co-localization was observed between the transferrin-568 and 1709 stains (Figure 15, A-D). This data strongly suggests that pY890-modified β-dystroglycan does not share a common endocytic compartment with the transferrin receptor during internalization or subsequent trafficking. To further verify this conclusion, the co-localization between internalized β-dystroglycan and a known compartment of transferrin receptor endocytosis was tested.

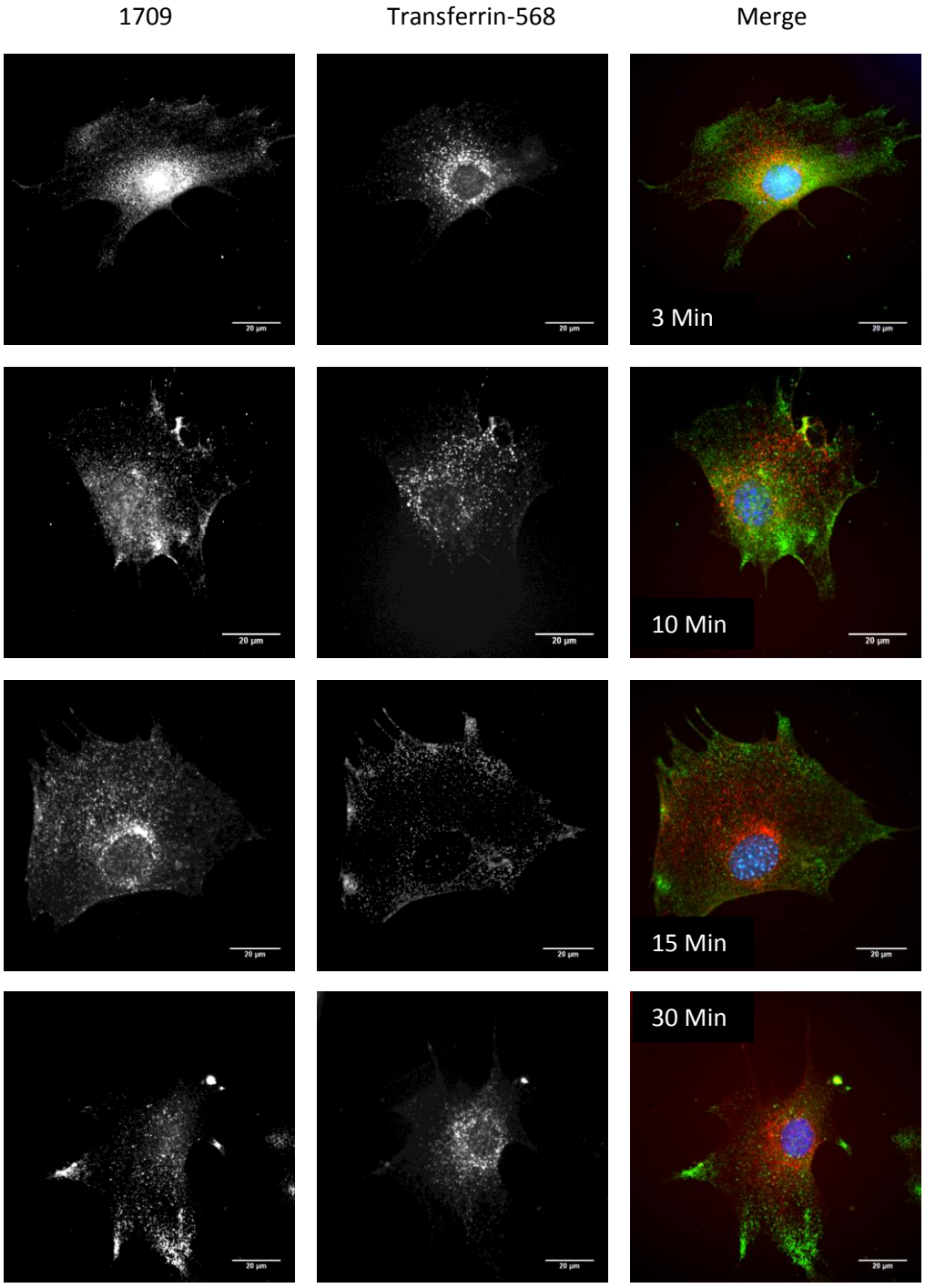

Figure 4: Representative images of 1709 (pY890-modified β-dystroglycan) and transferrin-568 co-staining of H2K myoblasts following a one minute transferrin-568 pulse and incubation at 37°C in growth media for the time points indicated. Following stripping of surface transferrin, H2K myoblasts were then processed for immunofluorescence as described in Materials and Methods. Shown are green channel (1709) fluorescence, red channel (Tfn-568) fluorescence and false colour merge (1709, Tfn-568, DAPI) images.

The early endosomal compartment, as defined by the presence of the Rab5 effector Early Endosomal Antigen 1 (EEA1), is a destination of the transferrin receptor during endocytosis (Mu et al., 1995 ; Rubino et al., 2000). Western blots of H2K myoblast lysates identified that EEA1 is expressed in this cell line (data not shown). Furthermore, staining H2K myoblasts with anti-EEA1 revealed a punctate staining throughout the cell, typical of the staining pattern observed in other experimental systems (Figures 5 and 6 and Stenmark et al., 1996). Co-immunostaining of H2K myoblasts for pY890-modified β-dystroglycan and EEA1 showed little co-localization between these proteins (Figure 5 and Figure 15, E), suggesting that internalized β-dystroglycan does not traffic via this compartment. Furthermore, the absence of co-localization between pY890-modified β-dystroglycan and the EEA1-positive early endosomal compartment, a known destination of internalized transferrin receptors, verifies the lack of co-localization observed between the pY890-modified β-dystroglycan and transferrin-568 stains (Figure 4).

These data suggest that the initial hypothesis is incorrect, and are in disagreement with the findings of Sotgia et al., (2003_a). Although this could be due to the improved resolution of the epifluorescence microscopy used in this study, it could also be due to abnormal transferrin receptor endocytosis or EEA1 staining in H2K myoblasts. To test if the latter was the case, H2K myoblasts were pulse-chased with transferrin-568 and co-stained with anti-EEA1 after a 3 minute incubation at 37°C. Assuming that the cytosolic fluorescent puncta predominantly observed during the early time points of transferrin-568 internalization represent internalizing vesicles or early endosomal compartments (Ghosh et al., 1994), then a co-localization between the transferrin-568 and EEA1 stains should be apparent at this time point. For this experiment a confocal fluorescence microscope was used to visualize stained H2K myoblasts, so that false co-localization due to spatial overlap in the z-plane could be excluded. Figure 6 contains a series of confocal slice images showing transferrin-568 and EEA1 staining at various positions within the z-plane. Whilst not all transferrin-568 puncta are EEA1-positive, the majority of EEA1-positive puncta are also positive for transferrin-568. This finding is in agreement with what one would expect to see if transferrin endocytosis were occurring as described in other experimental systems (Mu et al., 1995). When quantitatively analyzed, the two stains show a moderate level of co-localization, however a comparison of the individual average Manders coefficients (0.95 for EEA1 with transferrin-568, 0.6 for transferrin with EEA1) affirms the co-localization by eye, as well as explaining the relatively low overall co-localization (Figure 15, F,G,H). Together, these findings suggest that the lack of co-localization of these markers with pY890-modified β-dystroglycan is due to trafficking via different pathways, rather than any abnormal staining of these compartments in H2K myoblasts.

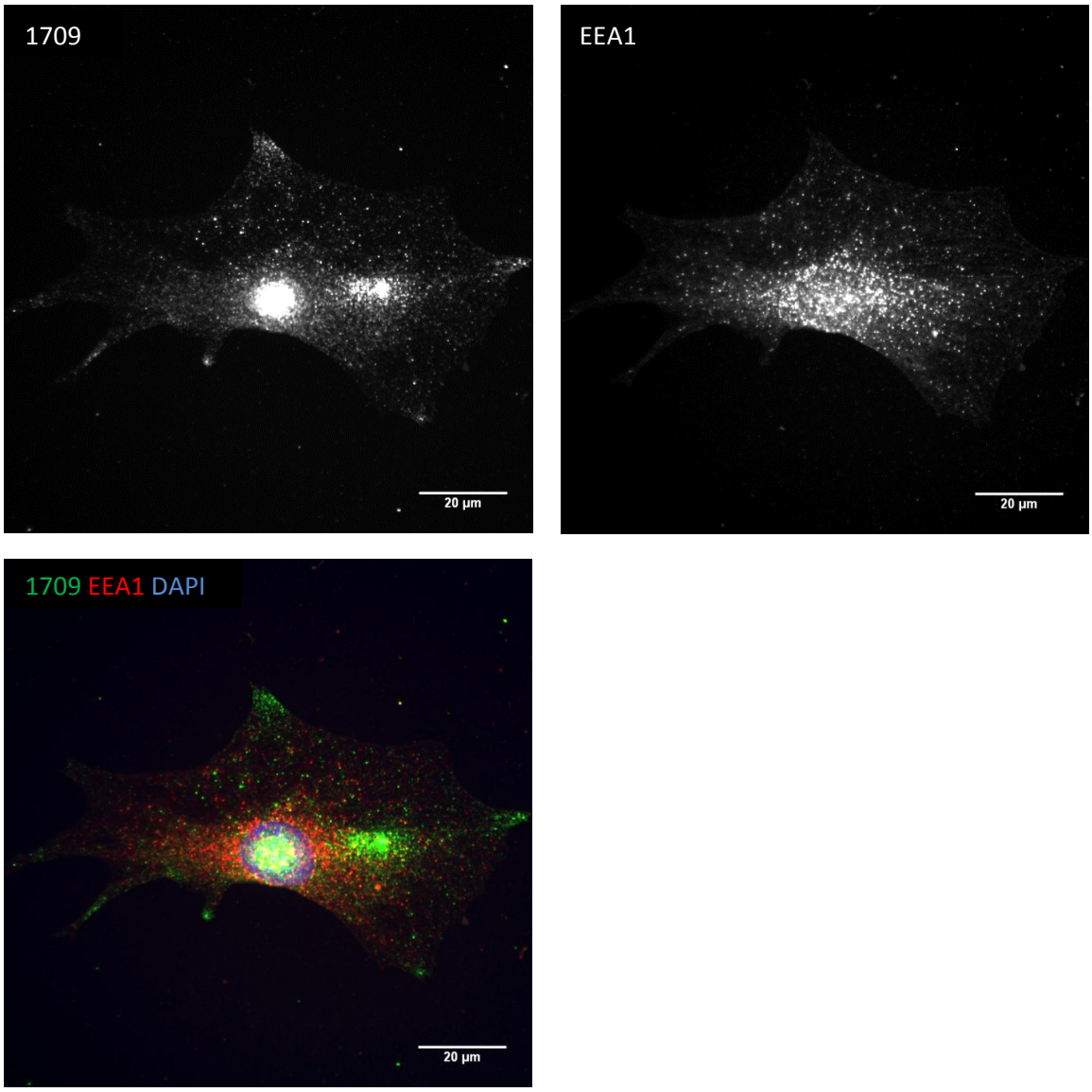

Figure 5: A representative image of 1709 (pY890-modified β-dystroglycan) and EEA1 co-immunostaining of H2K myoblasts. Shown are green channel (1709) fluorescence, red channel (EEA1) fluorescence and false colour merge (1709, EEA1, DAPI) images.

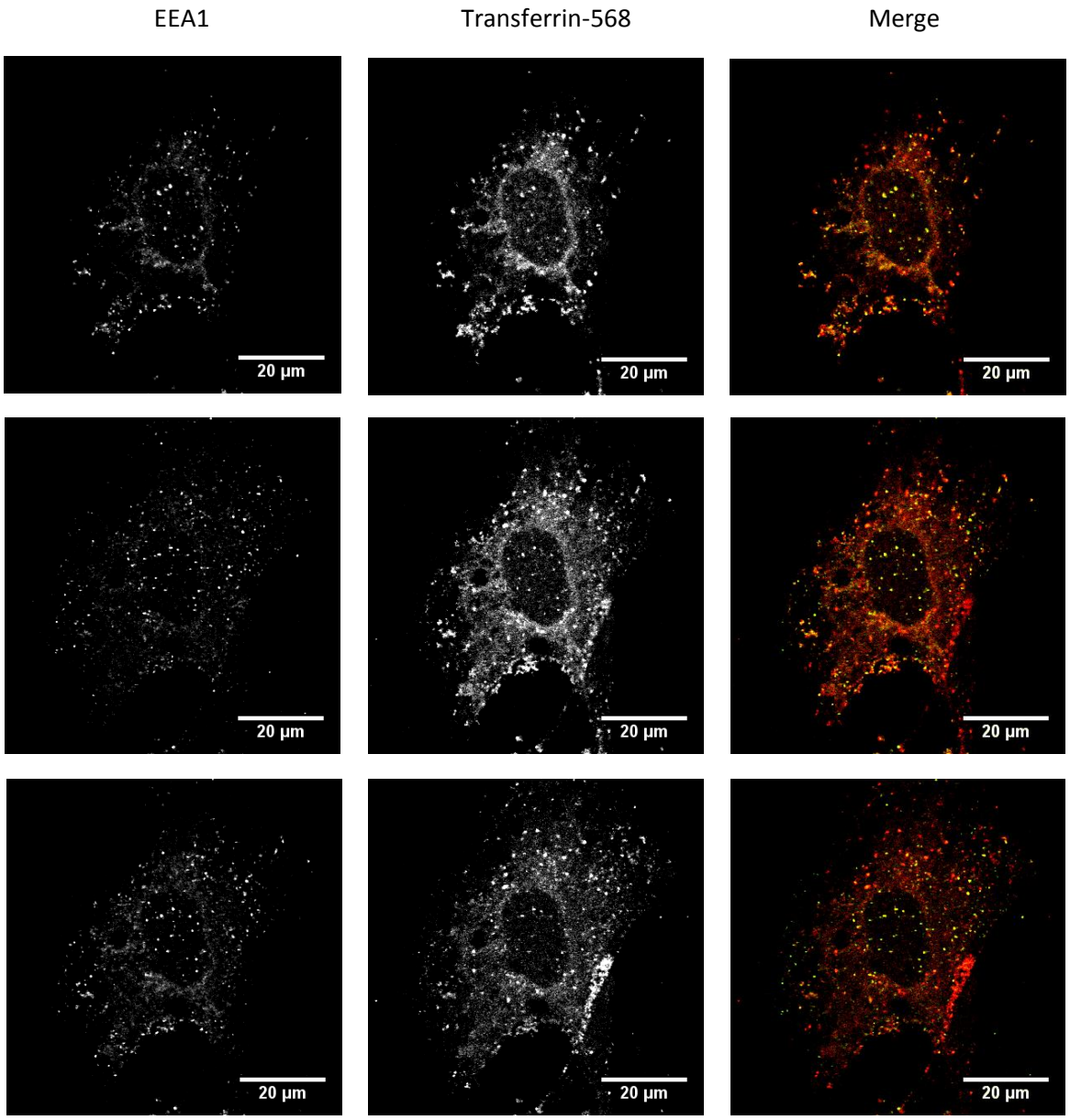

Figure 6: A representative series of Z-stack confocal immunofluorescence microscopy images of EEA1 (green) and transferrin-568 (red) co-staining of H2K myoblasts. Following a one minute transferrin-568 pulse and incubation at 37°C in growth media for a further two minutes, H2K myoblasts were transferred to 4°C, stripped and processed for immunofluorescence microscopy as described in Materials and Methods.

Although these data suggest that pY890-modified β-dystroglycan does not traffic via the pathways used by the transferrin, as internalized β-dystroglycan does not share a common compartment with the transferrin receptor or EEA1, they do not properly test if internalization occurs in a clathrin-dependent manner. It is conceivable that, following clathrin-dependent internalization, pY890-modified β-dystroglycan traffics via alternative endocytic compartments. If this is the case in H2K myoblasts then there should be some overlap between immunostains of pY890-modified β-dystroglycan and the clathrin heavy chain (CHC), an essential component of the clathrin lattice which coats internalized pits (Larkin et al., 1986). However, as shown in Figures 7 and 15 (I), these two immunostains show little or no overlap. In the face of these data it seemed unlikely that β-dystroglycan internalizes in either a clathrin-dependent manner, or traffics via any of the typical compartments downstream of clathrin-dependent internalization, so the initial hypothesis was revised.

5.2.4 Establishing the Use of 594-ChTxB in H2K Myoblasts

A plausible alternative is that β-dystroglycan internalizes using lipid rafts, potentially in association with caveolin-3. As discussed in the introduction, the argument for raft- or caveolar-dependent endocytosis of β-dystroglycan is not without justified criticism; however internalization via a pathway that does not utilize clathrin would explain the observed lack of co-localization of pY890-modified β-dystroglycan with the transferrin receptor, EEA1 and CHC stains. Thus, it was hypothesized that β-dystroglycan is endocytosed via a clathrin-independent mechanism. Beyond caveolar-mediated endocytosis, markers for these alternative pathways are not as robust or as well characterized as those of the "classical" clathrin-dependent pathway. However, one well-reported marker is the B subunit of the toxin from *V. cholerae*. Cholera toxin B subunit (ChTxB) selectively binds to GM1 gangliosides, which are present in lipid rafts in the plasma membrane, and has, by itself, little or no cytotoxicity (Nichols et al., 2001 ; Puri et al., 2001). For the experiments presented herein the fluorescently tagged Alexa Fluor 594-ChTxB (Invitrogen) was used.

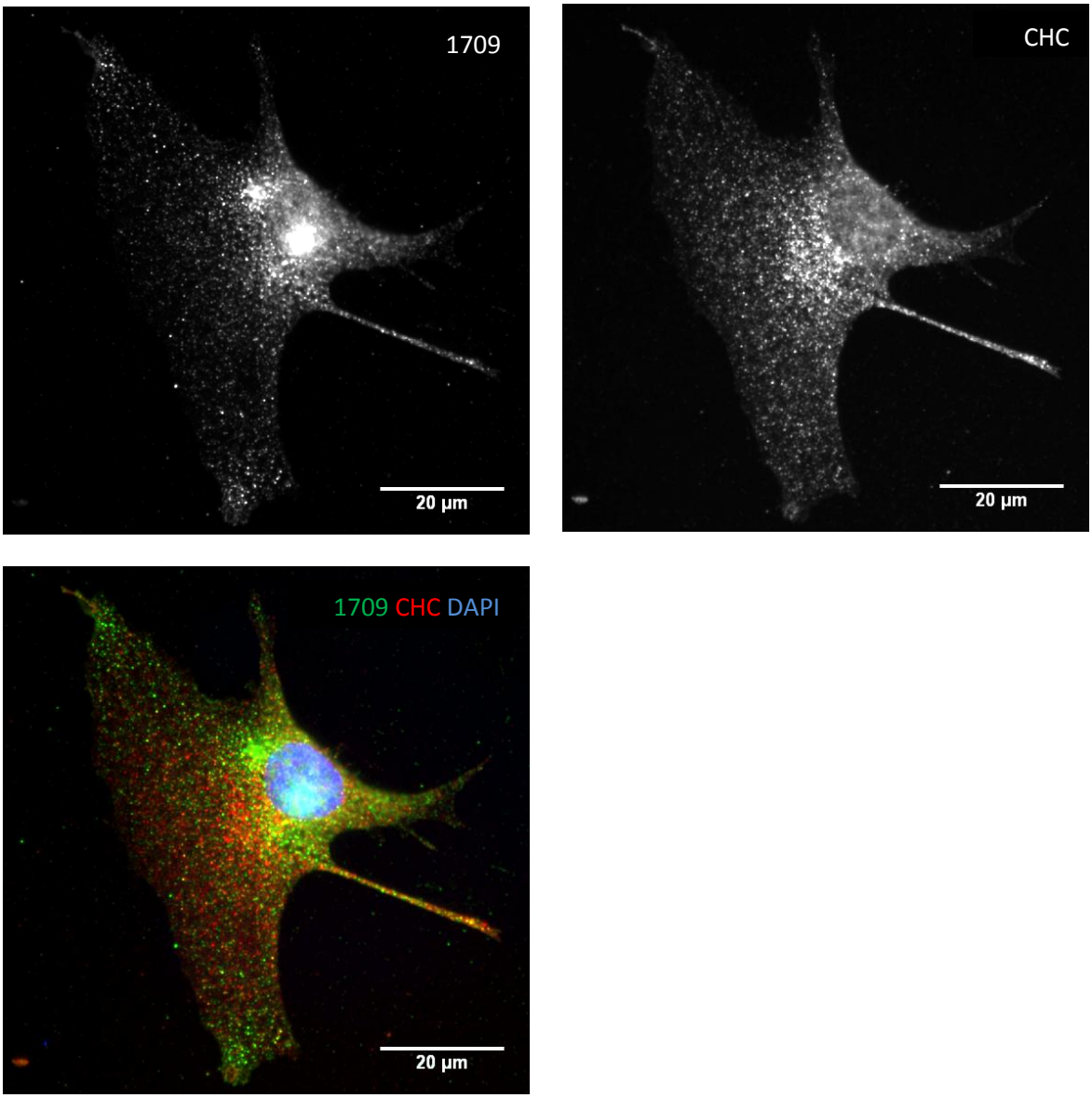

Figure 7: A representative image of 1709 (pY890-modified β-dystroglycan) and clathrin heavy chain co-immunostaining of H2K myoblasts. Shown are green channel fluorescence (1709), red channel (clathrin heavy chain) and false colour merge (1709, clathrin heavy chain and DAPI) images.

Initially, labelling conditions which gave adequate staining and stripping were determined. Figure 8 contains images depicting the typical stages of 594-ChTxB staining of H2K myoblasts. Incubation of myoblasts with growth media containing 1µg/ml 594-ChTxB for 30 minutes at 4°C produced a diffuse, patchy stain (Figure 8, A). Presumably, this is due to binding to GM1 gangliosides within the plasma membrane, with enriched membrane microdomains appearing as patches of more intense staining, although it is important to note that these patches do not appear as intense as the internalized puncta observed following incubation at 37°C (Figure 8, C). To ensure any membranous staining was excluded following internalization at 37°C, various stripping buffers and conditions were trialled (data not shown). The most optimal of these stripping conditions did not fully remove all membranous staining, however the remaining levels of 594-ChTxB staining were low enough to be disregarded from analysis as background (Figure 8,B). Thus, the use of stripping washes after incubation at 37°C permitted visualization of the internalized puncta, due to the large difference in staining intensity between residual membranous stain and internalized vesicles (Figure 8, C).

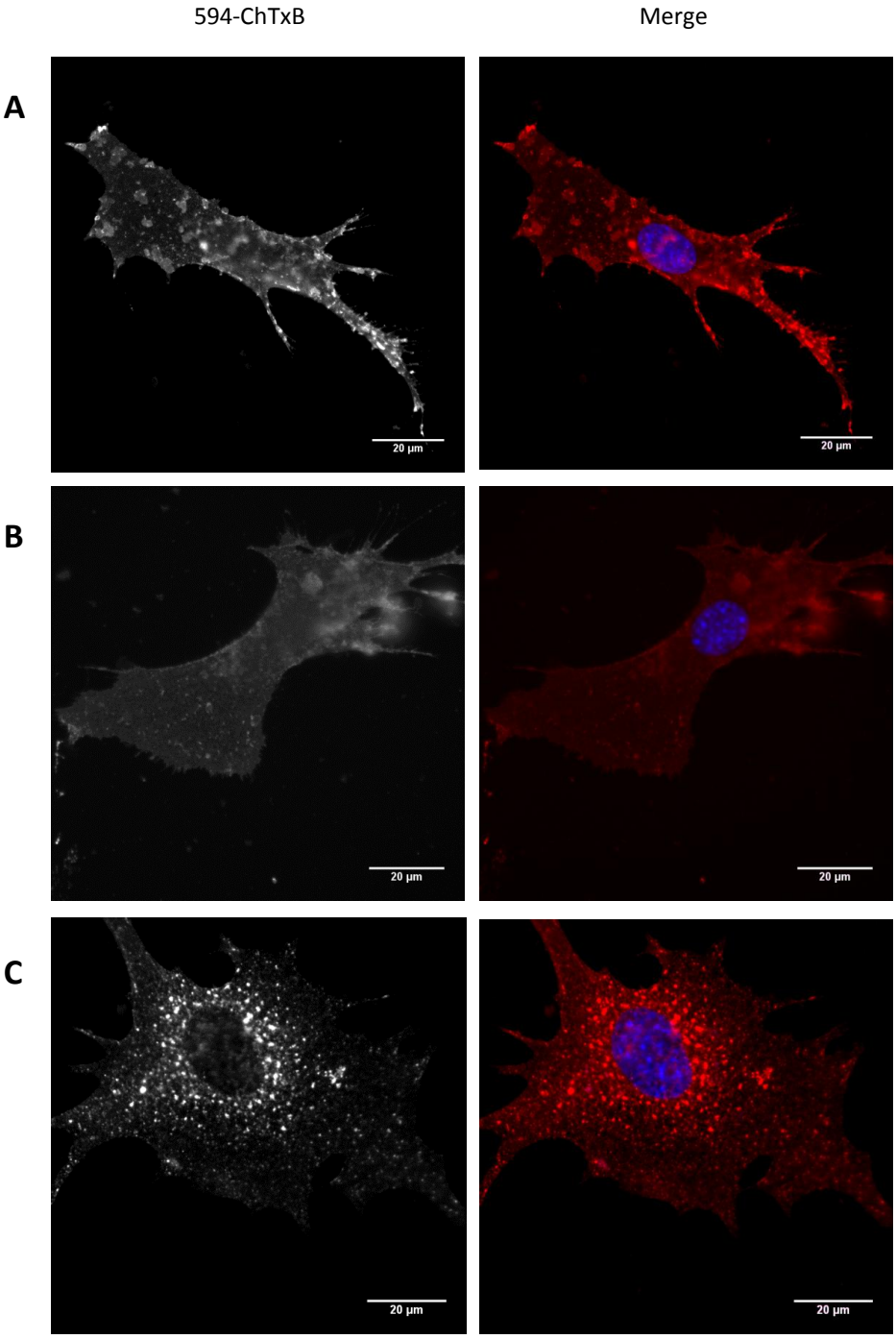

Figure 8: Representative images of H2K myoblasts stained with 594-ChTxB. Shown are red channel (594-ChTxB) and false colour (594-ChTxB and DAPI) merged images. (A) Surface labelling of H2K myoblasts at 4°C without subsequent internalization at 37°C gives a membranous, patchy stain. (B) As (A), but with a series of stripping washes at 4°C. The washes remove the majority of stain, but a residual stain is left. (C) Staining of H2K myoblasts with 594-ChTxB as described in Materials and Methods. In this instance, a ten minute incubation at 37°C was used.

5.2.5 β-Dystroglycan Does Not Traffic with Lipid Rafts Containing GM1

Having established conditions which gave suitable 594-ChTxB staining of H2K myoblasts, it was possible to visualize the vesicular compartments involved in endocytic pathways that utilise lipid rafts. As before with transferrin-568 staining, H2K myoblasts were labelled in a pulse chase manner: myoblasts were incubated with 1µg/ml 594-ChTxB at 4°C prior to switching to growth media without ChTxB and subsequent incubation at 37°C. With formalin fixation and co-immunostaining for pY890-modified β-dystroglycan after various 594-ChTxB incubation times, the extent of co-localization between these markers could be determined. At all of the time points examined (1, 3, 6, 10, 15, and 20 minutes), little or no co-localization was observed (Figures 9 and 15, J-O). This suggests that β-dystroglycan does not internalize via a pathway that involves lipid rafts that contain GM1.

Unlike the well-characterized transferrin receptor endocytic system, it was not possible to characterize the changes in staining observed with varying chase times following a 594-ChTxB pulse. Whilst there was an analogous transition of punctuate staining from peripheral to perinuclear compartments with time (Figure 9), exactly what these compartments are is harder to define. Furthermore, owing to the involvement of lipid rafts in multiple endocytic pathways, verification of the staining observed with 594-ChTxB in H2K myoblasts by co-localization with known markers was not possible. However, an important question to address, especially in light of the revised hypothesis, was whether this staining was a consequence of internalization in a clathrin-independent manner. To address this question, H2K myoblasts were pulsed with 594-ChTxB and chased for short times (30 and 60 seconds) in order to visualize the degree of co-localization with CHC, a bona fide marker of clathrin-dependent internalization. As shown in figures 10 and 15 (P,Q), 594-ChTxB staining does not co-localize with CHC immunostaining at these early time points, suggesting that labelling with 594-ChTxB does not visualize vesicles that internalize in a clathrin-dependent manner. Furthermore, the lack of co-localization between the pY890-modified β-dystroglycan and 594-ChTxB stains over the time points examined suggests that β-dystroglycan does not internalize or traffic via a pathway that involves lipid rafts.

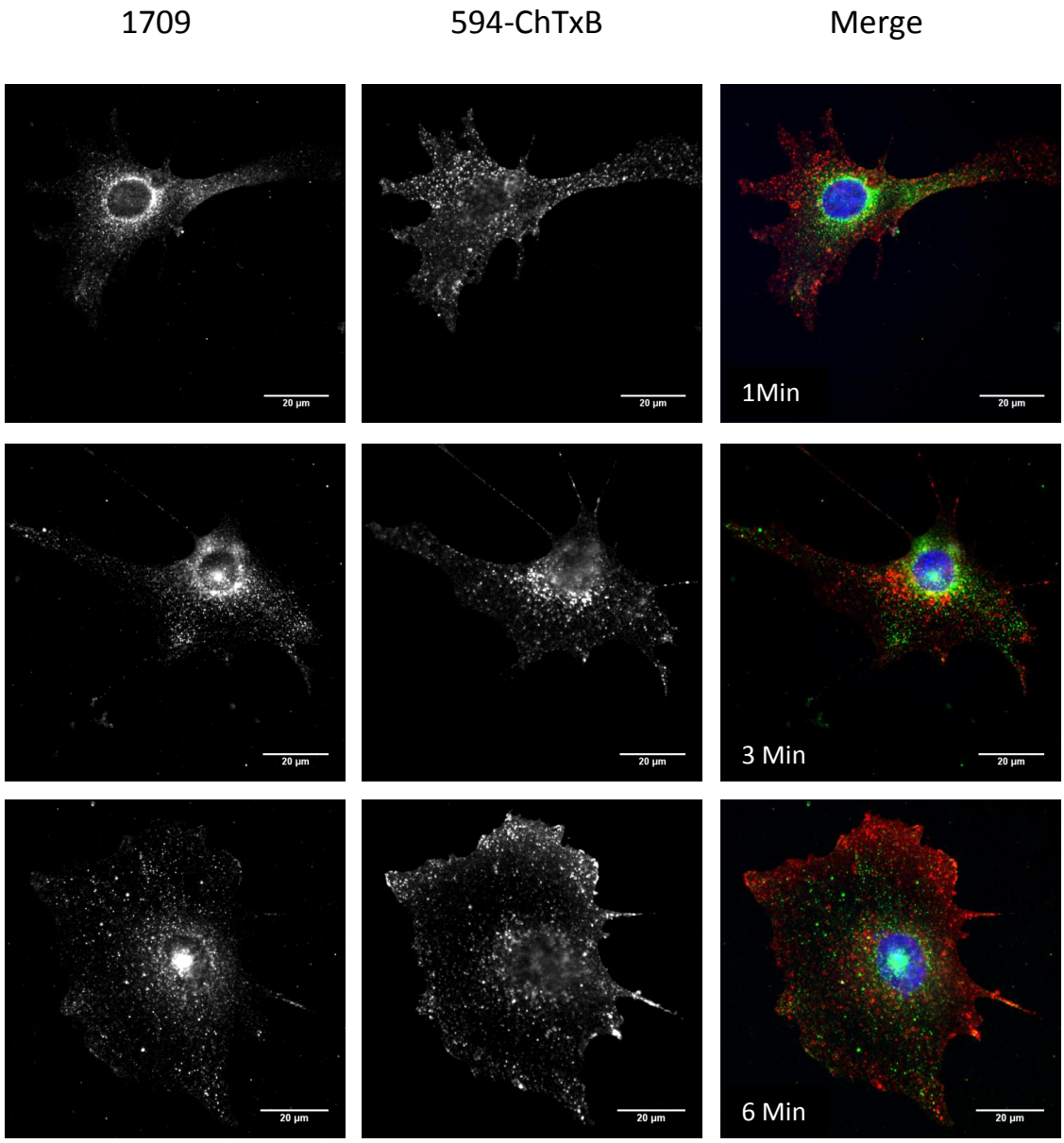

Figure 9: Representative images of H2K myoblasts pulse-chased with 594-ChTxB for the incubation times shown and then co-immunostained with 1709. Shown are green channel (1709), red channel (594-ChTxB) and false colour merged (1709, 594-ChTxB, DAPI) images. Figure continued on next page.

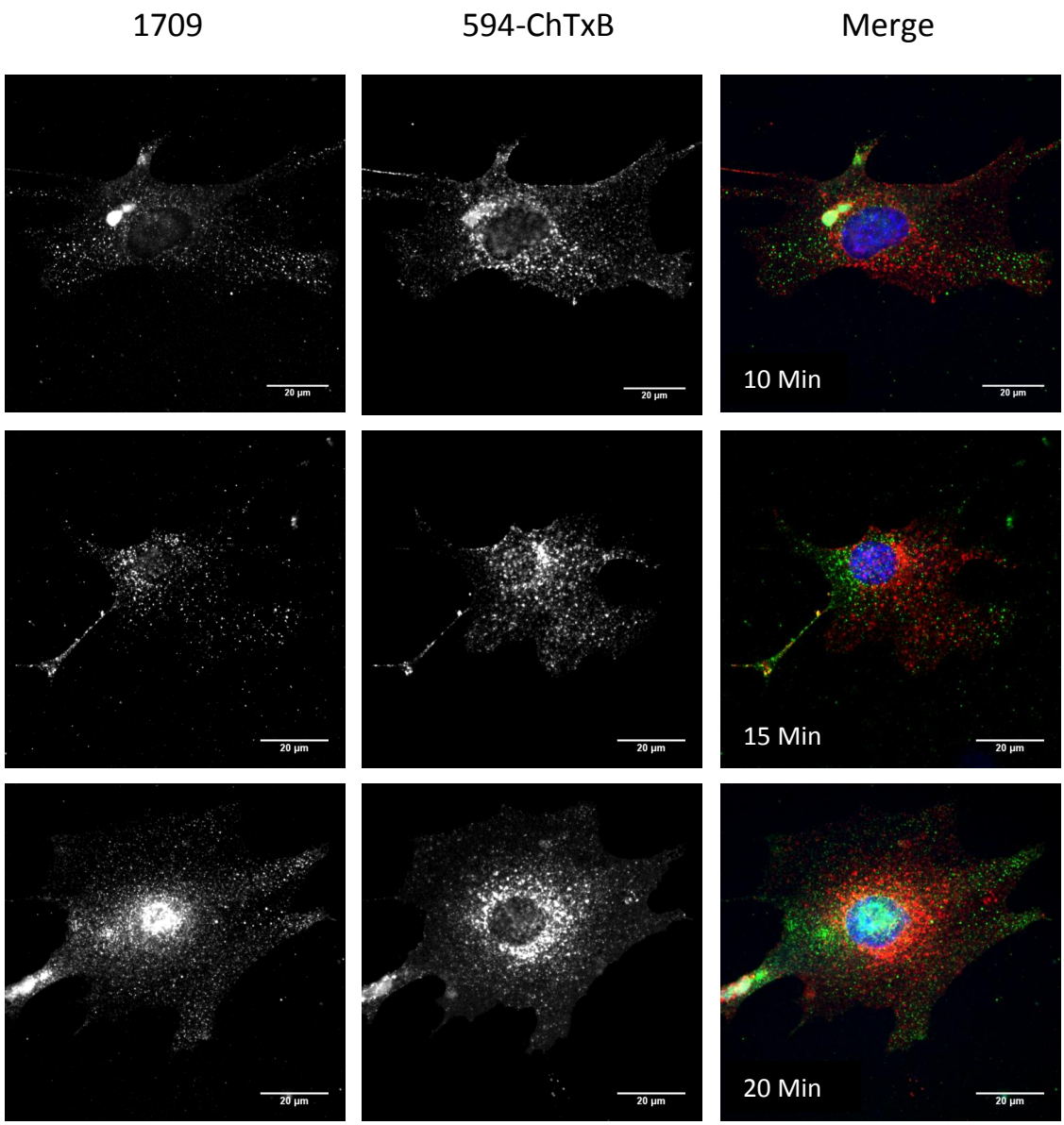

Figure 9: Continued from previous page.

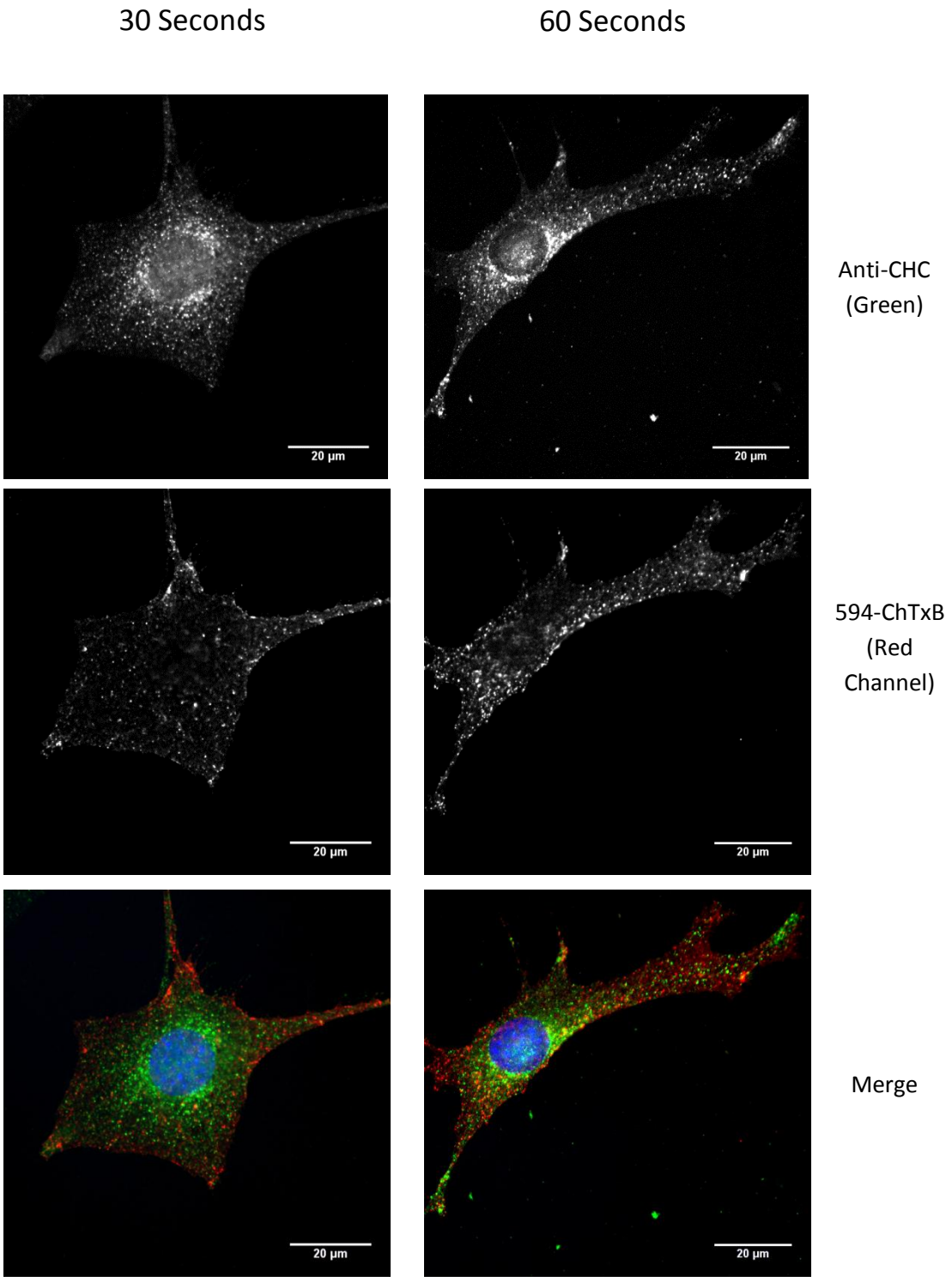

Figure 10: Representative images of H2K myoblasts pulse-chased with 594-ChTxB for the incubation times shown and then co-immunostained with anti-CHC. Shown are green channel (anti-CHC), red channel (594-ChTxB) and false colour merged (Anti-CHC, 594-ChTxB, DAPI) images.

5.2.6 Internalized β-Dystroglycan Does Not Traffic to the Lysosome

Being unable to establish a route of internalization for β-dystroglycan, the work focussed instead on the endocytic fate of β-dystroglycan. As described in Data Chapter 2, pY890-modified β-dystroglycan is also monoubiquitinated. Although the exact function of this monoubiquitination was not determined, it could be potentially involved in endolysosomal degradation, as is the case for the EGF receptor (Oved et al., 2006). Furthermore, the degradation of membrane proteins via endocytic delivery to the lysosomal compartment is a well documented and common process (Nichols et al., 2001). It was therefore of interest to see if a similar process occurs in H2K myoblasts and so, it was hypothesized that some of the internal β-dystroglycan staining observed was due to localization of this protein to the lysosomal compartment. Lysotracker™ Red DND-99 (Molecular Probes), hereafter referred to as "Lysotracker" was used to stain H2K myoblast lysosomes. In the literature involving the use of this dye, positive control experiments involving inhibition or neutralization of the lysosomal compartment are performed (Gotink et al., 2011). Neutralization of the lysosomal compartment by ammonium chloride treatment is a well-established protocol (Selgen et al., 1976 ; Ohkuma et al., 1978) and was adapted to establish correct staining of H2K myoblasts with Lysotracker. Pre-treatment of H2K myoblasts with growth media containing 50mM NH_4Cl for 2 hours abolishes the punctuate staining normally observed with lysotracker (Figure 11). In addition to a significant reduction in the number of puncta observed in H2K myoblasts stained with Lysotracker after NH_4Cl treatment, there is an increase in non-specific background staining and swollen vesicles are apparent (Figure 11). The swelling (or inhibition) of lysosomes in response to ammonium chloride neutralization is well-documented (Wibo et al., 1974 ; Selgen et al., 1976) and this observation, partnered with the loss of punctuate staining, suggests that Lysotracker can be used as a marker of the endolysosomal compartment in H2K myoblasts.

Having established the use of Lysotracker with H2K myoblasts, the co-localization of internalized β-dystroglycan with the lysosomal compartment was examined next. Co-staining with lysotracker and 1709 showed no co-localization overall (Figure 15, R), although some false co-localization, mainly due to excessive perinuclear signal in the green channel was apparent in several images (Figure 12).

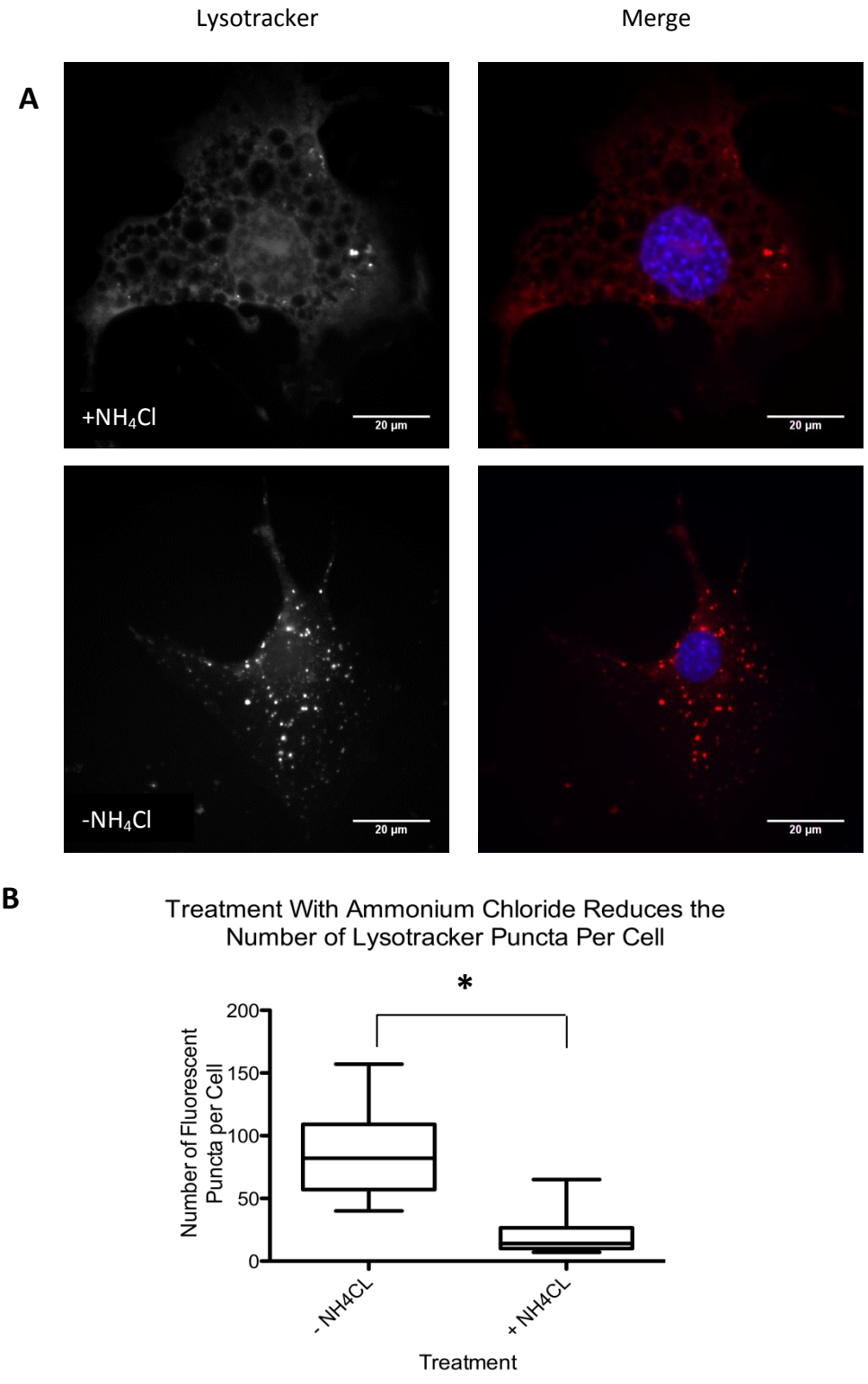

Figure 11: (A) Representative images of Lysotracker DND-99 staining of H2K myoblasts with and without 50mM ammonium chloride pre-treatment. Shown are red channel (lysotracker) and false colour merge images. (B) A scatter plot representation of the data. N=25 per treatment, with a significant difference between the means ($p<0.001$, Students t-test).

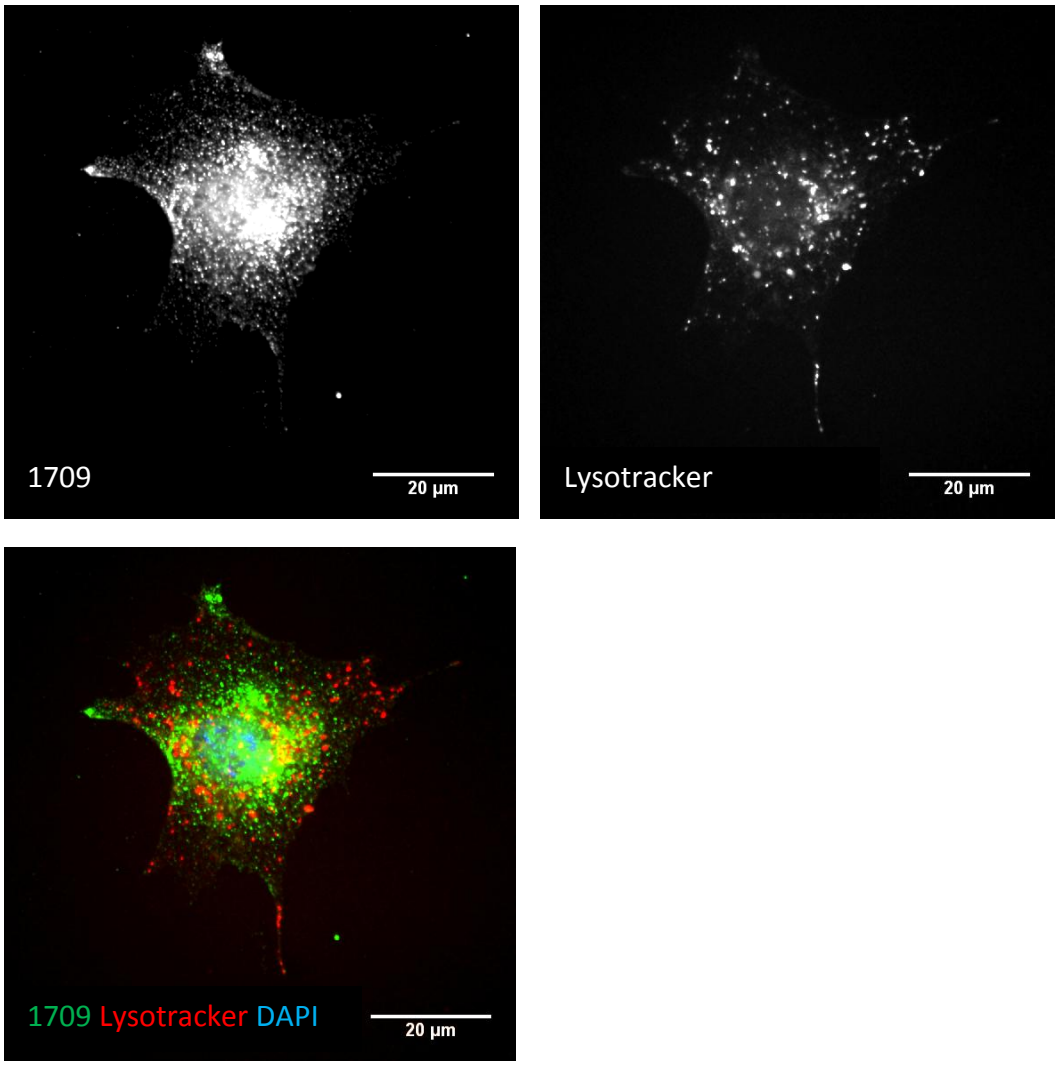

Figure 12: A representative image of 1709 and lysotracker staining of H2K myoblasts. H2K myoblasts were stained with Lysotracker as described in Materials and Methods, prior to processing for immunofluorescence microscopy and co-immunostaining with 1709. Shown are green channel (1709), red channel (Lysotracker) and false colour merge (1709, Lysotracker and DAPI).

However, even when this is included in the analysis the mean Manders coefficient for co-localization is 0.382, and this is not significantly different from other, negative co-localizations (Figure 15). Therefore, these data suggest that internalized, pY890-modified β-dystroglycan does not traffic to the endolysosomal compartment. However, the possibility exists that only a small proportion of pY890-modified β-dystroglycan would reside in this compartment, making detection of any potential co-localization difficult due to the sensitivity of this particular system. Therefore, alternative means of visualizing the lysosomal compartment in H2K myoblasts were employed to further test the hypothesis.

GFP-Sialin and Lamp1-mCherry are two markers of the lysosomal compartment, which have both been reported in the literature (Dozynkiewicz et al., 2012). Eukaryotic expression vectors containing either of these proteins were provided as generous gifts by Professor Jim Norman. H2K myoblasts were transfected with either one of the vectors expressing these proteins by electroporation. 24 hours after electroporation, H2K myoblasts were processed for immunofluorescence microscopy and immunostained for pY890-modified β-dystroglycan. For both GFP-Sialin and Lamp1-mCherry there is no co-localization with pY890-modified β-dystroglycan (Figures 13 and 15, S-T). The lack of co-localization could be interpreted as a verification of the experiments with Lysotracker, or could be due to improper localization of these two constructs. However, expression of both GFP-Sialin and Lamp1-mCherry in H2K myoblasts by electroporation results in almost complete co-localization (Figures 14 and 15, U), which makes the argument for improper localization of either tagged protein less likely. It is therefore more likely that a lack of co-localization with pY890-modified β-dystroglycan is due to these proteins residing in separate subcellular compartments. Hence, when the data from the Lysotracker, GFP-sialin and Lamp1-mCherry experiments are considered collectively, one can conclude that internalized β-dystroglycan does not traffic to the endolysosomal compartment or that the 1709-reactive epitope is lost early during the degradation process.

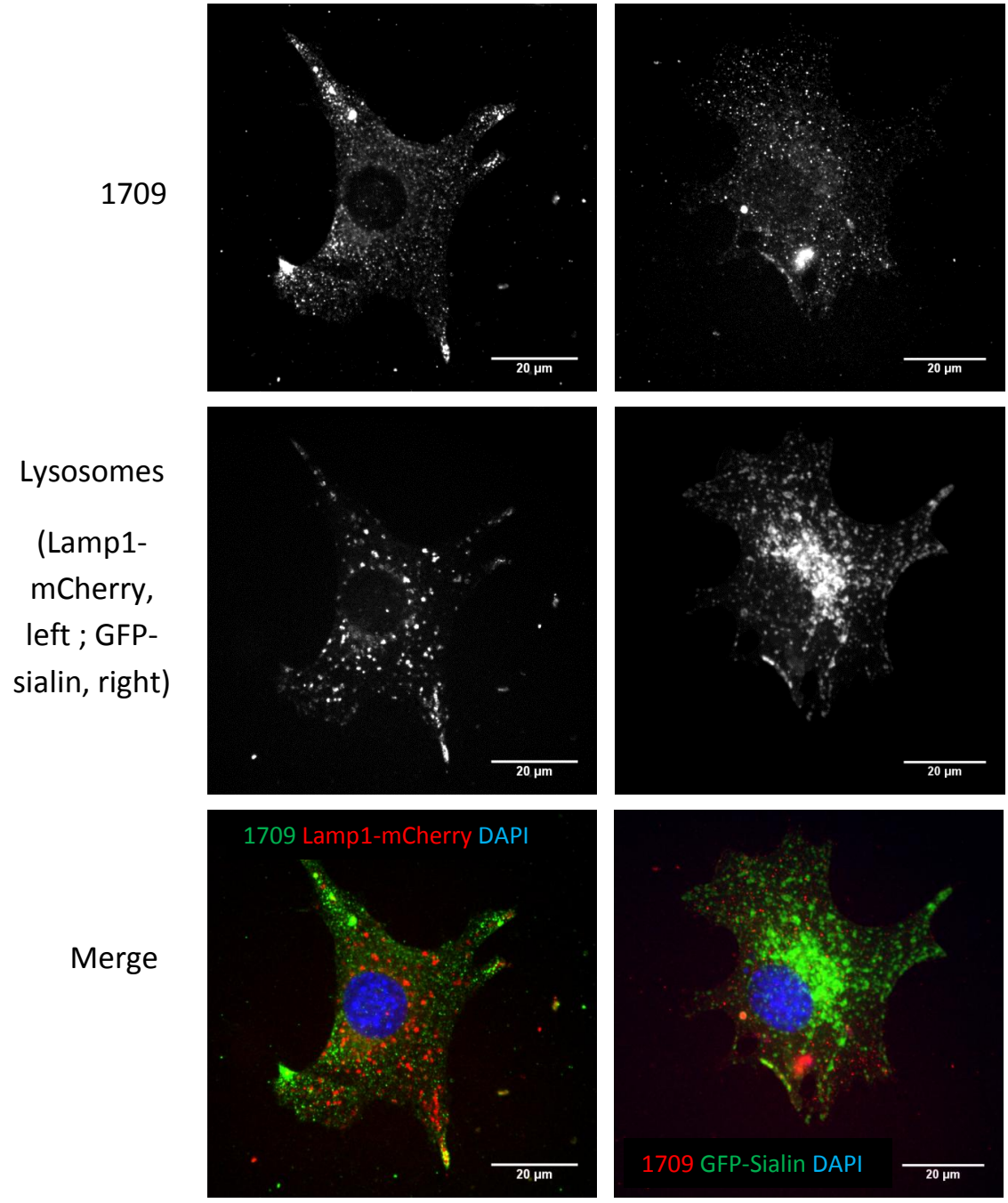

Figure 13: Representative images of H2K myoblasts transfected with either Lamp1-mCherry or GFP-sialin and co-immunostained with 1709. Shown are green channel (1709 or GFP-sialin), red channel (1709 or Lamp1-mcherry) and false colour merge images.

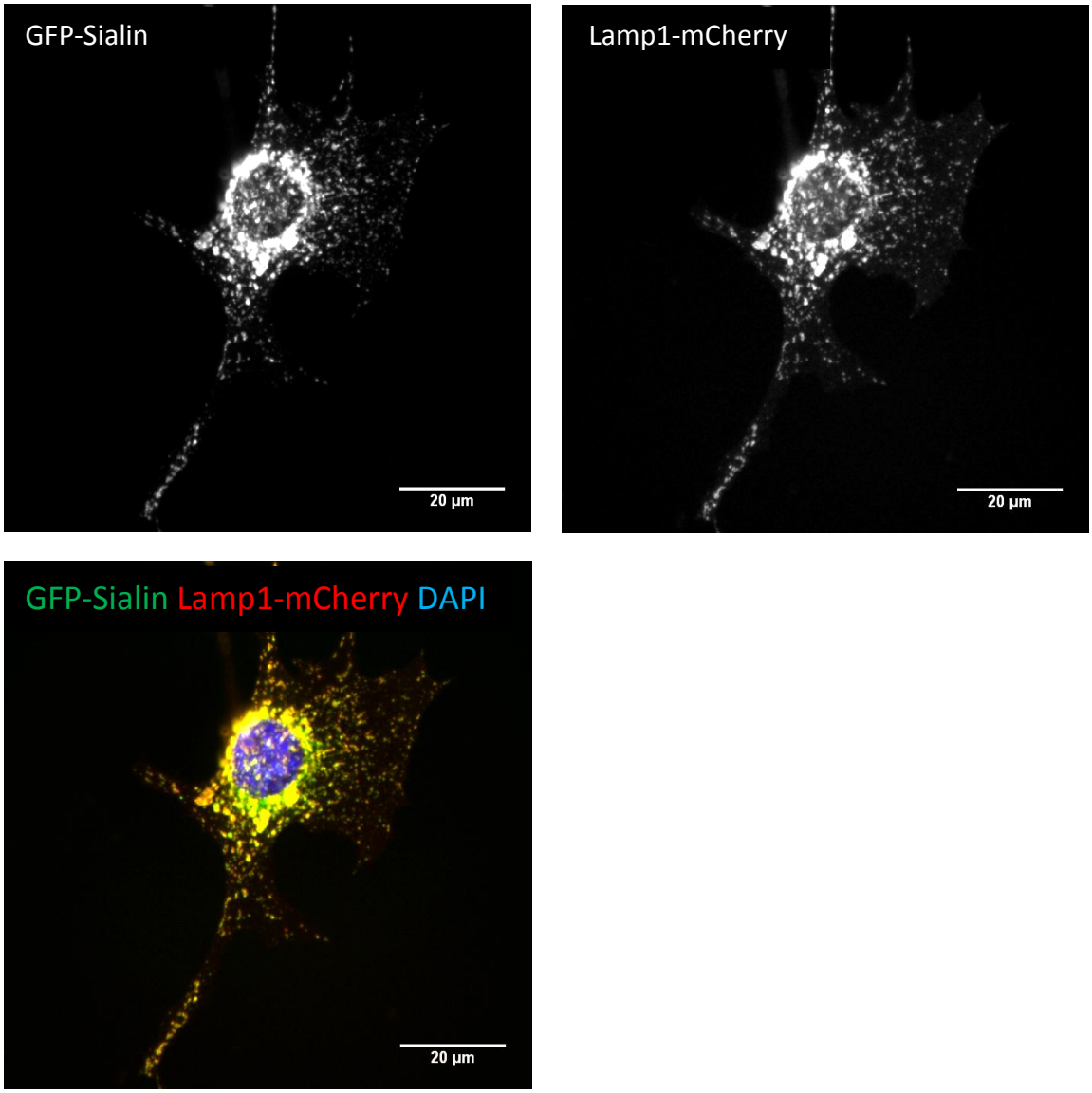

Figure 14: Representative images of H2K myoblasts transfected with Lamp1-mCherry and GFP-sialin. Shown are green channel (GFP-sialin), red channel (Lamp1-mcherry) and false colour merge images.

5.2.7 Quantification of Co-localization for All Experiments

Finally, a post-hoc co-localization analysis was performed using JACoP, as described in Materials and Methods (Bolte et al., 2006). Where appropriate, the Manders (co-localization) coefficients obtained from this analysis have been referred to in the text. Visually, one can see that there is limited variation between the negative co-localization results (A-E and I-T), whereas the positive results (F-H and U) are considerably higher. The non-zero value for negative co-localization can be attributed to the high perinuclear staining with 1709 and the relatively low resolution of epifluorescence microscopy used. The full implications of this are discussed later.

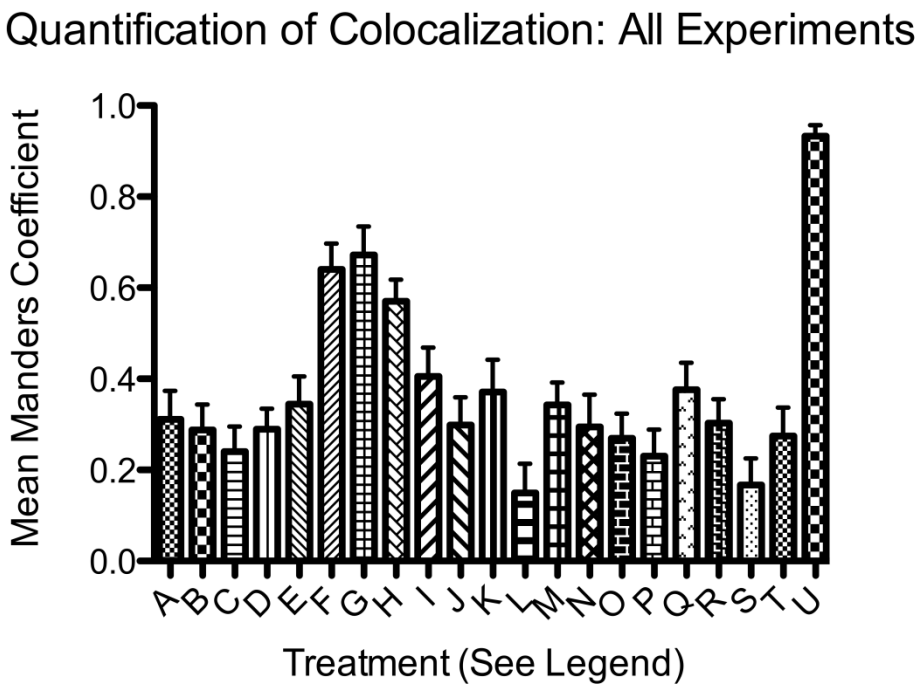

Figure 15: The mean Manders coefficient for all experiments shown in this chapter. N=30 per treatment. Transferrin-568 and 1709: 3 minutes (A), 10 minutes (B), 15 minutes (C), 30 minutes (D). 1709 and EEA1 (E). Transferrin-568 and EEA1 (F, G, H). 1709 and CHC (I). 1709 and 594-ChTxB: 1 minute (J), 3 minutes (K), 6 minutes (L), 10 minutes (M), 15 minutes (N), 20 minutes (O). 594-ChTxB and CHC: 30 seconds (P), 60 seconds (Q). 1709 and Lysotracker (R). 1709 and GFP-Sialin (S). 1709 and Lamp1-mCherry (T). GFP-Sialin and Lamp1-mCherry (U).

5.3.1 Examining β-Dystroglycan Internalization With Epifluorescence Microscopy

The internalization of β-dystroglycan is linked to Y890 phosphorylation (Chapter 3). In order to understand the mechanism governing this process, the endocytic route that β-dystroglycan internalization utilises was investigated. As seen throughout this chapter, the intracellular form of β-dystroglycan is readily detected by immunofluorescence microscopy and H2K myoblasts are amenable to the staining of endosomal compartments. Despite examining a wide range of likely endocytic routes, the mechanism of internalization was not identified by these approaches and exactly how β-dystroglycan internalizes in response to Y890 phosphorylation remains uncertain. However, it is now possible to rule out several pathways, which are present in H2K myoblasts and other cell lines, with a relatively high level of confidence.

The use of immunofluorescence microscopy as an approach can be justified on the basis that it does not suffer the same technical difficulties or caveats as other, contemporary methods. Establishing a method of genetic screening was unfortunately beyond the scope of this work and was therefore not pursued. The treatment of cell lines with inhibitors is widely used in the literature to examine the dependence of certain pathways in the endocytosis of proteins (Huth et al., 2006), and this approach could have been partnered with immunofluorescence microscopy or the internalization assay described previously. However, the utility of this approach has been recently called into question, owing to the lack of efficacy or specifity of inhibition: many, if not all inhibitors effect pathways other than those that they are supposed to selectively inhibit and therefore, the conclusions drawn from this approach are not always reliable (Anderson et al., 1996 ; Shogomori et al., 2001 ; Sharma et al., 2003 ; Vercauteren et al., 2010). For example, in Vercauteren et al., (2010), the inhibition of clathrin-independent endocytosis (as visualized by lactosylceramide uptake) by chlorpromazine, which is a supposedly specific inhibitor of clathrin-dependent uptake, is reported in several cell lines.

However, a drawback of the data presented in this chapter is the high level of peri-nuclear and nuclear staining with 1709. This problem arises primarily due to the use of epifluorescence microscopy, which cannot sufficiently resolve the fluorescent signals near the centre of the cell. The analysis of co-localization with JACoP was partially hampered by this, as fluorophores within this region did co-localize leading to a baseline Manders coefficient of approximately 0.35 (Figure 15). Whilst it was possible to distinguish positive co-localization (Figure 15, X,Y, and Z), one cannot deny that the sensitivity of analysis was affected by the method of microscopy used. Epifluorescence microscopy was chosen as a primary imaging method, as it was fast and readily available in the Winder lab. However, if

significant co-localization were observed, confocal fluorescence microscopy was used as a secondary imaging method, as was the case for the transferrin-568 and EEA1 co-stain (Figure 6). Due to the potentially limited extents of co-localization between sub-populations of pY890-modified β-dystroglycan and endocytic markers, future work may consider the use of confocal microscopy as a primary imaging method. This would improve the sensitivity of co-localization analysis and thus, provide a better means to test future hypotheses.

5.3.2 β-Dystroglycan and Transferrin Receptor Endocytosis

The endocytosis of the transferrin receptor is one of the most studied processes in the field of cellular biology and therefore, one can ascertain the reliability of the co-localization experiments presented here by a comparison with what is known in other experimental systems. The internalization of the transferrin receptor in H2K myoblasts is rapid and occurs within 60 seconds (Figure 2), which is in agreement with kinetics reported in the literature (Klausner et al., 1983 ; Ghosh et al., 1994). This internalization is clathrin-dependent and saturation of the system and subsequent release of transferrin occurs within 20-30 minutes (Harding et al., 1983, Hopkins et al., 1983). Although recycling was not accessed, as internalization was the focus of this work, the transition of transferrin-568 staining, from peripheral to perinuclear sub-cellular regions and eventually both, occurred within a time frame in H2K myoblasts (Figure 3). Presumably, the changes in stain represent changes from early to late and recycling endosomal compartments (Trischler et al., 1999 ; Piper et al., 2001), owing to the proposed localization of these compartments in muscle fibres (Kaisto et al., 1999). Whether this is the case was not addressed fully and future work may further verify the endocytosis of the transferrin receptor in H2K myoblasts by examining co-localization with rab 11 and the mannose-phosphate receptor (Dozynkiewicz et al., 2012). However, one can conclude that the internalization and early endocytic processing of the transferrin receptor is typical of other systems owing to the high degree of co-localization with EEA1 after a 3 minute pulse-chase (Figure 6 ; Mu et al., 1995). Hence, staining with transferrin-568 and for EEA1 were suitable approaches for testing if the internalization of β-dystroglycan is clathrin-dependent.

The lack of any co-localization between 1709 and transferrin-568 at any of the pulse-chase time points examined suggests that pY890-modified β-dystroglycan does not internalize in a clathrin-dependent manner, or traffic via the compartments that house the transferrin receptor (Figure 4). These conclusions are supported by the lack of any significant co-localization with clathrin heavy chain or EEA1 immunostaining (Figures 5 and 7). These findings are in direct opposition to those of Sotgia et al., (2003_a) and may reflect variability between the

different cell lines used, artefacts of overexpression or the limited resolution of the light microscopy employed in the publication. The data presented here does not use transgenic expression of β-dystroglycan tagged with alkaline phosphatise, and is of a higher resolution, which together make the conclusions one draws seem more favourable. However, one cannot exclude variability between cell lines and consequent alterations in endocytic mechanisms, as is the case for ChTxB endocytosis (Shogomori et al., 2001). Ultimately, an analysis of further cell lines will be required before any definite conclusions can be made, but from the data presented here it seems that pY890-modified β-dystroglycan uses an alternative internalization mechanism to that of the transferrin receptor in H2K myoblasts.

5.3.3 β-Dystroglycan and Lipid Raft Endocytosis

Having tested clathrin-dependent endocytosis, the focus of the work moved to clathrin-independent mechanisms. Several endocytic pathways use lipid rafts, as determined by a requirement for cholesterol and insensitivity to clathrin-dependent endocytic inhibition, and these include caveolar- and flotillin-dependent endocytosis (Anderson et al., 1996 ; Nichols et al., 2001 ; Pelkmans et al., 2002 ; Kokuba et al., 2003 ; Glebov et al., 2006). ChTxB selectively binds to GM1 gangliosides that are present in lipid rafts and can be used to follow the endocytosis of proteins dependent on these rafts (Puri et al., 2001; Shogomori et al., 2001). Although there is some dispute over how selective this marker is for clathrin-independent endocytosis, owing to the variability of the pathways used between cell lines and the potential incorporation of lipid rafts into clathrin-coated pits (Torgersen et al., 2001 ; Singh et al., 2003 ; Huth et al. 2006), these criticisms are equally applicable to alternative markers, such as the fluorescently-tagged lactosylceramides (Sharma et al., 2003 ; Marks et al., 2005). These issues could represent the passive accumulation of lipid rafts in clathrin-coated pits (Chang et al., 1992), or a minor requirement for cholesterol in clathrin-mediated endocytosis (Rodal et al., 1999). Either way, this issue raises the requirement for verification of ChTxB staining in experimental systems and so, co-localization with clathrin-positive vesicles was tested in H2K myoblasts. After 30 or 60 seconds of incubation at 37°C, internalized vesicles positive for 594-ChTxB do not co-localize with clathrin-positive vesicles (Figure 10). This suggests that ChTxB can be used as a valid marker for clathrin-independent endocytosis in the H2K myoblast cell line, as internalization does not occur within clathrin-coated vesicles.

Owing to the labelling of multiple pathways with 594-ChTxB, an examination of changes to the visual phenotype of staining was not performed. However, an examination of the data presented in Figure 9, as well as the other images presented in this chapter, shows a similar pattern to transferrin-568 staining: namely a progression from cytosolic to peri-nuclear accumulation. This suggests that clathrin-independent endocytosis functions in a typical manner in H2K myoblasts, although future work may attempt to verify this by examining the co-localization with established markers, such as cavin-1 (Hertzog et al., 2012). When co-immunostained with 1709, the lipid raft-positive vesicles did not co-localize with the β-dystroglycan stain at any of the time points examined. This suggests that β-dystroglycan does not internalize or traffic via a pathway using lipid rafts. As discussed earlier, whilst there is evidence in the literature suggesting an association of β-dystroglycan with components of raft-mediated endocytosis or lipid rafts themselves (Song et al., 1996 ; Vega-Moreno et al., 2012), these associations are contentious (Crosbie et al., 1998 ; Shah et al., 2006). A possible resolution of this argument would be to investigate the presence of pY890-modified β-dystroglycan in cold Triton-insoluble rafts. However, previous experiments from the Winder lab and other groups have indicated that β-dystroglycan (either native or pY890-modified) is not present in such fractions (Steve Winder, personal communication).

Collectively, both the 594-ChTxB and transferrin-568 experiments may also be criticized on the basis of temporal resolution. Although the pulse-chase and incubation conditions were used to examine a wide range of time points, there is the potential that co-localization between internal, pY890-modified β-dystroglycan occurs at time points not studied by this work. Furthermore, the endocytosis of a surface protein does not necessarily take a linear route and can switch between multiple compartments and pathways, as is the case for neuropilin 1 (Dang et al., 2012). Hence it is possible that internalized β-dystroglycan exhibits a transient association with the compartments stained by transferrin-568 and 594-ChTxB that is not detected with the time points used in this work. Although one can counter this argument with the fact that, over a large sample of imaged cells, there is a variation in the compartments stained with these pulse-chase markers and hence, one would expect to see some co-localization, this may have been below the sensitivity of the analysis used, or be simply indiscriminate to the eye.

5.3.4 β-Dystroglycan and the Lysosomal Compartment

Being unable to establish a mechanism of internalization, the work instead focussed on the potential importance of monoubiquitylation of pY890-modified β-dystroglycan (Data Chapter 2). Although this post-translational modification is traditionally associated with degradation (Jentsch et al., 1995), there is a growing body of evidence that it can direct lysosomal degradation, as is the case for the EGFR (Oved et al., 2006). Given the proposed link between β-dystroglycan internalization and degradation as a mechanism for the sarcolemmal loss of the protein in the *mdx* and DMD pathologies, it was of interest to examine the co-localization with the lysosomal compartment. Two methods of visualizing this compartment were available: Lysotracker™-DND-99 staining and transfection with fluorescently-tagged lamp1 and sialin. Both of these methods to visualize lysosomes have been previously reported in the literature (Pelkmans et al., 2001 ; Gotink et al., 2011 ; Dozynkiewicz et al., 2012), and both were demonstrated to give correct staining in H2K myoblasts, on account of the ability to inhibit staining with NH_4Cl treatment (Figure 11 and Ohkuma et al., 1978), or the high degree of co-localization between the two fluorescently-tagged markers (Figure 14). Whilst Lysotracker binding is pH-dependent and hence, Lysotracker can stain endocytic compartments that are late endosomes, the fluorescently-tagged proteins served as positive controls for any co-localization observed.

As shown in Figures 12 and 13, the immunostaining for pY890-modified β-dystroglycan did not co-localize with lysosomal staining with either approach. The interpretation of these findings is complicated by the fact that the epitope detected by 1709 immunostaining may be degraded by the action of the resident proteases of the lysosomal compartment (Seglen et al., 1976). Hence, it is not possible to conclusively disprove the lysosomal degradation of β-dystroglycan with these data. However, lysosomal inhibition could inhibit the internalization of β-dystroglycan, which could be visualized with the internalization assay described in Data Chapter 1. Unfortunately this experiment was not pursued due to time constraints and, therefore, it is only possible to form the limited conclusion that pY890-modified β-dystroglycan is not targeted to the lysosomal compartment.

5.3.5 The Endocytosis of β-dystroglycan in H2K Myoblasts

Whilst the data presented here does not support any of the proposed hypotheses for the internalization of β-dystroglycan, it is possible to discern a more likely mechanism from this work. The internalization of β-dystroglycan is unlikely to be clathrin-dependent or involve lipid rafts that contain GM1, as chiefly determined by transferrin-568 and 594-ChTxB staining respectively. It could however, involve one of the less well characterized endocytic mechanisms that also exist (Huth et al., 2006). During the writing of this thesis, preliminary data was reported suggesting that β-dystroglycan co-traffics with the low density lipoprotein (LDL) receptor (Qi Lu, personal communication). Binding to the LDL receptor enables the co-trafficking of the urokinase receptor (Czekay et al., 2001) and one can speculate that a similar direct or indirect interaction with the pY890-modified form of β-dystroglycan also mediates internalization. A potential flaw of this hypothesis is that the LDL receptor, like the transferrin receptor, is classically thought of as a marker of the clathrin-mediated endocytic pathway (Garcia et al., 1996), which would be in conflict with the data presented here. However, there is a growing body of evidence to suggest that the LDL receptor also utilizes a non-constitutive pathway that is clathrin-, caveolae- and dynamin-independent (Wu et al., 2005 ; Sorrentino et al., 2013 ; Scotti et al., 2013). Thus, on the basis of these findings and the data presented in this chapter, one can hypothesize that β-dystroglycan might co-traffic with the LDL receptor, and this hypothesis can form the basis of future work studying the mechanism of β-dystroglycan internalization in H2K myoblasts.

5.3.6 Summary

The data presented in this chapter can be summarized as follows:

1. pY890-modified β-dystroglycan does not internalize in a clathrin-dependent manner, or utilize compartments containing the transferrin receptor during subsequent endocytosis.
2. pY890-modified β-dystroglycan does not internalize with lipid rafts containing GM1, or utilize compartments containing this marker during subsequent endocytosis.
3. It is unlikely that pY890-modified β-dystroglycan is targeted to lysosomal compartment for degradation.

Chapter 6:
Discussion

6.1.1 A Model for the Internalization of β-Dystroglycan

From the data presented in the preceding chapters, several conclusions may be drawn. In H2K myoblasts, β-dystroglycan is internalized in response to Y890 phosphorylation. Without this particular post-translational modification, β-dystroglycan remains at the plasma membrane. Furthermore, there is a clear distinction between the localization of forms of β-dystroglycan with and without this modification. The internalization of β-dystroglycan may be linked to other phosphorylation events, however these are not solely responsible for the additional species detected on western blots of the internalized protein. Whilst it was not possible to demonstrate that internalized β-dystroglycan is ubiquitylated, the data presented here suggests a link between the processes of Y890 phosphorylation and ubiquitylation. Given this link, and that both the ubiquitylated and internalized forms of β-dystroglycan have similar electrophoretic mobilities, one can assume that ubiquitylation is also linked to internalization. The lead candidate ubiquitin E3-ligase for β-dystroglycan, Nedd4L, does not appear to directly bind β-dystroglycan, despite previous *in vitro* and screening data suggesting otherwise. It remains unresolved whether this ubiquitylation drives endocytic trafficking, or permits subsequent polyubiquitylation and degradation. From kinetic, spatial and co-localization analysis, one can conclude that the endosomal systems involving the transferrin receptor and GM1-positive lipid rafts within H2K myoblasts are not atypical, and that labelling of the compartments containing these trafficking proteins, as well as the endolysosomal compartment, was possible. However, despite examining a range of time points β-dystroglycan does not internalize or traffic with these markers, suggesting that an alternative mechanism of endocytosis is used.

These data, when combined with more established findings, can be summarized diagrammatically as the model shown in Figure 1. From an examination of this overview, several key criticisms and questions arise, which will be discussed in the next section.

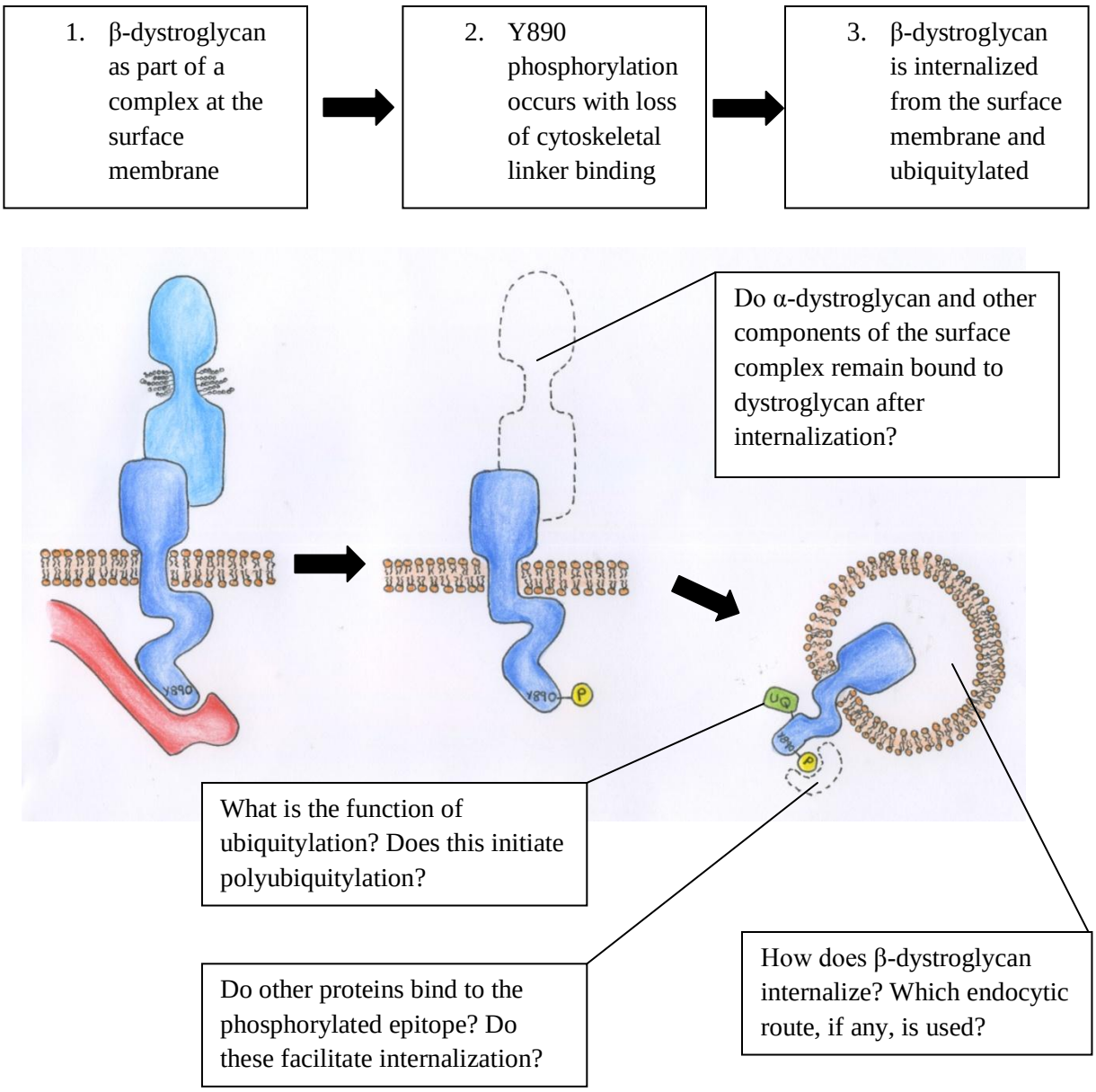

Figure 1: A model for the internalization of β-dystroglycan and questions that arise from this model. From the data presented in this thesis, one can conclude that Y890 phosphorylation causes internalization and subsequent ubiquitylation, but the mechanism for this process, as well as the involvement of other proteins is unclear. All artwork provided as a generous gift by Sarah Palmer.

6.1.2 Key Criticisms and Future Directions

The chief and main criticism of these findings is that they are not supported by replicate experiments in other cell lines. Whilst the H2K myoblast system was chosen on a basis that it most closely mimics primary myoblasts *in vivo* (see Chapter 1, Section 1.3.1), and could be used to support findings from contemporary projects in the Winder lab, it is by no means an exhaustive method of investigation in itself. The H2K myoblast system can be criticized as an *in vitro* model, along with other myoblast cell lines, as several components of the DGC are not expressed (Sen et al., 2011). Whilst H2K myoblasts do express other components and even form the closely related UGC (Thompson et al., 2008), and an altered localization of Y890 phosphorylated β-dystroglycan is reported in skeletal muscle sections (Sotgia et al., 2003_a), the data presented in this thesis are only suggestive of mechanisms present within skeletal muscle. Potential *in vitro* discrepancies can be reduced by testing these hypotheses in either myoblast cell lines that express dystrophin, as used in Goyenvalle et al. (2009), or in myotubes: myoblasts that have fused and differentiated *in vitro* and hence, more closely resemble mature skeletal muscle tissue (Yaffe et al., 1965). Furthermore, assuming that the process of internalization is a key feature of dystrophic pathology, it would be beneficial to verify these findings in either *mdx* or DMD patient myoblasts (Morgan et al., 1994). Whilst the findings described here are supported by observations from the Y890F/mdx mouse (discussed later), a direct examination of this process in skeletal muscle has not been performed. Thus, pursuing these options, as well as utilizing other experimental systems that express β-dystroglycan, would only serve to strengthen any conclusions drawn from the H2K myoblast data presented here.

The data supporting a link between the internalization and ubiquitylation of β-dystroglycan is suggestive, and is certainly not conclusive. As described in Chapter 4 (Section 4.3.2), an experiment was designed to test this hypothesis, however this gave no conclusive result. In addition, whether the proposed mono-ubiquitylation was linked to subsequent poly-ubiquitylation and degradation was not ascertained. As previously described, there is a large body of evidence suggesting a link between β-dystroglycan internalization and degradation by the proteasome (Ohlendieck et al., 1991_a ; Kämper et al., 1992 ; Ohlendieck et al., 1993 ; Sotgia et al., 2001 ; Bonnuccelli et al., 2003 ; Assereto et al., 2005 ; Bonnuccelli et al., 2007). A key step in testing the hypothesis that β-dystroglycan internalization is linked to proteasomal degradation would involve the detection of poly-ubiquitylated forms of the pY890-modified protein. Owing to the transient and minimal presence of poly-ubiquitylated protein species within the cell, it is possible that further ubiquitylations of β-dystroglycan were below the sensitivity of detection. The experiments performed in this thesis did not involve proteasomal inhibition, but repeating these experiments in the presence of proteasomal

inhibitors, such as velcade or MG-132, may allow the detection of such species. Furthermore the veracity of ubiquitylation, as well as an involvement in degradation, could also be tested by lysine mutagenesis. Indeed, the site of ubiquitylation for β-dystroglycan is not described in this thesis, but data from mass spectrometry analyses have positively identified K806 as a site of ubiquitylation (Derek Blake, personal communication). In addition to his, K791 and K792 have also been identified as potential ubiquitylation sites through proteomic screening (Kim et al., 2011). Hence, future work could utilize proteasomal inhibition and mutagenesis of these sites to test the involvement of ubiquitylation in the internalization of β-dystroglycan further.

Currently, the endocytic route or method of internalization for Y890-phosphorylated β-dystroglycan is unknown, although this work permits the exclusion of several possible pathways. It is unlikely that clathrin-dependent internalization occurs, and the lack of co-localization with the transferrin receptor at later time points suggests that compartments of this pathway, such as EEA1-positive early endosomes, do not house internalized β-dystroglycan (Mu et al., 1995 ; Rubino et al., 2000). Similarly, the lack of co-localization with GM1-positive rafts suggests that β-dystroglycan does not internalize via a caveolar- or flotillin-dependent mechanism and does not traffic via the caveosome or golgi compartments (Volonte et al., 1999 ; Nichols et al., 2001 ; Puri et al., 2001 ; Glebov et al., 2006 ; Huth et al., 2006 ; Hernandez-Deviez et al., 2007). Given the reported interaction of Y890-phosphorylated β-dystroglycan with caveolin-3 (Illsey et al., 2002), or the reported co-localization with the transferrin receptor (Sotgia et al., 2003_a), one might expect β-dystroglycan trafficking in H2K myoblasts to occur via the mechanisms mentioned above. However, the differences reported here may reflect variation between experimental systems: whilst expression of caveolin-3 in primary myoblasts has been demonstrated (Parton et al., 1997), other myoblast cell lines do not express this protein until after differentiation, although the functionally equivalent caveolin-1 is expressed during proliferation (Song et al. 1996). The expression of either caveolin-1 or caveolin-3 in H2K myoblasts is not examined in this thesis. Hence, the establishment of whether either of these proteins is expressed, as well as components of other endocytic pathways, would be of benefit to future studies. Furthermore, demonstrating an interaction, by co-immunoprecipitation for example, between specific components of endocytic pathways and Y890-phosphorylated β-dystroglycan may provide a better basis for subsequent microscopic investigation.

In addition, there are still alternative compartments which could contain internalized β-dystroglycan that were not examined in this study. For example, the alternative early endosomal compartment defined by APPL1 (Zoncu et al., 2009), or later compartments defined by the mannose-6-phosphate receptor (Trischler et al., 1999 ; Piper et al., 2001), may house internalized β-dystroglycan. Similarly,

endocytic trafficking may occur by alternative raft-mediated pathways that do not contain GM1 and thus, are not visualized by 594-ChTxB staining (Nichols et al., 2001 ; Puri et al., 2001). To address this, one could perform similar pulse-chase experiments with alternative markers of raft-mediated endocytosis, such as fluorophore-conjugated lactosylceramide (Singh et al., 2003 ; Marks et al., 2005), and test for co-localization with Y890-phosphorylated β-dystroglycan. Furthermore, the internalization and trafficking of β-dystroglycan may not be initiated by the protein alone, but occur together with other proteins, or as part of a larger process. As described earlier (Chapter 5, Section 5.3.5), co-trafficking with the LDL receptor via a clathrin-, caveolin- and dynamin-independent mechanism would fit with the data presented in this thesis, and is a possible avenue of future investigation (Qi Lu, personal communication). Finally, the internalization of β-dystroglycan may be part of a larger, macropinocytic mechanism. In support of this β-dystroglycan has been detected in membrane ruffles, where it is proposed to functionally interact with dynamin and ERK (Spence et al., 2004 ; Zhan et al., 2005). In these instances β-dystroglycan trafficking may not have a strict pathway dependence and this possibility is worth considering in future investigations of the mechanism of internalization.

The model is also hampered by the lack of a definite kinase responsible for the phosphorylation of Y890. Many phosphorylation pathways are altered in the dystrophic state (Batchelor et al., 2006 ; Peter et al., 2006 ; Sen et al., 2011), possibly as a consequence rather than a cause of the loss of sarcolemmal β-dystroglycan, which is proposed to act as signaling scaffold (Oak et al., 2003 ; Spence et al., 2004 ; Batchelor et al., 2006 ; Thompson et al., 2008). Thus, it is not possible to elucidate a candidate kinase from an examination of the state in which β-dystroglycan is lost from the sarcolemma (Ohlendieck et al., 1991_a ; Ohlendieck et al., 1993). Alternative approaches identifying kinases linked to β-dystroglycan phosphorylation also fail to identify a single, likely candidate. Whilst phosphorylation downstream of c-Src activation is evident from a number of studies and is suggestively associated with β-dystroglycan internalization (Sotgia et al., 2001 ; Sotgia et al., 2003_a ; Thompson et al., 2010), there is no evidence to suggest a single effector of the Src family kinases, or a downstream target thereof, as being responsible for Y890 phosphorylation. The identification of the kinase responsible for β-dystroglycan internalization would not only serve to expand and verify the model presented here, but would provide a basis for future therapeutic intervention in dystrophic pathology and as such, is an important focus of future work.

A question arising from this model is whether β-dystroglycan co-traffics with other proteins normally associated with complexes containing dystroglycan. As described earlier, β-dystroglycan is seldom observed in isolation; it is only through a myriad of associated and interacting proteins that this protein exerts a biological

function (see Chapter 1, Sections 1.1.3 and 1.1.4). Furthermore, these components are held together by various intermolecular contacts, and are lost together from the sarcolemma in various dystrophies (see Chapter 1, Sections 1.2.1 to 1.2.4). Admittedly, one can postulate that the regulation and internalization of each of these components is separate and that the loss of these components from the sarcolemma in dystrophic pathology may occur in a sequential nature. In support of this, the levels of α- and β-dystroglycan present at the surface membrane in cancer tissue and cell lines are not always correlative, which suggests post-translational regulation of these two proteins by separate mechanisms. However, one cannot dismiss the possibility that components of the dystroglycan complexes are co-trafficking with β-dystroglycan, and this hypothesis should therefore be addressed.

It is conceivable that complex components and transiently associated proteins, such as α-dystrobrevin-3, sarcospan, Grb2 and the syntrophins, could specify a membrane microdomain around internalized β-dystroglycan, with signaling functions separate to those suggested at the surface membrane. In the study of other surface receptors that undergo endocytic regulation, these internal microdomains are referred to as signalosomes and are an expanding field of cell biology. For example, the neurokinin 1 receptor initiates endosomal signaling from a microdomain defined by β-arrestin and substance P (Pelayo et al., 2011). From the work presented in this thesis it would be easy to extend the experiments and test this hypothesis, for example by co-immunoprecipitation or immunofluorescent co-localization of these complex components with 1709 staining. Furthermore, proteins that traffic with β-dystroglycan may control the endocytic route of this protein and an understanding of how these proteins function in this regard may provide new insights into the pathology of muscular dystrophies.

In a similar vein, one also can not dismiss the importance of scaffolding proteins, which are specifically recruited to the Y890-phosphorylated form of β-dystroglycan, in extending the current model. For example, the data presented in Chapter 4 did not demonstrate a direct interaction between β-dystroglycan and the candidate E3-ubiquitin ligase, Nedd4L. However, the data presented does not disprove the hypothesis that Y890-phosphorylated β-dystroglycan indirectly interacts with this ligase through an additional binding partner, as is proposed for other atypical β-dystroglycan complexes: the β-dystroglycan-Grb2-dynamin complex (Zhan et al., 2005), and the β-dystroglycan-ezrin-Cdc42 complex (Higginson et al., 2008). The phosphorylation of Y890 generates an SH2 (Src Homology 2) domain binding site (Russel et al. 1992) and indeed, the SH2 domain of c-Src has been demonstrated to bind this motif *in vitro* and *in vivo* (Sotgia et al., 2001). Whilst it is possible to view Y890 phosphorylation as key in the mechanism of internalization of β-dystroglycan, owing to the lack of internalized, unphosphorylated protein, Y890 phosphorylation may just act as an initiator for

the process. In this model, “free” cytoplasmic tails of β-dystroglycan are tagged for internalization by Y890 phosphorylation, but it is only the subsequent recruitment of scaffolding proteins and kinases, potentially through SH2 interactions, that initiates the endocytic process. This idea is significant in the interpretation of the data presented in this thesis, as one can only draw a correlative link between the processes of Y890 phosphorylation and internalization; although all internalized β-dystroglycan is phosphorylated on Y890, phosphorylation of Y890 does not necessarily cause internalization. Hence, future work should also establish the importance of additional binding factors in the internalization of β-dystroglycan.

6.1.3 β-Dystroglycan Internalization and Nuclear Translocation

Although not addressed in this thesis until now, any model dealing with the internalization of β-dystroglycan has to take into account a recently identified phenomenon: the translocation of β-dystroglycan to the nucleus. Evidence for this process is still emerging, but from an examination of various systems a common mechanism can be suggested. β-dystroglycan has been observed in the nucleus of LnCaP (Mitchell et al., 2013), HeLa (Fuentes-Mara et al., 2006), Hepa-1, A549 (Lara-Chacón et al., 2010) and C2C12 cells (Martinez-Vieyra et al., 2013). The exact function of β-dystroglycan in this sub-cellular context is unknown, however nuclear translocation has been proposed to be under cell cycle control (Grinu Mathew, PhD Thesis, Sheffield 2011). In support of this, the modulation of β-dystroglycan levels alters cell cycle progression (Sgambato et al., 2004 ; Sgambato et al., 2006) and alters the stability of nuclear components, such as lamin B1, which has a role in the organization of the nuclear organelle (Martinez-Vieyra et al., 2013). Furthermore, the presence of β-dystroglycan within the nucleus alters the expression of several genes, as determined by microarray analysis (Grinu Mathew, PhD Thesis, 2011). Thus, although how β-dystroglycan functions within the nucleus is unknown, that some nuclear function is exerted by the presence of the protein in this organelle is almost certain.

The translocation of β-dystroglycan to the nucleus is dependent on a nuclear localization sequence (NLS) between residues 776-782 (see Chapter 1, Figure 1) and is independent of α-dystroglycan (Oppizzi et al., 2008 ; Lara-Chacón et al., 2010 ; Mitchell et al., 2013). Entry occurs via the nuclear pore complex and involves α- and β-importin (Lara-Chacón et al., 2010). It is conceivable that import into the nucleus occurs after tyrosine phosphorylation and internalization from the membrane and indeed, treatment with orthovanadate has been shown to increase the levels of β-dystroglycan within the nucleus (Lara-Chacón et al., 2010).

However, Y890F mutagenesis promotes nuclear accumulation of β-dystroglycan (Lara-Chacón et al., 2010). This observation would appear to be in direct opposition to the hypothesis that internalization is dependent on phosphorylation of this residue, as nuclear localization must occur downstream of loss from the surface membrane. This finding, however, is not without several important caveats.

Lara-Chacón et al. (2010) report that the Y890F mutant is expressed within an artificial construct containing the cytoplasmic domain of β-dystroglycan fused to a c-terminal GFP tag. One would assume that such a construct, which lacks the transmembrane and ecto domains of β-dystroglycan, would not be anchored to the surface membrane to begin with and hence, according to the model presented in this thesis, Y890 phosphorylation is not required for internalization. Furthermore, assuming that this construct is localized at the surface membrane by binding to other proteins, the presence of the c-terminal GFP tag could impair any dependence on Y890 phosphorylation for internalization. Indeed, biotinylation experiments performed with c-terminally GFP-tagged Y890E and Y890F constructs in H2K myoblasts support this idea, as the internalization of β-dystroglycan appears to occur constitutively in the presence of this tag (Data not shown and Steve Winder, personal communication). However, there still remains a discrepancy in the data presented in Lara-Chacón et al. (2010): if orthovanadate treatment (and presumably Y890 phosphorylation) increases nuclear accumulation, why would Y890F mutagenesis also enhance this?

With the data presented in this thesis it is possible to propose an answer to this question and, more importantly, arrive at a model which links the processes of internalization from the surface membrane and nuclear translocation. The nuclear translocation of β-dystroglycan appears to be a dynamic process (Oppizzi et al., 2008), and, at steady-state conditions, a split distribution of cytoplasmic and nuclear protein is always observed (Lara-Chacón et al., 2010 ; Mitchell et al., 2013 ; Martinez-Vieyra et al., 2013 ; Grinu Mathew, personal communication). In contrast, Y890F mutagenesis appears to cause a single localization of β-dystroglycan to the nucleus, with no protein in the cytoplasm (Lara-Chacón et al., 2010). This localization would suggest that either a factor responsible for nuclear export, or a factor promoting cytoplasmic retention, is lost. The data presented in Data Chapter 2 suggests that the ubiquitylation of β-dystroglycan is exclusively linked to Y890 phosphorylation, thus one could hypothesize that a Y890F mutant would not be ubiquitylated. As discussed previously, the monoubiquitylation of β-dystroglycan may control the nuclear localization of the protein, especially if this modification occurs within or near an NLS (Li et al., 2003 ; Yurchenko et al., 2006 ; Chen et al., 2009 ; Cai et al., 2010 ; Wang et al., 2012). This is possible as ubiquitylation has been proposed to occur at K806, which is near the NLS (residues 776-782) (Derek Blake, personal communication).

The modified model would then occur as follows: β-dystroglycan is internalized from the surface membrane following Y890 phosphorylation and is subsequently sorted for nuclear transport, degradation or subsequent trafficking by ubiquitylation. It is interesting to note that the reports of endogenous β-dystroglycan in the nucleus mostly involve the use of antibodies raised against the unphosphorylated, Y890 epitope, suggesting that Y890 phosphorylation is dispensable for nuclear localization. In this instance, one can then predict that the kinase responsible for Y890 phosphorylation and the initiation of this process is localized exclusively to the cytoplasm; this prediction serves as a means to identify candidate kinases for Y890 phosphorylation, and is an important test of the model described. However, the model is not without an important caveat, which should be considered.

As mentioned earlier, orthovanadate treatment increases the levels of nuclear β-dystroglycan in HeLa cells, which would suggest that ubiquitylation is not important for cytoplasmic retention (Lara-Chacón et al., 2010). However, the increase in levels of nuclear protein does not occur with a concomitant reduction in the levels of cytoplasmic protein (Lara-Chacón et al., 2010). In this instance one can then suggest that the global level of internalized β-dystroglycan is increased by orthovanadate treatment, but the extent of ubiquitylation is unaltered and the excess internalized protein is localized to the nuclear compartment, appearing as an increase in nuclear accumulation in the steady state. This suggestion relies on the assumption that global levels of ubiquitin and the activity of the E3-ubiquitin ligase that targets β-dystroglycan are unaltered by orthovanadate treatment, but this assumption can be tested by future investigation using this model.

Nonetheless, an examination of the related field of nuclear β-dystroglycan prompts an extension of the model presented in this thesis, as well as instigating the basis of future investigation. In light of the predictions outlined above, it is equally possible that the mechanisms governing nuclear trafficking are entirely separate from the findings presented here. Indeed, whilst the establishment of nuclear β-dystroglycan in C2C12 myoblasts (Lara-Chacón et al., 2010 ; Martinez-Vieyra et al., 2013) suggests that this process also occurs in H2K myoblasts, there is no conclusive data to confirm this. The high levels of perinuclear β-dystroglycan immunoreactivity observed with epifluorescence microscopy (see Chapter 5) may be linked to nuclear import in the H2K myoblast system, but this could equally represent localization in a late endosomal compartment, as discussed previously. Furthermore, the *in vivo* relevance of this process is, as of yet, unresolved.

6.2.1 The in vivo Relevance of Y890 Phosphorylation

As mentioned earlier, the findings presented in this thesis are not directly supported by equivalent experiment performed *in vivo*, or even in an *ex vivo* system, such as isolated muscle fibres, yet several inferences can be drawn from the associated study of the β-dystroglycan Y890F knock-in mouse (Miller et al., 2012). The Y890F knock-in mouse displays no overt phenotype and, excepting the absence of any Y890-phosphorylated β-dystroglycan, is indistinguishable from control littermates. Homozygous Y890F mice were crossed with *mdx* mice to obtain Dag1$^{Y890F/Y890F}$:*mdx* mice. As Y890 phosphorylation causes the loss of β-dystroglycan from the surface membrane, and DMD pathology is characterized by the loss of β-dystroglycan from the sarcolemma (Ohlendieck et al., 1993), a phospho-null form of β-dystroglycan should be retained at the sarcolemma and, through the formation of alternative adhesion complexes, such as the UGC, be able to ameliorate dystrophic pathology. Findings from Dag1$^{Y890F/Y890F}$:*mdx* mice suggest that this is the case as parameters of muscle of histopathology are reduced, relative to *mdx* mice, and components of the DGC, including α-sarcoglycan and sarcospan, are restored to the sarcolemma (Miller et al., 2012). Furthermore, physiological parameters, specifically the force drop in response to eccentric contractions, are improved in Dag1$^{Y890F/Y890F}$:*mdx* mice and the increased levels of sarcolemmal plectin 1f, an alternative cytoskeletal protein that binds β-dystroglycan (Rezniczek et al., 2007), suggest that the formation of alternative adhesion complexes is critical in this process.

From these data one can infer that the internalization in response to Y890 phosphorylation described in H2K myoblasts is also a process present *in vivo* in skeletal muscle fibres and is an important step in the pathology of DMD. The key nature of this process is evidenced by the fact that all developing therapies for muscular dystrophy to date, which cause a restoration of β-dystroglycan to the sarcolemma, involve the blockade of Y890 phosphorylation. Whilst the route of administration or mechanism of action varies, these therapies commonly involve the expression of a protein containing a domain which binds to and prevents the phosphorylation of Y890. These therapies include: transgenic expression of utrophin or dystrophin (Cox et al., 1993 ; Phelps et al., 1995 ; Rafael et al., 1998), adenoviral delivery of truncated utrophin or dystrophin genes (Gilbert et al., 1998 ; Wang et al., 2000 ; Wakefield et al., 2000), induction of utrophin overexpression by trophic factors (Krag et al., 2004), small molecules (Tinsley et al., 2011) or artificial transcription factors (Onori et al., 2013), and skipping or directed splicing of mutated exons (Goyenvalle et al., 2004 ; Aartsma-Rus et al., 2004$_a$). Before, this was presumed to be due to a scaffolding effect: that binding localized β-dystroglycan to the surface membrane but, in light of the data presented in this thesis, one can now propose that the blockade of Y890 phosphorylation drives membranous localization. Furthermore, the deletion of the very c-terminus of

dystrophin, the region after the β-dystroglycan binding region, produces no obvious histological or physiological defects in mice (Rafael et al., 1994). Conversely, small lesions in the β-dystroglycan binding domain almost always cause DMD (Aartsma-Rus et al., 2006). Thus, together these data suggest that prevention of Y890 phosphorylation, in these examples by steric protection within a binding domain, is critical in DMD pathology and support the *in vivo* relevance of Y890 phosphorylation in this process.

However, one cannot only stress the importance of the Y890 phosphorylation of β-dystroglycan in dystrophic pathology. Transgenic overexpression of dystrophin isoforms that include the β-dystroglycan binding region, which omit the N-terminal actin binding domain, on the *mdx* background worsen dystrophic pathology (Cox et al., 1994 ; Judge et al., 2006). Similarly, genetic lesions within the actin binding domain of dystrophin present as DMD in patients (Beggs et al., 1991 ; Corrado et al., 1996 ; Aartsma-Rus et al., 2006), indicating the importance of not only Y890 phosphorylation and β-dystroglycan loss, but the mechanical link mediated by dystroglycan complexes within muscle fibres. In addition to this, one only has to examine the wide range of developing therapies that do not involve a restoration of β-dystroglycan to the sarcolemma to understand the importance of other mechanisms in dystrophic pathology.

For example, alterations in the calcium handling of dystrophic muscle fibres has been demonstrated, and these are proposed to result in enhance proteolysis (Kämper et al., 1992 ; Spencer et al., 1995; Dowling et al., 2003), and the inhibition of calcium-dependent proteases, blockade of calcium channels, or transgenic expression of proteins involved in calcium regulation have been demonstrated to ameliorate dystrophic pathology (Kämper et al., 1992 ; Badalamente et al., 2000 ; Goonaserka et al., 2011). In addition, in dystrophic pathology one must also consider the importance of: altered iNOS and nNOS activity and signaling (Louboutin et al., 2001 ; Wehling et al., 2001 ; Ito et al., 2013_b ; Ramachandran et al., 2013), tissue fibrosis (Ito et al., 2013_a), changes to the stem cell niche and impaired regeneration (Mendell et al., 1995 ; Nguyen et al., 2002 ; Griffin et al., 2009 ; Beffy et al., 2010; Boldrin et al., 2012 ; Lin et al., 2013), growth factor signaling and muscle differentiation (Maltzahn et al., 2012 ; Mikami et al., 2012), Akt signaling and the hypertrophic response (Peter et al., 2006 ; Peter et al., 2009 ; Marshall et al., 2012_a), NF-κB activation and the inflammatory response (Louboutin et al., 2001 ; Bonnuccelli et al., 2007), the stabilization of the DGC by components of the ECM (Amenta et al., 2011), sphingosine-1-phosphate signaling (Pantoja et al., 2013), integrin regulation and signaling (Burkin et al., 2001 ; Liu et al., 2011 ; Sen et al., 2011) and matrix metalloproteinase cleavage of β-dystroglycan (Matsumara et al., 2005 ; Michaluk et al., 2007 ; Delfin et al., 2011 ; Taniquiti et al., 2012).

Arguably, this long list of additional mechanisms within dystrophic pathology is a consequence of the loss of β-dystroglycan and the DGC from the sarcolemma. Microlesions in the sarcolemma, due to impaired sarcolemmal integrity in the absence of the DGC, are proposed to be responsible for altered calcium homeostasis and NOS signaling, which lead to necrosis and the hypertrophic response (Collet et al., 1999 ; Batchelor et al., 2006 ; Tinsley et al., 2011 ; Ito et al., 2013_b). These responses could then lead to the impaired regeneration, exhaustion of the stem cell niche and fibrosis observed in dystrophic muscle tissue (Coulton et al., 1988 ; Mendell et al., 1995). Furthermore, one would expect to see large changes in cellular signaling in the absence of β-dystroglycan, which acts as a scaffold for various signaling proteins, and indeed this is the case (Oak et al., 2003 ; Spence et al., 2004 ; Peter et al., 2006 ; Thompson et al., 2008 ; Sen et al., 2011). However, if the loss of β-dystroglycan from the sarcolemma were of such importance, why does the blockade of Y890 phosphorylation not fully prevent all dystrophic pathology? In the case of gene or molecular therapy trials one might cite the age at which a therapy is administered and an inability to prevent pathological changes that have occurred during development (McDonald et al., 2010 ; Cirak et al., 2011; Goemans et al., 2011 ; Malerba et al., 2011). Yet, to return to the Y890F knock-in mouse data, if this is true why does the blockade of Y890 phosphorylation from the embryonic stages of development not fully cure the relatively mild *mdx* pathology (Miller et al., 2012)?

6.2.2 Towards a Cure for Duchenne Muscular Dystrophy

The answer to this question is found upon re-examination of the complexes that involve β-dystroglycan in skeletal muscle tissue (see Chapter 1, Sections 1.13 and 1.1.4). In the *mdx* state Y890F β-dystroglycan is localized to the sarcolemma, where it presumably binds the alternative cytoskeletal linker protein plectin 1f (Rezniczek et al., 2007 ; Miller et al., 2012). Although plectin 1f binds to actin filaments and functionally substitutes dystrophin in mechanical linkage, it does not recruit the same accessory proteins that are associated with the DGC. In this regard, even the closely homologous protein utrophin does not fully recapitulate the functional capacity of dystrophin, as evidenced by the inability to fully cure dystrophic pathology with transgenic utrophin overexpression (Rafael et al., 1998). Specifically, this could be due to the absence of the nNOS binding site within the rod domain of utrophin, which is present in dystrophin (Lai et al., 2009 ; Lai et al., 2013). Thus, even the replacement of all lost DGCs with UGCs in the dystrophic state cannot elicit a full cure. In a similar vein, a DMD patient has been reported with a small deletion encompassing the syntrophin binding region of dystrophin (exons 72-73), which does not generate a premature stop (Suzuki et al. 1995 ; Béroud et al., 2007). As described previously, dystrophin contains various regions

that bind accessory proteins, namely the syntrophins and α-dystrobrevins, and these in turn recruit adaptors (Grb2 - Oak et al., 2001), channels (SkM1 and 2 – Gee et al., 1998), kinases (MAST and SAST – Lumeng et al., 1999) and can even control the stoichiometry of the complex (Newey et al., 2000_a). So, blocking Y890 phosphorylation of β-dystroglycan will not cure DMD or the *mdx* model, as it does not restore all the full DGC.

Hence, it is unsurprising that to date there is no cure for DMD, as each form of therapy carries similar caveats. Returning to gene therapy with truncated utrophins, which share a common strategy with the Y890F knock-in mutation, a complete amelioration of dystrophic pathology does not occur even with high levels of expression (Phelps et al., 1995 ; Wakefield et al., 2000 ; Gregorovic et al., 2006). One of the reasons for this is that these proteins do not scaffold the other components of the DGC. Therapeutic approaches which generate the re-expression of fully functional dystrophin, excepting a minor lesion, such as exon skipping and snRNA spliceosome targeting, are not applicable to all DMD patients, and at best can only produce a BMD or XDLC phenotype (Béroud et al., 2007). Furthermore, exon skipping efficiencies estimated *in vitro* are not the same as those observed *in vivo* (Aartsma-Rus et al., 2004_a ; Aartsma-Rus et al., 2004_b ; Mitrpant et al., 2009 ; Popplewell et al., 2010 ; Kayali et al., 2012). Similarly, the design of small molecules or artificial transcription factors is flawed by an incomplete knowledge of the factors governing *in vivo* specificity (Choo et al., 1997 ; Corbi et al., 2000 ; Chancellor et al., 2011 ; Tinsley et al., 2011 ; Onori et al., 2013). Therapies are also hindered by the route of delivery: for example the delivery of mini genes encapsulated within gutted adenoviral vectors or antisense oligonucleotides only transduces fibres near the site of injection (Goyenvalle et al., 2004 ; van Deutekom et al., 2007). Whilst the systemic delivery of antisense oligonucleotides is possible (Cirak et al., 2011), the efficacy of this route of administration is hard to predict (Yin et al., 2010_b).

In spite of these complications and difficulties, one can see evidence for the progression towards a functional cure for DMD. The delivery of genes or oligonucleotides has been enhanced by conjugation to cell penetrating peptides, which permit the specific targeting of skeletal muscle tissue with systemic delivery (Yin et al., 2008 ; Yin et al., 2009 ; Goyenvalle et al., 2010 ; Yin et al., 2010_a). Phage screening and testing within *mdx* mice, can be used to develop novel peptides, with a higher efficacy and specificity (Seow et al., 2010). Furthermore, the difficulties with adenoviral vector delivery can be overcome by selecting vectors with a higher tropism for skeletal muscle tissue (Goyenvalle et al., 2012). Indeed, the development of exon splicing therapy underscores how knowledge from other fields of biology can be used to augment and improve existing therapies (Goyenvalle et al., 2004 ; Goyenvalle et al., 2009 ; Goyenvalle et al., 2012). Dual therapy trials, exemplified by the combination of myostatin and micro-utrophin

delivery, also highlight the potential of combinatorial therapy (Sonnemann et al., 2009). Thus, whilst no therapy alone is fully curative, one can envisage how combined approaches, or the exchange of knowledge from similar fields, can improve therapies so that they accomplish this goal. In this light, one can fully evaluate the importance of the Y890F:*mdx* trial and also the importance of Y890 phosphorylation and the internalization of β-dystroglycan.

Although not curative, blocking Y890 phosphorylation and restoring β-dystroglycan to the sarcolemma does ameliorate dystrophic pathology (Miller et al., 2012). Assuming that this effect is caused by blocking the internalization of β-dystroglycan, as is observed in H2K myoblasts, then this knowledge provides the basis for alternative therapies. For example, inhibiting the kinase responsible for the phosphorylation of Y890 in dystrophic patients would extend the lifetime of β-dystroglycan at the sarcolemma, and one would predict this to enhance the effectiveness of other therapies. In addition, one could use small peptides which bind both the c-terminus of β-dystroglycan and dystrophin/utrophin/plectin 1f to block Y890 phosphorylation and maintain a mechanical link, in a manner similar to mini-agrin therapy (Moll et al., 2001). The synergy of combinatorial approaches has been used in other research fields, such as HIV treatment, to elicit better therapies and one would also expect this to be the case for DMD. Hence, any knowledge of the mechanism controlling sarcolemmal β-dystroglycan loss in dystrophic pathology can be utilized, in combination with other existing therapies, to provide better, or even full, cures for patients.

One criticism stands between this rose-tinted view of the future and reality and that is the heterogeneity of muscular dystrophies and genetic diseases in general. Studies of BMD patients with the same genetic lesion, but differing phenotypes, indicate the importance of the level of expression as well as the type of mutation of the *DMD* gene in dystrophic pathology (Corrado et al., 1996). Indeed, even within the genetic proximity of a family, one observes differences in the phenotype of muscular dystrophy presented by the same causative mutation (McNally et al., 1996 ; Melis et al., 1998 ; Aartsma-Rus et al., 2006). This genetic variation and the importance of other, unknown factors in dystrophic pathology may explain the variability of treatment efficacy in clinical trials for DMD (Cirak et al., 2011). Exome analyses have been used to identify additional genetic variants that may cause the differences in disease severity observed between consanguineous patients (McDonald et al., 2012), but how these variations effect disease is currently unknown. From the data presented in this thesis, one could predict that the activity of the kinase that phosphorylates Y890 may influence the severity of BMD and DMD, yet as of writing, the identity of this kinase is unknown. Thus, these findings only underscore the current limitation of knowledge regarding the processes involved in dystrophic pathology. Can a full cure for every DMD patient

be realized before the importance of every factor in dystrophic pathology is understood?

Hence, understanding the cellular biology of proteins such as β-dystroglycan, which have a key role in the formation of the DGC, is of paramount importance. To return to the model presented earlier, there are still many questions that remain unanswered concerning the mechanism of sarcolemmal β-dystroglycan loss. However, the research presented in this thesis provides a basis for future study and highlights the specific importance of Y890 phosphorylation in other processes, such as ubiquitylation. It is through research of this kind that the importance of other factors in dystrophic pathology can be addressed and hence, a full cure for DMD may be developed. Thus, future research into the mechanisms controlling β-dystroglycan, as well as being of scientific interest, is of benefit to the future of mankind, and is justified in both regards.

Bibliography

Aartsma-Rus, A., Kaman, W.E., Bremmer-Bout, M., Janson, A., Dunnen, den, J.T., van Ommen, G.B., and Van Deutekom, J. (2004a). Comparative analysis of antisense oligonucleotide analogs for targeted DMD exon 46 skipping in muscle cells. Gene Ther. *11*, 1391–1398.

Aartsma-Rus, A., Janson, A.A.M., Kaman, W.E., Bremmer-Bout, M., Van Ommen, G.-J.B., Dunnen, Den, J.T., and Van Deutekom, J.C.T. (2004b). Antisense-induced multiexon skipping for Duchenne muscular dystrophy makes more sense. Am. J. Hum. Genet. *74*, 83–92.

Aartsma-Rus, A., Van Deutekom, J.C.T., Fokkema, I.F., Van Ommen, G.-J.B., and Dunnen, Den, J.T. (2006). Entries in the Leiden Duchenne muscular dystrophy mutation database: An overview of mutation types and paradoxical cases that confirm the reading-frame rule. Muscle Nerve *34*, 135–144.

Adams, M.E., Butler, M.H., Dwyer, T.M., Peters, M.F., Murnane, A.A., and Froehner, S.C. (1993). Two forms of mouse syntrophin, a 58 kd dystrophin-associated protein, differ in primary structure and tissue distribution. Neuron *11*, 531–540.

Allikian, M.J., Hack, A.A., Mewborn, S., Mayer, U., and McNally, E.M. (2004). Genetic compensation for sarcoglycan loss by integrin alpha7beta1 in muscle. Journal of Cell Science *117*, 3821–3830.

Ambrose, H.J., Blake, D.J., Nawrotzki, R.A., and Davies, K.E. (1997). Genomic organization of the mouse dystrobrevin gene: comparative analysis with the dystrophin gene. Genomics *39*, 359–369.

Amenta, A.R., Yilmaz, A., Bogdanovich, S., McKechnie, B.A., Abedi, M., Khurana, T.S., and Fallon, J.R. (2011). Biglycan recruits utrophin to the sarcolemma and counters dystrophic pathology in mdx mice. Proceedings of the National Academy of Sciences *108*, 762–767.

Anderson, J.T., Rogers, R.P., and Jarrett, H.W. (1996). Ca-Calmodulin Binds to the Carboxyl-terminal Domain of Dystrophin. Journal of Biological Chemistry *271*, 6605–6610.

Anthony, K., Cirak, S., Torelli, S., Tasca, G., Feng, L., Arechavala-Gomeza, V., Armaroli, A., Guglieri, M., Straathof, C.S., Verschuuren, J.J., et al. (2011). Dystrophin quantification and clinical correlations in Becker muscular dystrophy: implications for clinical trials. Brain *134*, 3547–3559.

Aoki, T., Nomura, R., and Fujimoto, T. (1999). Tyrosine phosphorylation of caveolin-1 in the endothelium. Experimental Cell Research *253*, 629–636.

Araishi, K., Sasaoka, T., Imamura, M., Noguchi, S., Hama, H., Wakabayashi, E., Yoshida, M., Hori, T., and Ozawa, E. (1999). Loss of the sarcoglycan complex and sarcospan leads to muscular dystrophy in beta-sarcoglycan-deficient mice. Human Molecular Genetics *8*, 1589–1598.

Arechavala-Gomeza, V., Kinali, M., Feng, L., Guglieri, M., Edge, G., Main, M., Hunt, D., Lehovsky, J., Straub, V., Bushby, K., et al. (2010). Revertant fibres and dystrophin traces in Duchenne muscular dystrophy: Implication for clinical trials. Neuromuscular Disorders *20*, 295–301.

Armstrong, S.C., Latham, C.A., and Ganote, C.E. (2003). An ischemic beta-dystroglycan (betaDG) degradation product: correlation with irreversible injury in adult rabbit cardiomyocytes. Mol. Cell. Biochem. *242*, 71–79.

Assereto, S., Stringara, S., Sotgia, F., Bonuccelli, G., Broccolini, A., Pedemonte, M., Traverso, M., Biancheri, R., Zara, F., Bruno, C., et al. (2006). Pharmacological rescue of the dystrophin-glycoprotein complex in Duchenne and Becker skeletal muscle explants by proteasome inhibitor treatment. Am. J. Physiol., Cell Physiol. *290*, C577–C582.

Badalamente, M.A., and Stracher, A. (2000). Delay of muscle degeneration and necrosis in mdx mice by calpain inhibition. Muscle Nerve *23*, 106–111.

Barton, E.R., Morris, L., Kawana, M., Bish, L.T., and Toursel, T. (2005). Systemic administration of L-arginine benefits mdx skeletal muscle function. Muscle Nerve *32*, 751–760.

Batchelor, C.L., and Winder, S.J. (2006). Sparks, signals and shock absorbers: how dystrophin loss causes muscular dystrophy. Trends in Cell Biology *16*, 198–205.

Batchelor, C.L., Higginson, J.R., Chen, Y.-J., Vanni, C., Eva, A., and Winder, S.J. (2007). Recruitment of Dbl by ezrin and dystroglycan drives membrane proximal Cdc42 activation and filopodia formation. Cell Cycle *6*, 353–363.

Beffy, P., Del Carratore, R., Masini, M., Furling, D., Puymirat, J., Masiello, P., and Simili, M. (2010). Altered signal transduction pathways and induction of autophagy in human myotonic dystrophy type 1 myoblasts. International Journal of Biochemistry and Cell Biology *42*, 1973–1983.

Beggs, A.H., Hoffman, E.P., Snyder, J.R., Arahata, K., Specht, L., Shapiro, F., Angelini, C., Sugita, H., and Kunkel, L.M. (1991). Exploring the molecular basis for variability among patients with Becker muscular dystrophy: dystrophin gene and protein studies. Am. J. Hum. Genet. *49*, 54–67.

Béroud, C., Tuffery-Giraud, S., Matsuo, M., Hamroun, D., Humbertclaude, V., Monnier, N., Moizard, M.-P., Voelckel, M.-A., Calemard, L.M., Boisseau, P., et al. (2007). Multiexon skipping leading to an artificial DMD protein lacking amino acids from exons 45 through 55 could rescue up to 63% of patients with Duchenne muscular dystrophy. Hum. Mutat. *28*, 196–202.

Bies, R.D., Caskey, C.T., and Fenwick, R. (1992). An intact cysteine-rich domain is required for dystrophin function. J. Clin. Invest. *90*, 666–672.

Blake, D.J., Love, D.R., Tinsley, J., Morris, G.E., Turley, H., Gatter, K., Dickson, G., Edwards, Y.H., and Davies, K.E. (1992). Characterization of a 4.8kb transcript from the Duchenne muscular dystrophy locus expressed in Schwannoma cells. Human Molecular Genetics *1*, 103–109.

Blake, D.J., Nawrotzki, R., Peters, M.F., Froehner, S.C., and Davies, K.E. (1996). Isoform diversity of dystrobrevin, the murine 87-kDa postsynaptic protein. Journal of Biological Chemistry *271*, 7802–7810.

Blake, D.J., Nawrotzki, R., Loh, N.Y., Gorecki, D.C., and Davies, K.E. (1998). beta-dystrobrevin, a member of the dystrophin-related protein family. Proceedings of the National Academy of Sciences *95*, 241–246.

Boldrin, L., Neal, A., Zammit, P.S., Muntoni, F., and Morgan, J.E. (2012). Donor satellite cell engraftment is significantly augmented when the host niche is preserved and endogenous satellite cells are incapacitated. Stem Cells *30*, 1971–1984.

Bolte, S., and Cordelières, F.P. (2006). A guided tour into subcellular colocalization analysis in light microscopy. J Microsc *224*, 213–232.

Bonilla, E., Fischbeck, K., and Schotland, D.L. (1981). Freeze-fracture studies of muscle caveolae in human muscular dystrophy. The American Journal of Pathology *104*, 167–173.

Bonilla, E., Samitt, C.E., Miranda, A.F., Hays, A.P., Salviati, G., DiMauro, S., Kunkel, L.M., Hoffman, E.P., and Rowland, L.P. (1988). Duchenne muscular dystrophy: deficiency of dystrophin at the muscle cell surface. Cell *54*, 447–452.

Bonuccelli, G., Sotgia, F., Schubert, W., Park, D.S., Frank, P.G., Woodman, S.E., Insabato, L., Cammer, M., Minetti, C., and Lisanti, M.P. (2003). Proteasome inhibitor (MG-132) treatment of mdx mice rescues the expression and membrane localization of dystrophin and dystrophin-associated proteins. The American Journal of Pathology *163*, 1663–1675.

Bonuccelli, G., Sotgia, F., Capozza, F., Gazzerro, E., Minetti, C., and Lisanti, M.P. (2007). Localized treatment with a novel FDA-approved proteasome inhibitor blocks the degradation of dystrophin and dystrophin-associated proteins in mdx mice. Cell Cycle *6*, 1242–1248.

Boppart, M.D., Burkin, D.J., and Kaufman, S.J. (2006). Alpha7beta1-integrin regulates mechanotransduction and prevents skeletal muscle injury. Am. J. Physiol., Cell Physiol. *290*, C1660–C1665.

Bowe, M.A., Mendis, D.B., and Fallon, J.R. (2000). The small leucine-rich repeat proteoglycan biglycan binds to alpha-dystroglycan and is upregulated in dystrophic muscle. The Journal of Cell Biology *148*, 801–810.

Bradley, W.G., Fullthorpe, J.J. (1978). Studies of sarcolemmal integrity in myopathic muscle. Neurology *28*, 670-677.

Brenman, J.E., Chao, D.S., Gee, S.H., McGee, A.W., Craven, S.E., Santillano, D.R., Wu, Z., Huang, F., Xia, H., Peters, M.F., et al. (1996). Interaction of nitric oxide synthase with the postsynaptic density protein PSD-95 and alpha1-syntrophin mediated by PDZ domains. Cell *84*, 757–767.

Brown, S.C., Fassati, A., Popplewell, L., Page, A.M., Henry, M.D., Campbell, K.P., and Dickson, G. (1999). Dystrophic phenotype induced in vitro by antibody blockade of muscle alpha-dystroglycan-laminin interaction. Journal of Cell Science *112 (Pt 2)*, 209–216.

Brown, S.C., Torelli, S., Brockington, M., Yuva, Y., Jimenez, C., Feng, L., Anderson, L., Ugo, I., Kroger, S., Bushby, K., et al. (2004). Abnormalities in alpha-dystroglycan expression in MDC1C and LGMD2I muscular dystrophies. The American Journal of Pathology *164*, 727–737.

Bulfield, G., Siller, W.G., Wight, P.A., and Moore, K.J. (1984). X chromosome-linked muscular dystrophy (mdx) in the mouse. Proceedings of the National Academy of Sciences *81*, 1189–1192.

Burkin, D.J., Wallace, G.Q., Nicol, K.J., Kaufman, D.J., and Kaufman, S.J. (2001). Enhanced expression of the alpha 7 beta 1 integrin reduces muscular dystrophy and restores viability in dystrophic mice. The Journal of Cell Biology *152*, 1207–1218.

Cai, C., Weisleder, N., Ko, J.-K., Komazaki, S., Sunada, Y., Nishi, M., Takeshima, H., and Ma, J. (2009). Membrane repair defects in muscular dystrophy are linked to altered interaction between MG53, caveolin-3, and dysferlin. Journal of Biological Chemistry *284*, 15894–15902.

Cai, Q., and Robertson, E.S. (2010). Ubiquitin/SUMO modification regulates VHL protein stability and nucleocytoplasmic localization. PLoS ONE *5*, e12636.

Campbell, K.P. (1995). Three muscular dystrophies: loss of cytoskeleton-extracellular matrix linkage. Cell *80*, 675–679.

Carter, L.L., Redelmeier, T.E., Woollenweber, L.A., and Schmid, S.L. (1993). Multiple GTP-binding proteins participate in clathrin-coated vesicle-mediated endocytosis. The Journal of Cell Biology *120*, 37–45.

Cerecedo, D., Martínez-Rojas, D., Chávez, O., Martínez-Pérez, F., García-Sierra, F., Rendon, A., Mornet, D., and Mondragón, R. (2005). Platelet adhesion: structural and functional diversity of short dystrophin and utrophins in the formation of dystrophin-associated-protein complexes related to actin dynamics. Thromb. Haemost. *94*, 1203–1212.

Cerecedo, D., Cisneros, B., Suárez-Sánchez, R., Hernández-González, E., and Galván, I. (2008). beta-Dystroglycan modulates the interplay between actin and microtubules in human-adhered platelets. Br J Haematol *141*, 517–528.

Chancellor, D.R., Davies, K.E., De Moor, O., Dorgan, C.R., Johnson, P.D., Lambert, A.G., Lawrence, D., Lecci, C., Maillol, C., Middleton, P.J., et al. (2011). Discovery of 2-arylbenzoxazoles as upregulators of utrophin production for the treatment of Duchenne muscular dystrophy. J. Med. Chem. *54*, 3241–3250.

Chang, W.J., Rothberg, K.G., Kamen, B.A., and Anderson, R.G. (1992). Lowering the cholesterol content of MA104 cells inhibits receptor-mediated transport of folate. The Journal of Cell Biology *118*, 63–69.

Chen, B.B., and Mallampalli, R.K. (2009). Masking of a nuclear signal motif by monoubiquitination leads to mislocalization and degradation of the regulatory enzyme cytidylyltransferase. Molecular and Cellular Biology *29*, 3062–3075.

Chen, H.I., and Sudol, M. (1995). The WW domain of Yes-associated protein binds a proline-rich ligand that differs from the consensus established for Src homology 3-binding modules. Proceedings of the National Academy of Sciences *92*, 7819–7823.

Chockalingam, P.S., Cholera, R., Oak, S.A., Zheng, Y., Jarrett, H.W., and Thomason, D.B. (2002). Dystrophin-glycoprotein complex and Ras and Rho GTPase signaling are altered in muscle atrophy. Am. J. Physiol., Cell Physiol. *283*, C500–C511.

Choo, Y., and Klug, A. (1997). Physical basis of a protein-DNA recognition code. Curr. Opin. Struct. Biol. *7*, 117–125.

Chung, W., and Campanelli, J.T. (1999). WW and EF hand domains of dystrophin-family proteins mediate dystroglycan binding. Mol. Cell Biol. Res. Commun. *2*, 162–171.

Cirak, S., Arechavala-Gomeza, V., Guglieri, M., Feng, L., Torelli, S., Anthony, K., Abbs, S., Garralda, M.E., Bourke, J., Wells, D.J., et al. (2011). Exon skipping and dystrophin restoration in patients with Duchenne muscular dystrophy after systemic phosphorodiamidate morpholino oligomer treatment: an open-label, phase 2, dose-escalation study. Lancet *378*, 595–605.

Cohen, M.W., Jacobson, C., Yurchenco, P.D., Morris, G.E., and Carbonetto, S. (1997). Laminin-induced clustering of dystroglycan on embryonic muscle cells: comparison with agrin-induced clustering. The Journal of Cell Biology *136*, 1047–1058.

Cohn, R.D., Henry, M.D., Michele, D.E., Barresi, R., Saito, F., Moore, S.A., Flanagan, J.D., Skwarchuk, M.W., Robbins, M.E., Mendell, J.R., et al. (2002). Disruption of DAG1 in differentiated skeletal muscle reveals a role for dystroglycan in muscle regeneration. Cell *110*, 639–648.

Collet, C., Allard, B., Tourneur, Y., and Jacquemond, V. (1999). Intracellular calcium signals measured with indo-1 in isolated skeletal muscle fibres from control and mdx mice. The Journal of Physiology *520 Pt 2*, 417–429.

Corbi, N., Libri, V., Fanciulli, M., Tinsley, J.M., Davies, K.E., and Passananti, C. (2000). The artificial zinc finger coding gene "Jazz" binds the utrophin promoter and activates transcription. Gene Ther. *7*, 1076–1083.

Corrado, K., Mills, P.L., and Chamberlain, J.S. (1994). Deletion analysis of the dystrophin-actin binding domain. FEBS Letters *344*, 255–260.

Corrado, K., Rafael, J.A., Mills, P.L., Cole, N.M., Faulkner, J.A., Wang, K., and Chamberlain, J.S. (1996). Transgenic mdx mice expressing dystrophin with a deletion in the actin-binding domain display a "mild Becker" phenotype. The Journal of Cell Biology *134*, 873–884.

Costello, B.R., Shafiq, S.A. (1979). Freeze-fracture study of muscle plasmalemma in normal and dystrophic chickens. Muscle Nerve. *2*, 191-201.

Cote, P.D., Moukhles, H., Lindenbaum, M., and Carbonetto, S. (1999). Chimaeric mice deficient in dystroglycans develop muscular dystrophy and have disrupted myoneural synapses. Nat. Genet. *23*, 338–342.

Coulton, G.R., Morgan, J.E., Partridge, T.A., Sloper, J.C. (1988). The mdx mouse skeletal muscle myopathy: I. A histological, morphometric and biochemical investigation. Neuropathol. Appl. Neurobiol. *14*, 53-70.

Cox, G.A., Cole, N.M., Matsumura, K., Phelps, S.F., Hauschka, S.D., Campbell, K.P., Faulkner, J.A., and Chamberlain, J.S. (1993). Overexpression of dystrophin in transgenic mdx mice eliminates dystrophic symptoms without toxicity. Nature *364*, 725–729.

Cox, G.A., Sunada, Y., Campbell, K.P., and Chamberlain, J.S. (1994). Dp71 can restore the dystrophin-associated glycoprotein complex in muscle but fails to prevent dystrophy. Nat. Genet. *8*, 333–339.

Cox, S., Rosten, E., Monypenny, J., Jovanovic-Talisman, T., Burnette, D.T., Lippincott-Schwartz, J., Jones, G.E., and Heintzmann, R. (2012). Bayesian localization microscopy reveals nanoscale podosome dynamics. Nature Publishing Group *9*, 195–200.

Côté, P.D., Moukhles, H., and Carbonetto, S. (2002). Dystroglycan is not required for localization of dystrophin, syntrophin, and neuronal nitric-oxide synthase at the sarcolemma but regulates integrin alpha 7B expression and caveolin-3 distribution. Journal of Biological Chemistry *277*, 4672–4679.

Crisp, A., Yin, H., Goyenvalle, A., Betts, C., Moulton, H.M., Seow, Y., Babbs, A., Merritt, T., Saleh, A.F., Gait, M.J., et al. (2011). Diaphragm rescue alone prevents heart dysfunction in dystrophic mice. Human Molecular Genetics *20*, 413–421.

Crosbie, R.H., Heighway, J., Venzke, D.P., Lee, J.C., and Campbell, K.P. (1997). Sarcospan, the 25-kDa transmembrane component of the dystrophin-glycoprotein complex. Journal of Biological Chemistry *272*, 31221–31224.

Crosbie, R.H., Yamada, H., Venzke, D.P., Lisanti, M.P., and Campbell, K.P. (1998). Caveolin-3 is not an integral component of the dystrophin glycoprotein complex. FEBS Letters *427*, 279–282.

Crosbie, R.H., Lebakken, C.S., Holt, K.H., Venzke, D.P., Straub, V., Lee, J.C., Grady, R.M., Chamberlain, J.S., Sanes, J.R., and Campbell, K.P. (1999). Membrane targeting and stabilization of sarcospan is mediated by the sarcoglycan subcomplex. The Journal of Cell Biology *145*, 153–165.

Cross, S.S., Lippitt, J., Mitchell, A., Hollingsbury, F., Balasubramanian, S.P., Reed, M.W.R., Eaton, C., Catto, J.W., Hamdy, F., and Winder, S.J. (2008). Expression of beta-dystroglycan is reduced or absent in many human carcinomas. Histopathology *53*, 561–566.

Cullen, M.J., Walsh, J., Stevenson, S.A., Rothery, S., and Severs, N.J. (1998). Co-localization of dystrophin and beta-dystroglycan demonstrated in en face view by double immunogold labeling of freeze-fractured skeletal muscle. J. Histochem. Cytochem. *46*, 945–954.

Czekay, R.P., Kuemmel, T.A., Orlando, R.A., and Farquhar, M.G. (2001). Direct binding of occupied urokinase receptor (uPAR) to LDL receptor-related protein is required for endocytosis of uPAR and regulation of cell surface urokinase activity. Mol. Biol. Cell *12*, 1467–1479.

Daicho, T., Daisho, Y., Kojima, S., Takano, S., Tejima, Y., Marunouchi, T., Takagi, N., Takeo, S., and Tanonaka, K. (2009). Alterations in dystrophin-related glycoproteins in development of right ventricular failure in rats. J Pharmacol Sci *111*, 405–415.

Dang, P., Smythe, E., and Furley, A.J.W. (2012). TAG1 regulates the endocytic trafficking and signaling of the semaphorin3A receptor complex. Journal of Neuroscience *32*, 10370–10382.

Dangain, J., Vrbova, G. (1984). Muscle development in mdx mutant mice. Muscle Nerve. *7*, 700-704.

Deconinck, A.E., Potter, A.C., Tinsley, J.M., Wood, S.J., Vater, R., Young, C., Metzinger, L., Vincent, A., Slater, C.R., and Davies, K.E. (1997a). Postsynaptic abnormalities at the neuromuscular junctions of utrophin-deficient mice. The Journal of Cell Biology *136*, 883–894.

Deconinck, A.E., Rafael, J.A., Skinner, J.A., Brown, S.C., Potter, A.C., Metzinger, L., Watt, D.J., Dickson, J.G., Tinsley, J.M., and Davies, K.E. (1997b). Utrophin-dystrophin-deficient mice as a model for Duchenne muscular dystrophy. Cell *90*, 717–727.

Delfín, D.A., Zang, K.E., Schill, K.E., Patel, N.T., Janssen, P.M.L., Raman, S.V., and Rafael-Fortney, J.A. (2012). Cardiomyopathy in the dystrophin/utrophin-deficient mouse model of severe muscular dystrophy is characterized by dysregulation of matrix metalloproteinases. Neuromuscul. Disord. *22*, 1006–1014.

DelloRusso, C., Scott, J.M., Hartigan-O'Connor, D., Salvatori, G., Barjot, C., Robinson, A.S., Crawford, R.W., Brooks, S.V., and Chamberlain, J.S. (2002). Functional correction of adult mdx mouse muscle using gutted adenoviral vectors expressing full-length dystrophin. Proceedings of the National Academy of Sciences *99*, 12979–12984.

Deyst, K.A., Bowe, M.A., Leszyk, J.D., and Fallon, J.R. (1995). The α-Dystroglycan-β-Dystroglycan Complex MEMBRANE ORGANIZATION AND RELATIONSHIP TO AN AGRIN RECEPTOR. Journal of Biological Chemistry *270*, 25956–25959.

Dou, H., Huang, C., Singh, M., Carpenter, P.B., and Yeh, E.T.H. (2010). Regulation of DNA Repair through DeSUMOylation and SUMOylation of Replication Protein A Complex. Molecular Cell *39*, 333–345.

Dou, H., Huang, C., Van Nguyen, T., Lu, L.-S., and Yeh, E.T.H. (2011). SUMOylation and de-SUMOylation in response to DNA damage. FEBS Letters *585*, 2891–2896.

Dowling, P., Culligan, K., and Ohlendieck, K. (2002). Distal mdx muscle groups exhibiting up-regulation of utrophin and rescue of dystrophin-associated glycoproteins exemplify a protected phenotype in muscular dystrophy. Naturwissenschaften *89*, 75–78.

Dowling, P., Lohan, J., Ohlendieck, K. (2003). Comparative analysis of Dp427-deficient mdx tissues shows that the milder dystrophic phenotype of extraocular and toe muscle fibres is associated with a persistent expression of beta-dystroglycan. Eur. J. Cell Biol. *82*, 222-230.

Dozynkiewicz, M.A., Jamieson, N.B., MacPherson, I., Grindlay, J., van den Berghe, P.V.E., Thun, von, A., Morton, J.P., Gourley, C., Timpson, P., Nixon, C., et al. (2012). Rab25 and CLIC3 Collaborate to Promote Integrin Recycling from Late Endosomes/Lysosomes and Drive Cancer Progression. Developmental Cell *22*, 131–145.

Dreyfus, J.C., Schapira, G., and Schapira, F. (1954). Biochemical study of muscle in progressive muscular dystrophy. J. Clin. Invest. *33*, 794–797.
Duclos, F., Straub, V., Moore, S.A., Venzke, D.P., Hrstka, R.F., Crosbie, R.H.,

Durbeej, M., Larsson, E., Ibraghimov-Beskrovnaya, O., Roberds, S.L., Campbell, K.P., and Ekblom, P. (1995). Non-muscle alpha-dystroglycan is involved in epithelial development. The Journal of Cell Biology *130*, 79–91.

Durbeej, M., Lebakken, C.S., Ettinger, A.J., and van der Meulen, J. (1998). Progressive muscular dystrophy in α-sarcoglycan–deficient mice. The Journal of Cell Biology *142*, 1461–1471.

Durbeej, M., and Campbell, K.P. (1999). Biochemical characterization of the epithelial dystroglycan complex. Journal of Biological Chemistry *274*, 26609–26616.

Durbeej, M., Henry, M.D., Ferletta, M., Campbell, K.P., and Ekblom, P. (1998). Distribution of Dystroglycan in Normal Adult Mouse Tissues. Journal of Histochemistry & Cytochemistry *46*, 449–457.

Emery, A., Muntoni, F. (2003). Duchenne Muscular Dystrophy (2nd Ed.). *Oxford University Press*.

Ervasti, J.M., Ohlendieck, K., Kahl, S.D., Gaver, M.G., and Campbell, K.P. (1990). Deficiency of a glycoprotein component of the dystrophin complex in dystrophic muscle. Nature *345*, 315–319.

Ervasti, J.M., and Campbell, K.P. (1991). Membrane organization of the dystrophin-glycoprotein complex. Cell *66*, 1121–1131.

Ervasti, J.M., and Campbell, K.P. (1993). A role for the dystrophin-glycoprotein complex as a transmembrane linker between laminin and actin. The Journal of Cell Biology *122*, 809–823.

Ervasti, J.M., Kahl, S.D., and Campbell, K.P. (1991). Purification of dystrophin from skeletal muscle. Journal of Biological Chemistry *266*, 9161–9165.

Esser, A.K., Cohen, M.B., and Henry, M.D. (2010). Dystroglycan is not required for maintenance of the luminal epithelial basement membrane or cell polarity in the mouse prostate. Prostate n/a–n/a.

Ettinger, A.J., Feng, G., and Sanes, J.R. (1997). epsilon-Sarcoglycan, a broadly expressed homologue of the gene mutated in limb-girdle muscular dystrophy 2D. Journal of Biological Chemistry *272*, 32534–32538.

Eyermann, C., Czaplinski, K., and Colognato, H. (2012). Dystroglycan promotes filopodial formation and process branching in differentiating oligodendroglia. Journal of Neurochemistry*120*, 928-947.

Fall, A.M., Johnsen, R., Honeyman, K., Iversen, P., Fletcher, S., and Wilton, S.D. (2006). Induction of revertant fibres in the mdx mouse using antisense oligonucleotides. Genet Vaccines Ther *4*, 3.

Fernandez, K., Serinagaoglu, Y., Hammond, S., Martin, L.T., and Martin, P.T. (2010). Mice Lacking Dystrophin or Î± Sarcoglycan Spontaneously Develop Embryonal Rhabdomyosarcoma with Cancer-Associated p53 Mutations and Alternatively Spliced or Mutant Mdm2 Transcripts. The American Journal of Pathology *176*, 416–434.

Fischbeck, K.H., Bonilla, E., Schotland, D.L. (1983). Freeze-fracture analysis of plasma membrane cholesterol in Duchenne muscle. Ann. Neurol. *13*, 532-535.

Frost, A.R., hm, S.V.B.O., Sewduth, R.N., Josifova, D., Ogilvie, C.M., Izatt, L., and Roberts, R.G. (2010). Frost (2010). European Journal of Human Genetics *18*, 852–855.

Fuentes-Mera, L., Rodríguez-Muñoz, R., González-Ramírez, R., García-Sierra, F., González, E., Mornet, D., and Cisneros, B. (2006). Characterization of a novel Dp71 dystrophin-associated protein complex (DAPC) present in the nucleus of HeLa cells: Members of the nuclear DAPC associate with the nuclear matrix. Experimental Cell Research *312*, 3023–3035.

Garcia, A., Barbaras, R., Collet, X., Bogyo, A., Chap, H., and Perret, B. (1996). High-density lipoprotein 3 receptor-dependent endocytosis pathway in a human hepatoma cell line (HepG2). Biochemistry *35*, 13064–13071.

Gazzerro, E., Sotgia, F., Bruno, C., Lisanti, M.P., and Minetti, C. (2009). Gazerro (2010. European Journal of Human Genetics *18*, 137–145.

Gee, S.H., Blacher, R.W., Douville, P.J., Provost, P.R., Yurchenco, P.D., and Carbonetto, S. (1993). Laminin-binding protein 120 from brain is closely related to the dystrophin-associated glycoprotein, dystroglycan, and binds with high affinity to the major heparin binding domain of laminin. Journal of Biological Chemistry *268*, 14972–14980.

Gee, S.H., Madhavan, R., Levinson, S.R., Caldwell, J.H., Sealock, R., and Froehner, S.C. (1998). Interaction of muscle and brain sodium channels with multiple members of the syntrophin family of dystrophin-associated proteins. J. Neurosci. *18*, 128–137.

Ghosh, R.N., Gelman, D.L., and Maxfield, F.R. (1994). Quantification of low density lipoprotein and transferrin endocytic sorting HEp2 cells using confocal microscopy. Journal of Cell Science *107 (Pt 8)*, 2177–2189.

Gilbert, R., Nalbanoglu, J., Tinsley, J.M., Massie, B., Davies, K.E., and Karpati, G. (1998). Efficient Utrophin Expression Following Adenovirus Gene Transfer in Dystrophic Muscle. Biochemical and Biophysical Research Communications *242*, 244–247.

Glebov, O.O., Bright, N.A., and Nichols, B.J. (2005). Flotillin-1 defines a clathrin-independent endocytic pathway in mammalian cells. Nat Cell Biol *8*, 46–54.

Goemans, N.M., Tulinius, M., van den Akker, J.T., Burm, B.E., Ekhart, P.F., Heuvelmans, N., Holling, T., Janson, A.A., Platenburg, G.J., Sipkens, J.A., et al. (2011). Systemic Administration of PRO051 in Duchenne's Muscular Dystrophy. N Engl J Med *364*, 1513–1522.

Goldstein, G., Scheid, M., Hammerling, U., Schlesinger, D.H., Niall, H.D., and Boyse, E.A. (1975). Isolation of a polypeptide that has lymphocyte-differentiating properties and is probably represented universally in living cells. Proceedings of the National Academy of Sciences *72*, 11–15.

Goody, M.F., Kelly, M.W., Reynolds, C.J., Khalil, A., Crawford, B.D., and Henry, C.A. (2012). NAD+ Biosynthesis Ameliorates a Zebrafish Model of Muscular Dystrophy. PLoS Biol *10*, e1001409.

Goonasekera, S.A., Lam, C.K., Millay, D.P., Sargent, M.A., Hajjar, R.J., Kranias, E.G., and Molkentin, J.D. (2011). Mitigation of muscular dystrophy in mice by SERCA overexpression in skeletal muscle. J. Clin. Invest. *121*, 1044–1052.

Gotink, K.J., Broxterman, H.J., Labots, M., de Haas, R.R., Dekker, H., Honeywell, R.J., Rudek, M.A., Beerepoot, L.V., Musters, R.J., Jansen, G., et al. (2011). Lysosomal sequestration of sunitinib: a novel mechanism of drug resistance. Clin. Cancer Res. *17*, 7337–7346.

Goyenvalle, A., Vulin, A., Fougerousse, F., Leturcq, F., Kaplan, J.-C., Garcia, L., and Danos, O. (2004). Rescue of dystrophic muscle through U7 snRNA-mediated exon skipping. Science *306*, 1796–1799.

Goyenvalle, A., Babbs, A., Gert-Jan, B.V.O., Garcia, L., Davies, K.E. (2009). Enhanced Exon-skipping Induced by U7 snRNA Carrying a Splicing Silencer Sequence: Promising Tool for DMD Therapy. Molecular Therapy *17*, 1234-1240.

Goyenvalle, A., Babbs, A., Powell, D., Kole, R., Fletcher, S., Wilton, S.D., and Davies, K.E. (2010). Prevention of dystrophic pathology in severely affected dystrophin/utrophin-deficient mice by morpholino-oligomer-mediated exon-skipping. Mol. Ther. *18*, 198–205.

Goyenvalle, A., Wright, J., Babbs, A., Wilkins, V., Garcia, L., and Davies, K.E. (2012). Engineering Multiple U7snRNA Constructs to Induce Single and Multiexon-skipping for Duchenne Muscular Dystrophy. Molecular Therapy *20*, 1212–1221.

Grady, R.M., Zhou, H., Cunningham, J.M., Henry, M.D., Campbell, K.P., and Sanes, J.R. (2000). Maturation and maintenance of the neuromuscular synapse: genetic evidence for roles of the dystrophin--glycoprotein complex. Neuron *25*, 279–293.

Gramolini, A.O., Dennis, C.L., Tinsley, J.M., Robertson, G.S., Cartaud, J., Davies, K.E., and Jasmin, B.J. (1997). Local transcriptional control of utrophin expression at the neuromuscular synapse. Journal of Biological Chemistry *272*, 8117–8120.

Gramolini, A.O., Burton, E.A., Tinsley, J.M., Ferns, M.J., Cartaud, A., Cartaud, J., Davies, K.E., Lunde, J.A., and Jasmin, B.J. (1998). Muscle and neural isoforms of agrin increase utrophin expression in cultured myotubes via a transcriptional regulatory mechanism. Journal of Biological Chemistry *273*, 736–743.

Gramolini, A.O., Angus, L.M., Schaeffer, L., Burton, E.A., Tinsley, J.M., Davies, K.E., Changeux, J.P., and Jasmin, B.J. (1999). Induction of utrophin gene expression by heregulin in skeletal muscle cells: role of the N-box motif and GA binding protein. Proceedings of the National Academy of Sciences *96*, 3223–3227.

Gregorevic, P., Allen, J.M., Minami, E., Blankinship, M.J., Haraguchi, M., Meuse, L., Finn, E., Adams, M.E., Froehner, S.C., Murry, C.E., et al. (2006). rAAV6-microdystrophin preserves muscle function and extends lifespan in severely dystrophic mice. Nat Med *12*, 787–789.

Grewal, P.K., Holzfeind, P.J., Bittner, R.E., and Hewitt, J.E. (2001). Mutant glycosyltransferase and altered glycosylation of alpha-dystroglycan in the myodystrophy mouse. Nat. Genet. *28*, 151–154.

Griffin, C.A., Kafadar, K.A., and Pavlath, G.K. (2009). MOR23 Promotes Muscle Regeneration and Regulates Cell Adhesion and Migration. Developmental Cell *17*, 649–661.

Grisoni, K., Martin, E., Gieseler, K., Mariol, M.-C., and Ségalat, L. (2002). Genetic evidence for a dystrophin-glycoprotein complex (DGC) in Caenorhabditis elegans. Gene *294*, 77–86.

Gu, Z., Noss, E.H., Hsu, V.W., and Brenner, M.B. (2011). Integrins traffic rapidly via circular dorsal ruffles and macropinocytosis during stimulated cell migration. The Journal of Cell Biology *193*, 61–70.

Hammonds, R.G. (1987). Protein sequence of DMD gene is related to actin-binding domain of alpha-actinin. Cell *51*, 1.

Hara, Y., Balci-Hayta, B., Yoshida-Moriguchi, T., Kanagawa, M., Beltrán-Valero de Bernabé, D., Gündeşli, H., Willer, T., Satz, J.S., Crawford, R.W., Burden, S.J., et al. (2011). A dystroglycan mutation associated with limb-girdle muscular dystrophy. N Engl J Med *364*, 939–946.

Harding, C., Heuser, J., and Stahl, P. (1983). Receptor-mediated endocytosis of transferrin and recycling of the transferrin receptor in rat reticulocytes. The Journal of Cell Biology *97*, 329–339.

Heller, K.N., Montgomery, C.L., Janssen, P.M.L., Clark, K.R., Mendell, J.R., Rodino-Klapac, L.R. (2013). AAV-mediated Overexpression of Human α7 Integrin Leads to Histological and Functional Improvement in Dystrophic Mice. Mol. Therapy *21*, 520-525.

Helliwell, T.R., Ellis, J.M., Mountford, R.C., Appleton, R.E., and Morris, G.E. (1992). A truncated dystrophin lacking the C-terminal domains is localized at the muscle membrane. Am. J. Hum. Genet. *50*, 508–514.

Henry, M.D., and Campbell, K.P. (1998). A role for dystroglycan in basement membrane assembly. Cell *95*, 859–870.

Hernández-Deviez, D.J., Howes, M.T., Laval, S.H., Bushby, K., Hancock, J.F., and Parton, R.G. (2008). Caveolin regulates endocytosis of the muscle repair protein, dysferlin. Journal of Biological Chemistry *283*, 6476–6488.

Herrmann, R., Straub, V., Blank, M., Kutzick, C., Franke, N., Jacob, E.N., Lenard, H.G., Kröger, S., and Voit, T. (2000). Dissociation of the dystroglycan complex in caveolin-3-deficient limb girdle muscular dystrophy. Human Molecular Genetics *9*, 2335–2340.

Hertzog, M., Monteiro, P., Le Dez, G., and Chavrier, P. (2012). Exo70 Subunit of the Exocyst Complex Is Involved in Adhesion-Dependent Trafficking of Caveolin-1. PLoS ONE *7*, e52627.

Hezel, M., de Groat, W.C., and Galbiati, F. (2010). Caveolin-3 promotes nicotinic acetylcholine receptor clustering and regulates neuromuscular junction activity. Mol. Biol. Cell *21*, 302–310.

Higginson, J.R., Thompson, O., and Winder, S.J. (2008). Targeting of dystroglycan to the cleavage furrow and midbody in cytokinesis. The International Journal of Biochemistry & Cell Biology *40*, 892–900.

Hjerpe, R., Aillet, F., Lopitz-Otsoa, F., Lang, V., England, P., and Rodriguez, M.S. (2009). Hjerpe (2009). EMBO Reports *10*, 1250–1258.

Hoffman, E.P., Brown, R.H., and Kunkel, L.M. (1987). Dystrophin: the protein product of the Duchenne muscular dystrophy locus. Cell *51*, 919–928.

Hoffman, E.P., Watkins, S.C., Slayter, H.S., and Kunkel, L.M. (1989). Detection of a specific isoform of alpha-actinin with antisera directed against dystrophin. The Journal of Cell Biology *108*, 503–510.

Hochenester, E., Tisi, D., Talts, J.F., and Timpl, R. (1999). The crystal structure of a laminin G-like module reveals the molecular basis of alpha-dystroglycan binding to laminins, perlecan, and agrin. Molecular Cell *4*, 783–792.

Holt, K.H., and Campbell, K.P. (1998). Assembly of the sarcoglycan complex. Insights for muscular dystrophy. Journal of Biological Chemistry *273*, 34667–34670.

Holt, K.H., Lim, L.E., Straub, V., Venzke, D.P., Duclos, F., Anderson, R.D., Davidson, B.L., and Campbell, K.P. (1998). Functional rescue of the sarcoglycan complex in the BIO 14.6 hamster using delta-sarcoglycan gene transfer. Molecular Cell *1*, 841–848.

Hopkins, C.R., and Trowbridge, I.S. (1983). Internalization and processing of transferrin and the transferrin receptor in human carcinoma A431 cells. The Journal of Cell Biology *97*, 508–521.

Huang, X., Poy, F., Zhang, R., Joachimiak, A., Sudol, M., and Eck, M.J. (2000). Structure of a WW domain containing fragment of dystrophin in complex with beta-dystroglycan. Nat. Struct. Biol. *7*, 634–638.

Huth, U.S., Schubert, R., and Peschka-Süss, R. (2006). Investigating the uptake and intracellular fate of pH-sensitive liposomes by flow cytometry and spectral bio-imaging. Journal of Controlled Release *110*, 490–504.

Ibraghimov-Beskrovnaya, O., Ervasti, J.M., Leveille, C.J., Slaughter, C.A., Sernett, S.W., Campbell, K.P. (1992). Nature *355*, 696-702.

Ibraghimov-Beskrovnaya, O., Milatovich, A., Ozcelik, T., Yang, B., Koepnick, K., Francke, U., and Campbell, K.P. (1993). Human dystroglycan: skeletal muscle cDNA, genomic structure, origin of tissue specific isoforms and chromosomal localization. Human Molecular Genetics *2*, 1651–1657.

Ilsley, J.L., Sudol, M., and Winder, S.J. (2001). The interaction of dystrophin with β-dystroglycan is regulated by tyrosine phosphorylation. Cellular Signalling *13*, 625–632.

Ilsley, J.L., Sudol, M., and Winder, S.J. (2002). The WW domain: linking cell signalling to the membrane cytoskeleton. Cellular Signalling *14*, 183–189.

Imamura, M., Mochizuki, Y., Engvall, E., and Takeda, S. (2005). Epsilon-sarcoglycan compensates for lack of alpha-sarcoglycan in a mouse model of limb-girdle muscular dystrophy. Human Molecular Genetics *14*, 775–783.

Ito, N., Ruegg, U.T., Kudo, A., Miyagoe-Suzuki, Y., Takeda, S. (2013a) Activation of calcium signalling through Trpv1 by nNOS and peroxynitrite as a key trigger of skeletal muscle hypertrophy. Nat. Med., *19*, 101-106

Ito, T., Ogawa, R., Uezumi, A., Ohtani, T., Watanabe, Y., Tsujikawa, K., Miyagoe-Suzuki, Y., Takeda, S., Yamamoto, H., and Fukada, S.-I. (2013b). Imatinib attenuates severe mouse dystrophy and inhibits proliferation and fibrosis-marker expression in muscle mesenchymal progenitors. Neuromuscular Disorders *23*, 349–356.

James, M., Nuttall, A., Ilsley, J.L., Ottersbach, K., Tinsley, J.M., Sudol, M., and Winder, S.J. (2000). Adhesion-dependent tyrosine phosphorylation of (beta)-dystroglycan regulates its interaction with utrophin. Journal of Cell Science *113 (Pt 10)*, 1717–1726.

Jat, P.S., and Sharp, P.A. (1989). Cell lines established by a temperature-sensitive simian virus 40 large-T-antigen gene are growth restricted at the nonpermissive temperature. Molecular and Cellular Biology *9*, 1672–1681.

Jat, P.S., Noble, M.D., Ataliotis, P., Tanaka, Y., Yannoutsos, N., Larsen, L., and Kioussis, D. (1991). Direct derivation of conditionally immortal cell lines from an H-2Kb-tsA58 transgenic mouse. Proceedings of the National Academy of Sciences *88*, 5096–5100.

Jentsch, S., and Schlenker, S. (1995). Selective protein degradation: a journey's end within the proteasome. Cell *82*, 881–884.

Judge, L.M., Haraguchiln, M., and Chamberlain, J.S. (2006). Dissecting the signaling and mechanical functions of the dystrophin-glycoprotein complex. Journal of Cell Science *119*, 1537–1546.

Jung, D., Yang, B., Meyer, J., Chamberlain, J.S., and Campbell, K.P. (1995). Identification and characterization of the dystrophin anchoring site on beta-dystroglycan. Journal of Biological Chemistry *270*, 27305–27310.

Jung, D., Leturcq, F., Sunada, Y., Duclos, F., Tomé, F.M., Moomaw, C., Merlini, L., Azibi, K., Chaouch, M., Slaughter, C., et al. (1996). Absence of gamma-sarcoglycan (35 DAG) in autosomal recessive muscular dystrophy linked to chromosome 13q12. FEBS Letters *381*, 15–20.

Kachinsky, A.M., Froehner, S.C., and Milgram, S.L. (1999). A PDZ-containing scaffold related to the dystrophin complex at the basolateral membrane of epithelial cells. The Journal of Cell Biology *145*, 391–402.

Kaisto, T., Rahkila, P., Marjomäki, V., Parton, R.G., and Metsikkö, K. (1999). Endocytosis in skeletal muscle fibers. Experimental Cell Research *253*, 551–560.

Kang Y., Zhang, N., Koepp, D.M., Walters, K.J. (2007). Ubiquitin receptor proteins hHR23a and hPLIC2 interact. J. Mol. Biol. *365*, 1093-1101.

Karlsson, S., Kowanetz, K., Sandin, A., Persson, C., Ostman, A., Heldin, C.-H., and Hellberg, C. (2006). Loss of T-cell protein tyrosine phosphatase induces recycling of the platelet-derived growth factor (PDGF) beta-receptor but not the PDGF alpha-receptor. Mol. Biol. Cell *17*, 4846–4855.

Kay, B.K., Williamson, M.P., and Sudol, M. (2000). The importance of being proline: the interaction of proline-rich motifs in signaling proteins with their cognate domains. Faseb J. *14*, 231–241.

Kayali, R., Ku, J.-M., Khitrov, G., Jung, M.E., Prikhodko, O., and Bertoni, C. (2012). Read-through compound 13 restores dystrophin expression and improves muscle function in the mdx mouse model for Duchenne muscular dystrophy. Human Molecular Genetics *21*, 4007–4020.

Kämper, A., and Rodemann, H.P. (1992). Alterations of protein degradation and 2-D protein pattern in muscle cells of MDX and DMD origin. Biochemical and Biophysical Research Communications *189*, 1484–1490.

Khurana, T.S., Hoffman, E.P., and Kunkel, L.M. (1990). Identification of a chromosome 6-encoded dystrophin-related protein. Journal of Biological Chemistry *265*, 16717–16720.

Khurana, T.S., Watkins, S.C., Chafey, P., Chelly, J., Tomé, F.M., Fardeau, M., Kaplan, J.C., and Kunkel, L.M. (1991). Immunolocalization and developmental expression of dystrophin related protein in skeletal muscle. Neuromuscul. Disord. *1*, 185–194.

Kim, W., Bennett, E.J., Huttlin, E.L., Guo, A., Li, J., Possemato, A., Sowa, M.E., Rad, R., Rush, J., Comb, M.J., et al. (2011). Systematic and Quantitative Assessment of the Ubiquitin-Modified Proteome. Molecular Cell *44*, 325–340.

Kinali, M., Arechavala-Gomeza, V., Cirak, S., Glover, A., Guglieri, M., Feng, L., Hollingsworth, K.G., Hunt, D., Jungbluth, H., and Roper, H.P. (2011). Muscle histology vs MRI in Duchenne muscular dystrophy. Neurology *76*, 346–353.

Kingston, H.M., Sarfarazi, M., Thomas, N., and Harper, P.S. (1984). Localisation of the Becker muscular dystrophy gene on the short arm of the X chromosome by linkage to cloned DNA sequences. Human Genetics *67*, 6–17.

Klausner, R.D., Van Renswoude, J., Ashwell, G., Kempf, C., Schechter, A.N., Dean, A., and Bridges, K.R. (1983). Receptor-mediated endocytosis of transferrin in K562 cells. Journal of Biological Chemistry *258*, 4715–4724.

Koenig, M., Hoffman, E.P., Bertelson, C.J., Monaco, A.P., Feener, C., and Kunkel, L.M. (1987). Complete cloning of the Duchenne muscular dystrophy (DMD) cDNA and preliminary genomic organization of the DMD gene in normal and affected individuals. Cell *50*, 509–517.

Koenig, M., Monaco, A.P., and Kunkel, L.M. (1988). The complete sequence of dystrophin predicts a rod-shaped cytoskeletal protein. Cell *53*, 219–228.

Koenig, M., Beggs, A.H., Moyer, M., Scherpf, S., Heindrich, K., Bettecken, T., Meng, G., Müller, C.R., Lindlöf, M., and Kaariainen, H. (1989). The molecular basis for Duchenne versus Becker muscular dystrophy: correlation of severity with type of deletion. Am. J. Hum. Genet. *45*, 498–506.

Koenig, M., and Kunkel, L.M. (1990). Detailed analysis of the repeat domain of dystrophin reveals four potential hinge segments that may confer flexibility. Journal of Biological Chemistry *265*, 4560–4566.

Kokubo, H., Helms, J.B., Ohno-Iwashita, Y., Shimada, Y., Horikoshi, Y., and Yamaguchi, H. (2003). Ultrastructural localization of flotillin-1 to cholesterol-rich membrane microdomains, rafts, in rat brain tissue. Brain Research *965*, 83–90.

Krag, T.O.B., Bogdanovich, S., Jensen, C.J., Fischer, M.D., Hansen-Schwartz, J., Javazon, E.H., Flake, A.W., Edvinsson, L., and Khurana, T.S. (2004). Heregulin ameliorates the dystrophic phenotype in mdx mice. Proceedings of the National Academy of Sciences *101*, 13856–13860.

Kramarcy, N.R., and Sealock, R. (1990). Dystrophin as a focal adhesion protein. Collocalization with talin and the Mr 48,000 sarcolemmal protein in cultured Xenopus muscle. FEBS Letters *274*, 171–174.

Kramarcy, N.R., and Sealock, R. (2000). Syntrophin isoforms at the neuromuscular junction: developmental time course and differential localization. Mol. Cell. Neurosci. *15*, 262–274.

Kumar, S., Yoshida, Y., and Noda, M. (1993). Cloning of a cDNA which encodes a novel ubiquitin-like protein. Biochemical and Biophysical Research Communications *195*, 393–399.

Kumar, K.G.S., Barriere, H., Carbone, C.J., Liu, J., Swaminathan, G., Xu, P., Li, Y., Baker, D.P., Peng, J., Lukacs, G.L., et al. (2007). Site-specific ubiquitination exposes a linear motif to promote interferon- receptor endocytosis. The Journal of Cell Biology *179*, 935–950.

Kunz, S., Campbell, K.P., and Oldstone, M.B.A. (2003). Alpha-dystroglycan can mediate arenavirus infection in the absence of beta-dystroglycan. Virology *316*, 213–220.

Lai, Y., Thomas, G.D., Yue, Y., Yang, H.T., Li, D., Long, C., Judge, L., Bostick, B., Chamberlain, J.S., Terjung, R.L., et al. (2009). Dystrophins carrying spectrin-like repeats 16 and 17 anchor nNOS to the sarcolemma and enhance exercise performance in a mouse model of muscular dystrophy. J. Clin. Invest. *119*, 624–635.

Lai, Y., Zhao, J., Yue, Y., and Duan, D. (2013). α2 and α3 helices of dystrophin R16 and R17 frame a microdomain in the α1 helix of dystrophin R17 for neuronal NOS binding. Proc. Natl. Acad. Sci. U.S.a. *110*, 525–530.

Langenbach, K.J., and Rando, T.A. (2002). Inhibition of dystroglycan binding to laminin disrupts the PI3K/AKT pathway and survival signaling in muscle cells. Muscle Nerve *26*, 644–653.

Lara-Chacón, B., de León, M.B., Leocadio, D., Gómez, P., Fuentes-Mera, L., Martínez-Vieyra, I., Ortega, A., Jans, D.A., and Cisneros, B. (2010). Characterization of an Importin alpha/beta-recognized nuclear localization signal in beta-dystroglycan. J. Cell. Biochem. *110*, 706–717.

Larkin, J.M., Donzell, W.C., and Anderson, R.G. (1986). Potassium-dependent assembly of coated pits: new coated pits form as planar clathrin lattices. The Journal of Cell Biology *103*, 2619–2627.

Le, T.L., and Stow, J.L. (1999). Recycling of E-Cadherin A Potential Mechanism for Regulating Cadherin Dynamics. The Journal of Cell Biology *146*, 219–232.

Lei, H.-Y., and Chang, C.-P. (2009). Lectin of Concanavalin A as an anti-hepatoma therapeutic agent. J Biomed Sci *16*, 10.

Li, M., Brooks, C.L., Wu-Baer, F., Chen, D., Baer, R., and Gu, W. (2003). Mono- versus polyubiquitination: differential control of p53 fate by Mdm2. Science *302*, 1972–1975.

Lim, L.E., Duclos, F., Broux, O., Bourg, N., Sunada, Y., Allamand, V., Meyer, J., Richard, I., Moomaw, C., and Slaughter, C. (1995). Beta-sarcoglycan: characterization and role in limb-girdle muscular dystrophy linked to 4q12. Nat. Genet. *11*, 257–265.

Lin, X., Sun, B., Liang, M., Liang, Y.-Y., Gast, A., Hildebrand, J., Brunicardi, F.C., Melchior, F., and Feng, X.-H. (2003). Opposed regulation of corepressor CtBP by SUMOylation and PDZ binding. Molecular Cell *11*, 1389–1396.

Lin, C.H., MacGurn, J.A., Chu, T., Stefan, C.J., and Emr, S.D. (2008). Arrestin-Related Ubiquitin-Ligase Adaptors Regulate Endocytosis and Protein Turnover at the Cell Surface. Cell *135*, 714–725.

Lin, S., Shen, H., Jin, B., Gu, Y., Chen, Z., Cao, C., Hu, C., Keller, C., Pear, W.S., and Wu, L. (2013). Brief Report: Blockade of Notch Signaling in Muscle Stem Cells Causes Muscular Dystrophic Phenotype and Impaired Muscle Regeneration. Stem Cells *31*, 823–828.

Liu, J., Milner, D.J., Boppart, M.D., Ross, R.S., and Kaufman, S.J. (2012). β1D chain increases α7β1 integrin and laminin and protects against sarcolemmal damage in mdx mice. Human Molecular Genetics *21*, 1592–1603.

Loh, N.Y., Newey, S.E., Davies, K.E., and Blake, D.J. (2000). Assembly of multiple dystrobrevin-containing complexes in the kidney. Journal of Cell Science *113 (Pt 15)*, 2715–2724.

Louboutin, J.-P., Rouger, K., Tinsley, J.M., Halldorson, J., and Wilson, J.M. (2001). iNOS expression in dystrophinopathies can be reduced by somatic gene transfer of dystrophin or utrophin. Molecular Medicine-Cambridge Ma Then New York- *7*, 355–364.

Love, I.M., Shi, D., Grossman, S.R. (2013). P53 Ubiquitination and proteasomal degradation. Methods Mol. Biol. *962*, 63-73.

Lumeng, C., Phelps, S., Crawford, G.E., Walden, P.D., Barald, K., and Chamberlain, J.S. (1999). Interactions between beta 2-syntrophin and a family of microtubule-associated serine/threonine kinases. Nat. Neurosci. *2*, 611–617.

Malerba, A., Sharp, P.S., Graham, I.R., Arechavala-Gomeza, V., Foster, K., Muntoni, F., Wells, D.J., and Dickson, G. (2009). Malerba (2011)2. Molecular Therapy *19*, 345–354.

Maltzahn, von, J., Renaud, J.-M., Parise, G., and Rudnicki, M.A. (2012). Wnt7a treatment ameliorates muscular dystrophy. Proceedings of the National Academy of Sciences *109*, 20614–20619.

Mannen, H., Tseng, H.-M., Cho, C.-L., and Li, S.S.-L. (1996). Cloning and expression of human homolog HSMT3 to yeast SMT3 suppressor of MIF2 mutations in a centromere protein gene. Biochemical and Biophysical Research Communications *222*, 178–180.

Marks, D.L., Singh, R.D., Choudhury, A., Wheatley, C.L., and Pagano, R.E. (2005). Use of fluorescent sphingolipid analogs to study lipid transport along the endocytic pathway. Methods *36*, 186–195.

Marshall, J.L., Holmberg, J., Chou, E., Ocampo, A.C., Oh, J., Lee, J., Peter, A.K., Martin, P.T., and Crosbie-Watson, R.H. (2012a). Sarcospan-dependent Akt activation is required for utrophin expression and muscle regeneration. The Journal of Cell Biology *197*, 1009–1027.

Marshall, J.L., Chou, E., Oh, J., Kwok, A., Burkin, D.J., and Crosbie-Watson, R.H. (2012b). Dystrophin and utrophin expression require sarcospan: loss of α7 integrin exacerbates a newly discovered muscle phenotype in sarcospan-null mice. Human Molecular Genetics *21*, 4378–4393.

Martínez-Vieyra, I.A., Vásquez-Limeta, A., González-Ramírez, R., Morales-Lázaro, S.L., Mondragón, M., Mondragón, R., Ortega, A., Winder, S.J., and Cisneros, B. (2013). A role for β-dystroglycan in the organization and structure of the nucleus in myoblasts. BBA - Molecular Cell Research *1833*, 698–711.

Matsumura, K., Ervasti, J.M., Ohlendieck, K., Kahl, S.D., and Campbell, K.P. (1992a). Association of dystrophin-related protein with dystrophin-associated proteins in mdx mouse muscle. Nature *360*, 588–591.

Matsumura, K., Tome, F.M., Collin, H., Azibi, K., Chaouch, M., Kaplan, J.-C., Fardeau, M., and Campbell, K.P. (1992b). Deficiency of the 50 K dystrophin-associated glycoprotein in severe childhood autosomal recessive muscular dystrophy. Nature *359*, 320–322.

Matsumura, K., Zhong, D., Saito, F., Arai, K., Adachi, K., Kawai, H., Higuchi, I., Nishino, I., and Shimizu, T. (2005). Proteolysis of β-dystroglycan in muscular diseases. Neuromuscular Disorders *15*, 336–341.

Matsumura, K., Tomé, F.M., Ionasescu, V., Ervasti, J.M., Anderson, R.D., Romero, N.B., Simon, D., Recan, D., Kaplan, J.C., and Fardeau, M. (1993). Deficiency of dystrophin-associated proteins in Duchenne muscular dystrophy patients lacking COOH-terminal domains of dystrophin. J. Clin. Invest. *92*, 866.

Matunis, M.J., Coutavas, E., and Blobel, G. (1996). A novel ubiquitin-like modification modulates the partitioning of the Ran-GTPase-activating protein RanGAP1 between the cytosol and the nuclear pore complex. The Journal of Cell Biology *135*, 1457–1470.

McDearmon, E.L., Combs, A.C., and Ervasti, J.M. (2001). Differential Vicia villosa agglutinin reactivity identifies three distinct dystroglycan complexes in skeletal muscle. Journal of Biological Chemistry *276*, 35078–35086.

McDonald, C.M., Henricson, E.K., Han, J.J., Abresch, R.T., Nicorici, A., Atkinson, L., Elfring, G.L., Reha, A., and Miller, L.L. (2010). The 6-minute walk test in Duchenne/Becker muscular dystrophy: Longitudinal observations. Muscle Nerve *42*, 966–974.

McDonald, K.K., Stajich, J., Blach, C., Ashley-Koch, A.E., and Hauser, M.A. (2012). Exome analysis of two limb-girdle muscular dystrophy families: mutations identified and challenges encountered. PLoS ONE *7*, e48864.

McNally, E.M., Passos-Bueno, M.R., Bönnemann, C.G., Vainzof, M., de Sa Moreira, E., Lidov, H.G., Othmane, K.B., Denton, P.H., Vance, J.M., and Zatz, M. (1996). Mild and severe muscular dystrophy caused by a single gamma-sarcoglycan mutation. Am. J. Hum. Genet. *59*, 1040.

McNally, E.M., Ly, C.T., and Kunkel, L.M. (1998). Human epsilon-sarcoglycan is highly related to alpha-sarcoglycan (adhalin), the limb girdle muscular dystrophy 2D gene. FEBS Letters *422*, 27–32.

Melis, M.A., Cau, M., Muntoni, F., Mateddu, A., Galanello, R., Boccone, L., Deidda F., Loi, D., Cao, A. (1998). Elevation of serum creatine kinase as the only manifestation of an intragenic deletion of the dystrophin gene in three unrelated families. Eur. J. Paediatr. Neurol. *2*, 255-261.

Mendell, J.R., Kissel, J.T., Amato, A.A., King, W., Signore, L., Prior, T.W., Sahenk, Z., Benson, S., McAndrew, P.E., and Rice, R. (1995). Myoblast transfer in the treatment of Duchenne's muscular dystrophy. N Engl J Med *333*, 832–838.

Mercado, M.L., Amenta, A.R., Hagiwara, H., Rafii, M.S., Lechner, B., Owens, R.T., McQuillan, D.J., Froehner, S.C., and Fallon, J.R. (2006). Biglycan targets dystrobrevin, syntrophin and nNOS to the muscle cell membrane. The FASEB Journal: Official Publication of the Federation of American Societies for Experimental Biology *20*, 1724.

Mesa, L.E., Dubrovsky, A.L., Corderi, J., Marco, P., and Flores, D. (1991). Steroids in Duchenne muscular dystrophy--deflazacort trial. Neuromuscul. Disord. *1*, 261–266.

Metzinger, L., Blake, D.J., Squier, M.V., Anderson, L.V., Deconinck, A.E., Nawrotzki, R., Hilton-Jones, D., and Davies, K.E. (1997). Dystrobrevin deficiency at the sarcolemma of patients with muscular dystrophy. Human Molecular Genetics *6*, 1185–1191.

Michaluk, P., Kolodziej, L., Mioduszewska, B., Wilczynski, G.M., Dzwonek, J., Jaworski, J., Gorecki, D.C., Ottersen, O.P., and Kaczmarek, L. (2007a). beta-Dystroglycan as a Target for MMP-9, in Response to Enhanced Neuronal Activity. Journal of Biological Chemistry *282*, 16036–16041.

Michaluk, P., Kolodziej, L., Mioduszewska, B., Wilczynski, G.M., Dzwonek, J., Jaworski, J., Gorecki, D.C., Ottersen, O.P., and Kaczmarek, L. (2007b). Beta-dystroglycan as a target for MMP-9, in response to enhanced neuronal activity. Journal of Biological Chemistry *282*, 16036–16041.

Mikami, T., Koyama, S., Yabuta, Y., and Kitagawa, H. (2012). Chondroitin sulfate is a crucial determinant for skeletal muscle development/regeneration and improvement of muscular dystrophies. Journal of Biological Chemistry *287*, 38531–38542.

Miller, G., Wang, E.L., Nassar, K.L., Peter, A.K., and Crosbie, R.H. (2007). Structural and functional analysis of the sarcoglycan–sarcospan subcomplex. Experimental Cell Research *313*, 639–651.

Miller, G., Moore, C.J., Terry, R., La Riviere, T., Mitchell, A., Piggott, R., Dear, T.N., Wells, D.J., and Winder, S.J. (2012). Preventing phosphorylation of dystroglycan ameliorates the dystrophic phenotype in mdx mouse. Human Molecular Genetics *21*, 4508–4520.

Mitchell, A., Mathew, G., Jiang, T., Hamdy, F.C., Cross, S.S., Eaton, C., and Winder, S.J. (2013). Dystroglycan function is a novel determinant of tumor growth and behavior in prostate cancer. Prostate *73*, 398–408.

Mitrpant, C., Adams, A.M., Meloni, P.L., Muntoni, F., Fletcher, S., and Wilton, S.D. (2009). Molecular Therapy *17*, 1418–1426.

Mizuno, Y., Nonaka, I., Hirai, S., and Ozawa, E. (1993). Reciprocal expression of dystrophin and utrophin in muscles of Duchenne muscular dystrophy patients, female DMD-carriers and control subjects. Journal of the Neurological Sciences *119*, 43–52.

Moll, J., Barzaghi, P., Lin, S., Bezakova, G., Lochmüller, H., Engvall, E., Müller, U., and Ruegg, M.A. (2001). An agrin minigene rescues dystrophic symptoms in a mouse model for congenital muscular dystrophy. Nature *413*, 302–307.

Monaco, A.P., Bertelson, C.J., Liechti-Gallati, S., Moser, H., and Kunkel, L.M. (1988). An explanation for the phenotypic differences between patients bearing partial deletions of the DMD locus. Genomics *2*, 90–95.

Moraz, M.-L., Pythoud, C., Turk, R., Rothenberger, S., Pasquato, A., Campbell, K.P., and Kunz, S. (2012). Cell entry of Lassa virus induces tyrosine phosphorylation of dystroglycan. Cell Microbiol *15*, 689–700.

Morgan, J.E., Moore, S.E., Walsh, F.S., and Partridge, T.A. (1992). Formation of skeletal muscle in vivo from the mouse C2 cell line. Journal of Cell Science *102 (Pt 4)*, 779–787.

Morgan, J.E., Beauchamp, J.R., Pagel, C.N., Peckham, M., Ataliotis, P., Jat, P.S., Noble, M.D., Farmer, K., and Partridge, T.A. (1994). Myogenic cell lines derived from transgenic mice carrying a thermolabile T antigen: a model system for the derivation of tissue-specific and mutation-specific cell lines. Dev. Biol. *162*, 486–498.

Moser, H. (1984). Duchenne muscular dystrophy: pathogenetic aspects and genetic prevention. Hum. Genet. *66*, 17-40.

Mu, F.-T., Callaghan, J.M., Steele-Mortimer, O., Stenmark, H., Parton, R.G., Campbell, P.L., McCluskey, J., Yeo, J.-P., Tock, E.P., and Toh, B.-H. (1995). EEA1, an early endosome-associated protein. EEA1 is a conserved α-helical peripheral membrane protein flanked by cysteine “fingers” and contains a calmodulin-binding IQ motif. Journal of Biological Chemistry *270*, 13503–13511.

Nagpal, P., Plant, P.J., Correa, J., Bain, A., Takeda, M., Kawabe, H., Rotin, D., Bain, J.R., and Batt, J.A.E. (2012). The Ubiquitin Ligase Nedd4-1 Participates in Denervation-Induced Skeletal Muscle Atrophy in Mice. PLoS ONE *7*, e46427.

Nawrotzki, R., Loh, N.Y., Ruegg, M.A., Davies, K.E., and Blake, D.J. (1998). Characterisation of alpha-dystrobrevin in muscle. Journal of Cell Science *111*, 2595–2605.

Neri, M., Torelli, S., Brown, S., Ugo, I., Sabatelli, P., Merlini, L., Spitali, P., Rimessi, P., Gualandi, F., Sewry, C., et al. (2007). Dystrophin levels as low as 30% are sufficient to avoid muscular dystrophy in the human. Neuromuscul. Disord. *17*, 913–918.

Newey, S.E., Benson, M.A., Ponting, C.P., Davies, K.E., and Blake, D.J. (2000). Alternative splicing of dystrobrevin regulates the stoichiometry of syntrophin binding to the dystrophin protein complex. Curr. Biol. *10*, 1295–1298.

Newey, S.E., Howman, E.V., Ponting, C.P., Benson, M.A., Nawrotzki, R., Loh, N.Y., Davies, K.E., and Blake, D.J. (2001). Syncoilin, a novel member of the intermediate filament superfamily that interacts with alpha-dystrobrevin in skeletal muscle. Journal of Biological Chemistry *276*, 6645–6655.

Nguyen, H.H., Jayasinha, V., Xia, B., Hoyte, K., and Martin, P.T. (2002). Overexpression of the cytotoxic T cell GalNAc transferase in skeletal muscle inhibits muscular dystrophy in mdx mice. Proceedings of the National Academy of Sciences *99*, 5616–5621.

Nichols, B.J., and Lippincott-Schwartz, J. (2001). Endocytosis without clathrin coats. Trends in Cell Biology *11*, 406–412.

Nigro, V., de Sá Moreira, E., Piluso, G., Vainzof, M., Belsito, A., Politano, L., Puca, A.A., Passos-Bueno, M.R., and Zatz, M. (1996). Autosomal recessive limbgirdle muscular dystrophy, LGMD2F, is caused by a mutation in the δ–sarcoglycan gene. Nat. Genet. *14*, 195–198.

Nodari, A., Previtali, S.C., Dati, G., Occhi, S., Court, F.A., Colombelli, C., Zambroni, D., Dina, G., Del Carro, U., Campbell, K.P., et al. (2008). Alpha6beta4 integrin and dystroglycan cooperate to stabilize the myelin sheath. Journal of Neuroscience *28*, 6714–6719.

Oak, S.A., Russo, K., Petrucci, T.C., and Jarrett, H.W. (2002). Mouse α1-Syntrophin Binding to Grb2: Further Evidence of a Role for Syntrophin in Cell Signaling †. Biochemistry *40*, 11270–11278.

Oak, S.A., Zhou, Y.W., and Jarrett, H.W. (2003). Skeletal muscle signaling pathway through the dystrophin glycoprotein complex and Rac1. Journal of Biological Chemistry *278*, 39287–39295.

Odom, G.L., Gregorevic, P., Allen, J.M., Finn, E., and Chamberlain, J.S. (2008). Microutrophin Delivery Through rAAV6 Increases Lifespan and Improves Muscle Function in Dystrophic Dystrophin/Utrophin-deficient Mice. Molecular Therapy *16*, 1539–1545.

Ohkuma, S., Poole, B. (1978). Fluorescence probe measurement of the intralysosomal pH in living cells and the perturbation of pH by various agents. Proc. Natl. Acad. Sci. USA *75*, 3327-3331.

Ohlendieck, K., and Campbell, K.P. (1991a). Dystrophin-associated proteins are greatly reduced in skeletal muscle from mdx mice. The Journal of Cell Biology *115*, 1685–1694.

Ohlendieck, K., and Campbell, K.P. (1991b). Dystrophin constitutes 5% of membrane cytoskeleton in skeletal muscle. FEBS Letters *283*, 230–234.

Ohlendieck, K., Ervasti, J.M., Snook, J.B., and Campbell, K.P. (1991c). Dystrophin-glycoprotein complex is highly enriched in isolated skeletal muscle sarcolemma. The Journal of Cell Biology *112*, 135–148.

Ohlendieck, K., Matsumara, K., Ionasescu, W., Towbin, J.A., Bosch, E.P., Weinstein, S.L., Sernett, S.W., Campbell, K.P. (1993). Duchenne muscular dystrophy: deficiency of dystrophin-associated proteins in the sarcolemma. Neurology *43*, 795-800.

Onori, A., Pisani, C., Strimpakos, G., Monaco, L., Mattei, E., Passananti, C., and Corbi, N. (2013). Onori (2013). BMC Molecular Biology *14*, 1–1.

Oppizzi, M.L., Akhavan, A., Singh, M., Fata, J.E., and Muschler, J.L. (2008). Nuclear Translocation of β-Dystroglycan Reveals a Distinctive Trafficking Pattern of Autoproteolyzed Mucins. Traffic *9*, 2063–2072.

Oved, S., Mosesson, Y., Zwang, Y., Santonico, E., Shtiegman, K., Marmor, M.D., Kochupurakkal, B.S., Katz, M., Lavi, S., Cesareni, G., et al. (2006). Conjugation to Nedd8 instigates ubiquitylation and down-regulation of activated receptor tyrosine kinases. Journal of Biological Chemistry *281*, 21640–21651.

Pantoja, M., Fischer, K.A., Ieronimakis, N., Reyes, M., and Ruohola-Baker, H. (2012). Genetic elevation of Sphingosine 1-phosphate suppresses dystrophic muscle phenotypes in Drosophila. Development *140*, 136–146.

Parberry-Clark, C., Bury, J.P., Cross, S.S., and Winder, S.J. (2011). Loss of dystroglycan function in oesophageal cancer. Histopathology *59*, 180–187.

Parsons, M.J., Campos, I., Hirst, E.M.A., and Stemple, D.L. (2002). Removal of dystroglycan causes severe muscular dystrophy in zebrafish embryos. Development *129*, 3505–3512.

Parton, R.G., Joggerst, B., and Simons, K. (1994). Regulated internalization of caveolae. The Journal of Cell Biology *127*, 1199–1216.

Parton, R.G., Way, M., Zorzi, N., and Stang, E. (1997). Caveolin-3 associates with developing T-tubules during muscle differentiation. The Journal of Cell Biology *136*, 137–154.

Parton, R.G., and Simons, K. (2007). The multiple faces of caveolae. Nat Rev Mol Cell Biol *8*, 185–194.

Pasqual, G., Rojek, J.M., Masin, M., Chatton, J.-Y., and Kunz, S. (2011). Old World Arenaviruses Enter the Host Cell via the Multivesicular Body and Depend on the Endosomal Sorting Complex Required for Transport. PLoS Pathog *7*, e1002232.

Pasternak, C., Wong, S., and Elson, E.L. (1995). Mechanical function of dystrophin in muscle cells. The Journal of Cell Biology *128*, 355–361.

Pearce, M., Blake, D.J., Tinsley, J.M., Byth, B.C., Campbell, L., Monaco, A.P., and Davies, K.E. (1993). The utrophin and dystrophin genes share similarities in genomic structure. Human Molecular Genetics *2*, 1765–1772.

Pearse, B.M. (1976). Clathrin: a unique protein associated with intracellular transfer of membrane by coated vesicles. Proceedings of the National Academy of Sciences *73*, 1255–1259.

Pelayo, J.-C., Poole, D.P., Steinhoff, M., Cottrell, G.S., and Bunnett, N.W. (2011). Endothelin-converting enzyme-1 regulates trafficking and signalling of the neurokinin 1 receptor in endosomes of myenteric neurones. The Journal of Physiology *589*, 5213–5230.

Pelkmans, L., and Helenius, A. (2002). Endocytosis via caveolae. Traffic *3*, 311–320.

Pelkmans, L., Fava, E., Grabner, H., Hannus, M., Habermann, B., Krausz, E., and Zerial, M. (2005). Genome-wide analysis of human kinases in clathrin- and caveolae/raft-mediated endocytosis. Nature *436*, 78–86.

Peng, H.B., Ali, A.A., Daggett, D.F., Rauvala, H., Hassell, J.R., Smalheiser, N.R. (1998). The relationship between perlecan and dystroglycan and its implication in the formation of the neuromuscular junction. Cell Adhes. Commun. *5*, 475-489.

Percival, J.M., Gregorevic, P., Odom, G.L., Banks, G.B., Chamberlain, J.S., and Froehner, S.C. (2007). rAAV6-Microdystrophin Rescues Aberrant Golgi Complex Organization in mdx Skeletal Muscles. Traffic *8*, 1424–1439.

Persaud, A., Alberts, P., Hayes, M., Guettler, S., Clarke, I., Sicheri, F., Dirks, P., Ciruna, B., and Rotin, D. (2011). Hayes et al. (2011). The EMBO Journal *30*, 3259–3273.

Peter, A.K., and Crosbie, R.H. (2006). Hypertrophic response of Duchenne and limb-girdle muscular dystrophies is associated with activation of Akt pathway. Experimental Cell Research *312*, 2580–2591.

Peter, A.K., Ko, C.Y., Kim, M.H., Hsu, N., Ouchi, N., Rhie, S., Izumiya, Y., Zeng, L., Walsh, K., and Crosbie, R.H. (2009). Myogenic Akt signaling upregulates the utrophin-glycoprotein complex and promotes sarcolemma stability in muscular dystrophy. Human Molecular Genetics *18*, 318–327.

Petrof, B.J., Shrager, J.B., Stedman, H.H., Kelly, A.M., and Sweeney, H.L. (1993). Dystrophin protects the sarcolemma from stresses developed during muscle contraction. Proceedings of the National Academy of Sciences *90*, 3710–3714.

Phelps, S.F., Hauser, M.A., Cole, N.M., Rafael, J.A., Hinkle, R.T., Faulkner, J.A., and Chamberlain, J.S. (1995). Expression of full-length and truncated dystrophin mini-genes in transgenic mdx mice. Human Molecular Genetics *4*, 1251–1258.

Piper, R.C., and Luzio, J.P. (2001). Late endosomes: sorting and partitioning in multivesicular bodies. Traffic *2*, 612–621.

Pirozzi, G., McConnell, S.J., Uveges, A.J., Carter, J.M., Sparks, A.B., Kay, B.K., and Fowlkes, D.M. (1997). Identification of novel human WW domain-containing proteins by cloning of ligand targets. Journal of Biological Chemistry *272*, 14611–14616.

Popplewell, L.J., Adkin, C., Arechavala-Gomeza, V., Aartsma-Rus, A., de Winter, C.L., Wilton, S.D., Morgan, J.E., Muntoni, F., Graham, I.R., and Dickson, G. (2010). Comparative analysis of antisense oligonucleotide sequences targeting exon 53 of the human DMD gene: Implications for future clinical trials. Neuromuscular Disorders *20*, 102–110.

Puri, V., Watanabe, R., Singh, R.D., Dominguez, M., Brown, J.C., Wheatley, C.L., Marks, D.L., and Pagano, R.E. (2001). Clathrin-dependent and -independent internalization of plasma membrane sphingolipids initiates two Golgi targeting pathways. The Journal of Cell Biology *154*, 535–547.

Raasi, S., Varadan, R., Fushman, D., and Pickart, C.M. (2005). Diverse polyubiquitin interaction properties of ubiquitin-associated domains. Nat Struct Mol Biol *12*, 708–714.

Rabut, G., and Peter, M. (2008). Function and regulation of protein neddylation. "Protein modifications: beyond the usual suspects" review series. EMBO Reports *9*, 969–976.

Rafael, J.A., Sunada, Y., Cole, N.M., Campbell, K.P., Faulkner, J.A., and Chamberlain, J.S. (1994). Prevention of dystrophic pathology in mdx mice by a truncated dystrophin isoform. Human Molecular Genetics *3*, 1725–1733.

Rafael, J.A., Tinsley, J.M., Potter, A.C., Deconinck, A.E., and Davies, K.E. (1998). Skeletal muscle-specific expression of a utrophin transgene rescues utrophin-dystrophin deficient mice. Nat. Genet. *19*, 79–82.

Ramachandran, J., Schneider, J.S., Crassous, P.A., Zheng, R., Gonzalez, J.P., Xie, L.H., Beuve, A., Fraidenraich, D., and Peluffo, R.D. (2012). Nitric oxide signalling pathway in Duchenne muscular dystrophy mice: up-regulation of L-arginine transporters. Biochem. J. *449*, 133–142.

Rentschler, S., Linn, H., Deininger, K., Bedford, M.T., Espanel, X., and Sudol, M. (1999). The WW domain of dystrophin requires EF-hands region to interact with β-dystroglycan. Biological Chemistry *380*, 431–442.

Repetto, S., Bado, M., Broda, P., Lucania, G., Masetti, E., Sotgia, F., Carbone, I., Pavan, A., Bonilla, E., Cordone, G., et al. (1999). Increased number of caveolae and caveolin-3 overexpression in Duchenne muscular dystrophy. Biochemical and Biophysical Research Communications *261*, 547–550.

Rezniczek, G.A., Konieczny, P., Nikolic, B., Reipert, S., Schneller, D., Abrahamsberg, C., Davies, K.E., Winder, S.J., and Wiche, G. (2007). Plectin 1f scaffolding at the sarcolemma of dystrophic (mdx) muscle fibers through multiple interactions with -dystroglycan. The Journal of Cell Biology *176*, 965–977.

Roberds, S.L., Anderson, R.D., Ibraghimov-Beskrovnaya, O., and Campbell, K.P. (1993a). Primary structure and muscle-specific expression of the 50-kDa dystrophin-associated glycoprotein (adhalin). Journal of Biological Chemistry *268*, 23739–23742.

Roberds, S.L., Ervasti, J.M., Anderson, R.D., Ohlendieck, K., Kahl, S.D., Zoloto, D., and Campbell, K.P. (1993b). Disruption of the dystrophin-glycoprotein complex in the cardiomyopathic hamster. Journal of Biological Chemistry *268*, 11496–11499.

Roberds, S.L., Leturcq, F., Allamand, V., Piccolo, F., Jeanpierre, M., Anderson, R.D., Lim, L.E., Lee, J.C., Tomé, F.M., and Romero, N.B. (1994). Missense mutations in the adhalin gene linked to autosomal recessive muscular dystrophy. Cell *78*, 625–633.

Roberts, R.G., Bobrow, M., and Bentley, D.R. (1992). Point mutations in the dystrophin gene. Proceedings of the National Academy of Sciences *89*, 2331–2335.

Roberts, R.G., Freeman, T.C., Kendall, E., Vetrie, D.L., Dixon, A.K., Shaw-Smith, C., Bone, Q., and Bobrow, M. (1996). Characterization of DRP2, a novel human dystrophin homologue. Nat. Genet. *13*, 223–226.

Rodal, S.K., Skretting, G., Garred, O., Vilhardt, F., van Deurs, B., and Sandvig, K. (1999). Extraction of cholesterol with methyl-beta-cyclodextrin perturbs formation of clathrin-coated endocytic vesicles. Mol. Biol. Cell *10*, 961–974.

Rodriguez, M.S., Dargemont, C., and Hay, R.T. (2001). SUMO-1 conjugation in vivo requires both a consensus modification motif and nuclear targeting. Journal of Biological Chemistry *276*, 12654–12659.

Rojek, J.M., Perez, M., and Kunz, S. (2008). Cellular Entry of Lymphocytic Choriomeningitis Virus. Journal of Virology *82*, 1505–1517.

Rooney, J.E., Welser, J.V., Dechert, M.A., Flintoff-Dye, N.L., Kaufman, S.J., and Burkin, D.J. (2006). Severe muscular dystrophy in mice that lack dystrophin and alpha7 integrin. Journal of Cell Science *119*, 2185–2195.

Rothberg, K.G., Heuser, J.E., Donzell, W.C., Ying, Y.S., Glenney, J.R., and Anderson, R.G. (1992). Caveolin, a protein component of caveolae membrane coats. Cell *68*, 673–682.

Rubino, M., Miaczynska, M., Lippé, R., and Zerial, M. (2000). Selective membrane recruitment of EEA1 suggests a role in directional transport of clathrin-coated vesicles to early endosomes. Journal of Biological Chemistry *275*, 3745–3748.

Russell, R.B., Breed, J., and Barton, G.J. (1992). Conservation analysis and structure prediction of the SH2 family of phosphotyrosine binding domains. FEBS Letters *304*, 15–20.

Russo, K., Di Stasio, E., Macchia, G., Rosa, G., Brancaccio, A., and Corinna Petrucci, T. (2000). Characterization of the β-Dystroglycan–Growth Factor Receptor 2 (Grb2) Interaction. Biochemical and Biophysical Research Communications *274*, 93–98.

Rybakova, I.N., Amann, K.J., and Ervasti, J.M. (1996). A new model for the interaction of dystrophin with F-actin. The Journal of Cell Biology *135*, 661–672.
Rybakova, I.N., Patel, J.R., and Ervasti, J.M. (2000). The dystrophin complex forms a mechanically strong link between the sarcolemma and costameric actin. The Journal of Cell Biology *150*, 1209–1214.

Sacco, P., Jones, D.A., Dick, J.R., Vrbová, G. (1992). Contractile properties and susceptibility to exercise-induced damage of normal and mdx mouse tibialis anterior muscle. Clin. Sci. (Lond) *82*, 227-236.

Schofield, J.N., Blake, D.J., Simmons, C., Morris, G.E., Tinsley, J.M., Davies, K.E., and Edwards, Y.H. (1994). Apo-dystrophin-1 and apo-dystrophin-2, products of the Duchenne muscular dystrophy locus: expression during mouse embryogenesis and in cultured cell lines. Human Molecular Genetics *3*, 1309–1316.

Sciandra, F., Schneider, M., Giardina, B., Baumgartner, S., Petrucci, T.C., and Brancaccio, A. (2001). Identification of the β-dystroglycan binding epitope within the C-terminal region of α-dystroglycan. European Journal of Biochemistry *268*, 4590–4597.

Scotti, E., Calamai, M., Goulbourne, C.N., Zhang, L., Hong, C., Lin, R.R., Choi, J., Pilch, P.F., Fong, L.G., Zou, P., et al. (2013). IDOL stimulates clathrin-independent endocytosis and multivesicular body-mediated lysosomal degradation of the low-density lipoprotein receptor. Molecular and Cellular Biology *33*, 1503–1514.

Seglen, P.O., Reith, A. (1976). Ammonia inhibition of protein degradation in isolated rat hepatocytes. Exp. Cell Res. *100*, 276-280.

Semerdjieva, S., Shortt, B., Maxwell, E., Singh, S., Fonarev, P., Hansen, J., Schiavo, G., Grant, B.D., Smythe, E. (2008) Coordinated regulation of AP2 uncoating from clathrin-coated vesicles by rab5 and hRME-6. *J Cell Biol*, *183*, 499-511

Sen, S., Tewari, M., Zajac, A., Barton, E., Sweeney, H.L., and Discher, D.E. (2011). Upregulation of paxillin and focal adhesion signaling follows Dystroglycan Complex deletions and promotes a hypertensive state of differentiation. European Journal of Cell Biology *90*, 249–260.

Seow, Y., Yin, H., and Wood, M.J.A. (2010). Identification of a novel muscle targeting peptide in mdx mice. Peptides *31*, 1873–1877.

Sgambato, A., Camerini, A., Faraglia, B., Pavoni, E., Montanari, M., Spada, D., Losasso, C., Brancaccio, A., and Cittadini, A. (2004). Increased expression of dystroglycan inhibits the growth and tumorigenicity of human mammary epithelial cells. Cancer Biol. Ther. *3*, 967–975.

Sgambato, A., Di Salvatore, M.A., De Paola, B., Rettino, A., Faraglia, B., Boninsegna, A., Graziani, C., Camerini, A., Proietti, G., and Cittadini, A. (2006). Analysis of dystroglycan regulation and functions in mouse mammary epithelial cells and implications for mammary tumorigenesis. J. Cell. Physiol. *207*, 520–529.

Sgambato, A., Camerini, A., Amoroso, D., Genovese, G., De Luca, F., Cecchi, M., Migaldi, M., Rettino, A., Valsuani, C., Tartarelli, G., et al. (2007). Expression of dystroglycan correlates with tumor grade and predicts survival in renal cell carcinoma. Cancer Biol. Ther. *6*, 1840–1846.

Shabek, N., Herman-Bachinsky, Y., Buchsbaum, S., Lewinson, O., Haj-Yahya, M., Hejjaoui, M., Lashuel, H.A., Sommer, T., Brik, A., and Ciechanover, A. (2012). The Size of the Proteasomal Substrate Determines Whether Its Degradation Will Be Mediated by Mono- or Polyubiquitylation. Molecular Cell *48*, 87–97.

Shah, W.A., Peng, H., and Carbonetto, S. (2006). Role of non-raft cholesterol in lymphocytic choriomeningitis virus infection via alpha-dystroglycan. J. Gen. Virol. *87*, 673–678.

Sharma, D.K., Choudhury, A., Singh, R.D., Wheatley, C.L., Marks, D.L., and Pagano, R.E. (2003). Glycosphingolipids internalized via caveolar-related endocytosis rapidly merge with the clathrin pathway in early endosomes and form microdomains for recycling. Journal of Biological Chemistry *278*, 7564–7572.

Sharma, D.K., Brown, J.C., Cheng, Z., Holicky, E.L., Marks, D.L., and Pagano, R.E. (2005). The glycosphingolipid, lactosylceramide, regulates beta1-integrin clustering and endocytosis. Cancer Research *65*, 8233–8241.

Shen, J.G., Xu, C.Y., Li, X., Dong, M.J., Jiang, Z.N., Wang, J., and Wang, L.B. (2011). Dystroglycan is Associated with Tumor Progression and Patient Survival in Gastric Cancer. Pathol. Oncol. Res. *18*, 79–84.

Sherman, D.L., Wu, L.M.N., Grove, M., Gillespie, C.S., and Brophy, P.J. (2012). Drp2 and Periaxin Form Cajal Bands with Dystroglycan But Have Distinct Roles in Schwann Cell Growth. Journal of Neuroscience *32*, 9419–9428.

Shi, F., and Sottile, J. (2008). Caveolin-1-dependent 1 integrin endocytosis is a critical regulator of fibronectin turnover. Journal of Cell Science *121*, 2360–2371.

Shi, F., Harman, J., Fujiwara, K., and Sottile, J. (2010). Collagen I matrix turnover is regulated by fibronectin polymerization. AJP: Cell Physiology *298*, C1265–C1275.

Shiga, K., Yoshioka, H., Matsumiya, T., Kimura, I., Takeda, S., and Imamura, M. (2006). ζ-Sarcoglycan is a functional homologue of γ-sarcoglycan in the formation of the sarcoglycan complex. Experimental Cell Research *312*, 2083–2092.

Shogomori, H., and Futerman, A.H. (2001). Cholera toxin is found in detergent-insoluble rafts/domains at the cell surface of hippocampal neurons but is internalized via a raft-independent mechanism. Journal of Biological Chemistry *276*, 9182–9188.

Sicinski, P., Geng, Y., Ryder-Cook, A.S., Barnard, E.A., Darlison, M.G., Barnard, P.J. (1989). The molecular basis of muscular dystrophy in the mdx mouse: a point mutation. Science *244*, 1578-1580.

Singh, R.D., Puri, V., Valiyaveettil, J.T., Marks, D.L., Bittman, R., and Pagano, R.E. (2003). Selective Caveolin-1–dependent Endocytosis of Glycosphingolipids. Mol. Biol. Cell *14*, 3254–3265.

Smythe, E., Redelmeier, T.E., Schmid, S.L. (1992). Receptor-mediated endocytosis in semiintact cells. Methods Enzymol. *219*, 223-234.

Song, K.S., Scherer, P.E., Tang, Z., Okamoto, T., Li, S., Chafel, M., Chu, C., Kohtz, D.S., and Lisanti, M.P. (1996). Expression of caveolin-3 in skeletal, cardiac, and smooth muscle cells. Caveolin-3 is a component of the sarcolemma and co-fractionates with dystrophin and dystrophin-associated glycoproteins. Journal of Biological Chemistry *271*, 15160–15165.

Sonnemann, K.J., Heun-Johnson, H., Turner, A.J., Baltgalvis, K.A., Lowe, D.A., and Ervasti, J.M. (2009). Functional substitution by TAT-utrophin in dystrophin-deficient mice. PLoS Med *6*, e1000083.

Sorrentino, V., Nelson, J.K., Maspero, E., Marques, A.R., Scheer, L., Polo, S., Zelcer, N. (2013). The LXR-IDOL axis defines a clathrin-, caveolae-, and dynamin-independent endocytic route for LDLR internalization and lysosomal degradation. J. Lipid Res. *54*, 2174-2184.

Sotgia, F., Lee, H., Bedford, M.T., Petrucci, T., Sudol, M., and Lisanti, M.P. (2001). Tyrosine Phosphorylation of β-Dystroglycan at Its WW Domain Binding Motif, PPxY, Recruits SH2 Domain Containing Proteins †. Biochemistry *40*, 14585–14592.

Sotgia, F., Bonuccelli, G., Bedford, M., Brancaccio, A., Mayer, U., Wilson, M.T., Campos-Gonzalez, R., Brooks, J.W., Sudol, M., and Lisanti, M.P. (2003a). Localization of Phospho-β-dystroglycan (pY892) to an Intracellular Vesicular Compartment in Cultured Cells and Skeletal Muscle Fibers in Vivo †. Biochemistry *42*, 7110–7123.

Sotgia, F., Woodman, S.E., Bonuccelli, G., Capozza, F., Minetti, C., Scherer, P.E., and Lisanti, M.P. (2003b). Phenotypic behavior of caveolin-3 R26Q, a mutant associated with hyperCKemia, distal myopathy, and rippling muscle disease. AJP: Cell Physiology *285*, C1150–C1160.

Sotgia, F., Bonuccelli, G., Minetti, C., Woodman, S.E., Capozza, F., Kemp, R.G., Scherer, P.E., Lisanti, M.P. (2003c). Phosphofructokinase muscle-specific isoform requires caveolin-3 expression for plasma membrane recruitment and caveolar targeting: implications for the pathogenesis of caveolin-related muscle diseases. Am. J. Pathol. *163*, 2619-2134.

Spence, H.J., Dhillon, A.S., James, M., and Winder, S.J. (2004). Dystroglycan, a scaffold for the ERK-MAP kinase cascade. EMBO Reports *5*, 484–489.

Spencer, M.J., Croall, D.E., and Tidball, J.G. (1995). Calpains are activated in necrotic fibers from mdx dystrophic mice. Journal of Biological Chemistry *270*, 10909–10914.

Stenmark, H., Aasland, R., Toh, B.-H., and D'Arrigo, A. (1996). Endosomal localization of the autoantigen EEA1 is mediated by a zinc-binding FYVE finger. Journal of Biological Chemistry *271*, 24048–24054.

Stevenson, S., Rothery, S., Cullen, M.J., and Severs, N.J. (1998). Spatial Relationship of the C-Terminal Domains of Dystrophin and -Dystroglycan in Cardiac Muscle Support a Direct Molecular Interaction at the Plasma Membrane Interface. Circulation Research *82*, 82–93.

Straub, V., Rafael, J.A., Chamberlain, J.S., and Campbell, K.P. (1997). Animal models for muscular dystrophy show different patterns of sarcolemmal disruption. The Journal of Cell Biology *139*, 375–385.

Sunada, Y., Bernier, S.M., Kozak, C.A., Yamada, Y., and Campbell, K.P. (1994). Deficiency of merosin in dystrophic dy mice and genetic linkage of laminin M chain gene to dy locus. Journal of Biological Chemistry *269*, 13729–13732.

Suzuki, A., Yoshida, M., Yamamoto, H., and Ozawa, E. (1992). Glycoprotein-binding site of dystrophin is confined to the cysteine-rich domain and the first half of the carboxy-terminal domain. FEBS Letters *308*, 154–160.

Suzuki, A., Yoshida, M., Hayashi, K., Mizuno, Y., Hagiwara, Y., and Ozawa, E. (1994). Molecular organization at the glycoprotein-complex-binding site of dystrophin. Three dystrophin-associated proteins bind directly to the carboxy-terminal portion of dystrophin. Eur. J. Biochem. *220*, 283–292.

Suzuki, A., Yoshida, M., and Ozawa, E. (1995). Mammalian alpha 1- and beta 1-syntrophin bind to the alternative splice-prone region of the dystrophin COOH terminus. The Journal of Cell Biology *128*, 373–381.

Takemitsu, M., Ishiura, S., Koga, R., Kamakura, K., Arahata, K., Nonaka, I., and Sugita, H. (1991). Dystrophin-related protein in the fetal and denervated skeletal muscles of normal and mdx mice. Biochemical and Biophysical Research Communications *180*, 1179–1186.

Taniguti, A.P.T., Matsumura, C.Y., Rodrigues-Simioni, L., Neto, H.S., and Marques, M.J. (2012). Suramin affects metalloproteinase-9 activity and increases beta-dystroglycan levels in the diaphragm of the dystrophin-deficient mdxMOUSE. Muscle Nerve *46*, 810–813.

Taylor, J., Muntoni, F., Dubowitz, V., Sewry, C.A. (1997). The abnormal expression of utrophin in Duchenne and Becker muscular dystrophy is age related. Neuropathol. Appl. Neurobiol. *23*, 399-405.

thi Man, N., Helliwell, T.R., Simmons, C., Winder, S.J., Kendrick-Jones, J., Davies, K.E., and Morris, G.E. (1995). Full-length and short forms of utrophin, the dystrophin-related protein. FEBS Letters *358*, 262–266.

Thomas, G.H., Newbern, E.C., Korte, C.C., Bales, M.A., Muse, S.V., Clark, A.G., and Kiehart, D.P. (1997). Intragenic duplication and divergence in the spectrin superfamily of proteins. Mol. Biol. Evol. *14*, 1285–1295.

Thompson, O., Kleino, I., Crimaldi, L., Gimona, M., Saksela, K., and Winder, S.J. (2008). Dystroglycan, Tks5 and Src mediated assembly of podosomes in myoblasts. PLoS ONE *3*, e3638.

Thompson, O., Moore, C.J., Hussain, S.A., Kleino, I., Peckham, M., Hohenester, E., Ayscough, K.R., Saksela, K., and Winder, S.J. (2010). Modulation of cell spreading and cell-substrate adhesion dynamics by dystroglycan. Journal of Cell Science *123*, 118–127.

Thrower, J.S., Hoffman, L., Rechsteiner, M., and Pickart, C.M. (2000). Recognition of the polyubiquitin proteolytic signal. The EMBO Journal *19*, 94–102.

Tinsley, J.M., Blake, D.J., and Davies, K.E. (1993). Apo-dystrophin-3: a 2.2kb transcript from the DMD locus encoding the dystrophin glycoprotein binding site. Human Molecular Genetics *2*, 521–524.

Tinsley, J.M., Potter, A.C., Phelps, S.R., Fisher, R., Trickett, J.I., Davies, K.E. (1996). Amelioration of the dystrophic phenotype of mdx mice using a truncated utrophin transgene. Nature *384*, 349-353.

Tinsley, J., Deconinck, N., Fisher, R., Kahn, D., Phelps, S., Gillis, J.M., and Davies, K. (1998). Expression of full-length utrophin prevents muscular dystrophy in mdx mice. Nat Med *4*, 1441–1444.

Tinsley, J.M., Fairclough, R.J., Storer, R., Wilkes, F.J., Potter, A.C., Squire, S.E., Powell, A.C., Squire, S.E., Powell, D.S., Cozzoli, A., Capogrosso, R.F., Lambert, A., Wilson, F.X., Wren, S.P., De Luca, A., Davies, K.E. (2011). Daily treatment with SMTC1100, a novel small utrophin upregulator, dramatically reduces the dystrophic symptoms in the mdx mouse. PLoS One *6*, e19189

Torgersen, M.L., Skretting, G., van Deurs, B., and Sandvig, K. (2001). Internalization of cholera toxin by different endocytic mechanisms. Journal of Cell Science *114*, 3737–3747.

Trischler, M., Stoorvogel, W., and Ullrich, O. (1999). Biochemical analysis of distinct Rab5- and Rab11-positive endosomes along the transferrin pathway. Journal of Cell Science *112 (Pt 24)*, 4773–4783.

Trotman, L.C., Wang, X., Alimonti, A., Chen, Z., Teruya-Feldstein, J., Yang, H., Pavletich, N.P., Carver, B.S., Cordon-Cardo, C., Erdjument-Bromage, H., et al. (2007). Ubiquitination regulates PTEN nuclear import and tumor suppression. Cell *128*, 141–156.

Truong, K., Lee, T.D., Li, B., and Chen, Y. (2012). Sumoylation of SAE2 C Terminus Regulates SAE Nuclear Localization. Journal of Biological Chemistry *287*, 42611–42619.

Vaghy, P.L., Fang, J., Wu, W., and P Vaghy, L. (1998). Increased caveolin-3 levels in mdx mouse muscles. FEBS Letters *431*, 125–127.

Vainzof, M., Passos-Bueno, M.R., Canovas, M., Moreira, E.S., Pavanello, R.C., Marie, S.K., Anderson, L.V., Bönnemann, C.G., McNally, E.M., Nigro, V., et al. (1996). The sarcoglycan complex in the six autosomal recessive limb-girdle muscular dystrophies. Human Molecular Genetics *5*, 1963–1969.

van der Veen, A.G., and Ploegh, H.L. (2012). Ubiquitin-Like Proteins. Annu. Rev. Biochem. *81*, 323–357.

van Deutekom, J.C., Janson, A.A., Ginjaar, I.B., Frankhuizen, W.S., Aartsma-Rus, A., Bremmer-Bout, M., Dunnen, Den, J.T., Koop, K., van der Kooi, A.J., Goemans, N.M., et al. (2007). Local dystrophin restoration with antisense oligonucleotide PRO051. N Engl J Med *357*, 2677–2686.

Vega-Moreno, J., Tirado-Cortes, A., Álvarez, R., Irles, C., Mas-Oliva, J., and Ortega, A. (2012). Cholesterol depletion uncouples β-dystroglycans from discrete sarcolemmal domains, reducing the mechanical activity of skeletal muscle. Cell. Physiol. Biochem. *29*, 905–918.

Vercauteren, D., Vandenbroucke, R.E., Jones, A.T., Rejman, J., Demeester, J., De Smedt, S.C., Sanders, N.N., and Braeckmans, K. (2009). The use of inhibitors to study endocytic pathways of gene carriers: optimization and pitfalls. Molecular Therapy *18*, 561–569.

Vijay-Kumar, S., Bugg, C.E., Wilkinson, K.D., Vierstra, R.D., Hatfield, P.M., and Cook, W.J. (1987). Comparison of the three-dimensional structures of human, yeast, and oat ubiquitin. Journal of Biological Chemistry *262*, 6396–6399.

Voit, T., Haas, K., Léger, J.O., Pons, F., and Léger, J.J. (1991). Xp21 dystrophin and 6q dystrophin-related protein. Comparative immunolocalization using multiple antibodies. The American Journal of Pathology *139*, 969–976.

Volonté, D., Galbiati, F., Li, S., Nishiyama, K., Okamoto, T., and Lisanti, M.P. (1999). Flotillins/Cavatellins Are Differentially Expressed in Cells and Tissues and Form a Hetero-oligomeric Complex with Caveolins in Vivo CHARACTERIZATION AND EPITOPE-MAPPING OF A NOVEL FLOTILLIN-1 MONOCLONAL ANTIBODY PROBE. Journal of Biological Chemistry *274*, 12702–12709.

Wakefield, P.M., Tinsley, J.M., Wood, M.J., Gilbert, R., Karpati, G., and Davies, K.E. (2000). Prevention of the dystrophic phenotype in dystrophin/utrophin-deficient muscle following adenovirus-mediated transfer of a utrophin minigene. Gene Ther. *7*, 201–204.

Wang, B., Li, J., and Xiao, X. (2000). Adeno-associated virus vector carrying human minidystrophin genes effectively ameliorates muscular dystrophy in mdx mouse model. Proceedings of the National Academy of Sciences *97*, 13714–13719.

Wang, Q., Yin, H., Camelliti, P., Betts, C., Moulton, H., Lee, H., Saleh, A.F., Gait, M.J., and Wood, M.J.A. (2010). In vitro evaluation of novel antisense oligonucleotides is predictive of in vivo exon skipping activity for Duchenne muscular dystrophy. J Gene Med *12*, 354–364.

Wang, Y.E., Pernet, O., and Lee, B. (2011). Regulation of the nucleocytoplasmic trafficking of viral and cellular proteins by ubiquitin and small ubiquitin-related modifiers. Biology of the Cell *104*, 121–138.

Wehling, M., Spencer, M.J., and Tidball, J.G. (2001). A nitric oxide synthase transgene ameliorates muscular dystrophy in mdx mice. The Journal of Cell Biology *155*, 123–132.

Weller, S.G., Capitani, M., Cao, H., Micaroni, M., Luini, A., Sallese, M., and McNiven, M.A. (2010). Src kinase regulates the integrity and function of the Golgi apparatus via activation of dynamin 2. Proceedings of the National Academy of Sciences *107*, 5863–5868.

Whiteley, G., Collins, R.F., and Kitmitto, A. (2012). Characterization of the molecular architecture of human caveolin-3 and interaction with the skeletal muscle ryanodine receptor. J. Biol. Chem. *287*, 40302–40316.

Wibo, M., and Poole, B. (1974). Protein degradation in cultured cells. II. The uptake of chloroquine by rat fibroblasts and the inhibition of cellular protein degradation and cathepsin B1. The Journal of Cell Biology *63*, 430–440.

Wilkinson, K.D., and Audhya, T.K. (1981). Stimulation of ATP-dependent proteolysis requires ubiquitin with the COOH-terminal sequence Arg-Gly-Gly. Journal of Biological Chemistry *256*, 9235–9241.

Williamson, R.A., Henry, M.D., Daniels, K.J., Hrstka, R.F., Lee, J.C., Sunada, Y., Ibraghimov-Beskrovnaya, O., and Campbell, K.P. (1997). Dystroglycan is essential for early embryonic development: disruption of Reichert's membrane in Dag1-null mice. Human Molecular Genetics *6*, 831–841.

Wilson, M.D., Saponaro, M., Leidl, M.A. and Svesjstrup, J.Q. (2012). MultiDsk: A Ubiquitin-Specific Affinity Resin. *PLOS One*, *7*, e46398

Winder, S.J., and Kendrick-Jones, J. (1995). Calcium/calmodulin-dependent regulation of the NH2-terminal F-actin binding domain of utrophin. FEBS Letters *357*, 125–128.

Wright, W.E., Sassoon, D.A., and Lin, V.K. (1989). Myogenin, a factor regulating myogenesis, has a domain homologous to MyoD. Cell *56*, 607–617.
Wu, L., and Gonias, S.L. (2005). The low-density lipoprotein receptor-related protein-1 associates transiently with lipid rafts. J. Cell. Biochem. *96*, 1021–1033.

Yaffe, D., Feldman, M. (1965). The formation of hybrid multinucleated muscle fibres from myoblasts of different genetic origin. Dev. Biol. *11*, 300-317.

Yang, B., Jung, D., Motto, D., Meyer, J., Koretzky, G., and Campbell, K.P. (1995a). SH3 domain-mediated interaction of dystroglycan and Grb2. Journal of Biological Chemistry *270*, 11711–11714.

Yang, B., Jung, D., Rafael, J.A., Chamberlain, J.S., and Campbell, K.P. (1995b). Identification of α-syntrophin binding to syntrophin triplet, dystrophin, and utrophin. Journal of Biological Chemistry *270*, 4975–4978.

Yang, B., and Kumar, S. (2010). Nedd4 and Nedd4-2: closely related ubiquitin-protein ligases with distinct physiological functions. Cell Death and Differentiation *17*, 68–77.

Yatsenko, A.S., Kucherenko, M.M., Pantoja, M., Fischer, K.A., Madeoy, J., Deng, W.-M., Schneider, M., Baumgartner, S., Akey, J., Shcherbata, H.R., et al. (2009). The conserved WW-domain binding sites in Dystroglycan C-terminus are essential but partially redundant for Dystroglycan function. BMC Dev Biol *9*, 18.

Yin, H., Moulton, H.M., Seow, Y., Boyd, C., Boutilier, J., Iverson, P., and Wood, M.J.A. (2008). Cell-penetrating peptide-conjugated antisense oligonucleotides restore systemic muscle and cardiac dystrophin expression and function. Human Molecular Genetics *17*, 3909–3918.

Yin, H., Moulton, H.M., Betts, C., Seow, Y., Boutilier, J., Iverson, P.L., and Wood, M.J. (2009). A fusion peptide directs enhanced systemic dystrophin exon skipping and functional restoration in dystrophin-deficient mdx mice. Human Molecular Genetics *18*, 4405–4414.

Yin, H., Betts, C., Saleh, A.F., Ivanova, G.D., Lee, H., Seow, Y., Kim, D., Gait, M.J., and Wood, M.J. (2010a). Optimization of Peptide Nucleic Acid Antisense Oligonucleotides for Local and Systemic Dystrophin Splice Correction in the mdx Mouse. Molecular Therapy *18*, 819–827.

Yin, H., Moulton, H.M., Betts, C., Merritt, T., Seow, Y., Ashraf, S., Wang, Q., Boutilier, J., and Wood, M.J. (2010b). Functional rescue of dystrophin-deficient mdx mice by a chimeric peptide-PMO. Mol. Ther. *18*, 1822–1829.

Yoshida, M., and Ozawa, E. (1990). Glycoprotein complex anchoring dystrophin to sarcolemma. J. Biochem. *108*, 748–752.

Yoshida, M., Suzuki, A., Yamamoto, H., Noguchi, S., Mizuno, Y., and Ozawa, E. (1994). Dissociation of the complex of dystrophin and its associated proteins into several unique groups by n-octyl beta-D-glucoside. Eur. J. Biochem. *222*, 1055–1061.

Yoshida, T., Pan, Y., Hanada, H., Iwata, Y., and Shigekawa, M. (1998). Bidirectional signaling between sarcoglycans and the integrin adhesion system in cultured L6 myocytes. Journal of Biological Chemistry *273*, 1583–1590.

Yoshida, M., Hama, H., Ishikawa-Sakurai, M., Imamura, M., Mizuno, Y., Araishi, K., Wakabayashi-Takai, E., Noguchi, S., Sasaoka, T., and Ozawa, E. (2000). Biochemical evidence for association of dystrobrevin with the sarcoglycan-sarcospan complex as a basis for understanding sarcoglycanopathy. Human Molecular Genetics *9*, 1033–1040.

Yotsumoto, S., Fujiwara, H., Horton, J.H., Mosby, T.A., Wang, X., Cui, Y., and Ko, M.S. (1996). Cloning and expression analyses of mouse dystroglycan gene: specific expression in maternal decidua at the peri-implantation stage. Human Molecular Genetics *5*, 1259–1267.

Yurchenko, V., Xue, Z., and Sadofsky, M.J. (2006). SUMO modification of human XRCC4 regulates its localization and function in DNA double-strand break repair. Molecular and Cellular Biology *26*, 1786–1794.

Zaidel-Bar, R., Itzkovitz, S., Ma'ayan, A., Iyengar, R., and Geiger, B. (2007). Functional atlas of the integrin adhesome. Nat Cell Biol *9*, 858–867.

Zhan, Y., Tremblay, M.R., Melian, N., and Carbonetto, S. (2005). Evidence that dystroglycan is associated with dynamin and regulates endocytosis. Journal of Biological Chemistry *280*, 18015–18024.

Zoncu, R., Perera, R.M., Balkin, D.M., Pirruccello, M., Toomre, D., and De Camilli, P. (2009). A phosphoinositide switch controls the maturation and signaling properties of APPL endosomes. Cell *136*, 1110–1121.

Zovein, A.C., Luque, A., Turlo, K.A., Hofmann, J.J., Yee, K.M., Becker, M.S., Fassler, R., Mellman, I., Lane, T.F., and Iruela-Arispe, M.L. (2010). β1 integrin establishes endothelial cell polarity and arteriolar lumen formation via a Par3-dependent mechanism. Developmental Cell *18*, 39–51.